Welsh School of Pharmacy – Cardiff University
Tysgol Fferylliaeth – Prifysgol Caerdydd

CARDIFF
UNIVERSITY
PRIFYSGOL
CAERDYDD

A thesis submitted to the University of Wales for the degree of

Doctor of Philosophy

By

Nicholas Carpenter

Design and Synthesis of Inhibitors of Critical Target Proteins Implicated in Cellular Proliferation.

September 2005

Supervisor: Dr Alex W. White

UMI Number: U584163

All rights reserved

INFORMATION TO ALL USERS
The quality of this reproduction is dependent upon the quality of the copy submitted.

In the unlikely event that the author did not send a complete manuscript
and there are missing pages, these will be noted. Also, if material had to be removed,
a note will indicate the deletion.

UMI U584163
Published by ProQuest LLC 2013. Copyright in the Dissertation held by the Author.
Microform Edition © ProQuest LLC.
All rights reserved. This work is protected against
unauthorized copying under Title 17, United States Code.

ProQuest LLC
789 East Eisenhower Parkway
P.O. Box 1346
Ann Arbor, MI 48106-1346

CARDIFF
UNIVERSITY
PRIFYSGOL
CAERDYDD

BINDING SERVICES
Tel +44 (0)29 2087 4949
Fax +44 (0)29 20371921
e-mail bindery@cardiff.ac.uk

Acknowledgements

I would like to thank my supervisor for all his help during the project, especially his thorough knowledge of the subject area and attention to detail. I wish him all the best in his continued research in this field.

Many thanks also to the staff of the University for their advice and encouragement, and to Prof. Rob Nicholson, Denise Barrow, Carol Dutkowski and Richard McClelland of Tenovus, and KuDOS Pharmaceuticals Ltd, Cambridge, UK for their assistance with the biological assays.

Special thanks to project students Sarah, Tamsin and Kate for their contribution to this project. Also the AWW lab; Jerômé, Parinaz, Matt, Rupi and Andy, the McGuigan group and the Monday night footballers for their intellect, sense of humour, excellent cookery skills and discussion of the beautiful game.

Finally, thanks to Susan and my family; Mum, Dad, Dannie, Linny and Emily. Without your patience, love and support this would not have been possible.

Abstract

Cyclin-Dependent Kinases (CDKs) are a family of protein kinases that control progression through the eukaryotic cell cycle. CDKs become activated when they form a complex with the appropriate cyclin protein, and are fully activated by phosphorylation. CDK inhibitors regulate the activity of CDK/cyclin complexes through competitive inhibition with ATP for the active site. This inhibition prevents the CDK/cyclin complex phosphorylating its substrates and cell cycle progression stops.

Alterations in CDK control through cyclin overexpression, CDK inhibitor underexpression or CDK mutation are responsible for tumour development. Therefore CDK inhibition has become a novel therapeutic approach to cancer treatment.

Hymenialdisine and Kenpaullone have recently been identified as potent CDK inhibitors. The crystal structures of these two compounds as inhibitors of CDK2 show that Kenpaullone can form two hydrogen bonds to residue Leu83, while Hymenialdisine forms these two hydrogen bonds and a third to Glu81. These hydrogen bonds have been shown to be significant towards their potency, and are formed from the azepinone fused to a heterocycle feature of both structures.

The aim of this thesis is to explore the structure activity relationship associated with the novel azepinone motif of the two CDK inhibitors Kenpaullone and Hymenialdisine via analogues of the lead structure 3,4-dihydroazepino[3,4-*b*]indole-1,5(2*H*,10*H*)-dione, trivially named indoloazepinone. These analogues focus on alterations to the hydrogen bonding pattern, the size of the azepinone ring, extensions from the ketone functional group and bromination at the 7-posititon.

The compounds synthesized in the study were assayed against MCF-7 breast cancer and A549 non small cell lung cancer (NSCLC) cell lines showing good growth inhibition. An accumulation of proliferating cancer cells in the G_0/G_1 stage was demonstrated for a selected compound. Further assays against CDK2/cyclin A showed generally moderate inhibition, with good inhibition for one compound, while assays against Chk2 showed no inhibition.

Abbreviations

Δ (heat)
Ac (acetate)
ATM (ataxia-telengiectasia, mutated)
ATP (adenosine triphosphate)
ATR (ataxia-telengiectasia and Rad3-related)
aq (aqueous)
Bn (benzyl)
Bu (butyl)
CAK (CDK activating kinase)
CDC25 (cell division cycle 25)
CDK (cyclin-dependent kinase)
CDKI (cyclin-dependent kinase inhibitors)
Chk (checkpoint kinase)
Cip (CDK interacting protein)
DCC (1,3-dicyclohexylcarbodiimide)
DCM (dichloromethane)
DMAP (4-dimethylaminopyridine)
DMF (dimethylformamide)
DNA (deoxyribonucleic acid)
E2F (transcription factor)
EDCI (1-(3-dimethylaminopropyl)-3-ethylcarbodiimide hydrochloride)
Et (ethyl)
GI_{50} (50 % growth inhibition)
Gsk3 (glycogen synthase kinase 3)
HRMS (high resolution mass spectrometry)
IC_{50} (50 % inhibitory concentration)
INK4 (inhibitors of CDK4 and CDK6)
IUPAC (international union of pure and applied chemistry)
Kip (kinase inhibitory protein)
LDA (lithium diisopropylamide)
Me (methyl)
MOE (molecular operating environment)

MPF (mitotic promoting factor / M-phase promoting factor)
NBS (N-bromo succinamide)
NCI (national cancer institute)
NMR (nuclear magnetic resonance)
NOE (nuclear overhauser enhancement)
NOSEY (nuclear overhauser enhancement spectrometry)
NSCLC (non small cell lung cancer)
PDB (protein data bank)
Ph (phenyl)
PPA (polyphosphoric acid)
pRb (retinoblastoma protein)
psi (pounds per square inch)
Rb (retinoblastoma)
RNA (ribonucleic acid)
SEM (2-(trimethylsilyl)ethoxymethyl)
TEA (triethylamine)
TBAF (tetrabutylammonium fluoride)
TBDMS (tertiary-butyl dimethyl silyl)
tert (tertiary)
THF (tetrahydrofuran)
TLC (thin layer chromatography)
Ub (ubiquitin)

Table of Contents

1. INTRODUCTION 3

1.1 INTRODUCTION TO CANCER 3
1.2 THE CELL CYCLE 4
1.3 ENTRY TO THE G_1 PHASE 6
1.4 G_1 TO S PHASE TRANSITION 8
1.5 G_2 TO M PHASE TRANSITION 10
1.6 CDKS AND CYCLIN 12
  1.6.1 INK4 Family 15
  1.6.2 Cip/Kip Family 15
  1.6.3 CDK/Cyclin Location in the Cell 16
  1.6.4 CDK2 Structure, Cyclin Binding and Phosphorylation 16
  1.6.5 ATP Binding Site in Monomeric CDK2 21
1.7 CDK INHIBITORS 23
  1.7.1 Purine Based Inhibitors 24
  1.7.2 Flavones 26
  1.7.3 Paullones 27
  1.7.4 Hymenialdisine 29
  1.7.5 Other CDK Inhibitors 31

2. AIMS 33

2.1 SYNTHETIC AIMS 33
2.2 NOMENCLATURE 36

3. RESULTS AND DISCUSSION 38

3.1 INITIAL LEAD COMPOUND 38
3.2 SYNTHESIS OF N-METHYLINDOLOAZEPINONE 42
3.3 ALTERATIONS IN THE R POSITION 48
3.4 ALTERATIONS AT THE X-POSITION 57
3.5 ALTERATIONS IN THE Y POSITION 61

3.5.1 Hydrazone Extension 62

3.5.2 Oxime Extension 68

3.5.3 Extended Indoloazepinones 72

3.6 ALTERATIONS AT THE Z POSITION 83

3.7 MOLECULAR MODELLING 94

3.8. MOLECULAR DOCKING WITH MOE 99

3.8.1 Control Experiment 100

3.8.2 Docking Results 101

3.9 STEREOCHEMISTRY INVERSION 105

3.10 KENPAULLONE SYNTHESIS 108

3.11 SYNTHESIS CONCLUSIONS 110

4. BIOLOGICAL RESULTS 112

4.1 GROWTH INHIBITION ASSAYS 112

4.1.1 Reference compounds 113

4.1.2 Alterations in the X and R Positions 114

4.1.3 N-Methylindoloazepinone Analogues 117

4.1.4 Miscellaneous Compounds 120

4.1.5 Comparisons to Pyrrole Derivatives 121

4.2 CELL CYCLE ANALYSIS 122

4.3 CDK2/CYCLIN A INHIBITION 123

4.3.1 Reference Compounds 124

4.3.2 Synthesized Compounds 125

4.3.3 Comparisons to Pyrrole Derivatives 128

4.4 CHK2 INHIBITION 129

4.5 BIOLOGICAL CONCLUSIONS 132

5. CONCLUSION 133

6. EXPERIMENTAL 140

6.1 GENERAL METHODS 140

6.1.1 Thin Layer Chromatography 140

6.1.2 Column Chromatography......140

6.1.3 NMR Spectroscopy......140

6.1.4 Mass Spectrometry......140

6.1.5 Infrared Spectroscopy......141

6.1.6 Melting point......141

6.1.7 Cooling Baths......141

6.2 GENERAL PROCEDURES......142

Method A – Indole N protection......142

Method B – Amide bond formation (i)......142

Method C – Amide bond formation (ii)......143

Method D –Hydrolysis......143

Method E – Cyclization......143

Method F – Extension from ketone position (i)......144

Method G – Extension from ketone position (ii)......144

Method H – Extension from oxime......144

Method I - Bromination......145

Method J Cyclization (ii)......145

Method K Esterification......145

Ethyl 1H-indole-2-carboxylate [32]......146

1-Methyl-1H-indole-2-carboxylic acid [34]......146

1-Benzyl-1H-indole-2-carboxylic acid [39]......147

2,10-bis((2-(Trimethylsilyl)ethoxy)methyl)-3,4-dihydroazepino [3,4-b]indole-1,5(2H,10H)-dione [77]......147

3-Bromo-1-methyl-1H-indole-2-carboxylic acid [114]......148

1-(4-Methoxybenzyl)-1H-indole-2-carboxylic acid [80]......148

Ethyl 3-(1-methyl-1H-indole-2-carboxamido)propanoate [35]......148

Methyl 2-(1-methyl-1H-indole-2-carboxamido)benzoate [153]......149

Ethyl 3-(1-benzyl-1H-indole-2-carboxamido)propanoate [40]......149

Ethyl 3-(1H-indole-2-carboxamido)propanoate [52]......150

Ethyl 2-(1H-indole-2-carboxamido)acetate [117]......150

Ethyl 2-(1-methyl-1H-indole-2-carboxamido)acetate [154]......151

Ethyl 3-(3-bromo-1-methyl-1H-indole-2-carboxamido)propanoate [63]......151

Ethyl 3-(1-(4-methoxybenzyl)-1H-indole-2-carboxamido) propanoate [82]......152

Ethyl 4-(1H-indole-2-carboxamido)butanoate [120]......152

N-(2-(N-Methoxy-N-methylcarbamoyl)ethyl)-3-bromo-1-methyl-1H-indole-2-carboxamide [116] *153*
N-(3-(N-Methoxy-N-methylcarbamoyl)propyl)-3-bromo-1H-indole-2-carboxamide [121] *153*
N-((N-Methoxy-N-methylcarbamoyl)methyl)-3-bromo-1H-indole-2-carboxamide [118] *154*
N-(2-(N-Methoxy-N-methylcarbamoyl)ethyl)-3-bromo-1H-indole-2-carboxamide [119] *154*
3-(1-Methyl-1H-indole-2-carboxamido)propanoic acid [37] *155*
2-(1-Methyl-1H-indole-2-carboxamido)acetic acid [102] *155*
2-(1-Methyl-1H-indole-2-carboxamido)benzoic acid [103] *156*
3-(1H-Indole-2-carboxamido)propanoic acid [27] *156*
2-(1H-Indole-2-carboxamido)acetic acid [99] *156*
3-(3-Bromo-1H-indole-2-carboxamido)propanoic acid) [157] *157*
3-(3-Bromo-1-methyl-1H-indole-2-carboxamido)propanoic acid [115] *157*
4-(3-Bromo-1H-indole-2-carboxamido)butanoic acid [155] *158*
2-(3-Bromo-1H-indole-2-carboxamido)acetic acid [156] *158*
4-(1H-Indole-2-carboxamido)butanoic acid [100] *159*
3-(1-Benzyl-1H-indole-2-carboxamido)propanoic acid [41] *159*
3,4-Dihydro-10-methylazepino[3,4-b]indole-1,5(2H,10H)-dione [31] *160*
3,4-Dihydroazepino[3,4-b]indole-1,5(2H,10H)-dione [25] *160*
2,3-Dihydro-pyrazino[1,2-a]indole-1,4-dione [101] *161*
1-(1-methyl-1H-indole-2-carbonyl)benzo[b]azet-2(1H)-one [104] *161*
(E)-5-(2-Phenylhydrazono)-2,3,4,5-tetrahydro-10-methylazepino[3,4-b]indol-1(10H)-one [65] *162*
(E)-5-(2-(4-Fluorophenyl)hydrazono)-2,3,4,5-tetrahydro-10-methylazepino[3,4-b]indol-1(10H)-one [68] *162*
(E)-5-(2-(4-Carboxylic acid methyl ester)hydrazono)-2,3,4,5-tetrahydro-10-methylazepino[3,4-b]indol-1(10H)-one [72] *163*
(E)-2,3,4,5-Tetrahydro-5-(hydroxyimino)-10-methylazepino[3,4-b]indol-1(10H)-one [73] *164*
(E)-5-(2-Phenylhydrazono)-2,3,4,5-tetrahydroazepino[3,4-b]indol-1(10H)-one [64] *164*
(E)-2,3,4,5-Tetrahydro-5-(hydroxyimino)azepino[3,4-b]indol-1(10H)-one [87]165

(E)-7-Bromo-2,3,4,5-tetrahydro-5-(hydroxyimino)azepino[3,4-b]indol-1(10H)-one [86] *165*
(E)-5-(Benzyloxy)imino-2,3,4,5-tetrahydroazepino[3,4-b]indol-1(10H)-one[88]166
N-(2-(Benzyloxycarbamoyl)phenyl)-1-methyl-1H-indole-2-carboxamide [107].167
(E)-5-(benzyloxy)imino-2,3,4,5-tetrahydro-10-methylazepino[3,4-b]indol-1(10H)-one [75] *167*
(E)-5-(Cyclohexylmethoxy)imino-2,3,4,5-tetrahydroazepino[3,4-b]indol-1(10H)-one [76] *168*
Ethyl 3-(3-bromo-1H-indole-2-carboxamido)propanoate [56] *169*
7-Bromo-3,4-dihydro-2H,10H-azepino[3,4-b]indole-1,5-dione [57] *169*
Ethyl 3-bromo-1H-indole-2-carboxylate [113] *169*
Ethyl 4-(3-bromo-1H-indole-2-carboxamido)butanoate [158] *170*
Ethyl 2-(3-bromo-1H-indole-2-carboxamido)acetate [159] *170*
N-((Methoxycarbamoyl)methyl)-3-bromo-1H-indole-2-carboxamide [122] *171*
N-(3-(Methoxycarbamoyl)propyl)-3-bromo-1H-indole-2-carboxamide) [123] and 3-Bromo-N-(5,5-dimethyl-4-oxohexyl)-1H-indole-2-carboxamide [124] *171*
β-Alanine ethyl ester hydrochloride [36] *172*
Methyl 4-hydrazinylbenzoate hydrochloride [70] *172*
Ethyl 1-tosyl-1H-indole-2-carboxylate [44] *173*
Phenylmagnesium bromide [47] *173*
Diphenyl-4-pyridylmethanol [49] *174*
Diphenyl-4-pyridylmethyl Chloride Hydrochloride [50] *174*
Methyl 2-(3-Ethoxycarbonyl-propionylamino)-benzoate [137] *175*
4,5-Dihydro-1H-benzo[b]azepin-2(3H)-one [141] *175*
3,4-Dihydro-1H-benzo[b]azepine-2,5-dione [139] *176*
Kenpaullone [14] *176*
2-Phenoxyisoindoline-1,3-dione [135] *177*
BIOLOGICAL ASSAYS 177
Cellular Proliferation Assays *177*
CDK2/Cyclin A Assay *178*
Chk2 Assay *178*
Molecular Modelling *179*

REFERENCES 180

Outline of Thesis

In normal cells, growth is regulated in order to maintain the correct balance between proliferation and cell death. In cancer cells, the regulation of this vital balance is lost, resulting in excessive growth and reduced cell death. A family of serine/threonine protein kinases, the cyclin-dependent kinases (CDKs) play an influential role in progression through the cell cycle and cell proliferation. Misregulation of CDK activity is a common feature in many important tumours. The role of CDKs in controlling the cell cycle has presented an attractive target for the design of novel anti-cancer agents, and X-ray crystal structures of active and inactive CDK2, as well as inhibitor-CDK2 complexes have been established. A number of synthetic CDK inhibitors have been discovered, and good selectivity for CDKs over other kinases has been established. Selectivity between individual CDKs is also often observed.

This thesis will discuss the development of new potential anti-proliferative drugs designed as CDK2 inhibitors and based on the structure of known inhibitors Hymenialdisine and Kenpaullone. The aim of the study is to develop a new series of ATP competitive CDK2 inhibitors that could be used as anti-tumour agents. Chapter 1 will give a general background to the cell cycle, paying particular interest in the role of the CDKs. This is followed by detail of the activation of the CDK2/cyclin A complex, and a review of known synthetic CDK inhibitors. The chemical synthesis of the series of compounds is then discussed in chapter 3, followed by the biological evaluation in chapter 4. The conclusions to the project are summarized in chapter 5 and the experimental procedures of the work are in chapter 6.

1. INTRODUCTION 3

1.1 INTRODUCTION TO CANCER 3

1.2 THE CELL CYCLE 4

1.3 ENTRY TO THE G_1 PHASE 6

1.4 G_1 TO S PHASE TRANSITION 8

1.5 G_2 TO M PHASE TRANSITION 10

1.6 CDKS AND CYCLIN 12

1.6.1 INK4 Family 15

1.6.2 Cip/Kip Family 15

1.6.3 CDK/Cyclin Location in the Cell 16

1.6.4 CDK2 Structure, Cyclin Binding and Phosphorylation 16

1.6.5 ATP Binding Site in Monomeric CDK2 21

1.7 CDK INHIBITORS 23

1.7.1 Purine Based Inhibitors 24

1.7.2 Flavones 26

1.7.3 Paullones 27

1.7.4 Hymenialdisine 29

1.7.5 Other CDK Inhibitors 31

1. Introduction

1.1 Introduction to Cancer

Cancer is a major cause of death in the UK with more than three quarters of a million new cases registered in 2000. More than one in three people will be diagnosed with a cancer during their lifetime, with one in four dying from their disease.[1] Worldwide, cancer accounts for 12.5 % of deaths – over 7 million deaths a year.[2]

Cancer is not a single disease. It is a broad group characterized by uncontrolled cell proliferation. Most, if not all malignant tumours are the result of a deregulated cell cycle.[3] Every cell division has the potential to give rise to mutations that could result in onset of cancer. Therefore, not surprisingly, the risk of developing cancer rises significantly as an individual ages. Indeed, 65 % of all cases in the UK occur in people aged over 65.[1] In most cases, overactivity of positive, or underactivity of negative regulators of cell cycle components resulting in abnormal function is the root cause of the cancer development (table 1.1.1).

Protein	Alteration	Tumour
CDK4	Mutation	Melanoma
Cyclin D1	Overexpression	Breast and prostate cancer, parathyroid adenoma, gastric and esophagic carcinoma, multiple myeloma
Cyclin D2	Overexpression	Colorectal Carcinoma
Cyclin E	Overexpression	Breast, ovary and gastric carcinoma
Cyclin A	Overexpression	Hepatocellular carcinoma
CDC25A	Activation	Head and neck cancer, NSCLC
CDC25C	Activation	Breast cancer, lymphomas, head and neck cancer, NSCLC
$p27^{Kip1}$	Inactivation/ degradation	Colon, breast and prostate cancer
$p57^{Kip2}$	Deletion/ inactivation	Beekwith-Widemann syndrome
$p16^{INK4a}$	Deletion/ inactivation/ mutation	Melanoma, lymphomas, NSCLC, pancreatic carcinoma
$p15^{INK4b}$	Deletion/ inactivation	Leukaemia, lymphomas
pRb	Inactivation	Retinoblastoma, SCLC, sarcoma and bladder carcinoma

Table 1.1.1: Cell cycle regulatory elements involved in human neoplasia[3]

1.2 The Cell Cycle

The eukaryotic cell cycle can be separated into four distinct phases that occur in a defined order: G_1 (Gap 1), S (Synthesis), G_2 (Gap 2), and M (Mitosis) (fig 1.2.1). There is also a G_0 phase, known as quiescence where the cells are not progressing through the cell cycle. This is the most common phase for normal healthy cells.[4]

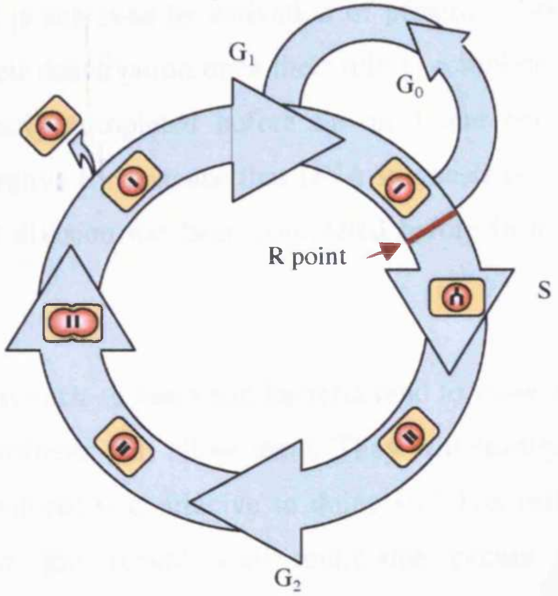

Fig 1.2.1: The cell cycle, showing the phases of the cycle and a representation of the cell's progress through division.

During the cell cycle, the DNA contained in the cell's nucleus is replicated then the cell divides.[5] During S phase DNA is replicated, and in M phase cell division occurs leading to the formation of two daughter cells. To ensure that these events occur without error, cells have developed surveillance mechanisms, known as cell cycle checkpoints. These occur in the two gap phases, with the most well defined being the restriction point, or R point in the G_1 phase.[6]

Mitosis itself is subdivided into five stages. Firstly Prophase, where units of a protein called tubulin join together to form microtubules, which bundle together in fibres to form what is known as the mitotic spindle. During Prometaphase, the chromosomes attach to the spindle and begin to align at the metaphase plate around the "equator" of the spindle. This process is completed during Metaphase, and the cell is then ready for division. Anaphase involves the chromosomes that were duplicated in the S phase dividing, and heading towards opposite poles of the nucleus. Finally Telophase; the spindle is broken down and a new nuclear envelope develops around the daughter chromosomes. The daughter cells are then separated by a process known as cytokinesis during which the cell membrane connecting the two cells is slowly constricted. The cytoplasm is then separated until two separate cells are formed.[7]

The cell cycle is controlled to ensure the correct order of the processes of cell division are maintained. This is achieved by activation of proteins responsible for carrying out each process, and their deactivation once their role is completed. Each stage of the cell cycle must be properly completed before the next one begins, and this is closely regulated. It is imperative for instance that DNA synthesis is completed before mitosis begins, and that cell division has been completed before further DNA replication can begin.[8]

Unicellular organisms such as yeast and bacteria tend to grow and proliferate as fast as the availability of nutrients will allow them. They will readily traverse the cell cycle assuming the environment is conducive to doing so.[9] The cell cycle in multi-cellular organisms differs in this regard. Cell replication occurs only when there is a requirement by the organism, either for growth or to replenish after cell loss. Cells in multi-cellular organisms must also receive an external stimulus before undergoing division. The cell cycle control system of multi-cellular organisms therefore plays a vital role in maintaining a healthy balance between proliferation and cell death, with deregulation having the potential to result in cancer.[10]

1.3 Entry to the G_1 Phase

In multi-cellular organisms, nutrition alone cannot initiate cell proliferation. As they are members of a highly organized and controlled community of cells, cell division must be regulated to avoid inappropriate proliferation. Therefore, cells also require appropriate chemical signals from other cells to traverse the cell cycle. These usually come from neighbouring cells, and enable the cell to overcome internal restraint and progress through the cell cycle.[10] These signals are in the form of growth factors such as epidermal growth factor, platelet-derived growth factor, estrogen, bombesin, and vasopressin.[11]

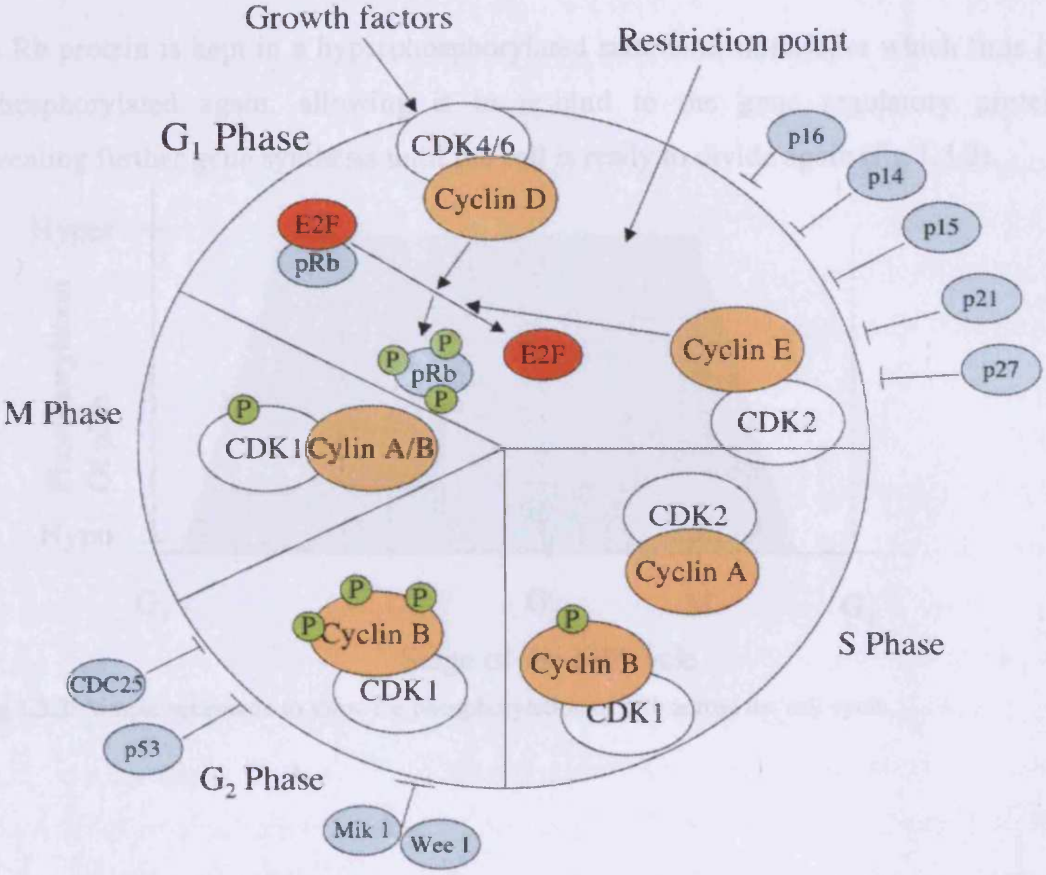
Growth factors
Restriction point
G1 Phase
CDK4/6
Cyclin D
p16
p14
p15
p21
p27
E2F
pRb
P
pRb
E2F
Cyclin E
CDK2
M Phase
CDK1
Cylin A/B
CDK2
Cyclin A
Cyclin B
CDK1
Cyclin B
CDK1
S Phase
CDC25
p53
G2 Phase
Mik 1
Wee 1

Fig 1.3.1: Key cell cycle regulators.

One important example of an internal restraint used by the cell to avoid unwanted proliferation is the retinoblastoma (Rb) protein.[10] This protein was first identified through studies of retinoblastoma, a rare eye tumour afflicting children, from which it derived its name. In this disease, the Rb protein is defective, or missing.

Later studies have shown that the Rb protein is, in fact abundant in all vertebrate cells where it binds to gene regulatory proteins, such as E2F, and prevents them from stimulating the synthesis of genes that are required for cell division.[12] The Rb protein is in a hypophosphorylated state during the early G_1 phase. It is then phosphorylated by CDK/cyclin complexes, after cyclin production is activated by external stimuli. Once the Rb protein is phosphorylated, its conformation changes liberating the bound proteins, including E2F, which are then able to begin cell proliferation.[13]

The Rb protein is kept in a hyperphosphorylated state until mitosis, at which time it is dephosphorylated again, allowing it to re-bind to the gene regulatory proteins, preventing further gene synthesis until the cell is ready to divide again (fig 1.3.2).

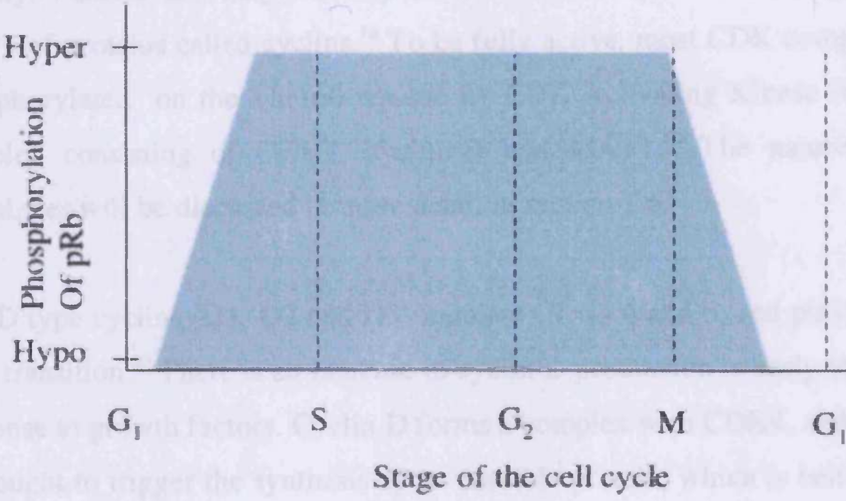

Fig 1.3.2: Simple schematic to show the phosphorylation of pRb across the cell cycle.

1.4 G_1 to S Phase Transition

Central to progression from the G_1 phase is the restriction point, or R point. This is a control mechanism, and if the correct conditions are not met then the cell returns to quiescence, rather than proceeding to the S phase. Once the R point has been passed, the cell is committed to undergoing the cell cycle, and no longer requires any external stimulus to continue the cell cycle.[14]

The cell cycle apparatus is controlled through the phosphorylation of proteins whose role is to initiate or regulate the key stages of the cell cycle, and this is carried out by a specific family of kinases, known as Cyclin-Dependent Kinases (CDKs).[15] Kinases are enzymes that transfer a phosphate group from adenosine triphosphate (ATP) to specific amino acid side chains on their target proteins,[16] rapidly and specifically altering their activity.[17] CDKs are enzymatically inactive until they form a complex with another family of proteins called cyclins.[18] To be fully active, most CDK complexes need to be phosphorylated on the Thr160 residue by CDK Activating Kinase (CAK). CAK is a complex consisting of CDK7, cyclin H and MAT1.[19] The nature of CDK/cyclin complexes will be discussed in more detail in section 1.6.

The D type cyclins (D1, D2 and D3) regulate CDKs 4 and 6, and play a key role in the G_1/S transition.[20] There is an increase in cyclin D production in early to mid G_1 phase in response to growth factors. Cyclin D forms a complex with CDK4, and activates it. This is thought to trigger the synthesis of an unstable protein, which is believed to be cyclin E. This is turn activates cyclin A production and DNA synthesis. Under inadequate conditions, synthesis of cyclin E does not keep up with loss, so this protein cannot be accumulated in a sufficient amount to move the cell through the R point into the S phase, and the cell returns to quiescence.[21] At this stage, distinctions between the functions of CDK 4 and 6 complexes have not been identified, although their expression patterns vary widely among different cell types, suggesting they may have distinct functions.[22]

The CDK4/cyclin D complex also phosphorylates the Rb protein.[23] As seen above, when the Rb protein is phosphorylated, it releases gene-activating proteins, including

E2F. If this is prevented, E2F is not active, the required concentration of cyclin E is not synthesized, and the cell cannot pass through the R point (fig 1.4.1). [24] In cells lacking the Rb protein, E2F is not controlled and the CDK4/cyclin D activity is not required for cells to progress through the R point.

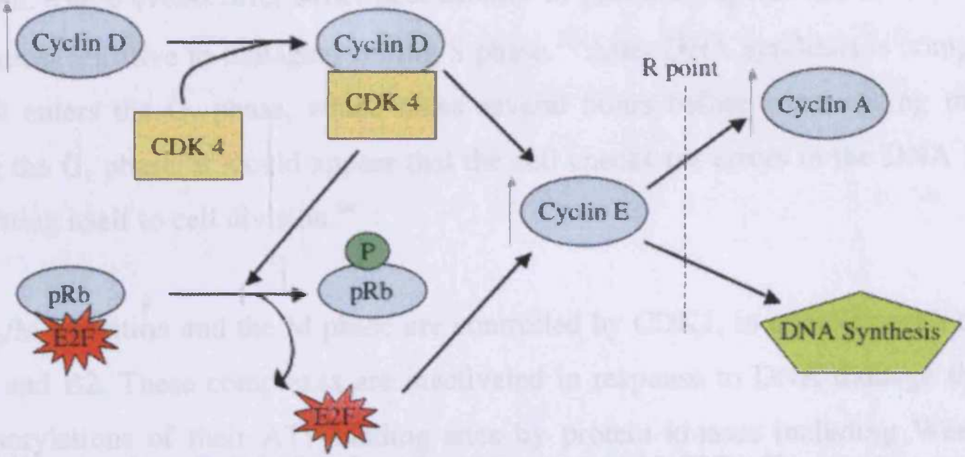

Fig 1.4.1: Increase in cyclin D leads to formation of its complex with CDK4. This complex increases the synthesis of cyclin E, and phosphorylates the Rb protein (pRb). pRb releases E2F, which also increases cyclin E. This leads to passage through the R point, synthesis of cyclin A, and the onset of DNA synthesis.

Cyclin E associates with CDK2 and this complex maintains the phosphorylated state of the Rb protein, creating a positive feedback loop that results in increases in E2F activity. CDK2/cyclin E (and many other CDK/cyclin complexes) also phosphorylates Histone 1, which plays an important role in chromatin rearrangement during DNA replication.

Cyclin A levels increase as the cell passes through the G_1/S transition and are maintained throughout the S phase. CDK2 complexes with cyclin A early in the S phase, while the CDK1/cyclin A complex is required for passage to the G_2 phase. Unlike cyclin E, cyclin A/CDK complexes participate in a negative feedback loop, regulating E2F. This is achieved via phosphorylation of the E2F heterodimerization partner, DP1.[25]

Alterations in the control of the G_1 phase of the cell cycle have been the most studied in respect to causes of cancer. The Rb protein pathway has been shown to be regularly mutated, with possibly over 90 % of human cancers containing mutations in this pathway. Overexpression of cyclins D and E have also been shown to be major factors in human cancer, as well as mutations to CDK4, which enable it to avoid inhibition by its natural control $p16^{INK4a}$, which will be discussed in section 1.6.1.

1.5 G_2 to M Phase Transition

During DNA replication, the chromatin is disassembled and the DNA double helix unwound. These events offer better accessibility to genotoxic agents and as a result the cell is most sensitive to mutagens during S phase.[26] After DNA synthesis is completed, the cell enters the G_2 phase, which takes several hours before commencing mitosis. During the G_2 phase, it would appear that the cell checks for errors in the DNA before committing itself to cell division.[24]

The G_2/M transition and the M phase are controlled by CDK1, in complex with cyclins A, B1 and B2. These complexes are inactivated in response to DNA damage through phosphorylations of their ATP-binding sites by protein kinases including Weel and Mikl.[27] CDKl/cyclin B is activated by CDC25C phosphatase, and accumulates in the cell nucleus. This is required for the G_2/M transition, while for mitosis to begin, dephosphorylation of these sites by CDC25 phosphatases must occur.[24] CDKl complexes have been shown to phosphorylate key proteins such as lamins and Histone 1, as well as components of the mitotic spindle.[28] CDK2 has also been shown to play a role in the formation of the mitotic spindle.[29]

For cells to complete mitosis, cyclin A and B must be degraded, which would appear to involve CDKl/cyclin B regulation. Once the daughter cell has separated, the cell reenters G_1/G_0 and the cell cycle begins again.

Current understanding is that the ATM/ATR kinases are activated by DNA damage in the G_2 phase,[30] these in turn instigate a signal pathway that results in Checkpoint kinase 1 and 2 (Chkl and Chk2) phosphorylating CDC25. This phosphorylation is thought to prevent CDC25 from activating CDK1, thus halting the cell cycle. Chkl and Chk2 can also phosphorylate Weel resulting in its inhibition of the CDKl/cyclin B complex.[27]

While the G_2/M transition has not been studied to the same level as G_1/S, G_2/M checkpoint inhibitors may also be valuable in cancer therapy to enhance the effectiveness of DNA-damaging agents in tumours with a defective G_1 DNA damage checkpoint, such as those with mutated p53. However, few G_2 checkpoint inhibitors are known. Those found so far include caffeine and caffeine analogues, and all have been shown to enhance the cytotoxicity of DNA-damaging agents.[31]

While Chk2 was only identified in 1994, and not reported in humans till 1998, defects in Chk2 have been shown to contribute to the development of both hereditary and sporadic human cancers.[32] Some current experiments also suggest that certain tumours may overexpress Chk2 suggesting that direct Chk2 inhibition alone may have some therapeutic value.[33] Coupled with its role in the G_2/M checkpoint, Chk2 has become an attractive target for drug discovery.

1.6 CDKs and Cyclin

As described above, the CDK/cyclin complexes play a key role in governing the cell cycle. Understanding how CDK activity is properly controlled is important for understanding cancer biology.[34]

CDKs were first identified in the 1970s when the cdc2 gene in *S. pombe* was shown to play a key role in the control of cell division. The corresponding human gene was isolated in 1987, and later named CDK1. Paul Nurse recently received the Nobel Prize for this work.[35] There are now 13 CDKs that have been identified, with 11 known to form complexes with cyclins. As can be seen, the function of these CDK/cyclin complexes is not limited to the cell cycle (table 1.6.1).

CDK	Complex formed with	Cell Cycle Regulation	Other Functions
CDK1	Cyclin A / B Cyclins (B1 & B2)	G_2/M Transition	Regulation of topoisomerase 2 / neuronal cell death
CDK2	Cyclin A / Cyclin E	G_1/S Transition / G_2 centrosome duplication	-
CDK3	Cyclin E	G_1/S Transition	-
CDK4	D Cyclins (D1, D2 & D3)	G_1 Phase progression	Neuronal cell death
CDK5	p35, p25, p29, p39, D Cyclins (D1, D2 & D3)	-	Neuronal differentiation / apoptosis
CDK6	Cyclin D	G_1 phase progression	Neuronal cell death
CDK7	Cyclin H	CDK1 & 2 activation	Transcription regulation
CDK8	Cyclin C	G_0/S Transition	Transcription regulation
CDK9	Cyclin K / Cyclin T	-	Transcription regulation / Signal transduction
CDK10	Ets2	G_2/M	Transcription regulation
CDK11	Cyclin L	-	Apoptosis

Table 1.6.1: The functions of human CDKs and cyclins.[3,36]

Although CDKs 1, 2, 3, 4, 6, 7 and 8 have been shown to have key roles, only CDKs 2 and 3 would appear to have exclusively cell cycle related function. While pharmacological inhibition of CDKs can cause apoptosis in dividing cells, CDKs 1, 4 and 6 play a key role in neuronal cell death, and their inhibition can result in neuroprotection. CDKs 4 and 11 also play an indirect function in apoptosis. CDK5 is important for neuronal survival by inhibiting apoptotic pathways.[37] Meanwhile CDKs 7, 8, 9 and 10 have been shown to regulate transcription. Although CDK10 is the most recently discovered of these and little is known about its exact function, overexpression of inactive CDK10 has been reported to cause G_2/M arrest and has been implicated in the regulation of this phase.[38] More is known of the function of CDKs 7, 8 and 9 which have been shown to catalyze phosphorylation of RNA polymerase II, on its carboxy-terminal domain. All three catalyze different sites though, which implies that they function via different mechanisms.

While the presence of CDKs remains constant throughout the cell cycle, their activity does not. They become active at the appropriate times in the cycle and then quickly become deactivated again in a cyclical pattern. Monomeric CDK is inactive, becoming activated on formation of a complex with the appropriate cyclin. It would appear that the cyclin plays a major role in substrate specificity, resulting in the same CDK undertaking differing roles when bound to different cyclin partners.[39] In order to bind to their CDK partner, all cyclins posses a common feature called a cyclin box, which is conserved throughout the cyclin family. On binding, there is crucial conformational change in the CDK that is required for activation.[40]

One example of this is the CDK1/cyclin A or B complex that is also known as M-phase or Mitotic Promoting Factor (MPF). MPF triggers mitosis, and its concentration fluctuates in accordance with the oscillating cyclin concentration across the cell cycle (fig 1.6.1).[41]

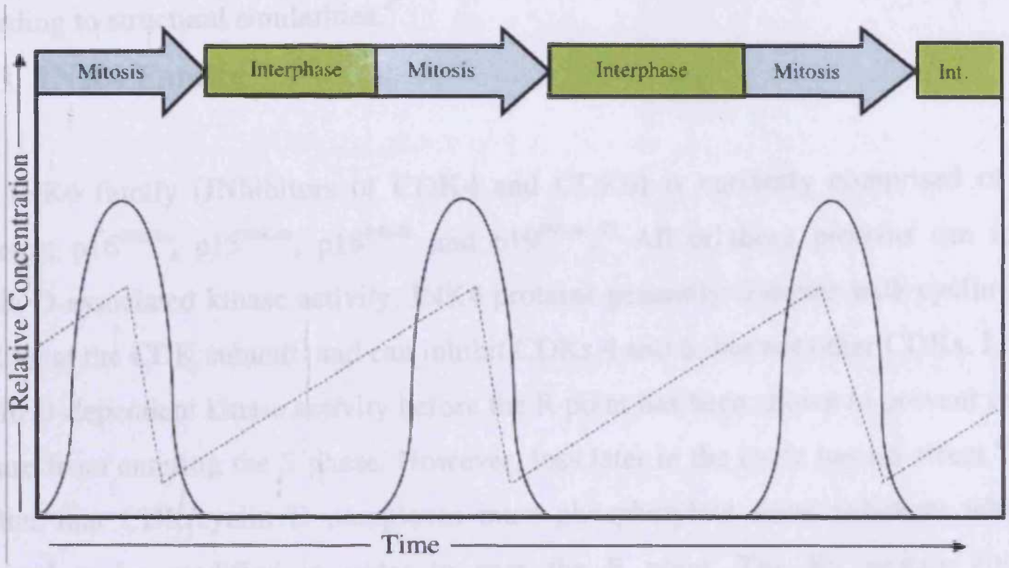

Fig 1.6.1: Graph of the concentration peaks of MPF (*solid line*) in mitosis against the cyclin concentration (*dotted line*) across the cell cycle.[41]

The availability of cyclins fluctuates throughout the cell cycle due to their synthesis by successive rounds of transcription when required during the progress of the cell cycle, and destruction by enzymes activated by the CDK/cyclin complex when they are no longer required.[42] Ubiquitin-mediated proteolysis is the main process by which proteins are degraded in the cell, and cyclins have been shown to undergo ubiquitin-dependent proteolysis.[43] This destruction has been shown to result in abrupt deactivation of the CDK function.[44]

Ubiquitin (Ub) is a 76 amino acid peptide that forms a marker on its substrate that is recognized by the 26S proteasome, which unfolds the substrate and rapidly degrades it into short peptides.[45] The ubiquitination requires three components. First Ub is activated by the ubiquitin activating enzyme (E1). The Ub is then transferred to the ubiquitin conjugating enzyme (E2), and then on to the specificity factor (E3) from where it is transferred to the protein to be degraded (e.g. cyclin).[46] Once a protein has been ubiquitinated, further Ub is added to the initial Ub forming a poly-Ub chain, and once this reaches four Ub in length, it is recognized by the 26S proteasome.

CDK function is also affected by their association with inhibitory proteins, known as CDKIs. These proteins either physically block activation, or block the access of substrates. The known CDKIs are grouped into two gene families, INK4 and Cip/Kip, according to structural similarities.[47]

1.6.1 INK4 Family

The INK4 family (INhibitors of CDK4 and CDK6) is currently comprised of four proteins; p16^{INK4a}, p15^{INK4b}, p18^{INK4c} and p19^{INK4d}.[48] All of these proteins can inhibit cyclin D-associated kinase activity. INK4 proteins generally compete with cyclin D for binding at the CDK subunit, and can inhibit CDKs 4 and 6, but not other CDKs. Loss of cyclin D-dependent kinase activity before the R point has been shown to prevent cells in culture from entering the S phase. However, loss later in the cycle has no effect.[49] This implies that CDK/cyclin D complexes must phosphorylate some substrate which is required to be modified in order to pass the R point. The Rb protein fits this description,[49] and it appears that p16^{INK4a} plays a key role in regulating the Rb protein. Indeed, in cells lacking the Rb protein, INK4 expression does not arrest the cell progression. P15^{INK4b} meanwhile is unaffected by the Rb protein, but is stimulated by the growth inhibitor TGF-β pathway. Furthermore, it has shown that p16^{INK4a} and p15^{INK4b} are commonly mutated or deleted in human cancer.[50]

1.6.2 Cip/Kip Family

There are currently three proteins comprising the Cip/Kip family (CDK interacting protein/ Kinase inhibitory protein): p21^{Cip1}, p27^{Kip1} and p57^{Kip2}.[21] These proteins share a homologous inhibitory domain, which is required for binding and inhibition of complexes of CDK 2 and 4. The Cip/Kip family share a broader range of inhibition than the INK4 family.[51]

p21^{Cip1} and p57^{Kip2} are involved in the G_1/S checkpoint,[24] whereas p27^{Kip1} is present in high abundance in quiescent cells. Its level slowly decreases as cells are stimulated to enter the cell cycle, primarily as a result of an accelerated degradation of the protein.[52] p27^{Kip1} is required for maintaining the appropriate levels of the D cyclins,[53] and it can also selectively cleave cyclin A.[54] p21^{Cip1} would appear to also play a role in G_2/M, with induced p21^{Cip1} expression causing cells to accumulate in both G_1 and G_2 phases, by inhibition of cyclins A, B and E.[55] Paradoxically, it has recently been shown that p21^{Cip1} also functions to cause cell cycle progression and protect cells from apoptosis.[56]

1.6.3 CDK/Cyclin Location in the Cell

The location of the CDK/cyclin complexes is also crucial, and CDK activity is mainly located in the cell's nucleus. The CDK and cyclin must form their complex, it must be activated, and it must be correctly positioned in order to function.

For example, cyclin D1 is known to be in the nucleus during mid G_1 phase, but it is transported to the cytoplasm at the onset of S phase. Failure to transport its complex with CDK4 into the nucleus has been shown to cause cell cycle arrest. The CDK1 complexes with cyclins A, B1 and B2 also display clear patterns in subcellular location. Cyclin A is located exclusively in the nucleus, while the B cyclins are synthesized in the cytoplasm. Cyclin B2 remains in the cytoplasm, while B1 is translocated to the nucleus at the onset of prophase. This observation would imply that CDK1 displays different behaviour when complexed to the different cyclins, phosphorylating different substrates in different intracellular locations.[57]

1.6.4 CDK2 Structure, Cyclin Binding and Phosphorylation

The crystal structures of CDK2 with (PDB ID: 1HCK)[58] and without (PDB ID: 1HCL)[59] ATP have been studied, as well as the CDK2/cyclin A complex with (PDB ID: 1JST)[60] and without (PDB ID: 1FIN)[61] phosphorylation, elucidating the nature of the binding.

Like other protein kinases, the core of human CDK2 displays two major subdomains. These are a β-sheet rich amino terminal lobe and a larger α-helix rich carboxy-terminal lobe. ATP binds in a deep cleft between these two lobes, and this is presumed to be the site of substrate binding and catalysis (fig 1.6.2).

Independently CDK2 is inactive, and the residues of the ATP-binding site are not correctly aligned to promote catalysis. This is mainly due to the orientation of two key structural elements known as the T loop (residues 146-166) and the PSTAIRE α-helix (residues 45-51).[62] In order to become active, CDK needs to form a complex with a cyclin (in this case CDK2/cyclin A, fig 1.6.3).

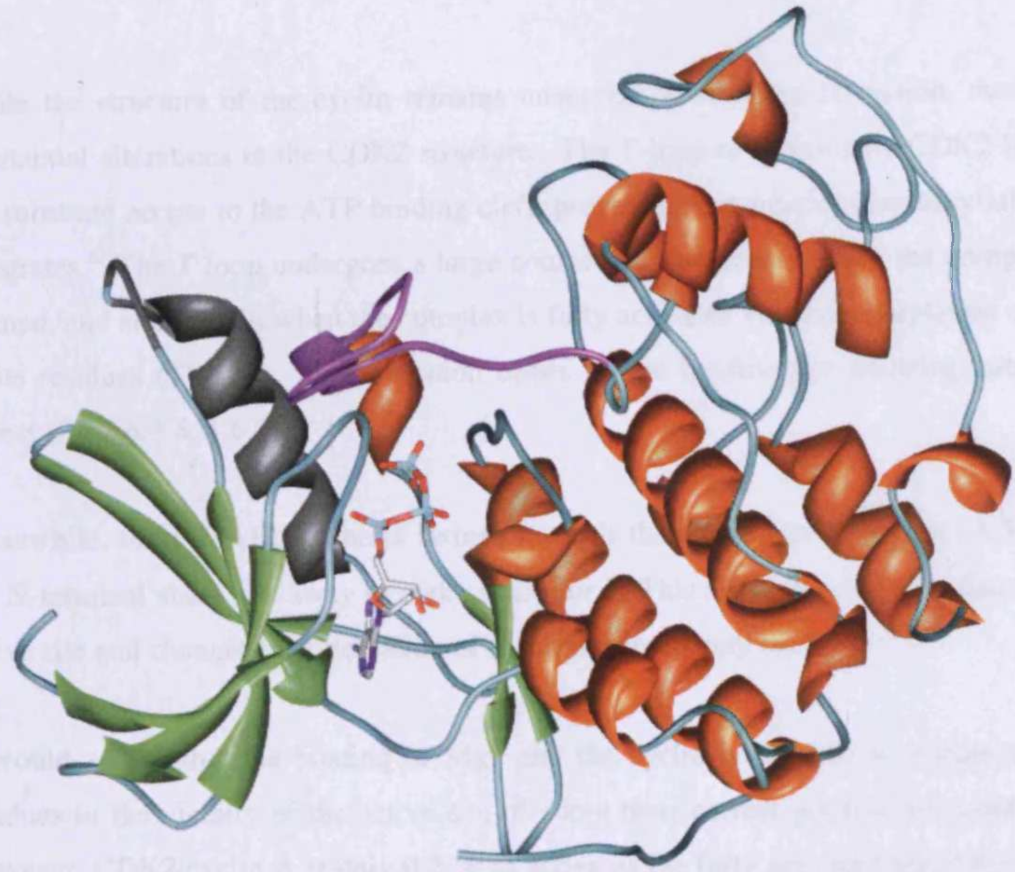

Fig 1.6.2: Representation of CDK2 (*light blue*) with ATP (PDB ID: 1HCK). β-sheets (*green*), α-helix (*orange*), ATP (*stick*), the T loop (*purple*) and PSTAIRE α-helix (*grey*) are highlighted.

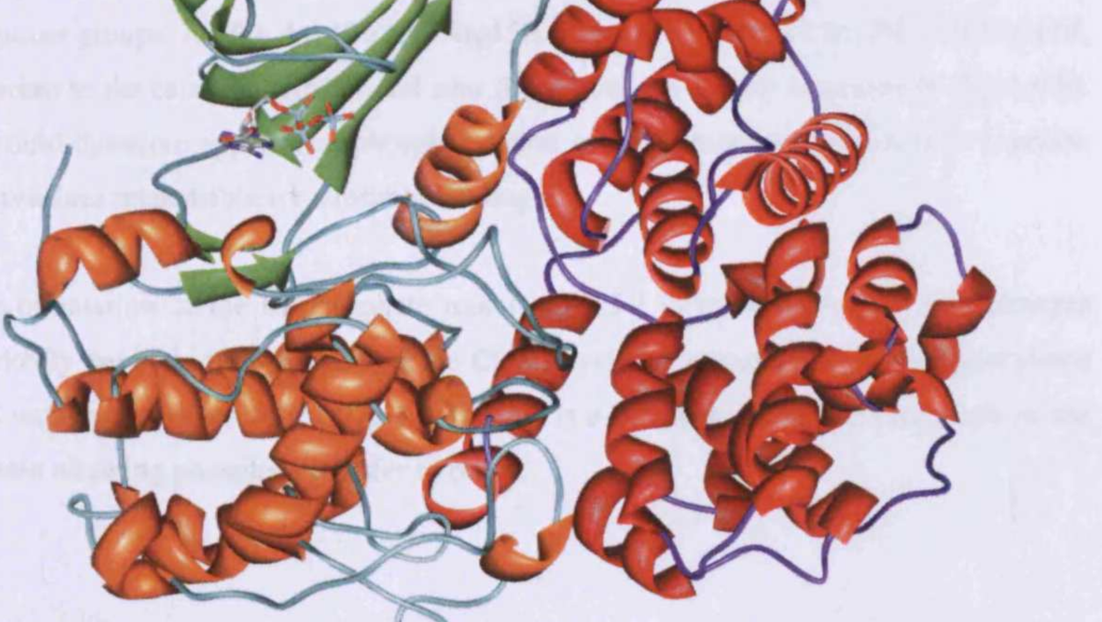

Fig 1.6.3: Representation of CDK2 (*light blue*) [β-sheets (*green*), α-helix (*orange*)], complexed with Cyclin A (*dark blue*) [α-helix (*red*)], with ATP (*stick*), (PDB ID: 1FIN).

While the structure of the cyclin remains unaltered on complex formation, there are substantial alterations in the CDK2 structure. The T-loop of monomeric CDK2 blocks the substrate access to the ATP binding cleft, preventing enzymatic phosphorylation of substrates.[63] The T loop undergoes a large conformational change when the complex is formed, and alters again when the complex is fully activated via phosphorylation of one of its residues (Thr160). This alteration opens up the binding site allowing substrate access (fig 1.6.4 & 1.6.5).

Meanwhile, the PSTAIRE α-helix swings towards the active site cleft (fig 1.6.5), and the N-terminal sheet tilts away to make space for it. This alters the conformation of the active site and changes the orientation of tri-phosphate moiety of ATP.

It would appear that the binding of Mg^{2+} and the cyclin is required to enable all the residues in the vicinity of the active site of adopt their correct position for catalysis.[64] However, CDK2/cyclin A is only 0.2 % as active as the fully activated phosphorylated complex,[62] while phosphorylated monomeric CDK2 is only 0.3 % as active.[65] While complex formation alters the conformation of the protein to allow activity, it is thought that phosphorylation allows the formation of the substrate binding site. Once phosphorylated, Thr160 turns towards the active site and into contact with three Arginine groups, Arg50, Arg126 and Arg150. These are located in the PSTAIRE motif, adjacent to the catalytic Asp127 and near the start of the T-loop respectively (fig 1.6.6). It would therefore appear that phosphorylation of the Threonine group acts to organise the residues responsible for substrate binding.

The orientation of the tri-phosphate moiety of ATP in the binding site also changes markedly between free CDK2 and the CDK2/cyclin A complex in its phosphorylated and unphosphorylated forms (fig 1.6.7). This is a direct result of the alterations in the protein allowing phosphate transfer to occur.

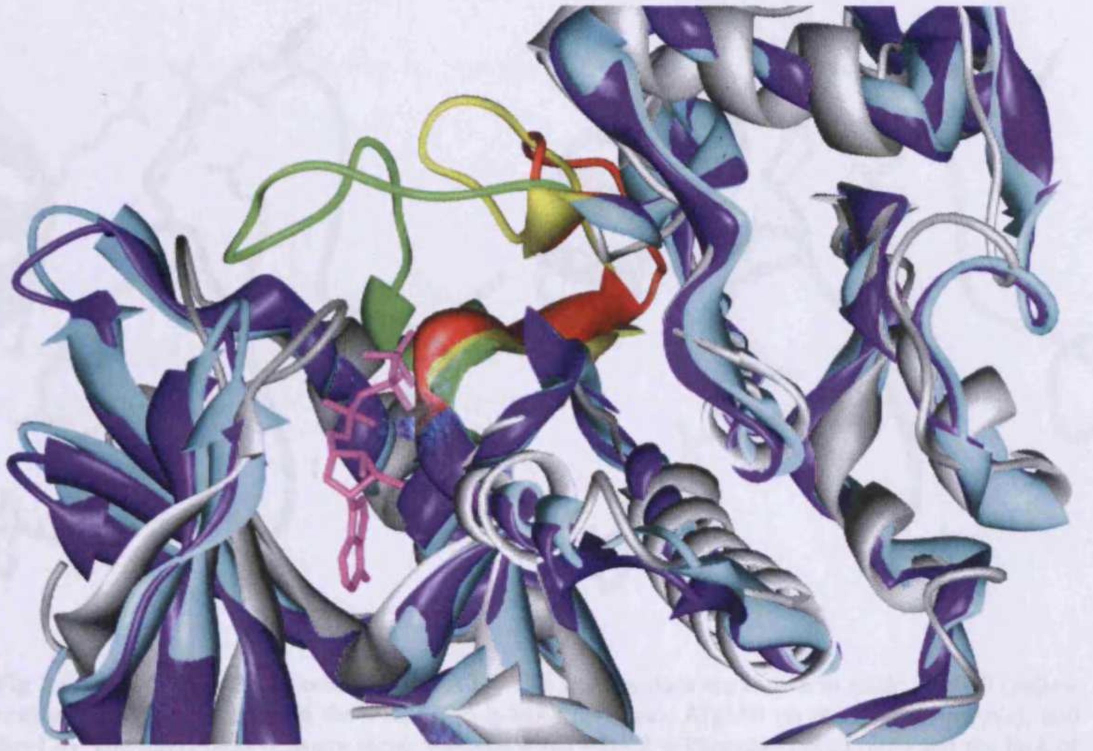

Fig 1.6.4: Superimposition of CDK2/ATP (*grey*, T-loop *green*) [1HCK], CDK2/cyclin A/ATP (*light blue*, T-loop *yellow*) [1FIN], and phosphorylated CDK2/cyclin A/ATP (*dark blue*, T-loop *red*) [1JST]. ATP of [1HCK] only shown (*purple*).

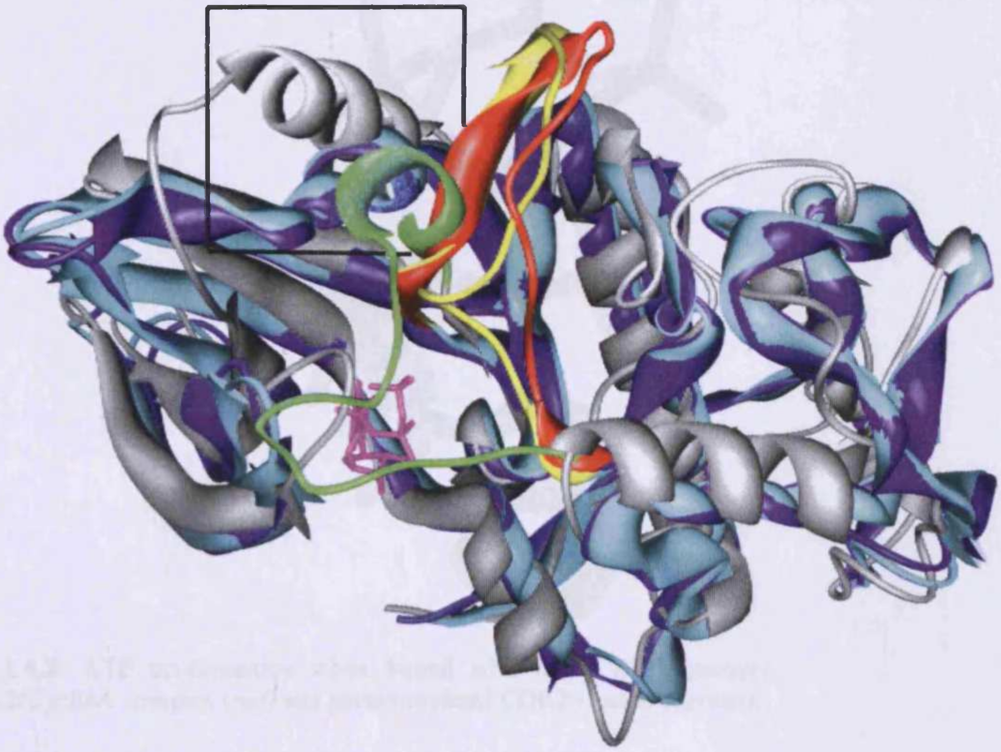

Fig 1.6.5: fig 1.6.4 rotated by 90° showing the effect of the T-loop on substrate access to ATP. Conformational change in the PSTAIRE α-helix of Monomeric CDK2 (*grey*) compared to cyclin-bound CKD2 is highlighted in the box.

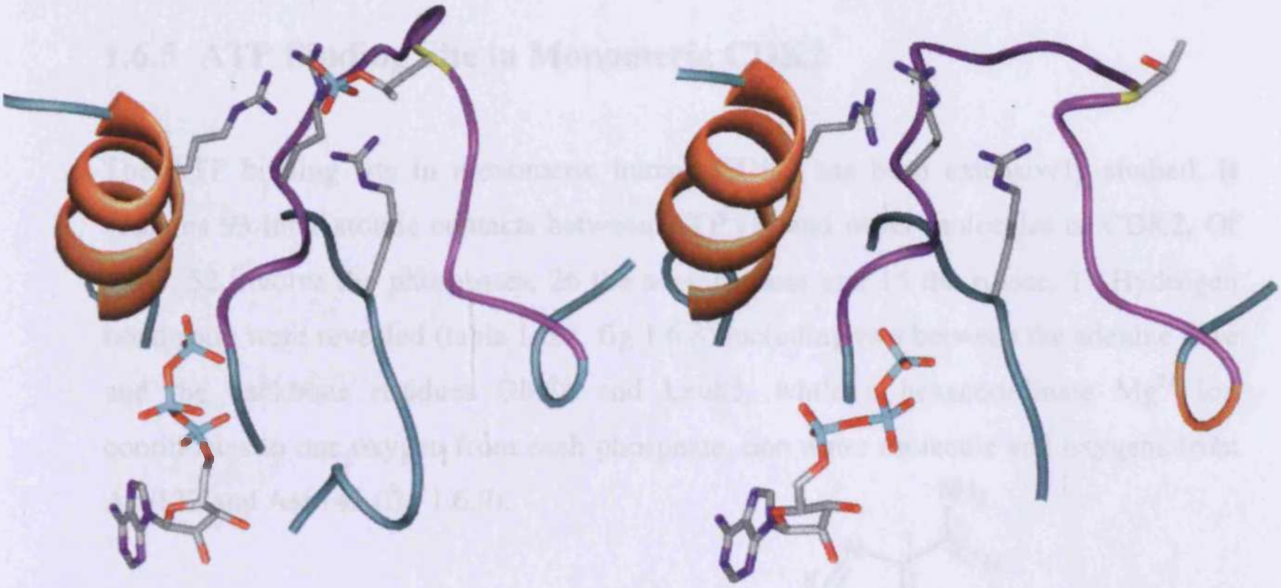

Fig 1.6.6: CDK2/Cyclin A complex with ATP. The key residues are shown in stick: Thr160 (*yellow residue on T-loop*) Arg50 on the PSTAIRE α-helix (*orange*), Arg150 on the T-loop (*purple*), and Arg126. The interaction between these residues when CDK2 is Phosphorylated (*left*) and the lack of interaction when unphosphorylated (*right*).

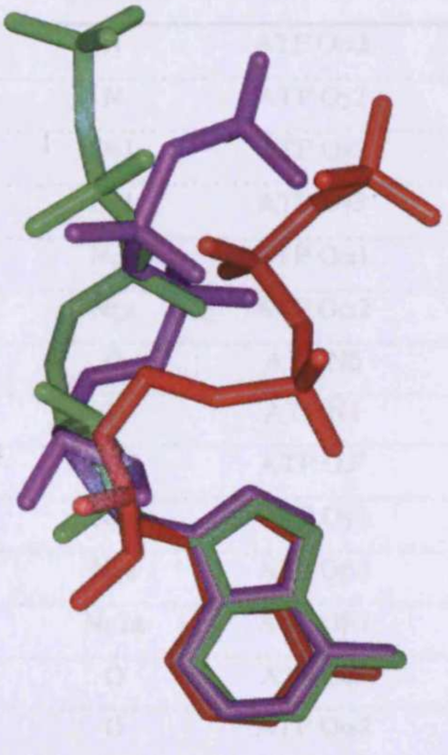

Fig 1.6.7: ATP conformation when bound with free CDK2 (*purple*), CDK2/CyclinA complex (*red*) and phosphorylated CDK2/CyclinA (*green*).

1.6.5 ATP Binding Site in Monomeric CDK2

The ATP binding site in monomeric human CDK2 has been extensively studied. It contains 93 inter-atomic contacts between ATP [1] and water molecules or CDK2. Of these, 52 involve the phosphates, 26 the adenine base and 15 the ribose. 17 Hydrogen bond pairs were revealed (table 1.6.2, fig 1.6.8) including two between the adenine base and the backbone residues Glu81 and Leu83, while a hexacoordinate Mg^{2+} ion coordinates to one oxygen from each phosphate, one water molecule and oxygens from Asn132 and Asp145 (fig 1.6.9).

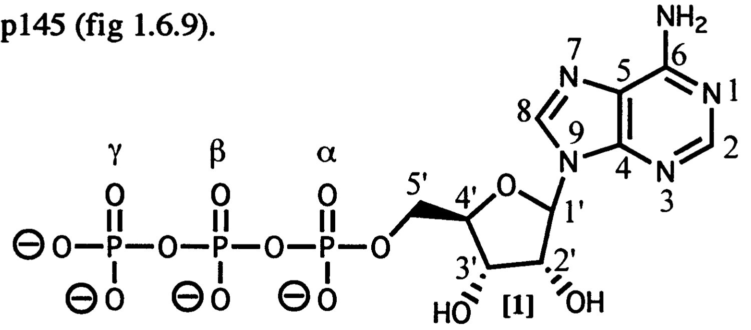

[1]

CDK2 residue	Hydrogen Bond Partners		ATP fragment
Gly13	N	ATP Oα2	Phosphate
Thr14	N	ATP Oγ2	Phosphate
Thr14	Oγ1	ATP Oγ2	Phosphate
Thr14	Oγ1	ATP Oγ3	Phosphate
Lys33	Nζa	ATP Oα1	Phosphate
Lys33	Nζa	ATP Oα2	Phosphate
Glu81	O	ATP N6	Adenine
Leu83	N	ATP N1	Adenine
Asp86	Oδ2	ATP O3'	Ribose
Lys129	Nζa	ATP Oγ3	Phosphate
Lys129	Nζa	ATP Oβ3	Phosphate
Gln131	Nε2a	ATP Oβ1	Phosphate
Gln131	O	ATP O2'	Ribose
Wat502	O	ATP Oα2	Phosphate
Wat502	O	ATP Oγ2	Phosphate
Wat503	O	ATP O5'	Ribose
Wat505	O	ATP N3	Adenine

Table 1.6.2: Hydrogen bond interactions between ATP and CDK2/water molecules identified from crystal structure (PDB ID: 1HCK)[59]

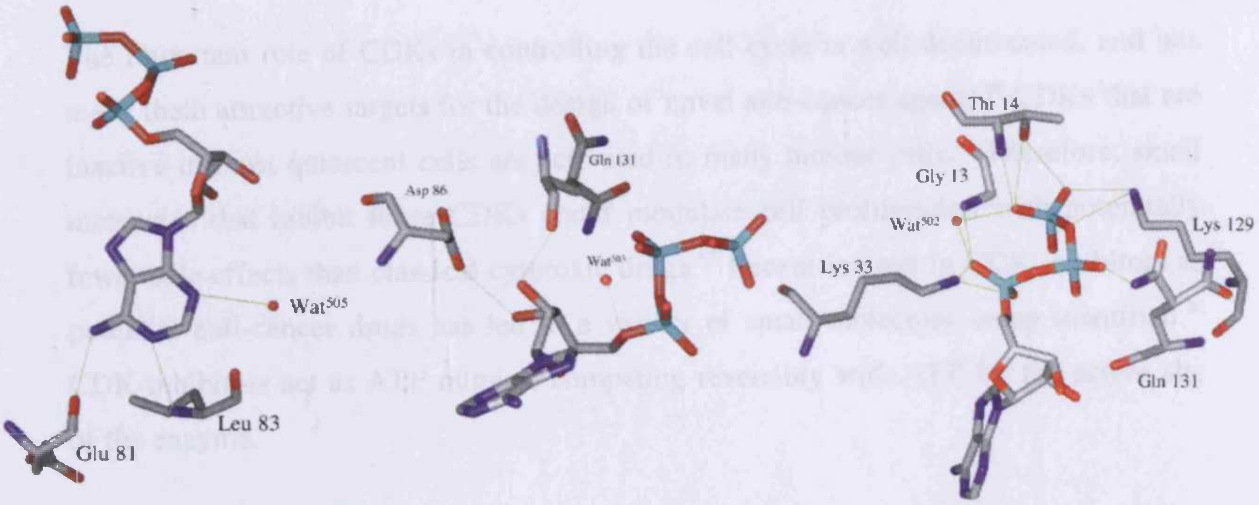
Thr 14
Gln 131
Asp 86
Gly 13
Wat^{502}
Lys 129
Wat^{503}
Lys 33
Wat^{505}
Gln 131
Leu 83
Glu 81

Fig 1.6.8: Hydrogen bonds of ATP in the active site: Between adenine and Glu81, Leu83 and Water^{505} (*left*), between ribose and Asp86, Gln131 and Water^{503} (*centre*) and between the tri-phosphate and Gly13, Thr14 (3), Lys33 (2), Lys129 (2), Gln131 and Water^{502} (2) (*right*).

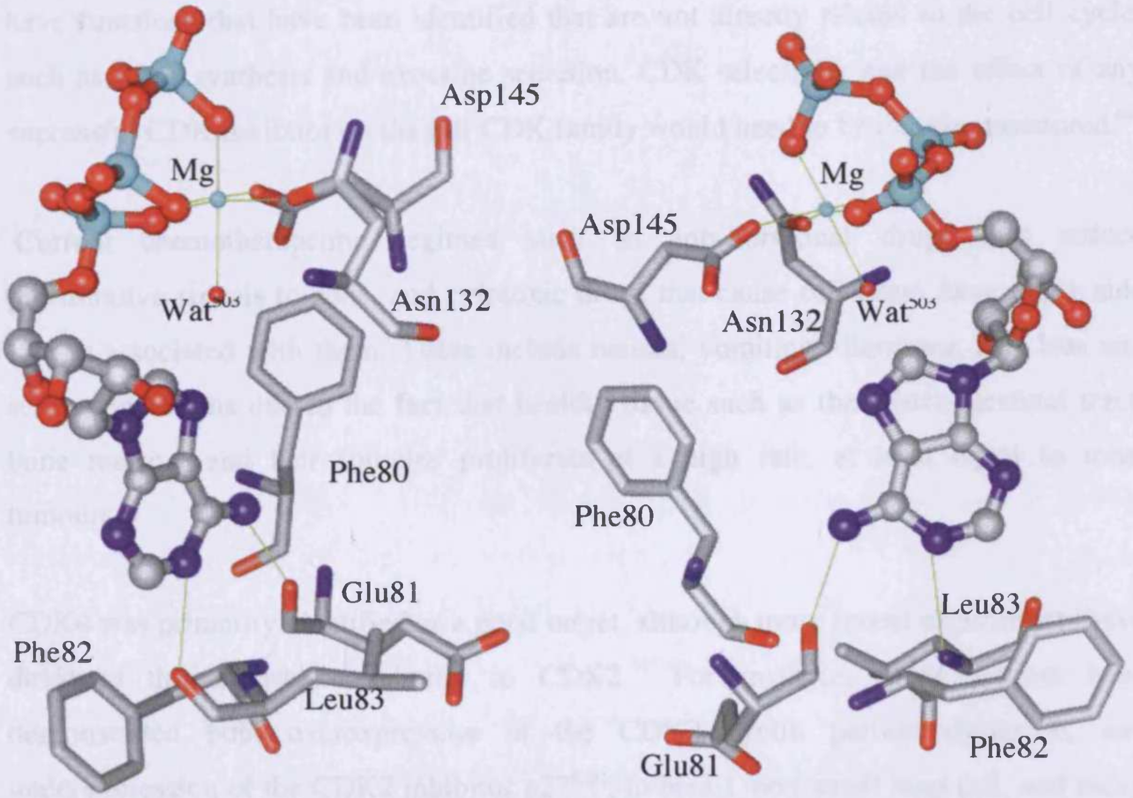
Asp145
Mg
Wat^{503}
Asn132
Phe80
Glu81
Phe82
Leu83
Mg
Asp145
Asn132
Wat^{503}
Phe80
Leu83
Glu81
Phe82

Fig 1.6.9: Two views of the hydrogen bonds of ATP to Glu81 and Leu83, and the hexacoordinate Mg ion.

1.7 CDK Inhibitors

The important role of CDKs in controlling the cell cycle is well documented, and has made them attractive targets for the design of novel anti-cancer agents.[66] CDKs that are inactive in most quiescent cells are activated in many tumour cells.[67] Therefore, small molecules that inhibit these CDKs could modulate cell proliferation with potentially fewer side effects than classical cytotoxic drugs.[67] Recent interest in CDK inhibitors as potential anti-cancer drugs has led to a variety of small molecules being identified.[36] CDK inhibitors act as ATP mimics, competing reversibly with ATP for the active site of the enzyme.

In order to have significant antitumour activity, small molecule CDK inhibitors may need to target multiple CDKs, as some CDK functions may be redundant in the tumour cells.[68] However, it is important to recognize that a number of CDK/cyclin complexes have functions that have been identified that are not directly related to the cell cycle, such as RNA synthesis and exocrine secretion. CDK selectivity and the effect of any successful CDK inhibitor on the full CDK family would need to be closely monitored.[69]

Current chemotherapeutic regimes such as anti-hormonal drugs that reduce proliferative signals to cells, and cytotoxic drugs that cause cell death have many side effects associated with them. These include nausea, vomiting, diarrhoea, hair loss and serious infections due to the fact that healthy tissue such as the gastrointestinal tract, bone marrow and hair follicles proliferate at a high rate, at least equal to most tumours.[70]

CDK4 was primarily identified as a good target, although more recent experiments have devalued this kinase in relation to CDK2.[71] For instance, many reports have demonstrated both overexpression of the CDK2 cyclin partner cyclin E, and underexpression of the CDK2 inhibitor $p27^{Kip1}$, in breast, non-small lung cell, and many other cancers. Their altered expression has been shown to correlate with increased CDK2 activity levels and poor overall survival. This observation makes CDK2 and its regulatory pathways credible targets for the development of novel chemotherapeutic agents.[72]

1.7.1 Purine Based Inhibitors

ATP, the natural ligand of CDKs, is a purine based molecule. As this can be regarded as a lead compound, the purine pharmacophore has been extensively investigated in structure based design of small molecule inhibitors of CDKs. Included in this category is the first compound identified as a CDK inhibitor, 6-Dimethylaminopurine [2].[73]

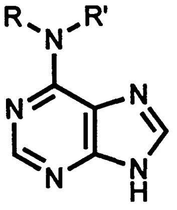

6-Dimethyl aminopurine [2] R=R'=CH_3
Isopentenyladenine [3] R=H, R'= 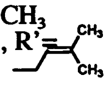

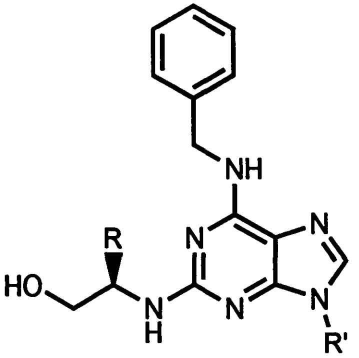

Olomoucine [4] R=H, R'=CH_3
(R)-Roscovitine [5] R=CH_2CH_3, R'=$CH(CH_3)_2$

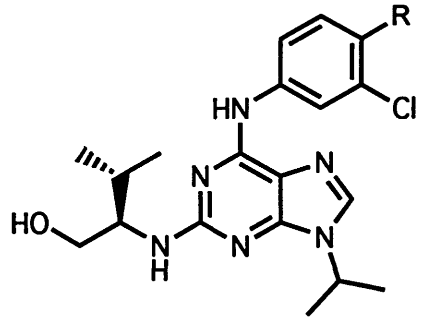

Purvalanol A [7] R=H
Purvalanol B [8] R=COOH

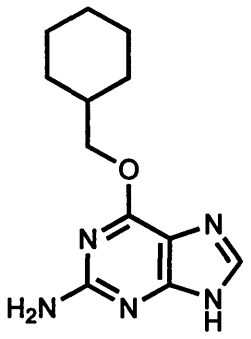

NU2058 [6]

6-Dimethylaminopurine was originally synthesized as an analogue of Puromycin, a protein synthesis inhibitor.[74] However, it was found to block mitosis in sea urchin embryos. The target of this action was identified as CDK1.[75] Derivatives of 6-Dimethylaminopurine were also found to be active CDK inhibitors, including Isopentenyladenine [3] and Olomoucine [4]. Olomoucine became a lead structure itself when it was discovered that it only displayed good inhibition against CDKs 1, 2 and 5, and the MAP kinase erk1 when screened against 35 different kinases.[76] One compound to result from this was *(R)*-Roscovitine [5]. Olomoucine and *(R)*-Roscovitine were the first purine inhibitors of CDKs to be evaluated extensively, and *(R)*-Roscovitine was found to be ten-fold more active than Olomoucine, with the same selectivity.

X-ray crystallography studies of these compounds revealed the binding of the compounds in the ATP active site of CDK2. Due to the large extensions from the 6- and 9-positions, the purine orientation is not the same as described for ATP. Not only is the corresponding purine in a completely different orientation, the hydrogen bonding interactions with the active site are different. Whereas ATP interacts with the backbone of Glu81 and Leu83, the purine-based inhibitors form two hydrogen bonds to the backbone of Leu83. Careful analysis of the crystal structure of Olomoucine, as well as *(R)*-Roscovitine and Isopentenyladenine have led to further purine based inhibitors such as NU2058 [6],[77] Purvalanol A [7] and Purvalanol B [8].[78] These compounds, particularly [7] and [8] were shown to be potent inhibitors of several CDKs, while NU2058 has been shown to be selective for CDKs 1 and 2 (table 1.7.1).

Inhibitor	**CDK1/ Cyclin B**	**CDK2/ Cyclin A**	**CDK2/ Cyclin E**	**CDK4/ Cyclin D**
6-Dimethylaminopurine[36] [2]	120	NR	NR	NR
Isopentenyladenine[79] [3]	55	NR	NR	NR
Olomoucine[79] [4]	7.0	7.0	7.0	Inactive
(*R*)-Roscovitine[80] [5]	0.65	0.7	0.7	> 100
NU2058[77] [6]	7	17	NR	NR
Purvalanol A[80] [7]	0.004	0.07	0.035	0.850
Purvalanol B[80] [8]	0.006	0.006	0.009	> 10

Table 1.7.1: IC_{50} values for purine based inhibitors, all values in μM. NR Not Reported.

1.7.2 Flavones

Flavopiridol **[9]** is a synthetic analogue of the naturally occurring Rohitukine alkaloid **[10]**, which was isolated from an ingredient of a traditional Indian folk medicine, *Dysoxylum binectariferum.*[81] Flavopiridol was originally identified as an inhibitor for a number of other kinases, such as the tyrosine kinase receptor family and receptor associated kinases. However, its greatest activity was found against the CDKs. Unlike the purine-based inhibitors which display most activity against CDK1 and CDK2, Flavopiridol shows equipotent inhibition of CDKs 2 and 4.[82] It was found that selectivity for CDK1/cyclin B could be achieved via addition of a sulfur or oxygen linker; Thioflavopiridol **[11]** or Oxoflavopiridol **[12]**.[83]

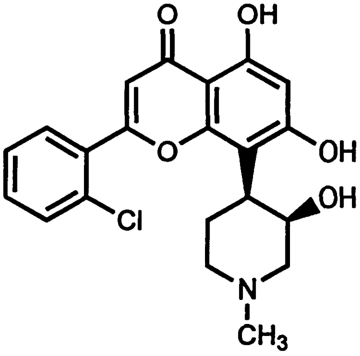

Flavopiridol **[9]**

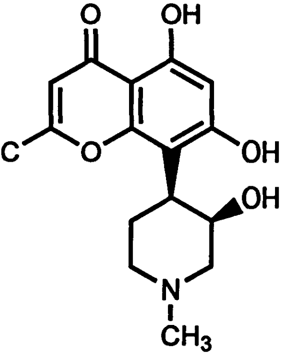

Rohitukine **[10]**

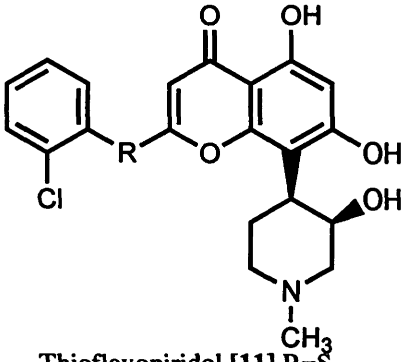

Thioflavopiridol **[11]** R=S
Oxoflavopiridol **[12]** R=O

Inhibitor	**CDK1/Cyclin B**	**CDK2/Cyclin E**	**CDK4/Cyclin D1**
Flavopiridol[79,17] [9]	0.4/ 0.2	0.1	0.4/ 0.2
Thioflavopiridol[17] [11]	0.11	2.10	16.2
Oxoflavopiridol[17] [12]	013	2.11	6.15

Table 1.7.2: IC$_{50}$ values for purine based inhibitors, all values in μM.

Flavopiridol is the most studied CDK inhibitor, was the first CDK modulator tested in clinical trials, and is currently in phase II. Early results suggest anti-tumour activity against renal, prostate and colon cancer as well as non-Hodgkin's lymphoma.[84]

It has also been noted that Flavopiridol was most effective when it was used following treatment with other chemotherapy drugs, as it can enhance the cell death resulting from other drugs such as Cisplatin, Etoposide, and Paclitaxel.[85] Therefore, it is being considered for further testing as a combination agent with drugs such as Paclitaxel, Cytarabine, Topotecan, Doxorubicin, Etoposide, 5- Fluorouracil, and Cisplatin.[86]

1.7.3 Paullones

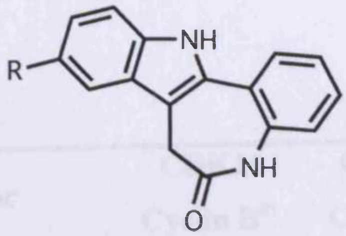

Paullone **[13]** R=H
Kenpaullone **[14]** R=Br
Alsterpaullone **[15]** R=NO_2
[16] R=CN

When Flavopiridol was used in a COMPARE search performed at the National Cancer Institute (NCI), Kenpaullone **[14]** was identified as a potential CDK inhibitor.[87] It was shown that Kenpaullone acts as an ATP competitive inhibitor of CDK1/cyclin B. While Kenpaullone is as potent as Flavopiridol against CDK1/cyclin B, it was much less active *in vitro* compared to Flavopiridol.[88] Analogues were synthesized, and more potent substances found by varying the 9-substitutent from Br to NO_2 **[15]** and CN **[16]** (table 1.7.3).

Elucidation of the crystal structure of Paullone (fig 1.7.1) showed that like Olomoucine, Paullone forms two hydrogen bonds to the Leu83 backbone, rather than one to Leu83 and one to Glu81 as ATP does.

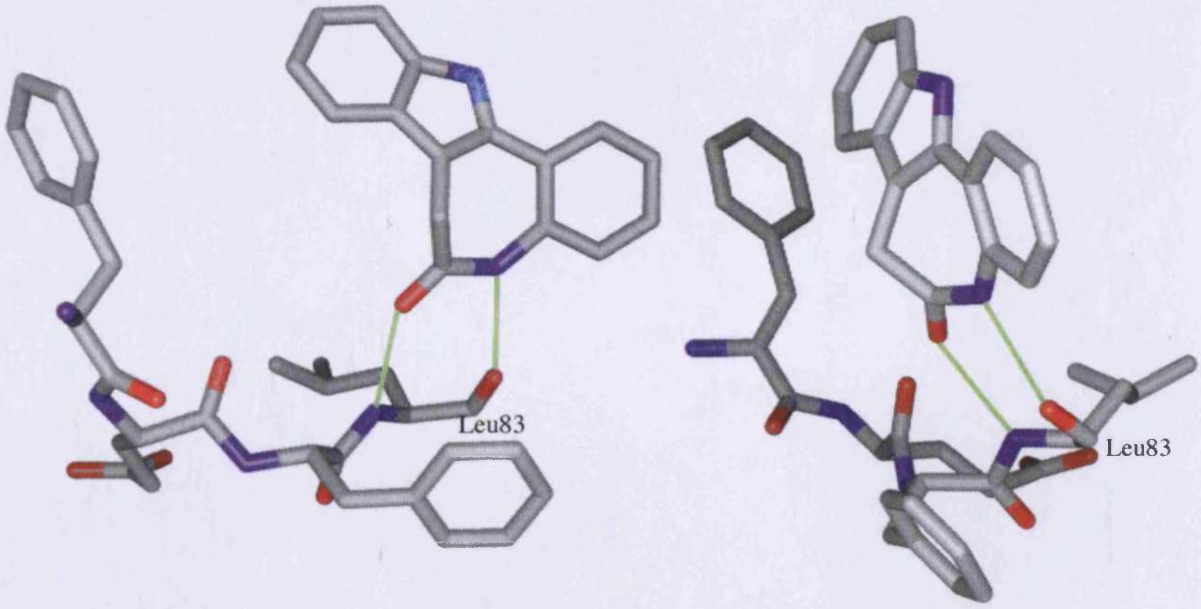

Fig 1.7.1: Hydrogen bonding pattern of Paullone in the active site of CDK2. Residues Phe80 (*far left*) to Leu83 are shown, with the two hydrogen bonds displayed (*green*).

Inhibitor	CDK1/ Cyclin B[87]	CDK2/ Cyclin A	CDK2/ Cyclin E	CDK4/ Cyclin D1
Paullone [13]	7	NR	NR	NR
Kenpaullone[89] [14]	0.4	0.68	7.5	> 100
Alsterpaullone [15]	0.035	0.015	0.2	> 10
[16]	0.024	NR	NR	NR

Table 1.7.3: Activity of the Paullone family. All values in μM. NR Not Reported.

Alterations by modification of the lactam ring did not increase activity, but substitution on the fused benzene ring showed promise and is being investigated further. The crystal structure showed these two rings lie between the sidechains of Ile10 and Leu134, while the other benzene ring is positioned in a hydrophobic pocket resulting from residues Phe80 and Ala144.[90]

1.7.4 Hymenialdisine

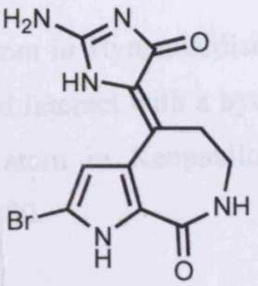

Hymenialdisine [17]

The natural product Hymenialdisine [17] has been isolated from Pacific marine sponges from the *Agelasidae, Axinellidae* and *Halichondriidae* families.[91] Hymenialdisine is a potent CDK inhibitor, and is an order of magnitude more active against CDK1 than Olomoucine. Unlike Olomoucine, Paullone or the natural ligand ATP, a crystal structure of the CDK2-Hymenialdisine complex (fig 1.7.2) shows that Hymenialdisine can form three hydrogen bonds to the Glu81 and Leu83 residues of CDK2, rather than just two.[92] There is also a fourth hydrogen bond from the guanidinone ring to Asp145 and a fifth to Gln131 via a water molecule.

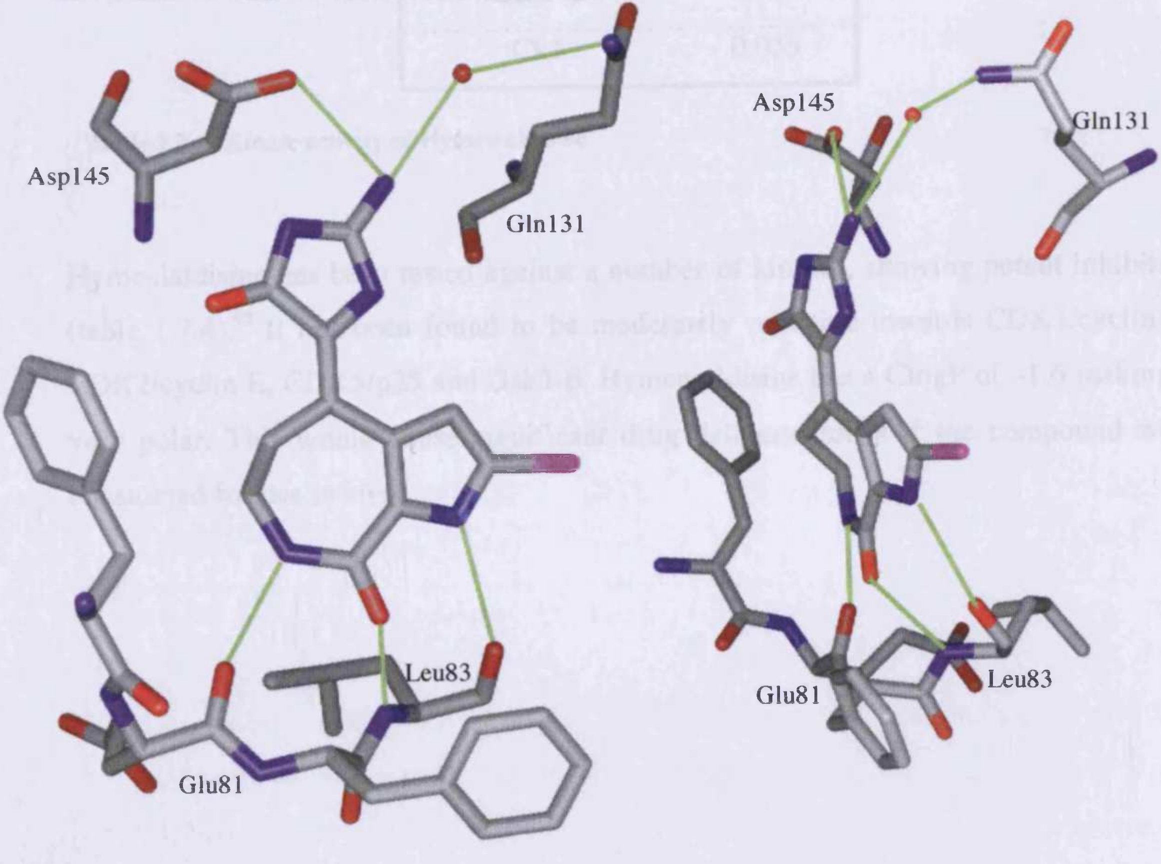

Fig 1.7.2: Crystal structure of Hymenialdisine in the active site of CDK2, showing the orientation and the hydrogen bonding to Glu81 and Leu83.

Interestingly, the bromine atom in Hymenialdisine was found to orientate towards the entrance to the active site and interact with a hydrophobic region formed by Phe82 and Ile10, unlike the bromine atom in Kenpaullone, which is orientated towards the hydrophobic pocket near Phe80.

Enzyme	IC_{50} (μM)
CDK1/Cyclin B	0.022
CDK2/Cyclin A	0.070
CDK2/Cyclin E	0.040
CDK3/Cyclin E	0.100
CDK4/Cyclin D1	0.600
CDK5/p25	0.028
CDK6/Cyclin D2	0.700
Gsk3-β	0.010
Ck1	0.035

Table 1.7.4: Kinase activity of Hymenialdisine

Hymenialdisine has been tested against a number of kinases, showing potent inhibition (table 1.7.4).[92] It has been found to be moderately selective towards CDK1/cyclin B, CDK2/cyclin E, CDK5/p25 and Gsk3-β. Hymenialdisine has a ClogP of –1.6 making it very polar. This would cause significant drug delivery issues if the compound were considered for use *in vivo*.

1.7.5 Other CDK Inhibitors

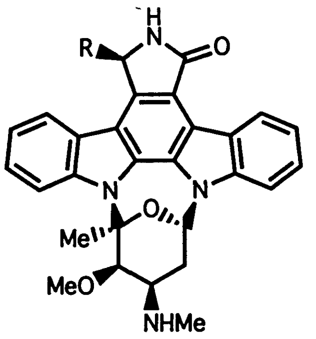

Staurosporine [18] R=H
UCN-01 [19] R=OH

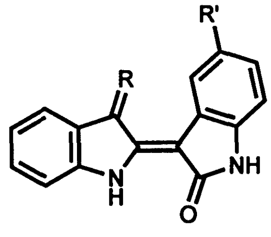

Indirubin [20] R=O, R'=H
5-Chloro-indibubin [21] R=O, R'=Cl
Indirubin-5-sulphonic acid [22] R=O, R'=SO_3H
Indirubin-3'-mono oxime [23] R=NOH, R'=H

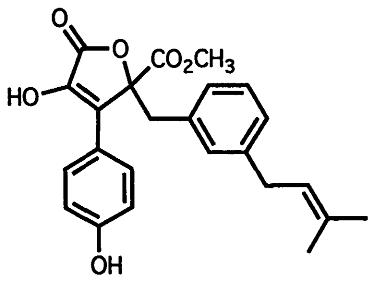

Butyrolactone I [24]

Other inhibitors include the second CDK modulator tested in clinical trials, the natural product Staurosporine [18], which was isolated from *Streptomyces staurosporeus*, and the hydroxy analogue, UCN-01 [19]. UCN-01 blocks cell cycle progression, promotes apoptosis and although it is very non-selective and inhibits a wide range of kinases is currently in phase II clinical trials.[93]

Inhibitor	CDK1/ Cyclin B	CDK2/ Cyclin A	CDK2/ Cyclin E	CDK4/ Cyclin D1
Staurosporine[17,36,94] [18]	0.006	0.007	NR	0.120
UCN-01[17,36,94] [19]	0.031/ 0.100	0.030	NR	0.032
Indirubin[95] [20]	10.0	2.2	7.5	12.0
5-Chloro-indibubin[95] [21]	0.4	0.75	0.55	6.5
Indirubin-5-sulphonic acid[95] [22]	0.055	0.035	0.15	0.3
Indirubin-3'-mono oxime[95] [23]	0.18	0.44	0.25	3.33
Butyrolactone I[79] [24]	0.68	0.82	NR	NR

Table 1.7.5: Activity of other inhibitors. All values in μM. NR Not Reported

Danggui Longhui Wan is a traditional Chinese herbal remedy used to treat leukaemia. The active ingredient was found to be Indirubin [20].[96] Along with analogues 5-chloro- [21], 5-sulphonic acid [22] and 3'-mono oxime [23], Indirubin was found to inhibit Rb phosphorylation, as well as cell proliferation in the G_1 phase, and the G_2/M transition.

While **[20]** inhibits all CDKs equally well, **[21]** and **[22]** were shown to express greater specificity for CDKs 1, 2 and 5 over CDK4. Meanwhile **[23]** has been shown to cause G_2/M arrest.[95] Growth inhibition assays of these compounds against the MCF-7 cell line displayed good inhibition by **[20]** (4.0 μM) and **[23]** (3.3 μM).[97]

Butyrolactone I **[24]** was identified as an inhibitor of CDKs 1 and 2, but showed no inhibition when tested against other kinases such as MAPK, PKC and EGFR. Compound **[24]** also prevented phosphorylation of the Rb protein, as well as Histone H1.[79]

Cell cycle arrest was also observed at the G_1/S and G_2/M phase transitions, which is consistent with CDK2 and CDK1 inhibition respectively.[98]

2. AIMS

2.1 Synthetic Aims

The aim of this project was to synthesize a novel series of compounds to explore the structure activity relationships associated with the 7-membered azepinone ring fused to an aromatic heterocycle common to both known inhibitors Paullone [13] and Hymenialdisine [17].

There has been substantial progress in the understanding of how inhibitors interact with the target protein CDK2 as a result of the crystallisation of CDK2-inhibitor complexes.[99] This knowledge would be used to assist the design of analogues to optimize the CDK binding. Molecular modelling programs, such as MOE and SYBYL, and visualization software (WebLab™ Viewer, Swiss-Pdb Viewer, iMol and Chimera) would be utilized to analyze the results of docking experiments carried out on the synthesized and proposed structures in order to better understand the impact on binding affinity that different alterations to the lead molecule would have.

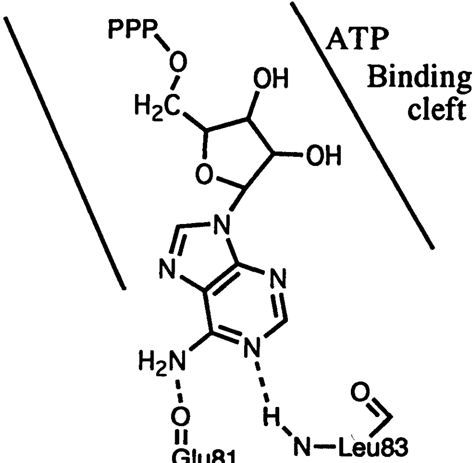

[1]

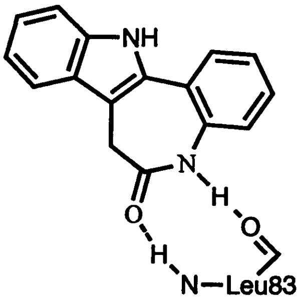

[13]

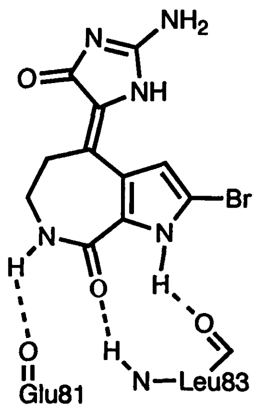

[17]

The ability to form two or three hydrogen bonds to the backbone of residues Leu83 and Glu81 is a common feature in the binding of all crystallographically determined CDK2 inhibitors, as well as the natural substrate ATP [1], emphasising the anchoring nature of these interactions.[100]

While the bromine of Hymenialdisine had been shown to increase its potency, initial work in our laboratory had shown that the synthesis of bromopyrrole derivatives in order to produce direct analogues of Hymenialdisine resulted in a complex mixture of products. As a benzene ring is only slightly more bulky than the bromine atom of Hymenialdisine and has good similarity in lipophilic character, the indoloazepinone structure was selected as the basic scaffold of the novel series of compounds. The synthesis of **[25]** and analogues to explore the structure activity relationships thereof would be the basis to the project.

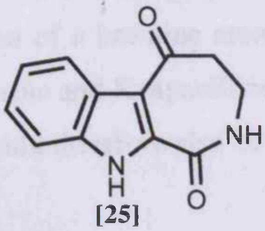

[25]

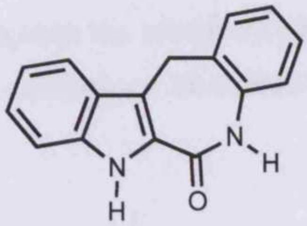

[26]

Inverting the indole of Paullone **[13]** would potentially bring the aromatic nitrogen into a position to interact with Glu81, in the same way as seen with Hymenialdisine **[17]**, thus improving the binding potential of the molecule **[26]**.

By overlapping this structure and Hymenialdisine **[17]**, it is clear that the "inverted Paullone" structure shares the Hymenialdisine motif, again with an indole rather than bromopyrrole fused to the lactam ring (fig 2.1.1).

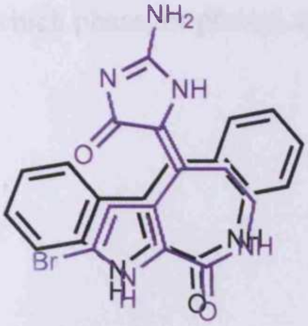

Fig 2.1.1: "Inverted Paullone" **[26]** (*black*) overlapped by Hymenialdisine **[17]** (*blue*).

Hymenialdisine has a guanidinone extension that has been shown by crystal structure analysis to be advantageous to its binding affinity in the CDK2 active site. However, this group is very polar, giving the molecule a ClogP of –1.6 that would lead to drug delivery issues with this molecule. Investigation of alternative extensions from this position would be an important part of the project, so a ketone was incorporated in this position. This group could be used as a convenient starting point for exploration into interactions between the active site and the phosphate moiety of ATP that could be advantageous for the affinity of the molecule for the active site of CDK2.

The ability of Hymenialdisine to form three hydrogen bonds would appear to be advantageous, so the novel series would want to determine the inhibitory importance of forming three rather than two hydrogen bonds. This would be assessed by blocking one of the hydrogen bonding positions.

Incorporation of a bromine atom was shown to improve the inhibitory effects of both Hymenialdisine and Kenpaullone, despite different orientations. Modification to include bromine would therefore also be investigated.

The importance of the 7-membered azepinone, or ε-lactam ring would also be investigated to determine how reduction or expansion affects the inhibitory potential of the molecule, with derivatives of the "inverted Paullone" [26] also a target.

The series of compounds would be subjected to a series of assays to discover the potency of the compounds. The compounds would be screened against cancer cell lines *in vitro*, and any compounds displaying promising inhibition would be further scrutinized by assays against the target protein complex, CDK2/cyclin A, as well as cell cycle analysis to determine in which phase, or phases, activity occurred.

2.2 Nomenclature

The synthesized compounds were named according to the "Hantzsch-Widman Nomenclature for Heteromonocyclic rings" with the "Fused Ring Nomenclature" as described by the International Union of Pure and Applied Chemistry (IUPAC) nomenclature system.[101]

According to this system, **[25]** is 1*H*-indole (the parent component) fused to 1*H*-azepine-2,5-dione. The common bond is therefore [3,4-*b*] (fig 2.2.1).

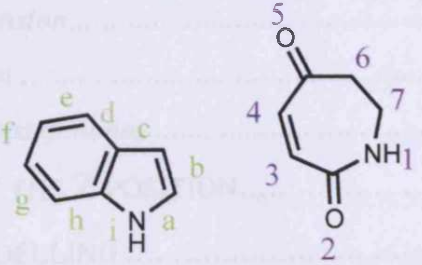

Fig 2.2.1: The appropriate letter locants for parent component, 1*H*-indole (*green*), and numerical locants for the attached component, 1*H*-azepine-2,5-dione (*blue*) as described by the IUPAC nomenclature system.

Based on this system, pre-cyclization compounds were numbered anti-clockwise around the indole ring from N being position 1, while in the cyclized compounds the indole N is position 10 (fig 2.2.2).

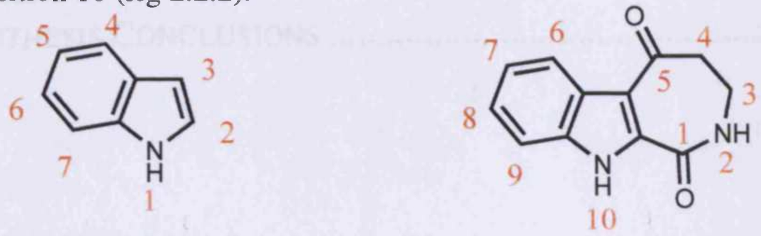

Fig 2.2.2: Numbering system used for precyclized compounds (*left*) and cyclized compounds (*right*).

Therefore the name for **[25]** was 3,4-dihydroazepino[3,4-*b*]indole-1,5(2*H*,10*H*)-dione. This structure was trivially named indoloazepinone, and is reported by that name throughout this thesis.

3. RESULTS AND DISCUSSION 38

3.1 INITIAL LEAD COMPOUND 38

3.2 SYNTHESIS OF N-METHYLINDOLOAZEPINONE 42

3.3 ALTERATIONS IN THE R POSITION 48

3.4 ALTERATIONS AT THE X-POSITION 57

3.5 ALTERATIONS IN THE Y POSITION 61

3.5.1 Hydrazone Extension *62*

3.5.2 Oxime Extension *68*

3.5.3 Extended Indoloazepinones *72*

3.6 ALTERATIONS AT THE Z POSITION 83

3.7 MOLECULAR MODELLING 94

3.8. MOLECULAR DOCKING WITH MOE 99

3.8.1 Control Experiment *100*

3.8.2 Docking Results *101*

3.9 STEREOCHEMISTRY INVERSION 105

3.10 KENPAULLONE SYNTHESIS 108

3.11 SYNTHESIS CONCLUSIONS 110

3. Results and Discussion

3.1 Initial Lead Compound

The primary synthetic target for this study was indoloazepinone [25], and derivatives of this compound.

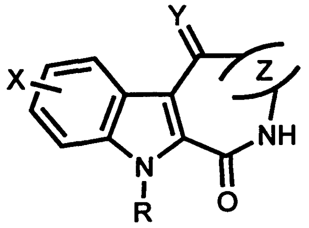

Fig 3.1.1: The four key areas of the molecule

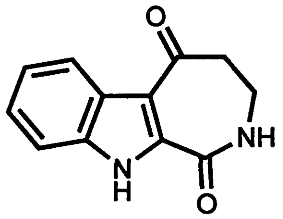

[25]

The study has focused on investigating four key areas of the molecule to evaluate their impact on the binding of the molecule in the active site of CDK2 (fig 3.1.1); X – extensions from the indole benzene ring towards the exterior of the protein, Y – extensions from the ketone position into the cleft of the active site, Z – the size of the lactam ring and R – blockage of a potential hydrogen bonding position.

Retrosynthetic analysis (fig 3.1.2) showed that the lead compound could be made with commercially available indole-2-carboxylic acid [28] and β-alanine [29] as the starting materials.

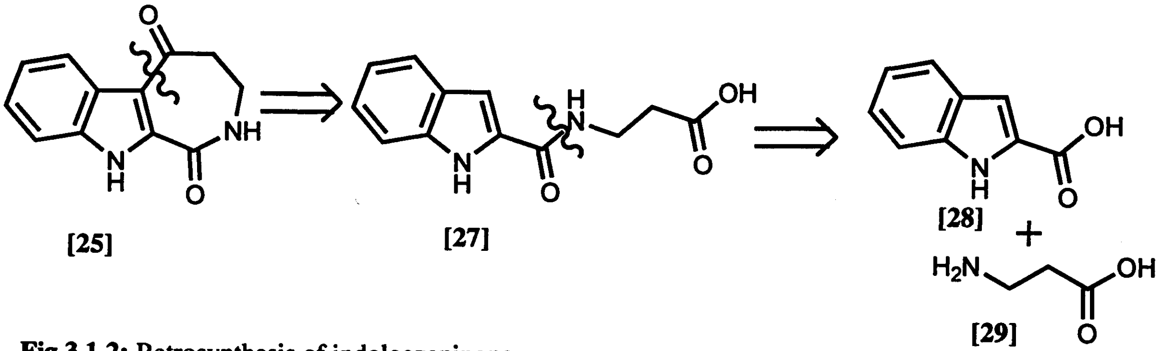

Fig 3.1.2: Retrosynthesis of indoloazepinone

Therefore, there were two key reactions in the synthetic route – the amide bond forming reaction (step A), and the cyclization step (step B) (fig 3.1.3).

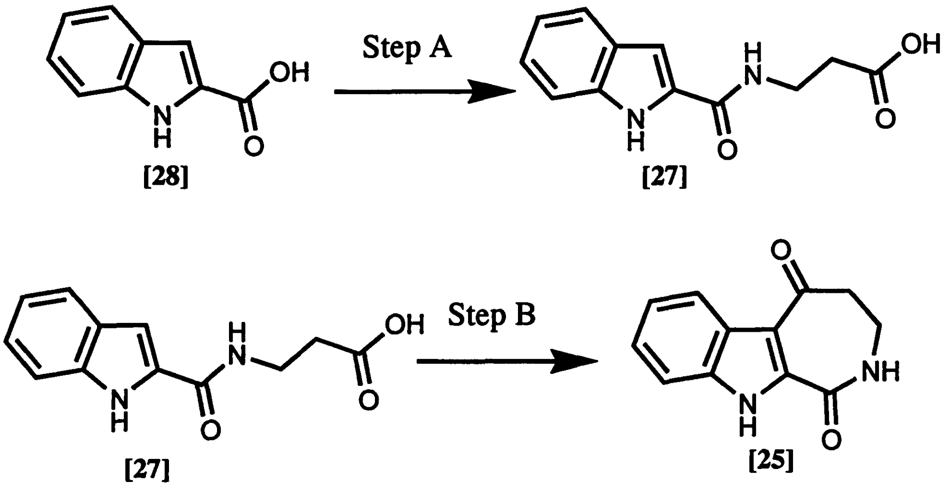

Fig 3.1.3: The proposed synthetic steps for the formation of indoloazepinone **[25]** from indole-2-carboxylic acid **[28]** through an amide bond forming reaction (step A) and a cyclization step (step B).

Previous work in our laboratory had developed a method to form the amide bond, via an acid chloride (see fig 3.2.5 page 43).[102] However, it had also been shown that if the reaction was carried out on the N-unsubstituted indole **[28]**, the unprotected nitrogen would react with a molecule of the acid chloride, and the main product of the reaction would be the dimer **[30]** (fig 3.1.4).[102]

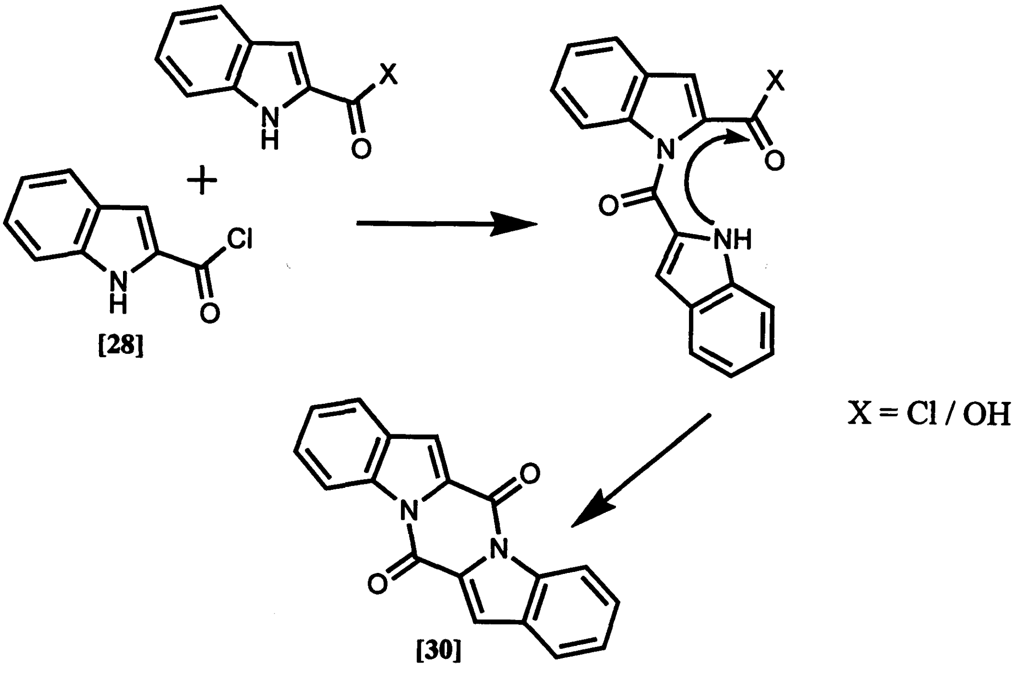

Fig 3.1.4: Formation of the unwanted side product **[30]** when the amide bond forming reaction is carried out on the free NH indole.

Therefore, it was necessary to protect this nitrogen for the amide bond forming reaction to be successful.

The aim of investigation at the R position (fig 3.1.1) was to evaluate the importance of the potential hydrogen bond to the activity of the molecule. As seen previously (page 34), **[25]** would be expected to from three hydrogen bonds to the CDK2 backbone residues Glu81 and Leu83. By placing a small group in the R position, such as a methyl group, the molecule would only be able to make two hydrogen bonds. As the methyl group is relatively small compared to other potential protecting groups, it would hopefully have minimal effect on the binding of the rest of the molecule in the active site of CDK2. Therefore the two hydrogen bonds to the oxygen of Glu81, and the nitrogen of Leu83 could still be formed.

Comparison of the activity of the two molecules (R=H and R=CH_3) would give an indication of the effect of the third hydrogen bond. To avoid the synthetic complications outlined above, it was therefore logical to put this group in place prior to the amide bond forming reaction.

The natural substrate, ATP also only has these two hydrogen bonds, so, only taking the hydrogen bonding in this area of the active site into account, **[31]** should theoretically still be a competitive inhibitor (fig 3.1.5).

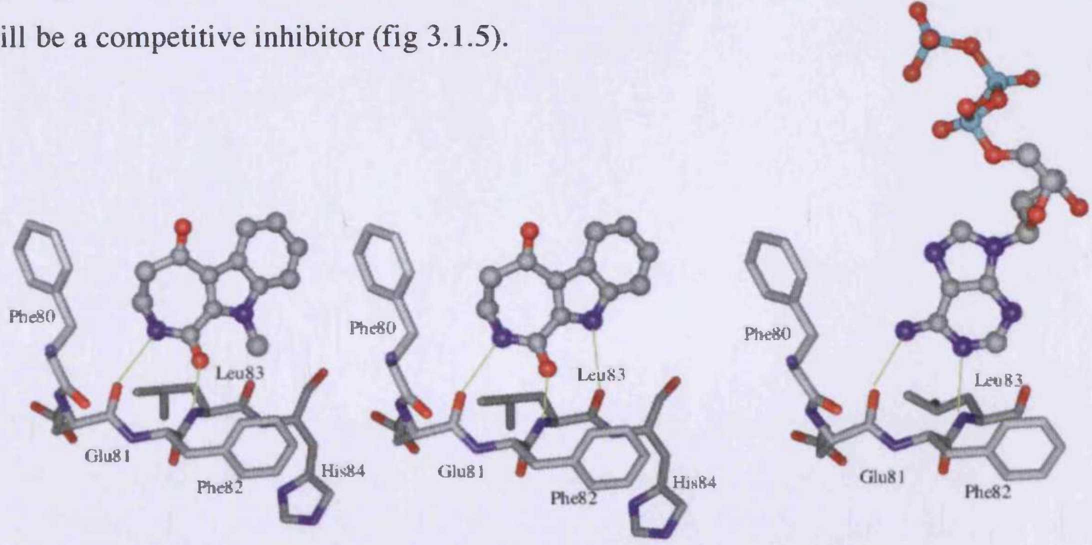

Fig 3.1.5: The hydrogen bonds (*green*) for the binding in the CDK2 active site of ATP **[1]** (*right*), and the theoretical hydrogen bonding for **[31]** (*left*) and **[25]** (*centre*).

The methyl group was also very stable; it would be more accurate to describe it as a blocking group than as a protecting group, which made the methyl analogue ideal to develop the chemistry with. Once a reliable synthetic pathway had been ascertained, other protecting groups could be utilized, and removed after cyclization to afford the free NH analogue. Therefore, N-methylindoloazepinone [31] became an additional target molecule.

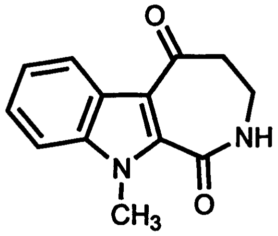

[31]

3.2 Synthesis of N-Methylindoloazepinone

Before the methyl group could be added, the carboxylic acid functional group had to be protected. This was done by synthesizing the ester **[32]**. This reaction was easy to carry out, and had excellent yields of over 90 % (fig 3.2.1), which did not change significantly when the reaction was carried out at scales between 2 g and 20 g of the carboxylic acid.

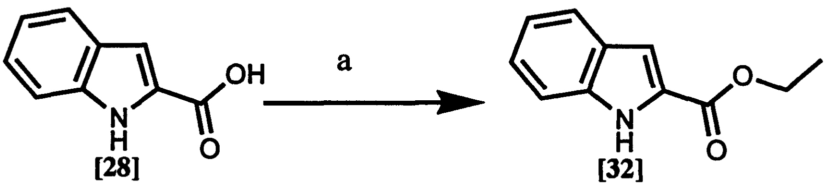

Fig 3.2.1: a: EtOH, H_2SO_4, Δ 23 hrs, 93 %

For the methyl protecting reaction, producing **[33]**, initially low yields of around 30 % were obtained using the stated conditions (fig 3.2.2 – a).

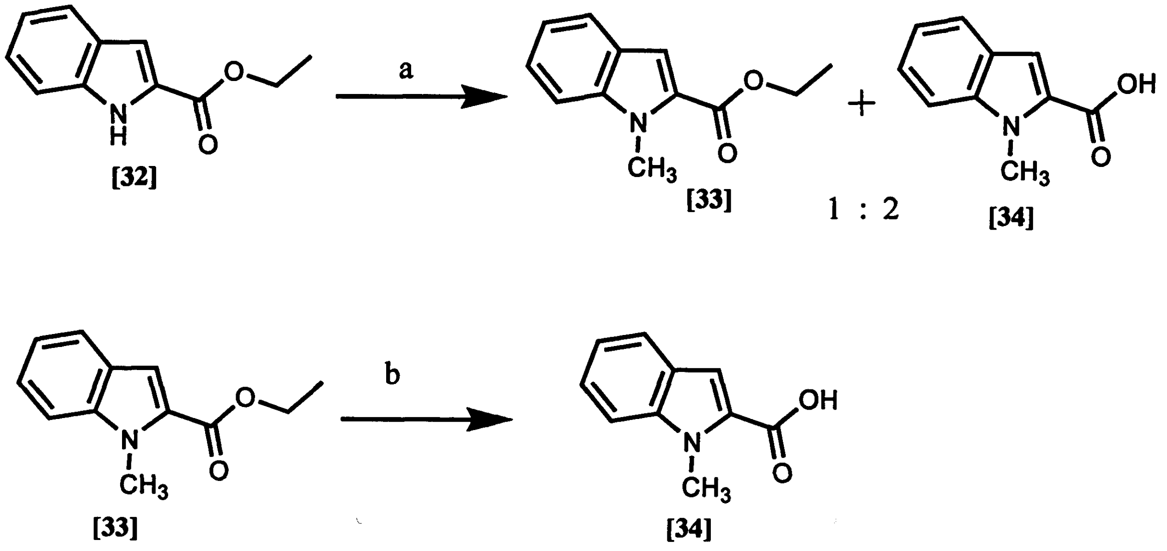

Fig 3.2.2: a: i. NaH, THF, ii. MeI, THF, 29 % ([33]) 65 % ([34]), b: NaOH(aq), MeOH, 60 °C, 88 %

However, the workup procedure of the methylating reaction was modified allowing recovery of the carboxylic acid and approximately 2 : 1 **[34]** : **[33]** was recovered. Hydrolysis of the ester to afford the indole (N-methyl) carboxylic acid **[34]** also yielded over 85 % (fig 3.2.2 – b).

Therefore, logically, there was no need to isolate **[33]**, and the two steps could be combined. This proved to be the case (fig 3.2.3), and the synthesis of **[34]** consistently yielded over 85 %.

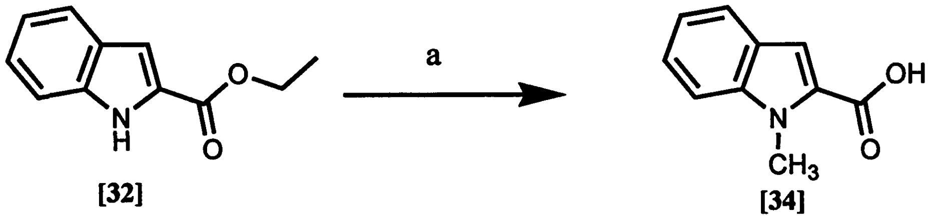

Fig 3.2.3: a: i. NaH, THF, ii. MeI, THF, iii. NaOH (aq), MeOH, 60 °C, 88 %

To form carboxylic acid ester **[35]**, β-alanine **[29]** needed to be coupled to the carboxylic acid **[34]**. Again, it was necessary to protect the β-alanine carboxylic acid group to avoid unwanted side reactions. This was converted into the hydrochloride salt of the ester **[36]** (fig .3.2.4).[103]

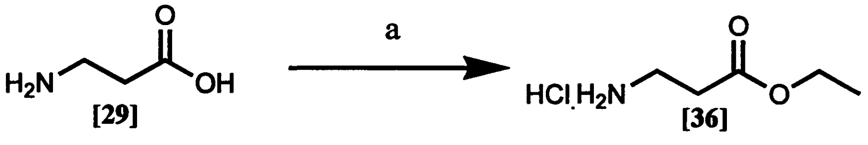

Fig 3.2.4: a. $SOCl_2$, EtOH, Δ 10 h, 96 %

The amide bond forming reaction to produce **[35]** was very effective (fig 3.2.5), and proceeded in high yield.

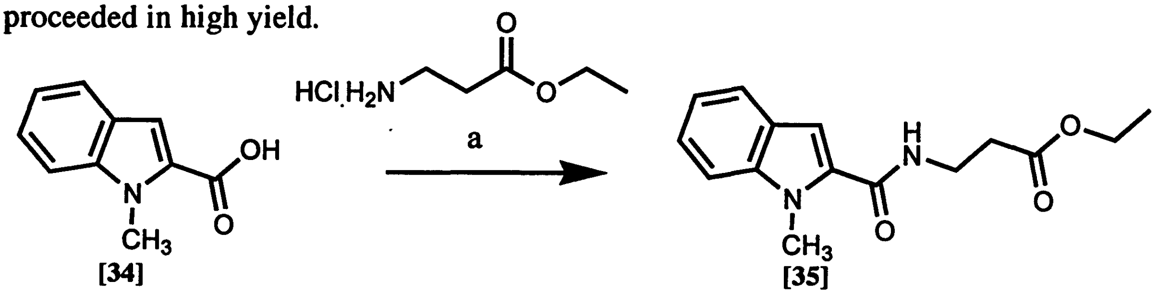

Fig 3.2.5: a. i. TEA, oxalyl chloride, THF, 0 °C
ii. β-alanine ethyl ester hydrochloride, TEA, THF, 80 %

The hydrolysis of the ester to form the cyclization pre-cursor **[37]** was effectively the same reaction used to produce **[34]** from **[33]** (fig 3.2.3), and not surprisingly, high yields were again produced (fig 3.2.6 -a).

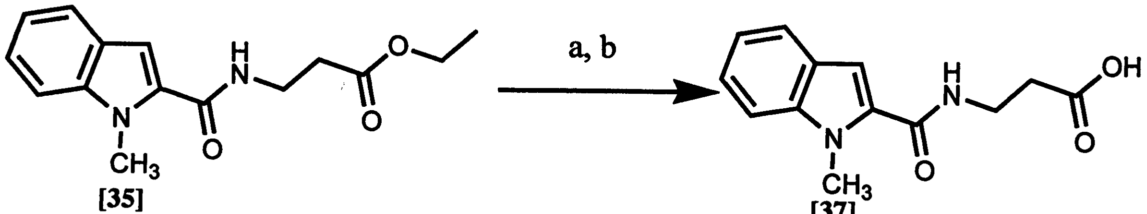

Fig 3.2.6: a: MeOH, NaOH (aq), 60 °C 4 h, 81 %,
b: $LiOH.H_2O$, THF, 97 %

These conditions were strongly basic and the indole (N-methyl) carboxylic acid [34] was often evident in the crude product, sometimes in significant quantities, indicating cleavage of the amide bond. Therefore a milder reaction using lithium hydroxide monohydrate (LiOH.H_2O) was used (fig 3.2.6 -b). Amide bond cleavage was no longer observed using this method, and yields improved.

The molecule was now ready for the second key step – the cyclization step to form N-methylindoloazepinone [31] (fig 3.2.7). This was an acid catalyzed cyclodehydration reaction, with phosphorus pentoxide used to extract the resultant water.104

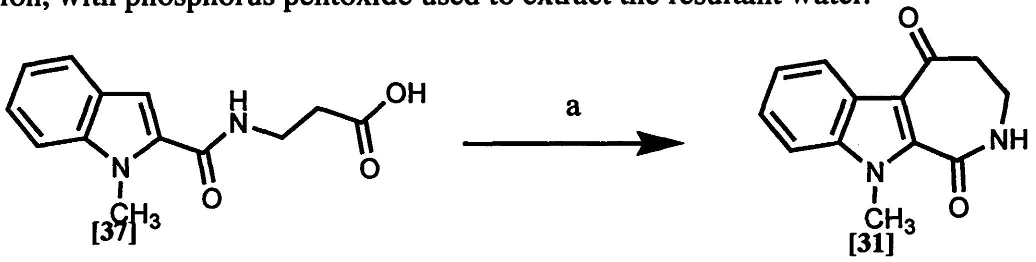

Fig 3.2.7: a: Phosphorus pentoxide, methane sulfonic acid, 80 °C, 81 %

This reaction was preferable to the alternative cyclization method using polyphosphoric acid (PPA),105 as the reagents were easier to handle than the highly viscous PPA.104 Nevertheless, after quenching with ice, the resulting residue was both extremely messy and time consuming to extract. On small scale, the yield was far from impressive; under 40 % after purification. It was found, however, that the reaction scaled up extremely well, and reaction scales on more than 1 g yielded around 80 % of analytically pure product without needing purification.

^1H NMR was a powerful tool to show that the cyclization had been successful. There were two key areas of the spectrum that gave evidence for cyclization. Firstly, the aromatic region changed markedly. Before cyclization, the aromatic region showed five peaks: 1 singlet, 2 doublets and 2 double doublets. After cyclization, the singlet disappeared (as would be expected), and the other peaks moved slightly upfield, with the doublet nearest the position of the cyclization moving 0.7 ppm as a result of the deshielding effects of the newly introduced carbonyl group (fig 3.2.8). This property was found to be a common feature of all the cyclized compounds and was a reliable marker to show whether or not the reaction had been successful.

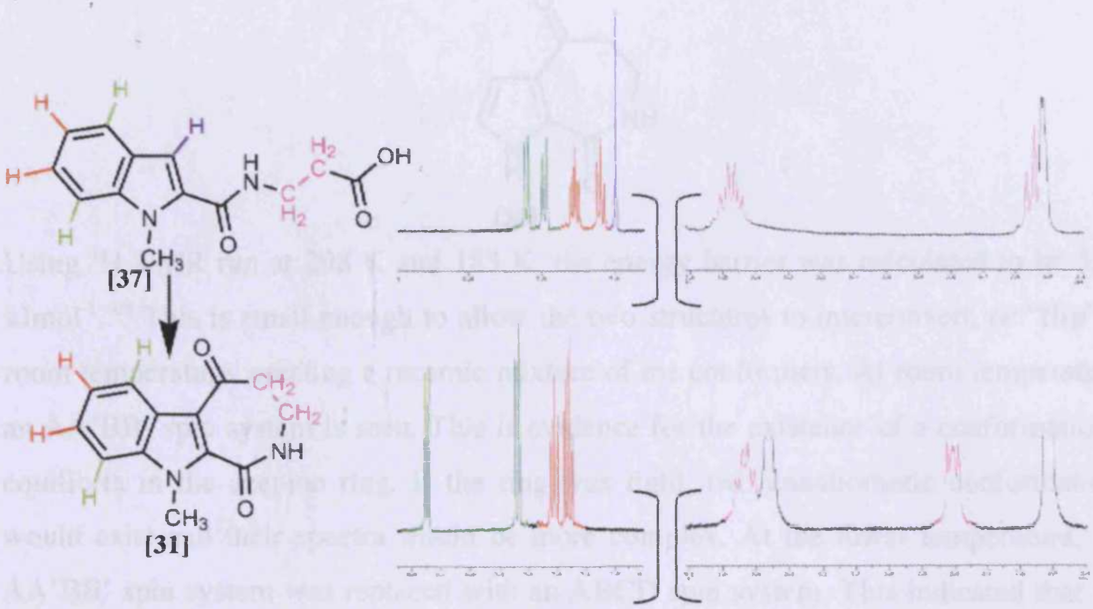

Fig 3.2.8: The ^{1}H NMR signals of the pre and post cyclization compounds in d6-DMSO. The aromatic singlet is (*blue*), doublets (*green*) and double-doublets (*red*) are shown. The aliphatic CH_2 groups (*magenta*) are also shown. The regions 6.8-8.5 ppm, and 2.4-3.6 ppm are displayed.

The other key alteration was the two CH_2 groups in the newly formed ring. In the ring opened compound, they were a classic quartet and triplet, but in the cyclized compound, an unusual multiplet was observed, with the outside peaks actually taller than the central peak (fig 3.2.9).

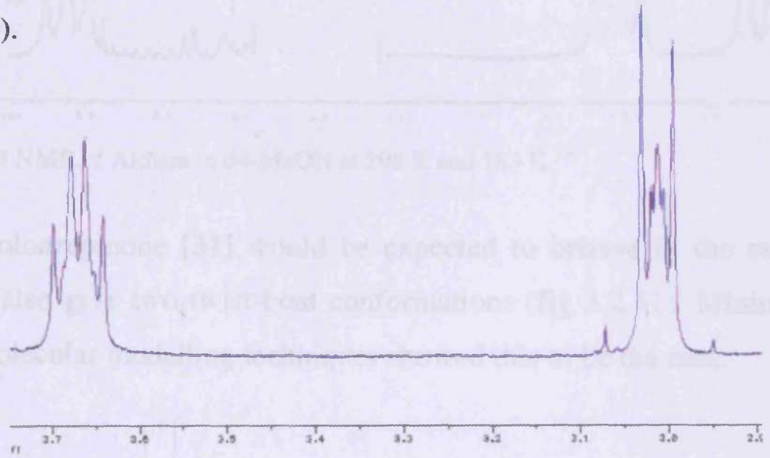

Fig 3.2.9: ^{1}H NMR signals of **[31]** in $CDCl_3$ for the two aliphatic CH_2 groups. The region 2.9 ppm to 3.8 ppm is shown.

The pyrrole (NH) equivalent, a natural product trivially named Aldisin **[38]** has been studied by Latypovt et al., and it was deduced that there are two distinct twist-boat conformations possible. [106]

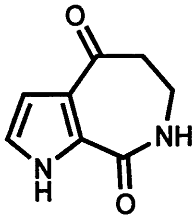

[38]

Using ^1H NMR run at 298 K and 183 K, the energy barrier was calculated to be 52.3 $kJmol^{-1}$.[106] This is small enough to allow the two structures to interconvert, or “flip” at room temperature, creating a racemic mixture of the conformers. At room temperature, an AA’BB’ spin system is seen. This is evidence for the existence of a conformational equilibria in the azepine ring. If the ring was rigid, two enantiomeric conformations would exist and their spectra would be more complex. At the lower temperature, the AA’BB’ spin system was replaced with an ABCD spin system. This indicated that the conformational equilibria was reduced at the lower temperature (fig 3.2.10).

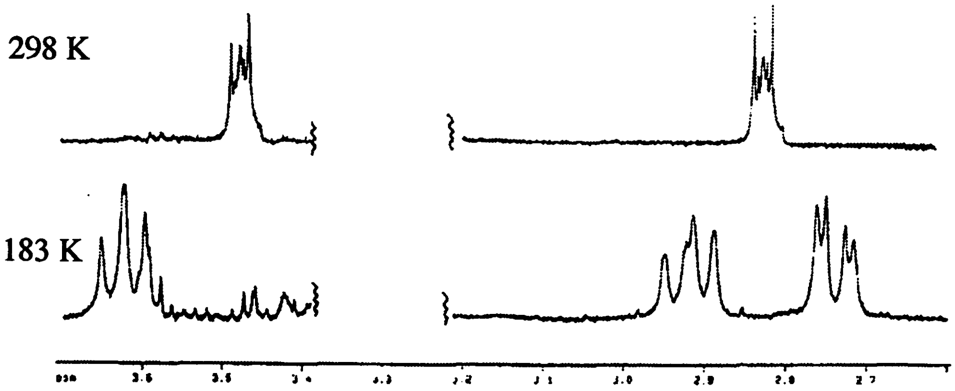

Fig 3.2.10: 1H NMR of Aldisin in d4-MeOH at 298 K and 183 K.[106]

N-Methylindoloazepinone [31] would be expected to behave in the same manner as Aldisin, and also give two twist-boat conformations (fig 3.2.11). Minimisation with a number of molecular modelling techniques showed this to be the case.

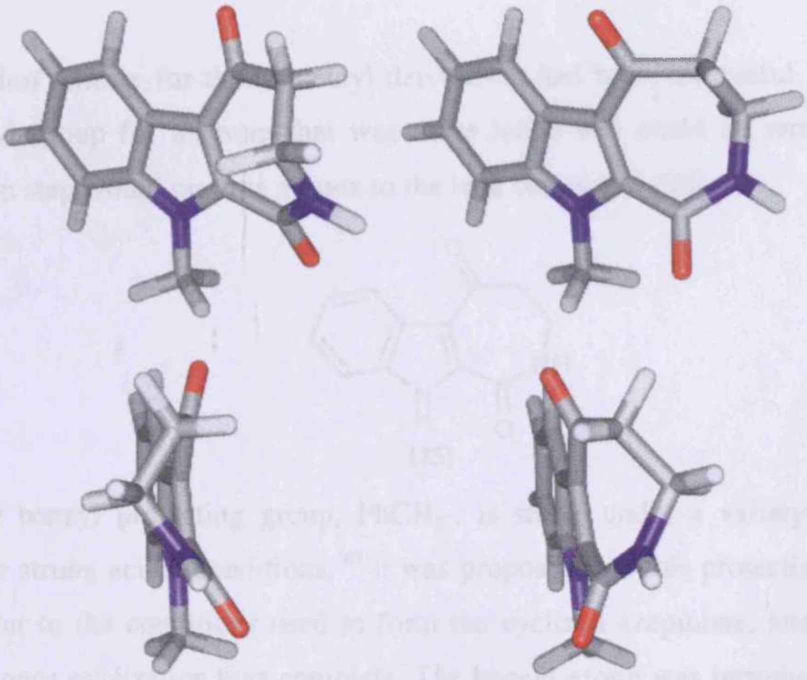

Fig 3.2.11: 3D representations of the two twist-boat conformations of N-methylindoloazepinone **[31]** minimized using MM2 minimisation in Chemdraw 3D.

N-Methylindoloazepinone **[31]** had been synthesized successfully from the commercially available starting material indole-2-carboxylic acid **[28]** in an overall yield of 51 % (fig 3.2.12). All the reactions were reproducible and, with the exception of the significant improvement with scale-up of the final stage, the percentage yields remained reasonably constant for the individual steps.

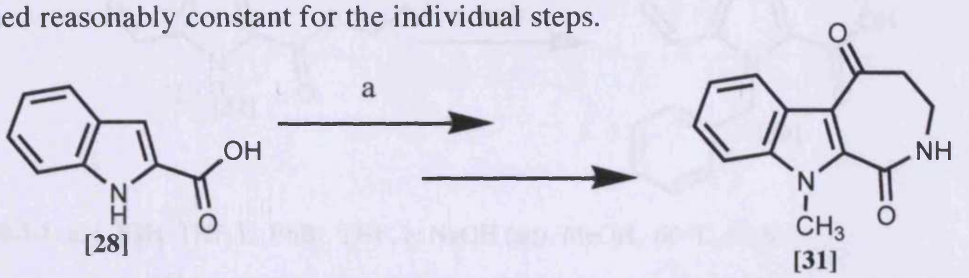

[28] [31]

Fig 3.2.12: a: Overall synthesis of N-methylindoloazepinone **[31]** from indole-2-carboxylic acid **[28]**; 51 %

3.3 Alterations in the R position

The reaction scheme for the N-methyl derivatives had been successful, so exchanging the methyl group for a group that was more labile and could be removed after the cyclization step would provide a route to the lead compound **[25]**.

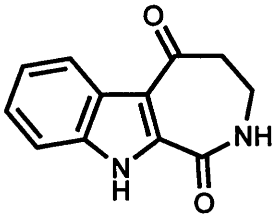

[25]

Since the benzyl protecting group, $PhCH_2$-, is stable under a variety of conditions, except for strong acidic conditions,[107] it was proposed that this protecting group would be resistant to the conditions used to form the cyclized azepinone, and could then be removed once cyclization was complete. The benzyl group was introduced at the same point in the synthesis as the methyl group (as described above), and the reaction worked reasonably well, although some difficulties were encountered separating unreacted benzyl bromide. The hydrolysis to afford **[39]** proceeded in comparable yield to the methyl-protected equivalent and the workup conditions for this reaction removed the benzyl bromide impurity from the previous step. It was also shown that, similar to the methyl analogue, there was no need to isolate the intermediate (fig 3.3.1).

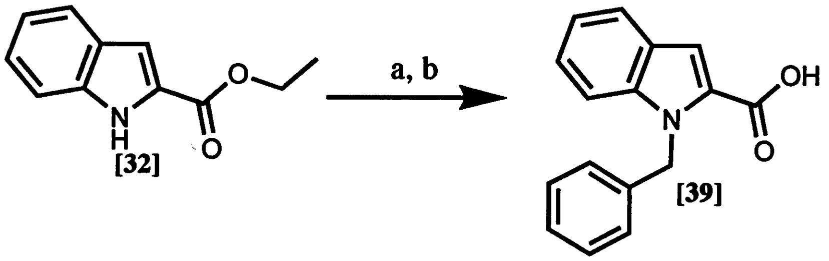

Fig 3.3.1: a: i. NaH, THF, ii. BnBr, THF, b: NaOH (aq), MeOH, 60 °C, 81 %

The formation of the amide bond to afford **[40]**, and the subsequent hydrolysis to form the carboxylic acid **[41]** were both achieved in comparative yields to their methyl equivalent (fig 3.3.2).

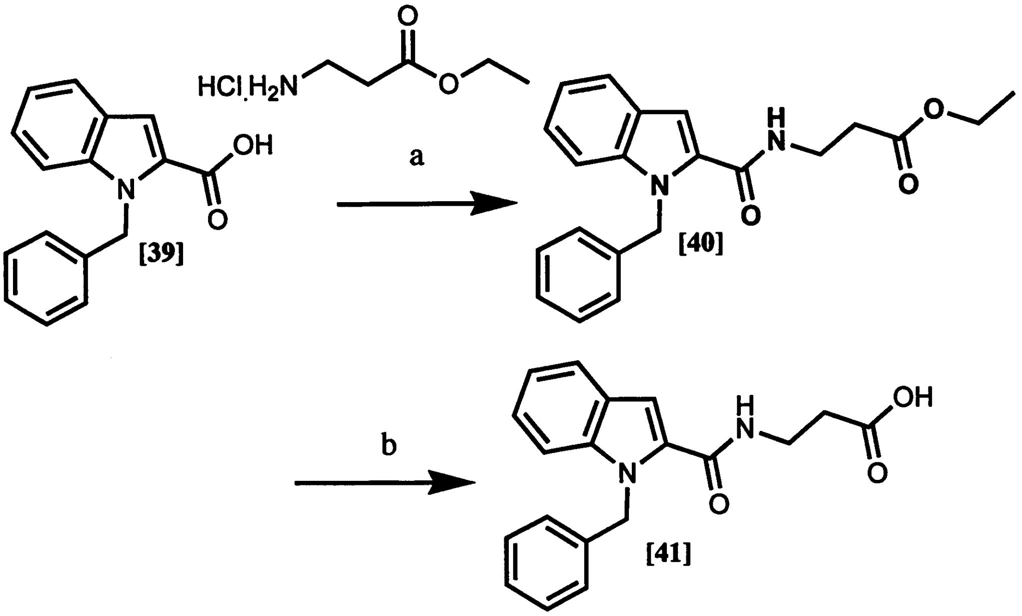

Fig 3.3.2: a: i. TEA, oxalyl chloride, THF, 0 °C, ii. β-alanine ethyl ester hydrochloride, THF, 91 %. b: NaOH (aq), MeOH, 82 %

It was interesting to note the ^{13}C NMR of these compounds. 12 Peaks would be expected for the aromatic portion of the molecule; 8 for the indole and 4 for the phenyl ring and this was the case with **[39]**. Once the amide bond had been formed to give **[40]** however, it would appear that the extension forced the benzyl group into a more conformationally restricted position, making all 6 carbons non-equivalent (table 3.3.1).

Compound number	Aromatic peaks in ^{13}C NMR
[39]	110.8, 111.6, 121.0, 122.7,125.3,125.9,126.6, 127.3, 128.5, 128.8, 139.0, 139.3
[40]	105.5, 111.4, 120.7, 122.0, 124.1, 126.2, 127.0, 127.3, 127.8, 127.9, 128.7, 132.0, 138.2, 139.1

Table 3.3.1: The carbon peaks for the aromatic region of **[39]** and **[40]**.
^{13}C NMR carried out in d-6 DMSO.

This set up the cyclization step to form N-benzyl indoloazepinone [42] (fig 3.3.3).

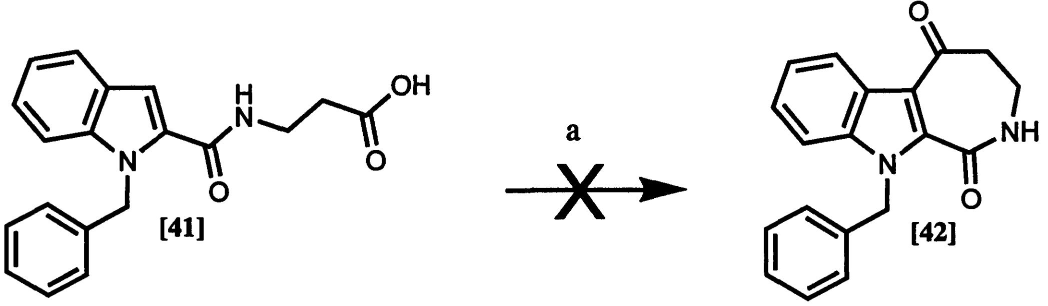

Fig 3.3.3: a: Phosphorus pentoxide, methyl sulfonic acid, 80 °C, 0 %

However the reaction was not successful, and it was not possible to isolate any of the reaction products from the residue. Crude analysis suggested that the strong acidic conditions may have cleaved the benzyl group and subjected the compound to further degradation.

Alternative methods were therefore attempted to cyclize the benzyl-protected precursor [41]. Acid chlorides are known to acylate the 3 position of indoles,[108,109,110] so if the carboxylic acid was converted to an acid chloride, the molecule could be more prone to cyclization. Therefore, [41] was treated with thionyl chloride to form the acid chloride. This was then heated with methane sulfonic acid in DMSO as acidic conditions and heat seemed to be important according to the literature.[109] However, again nothing could be identified from the crude product. Again it seemed that the harsh conditions may have broken the molecule down, therefore a milder method of forming the acid chloride was attempted. The same method as used to form the acid chloride for the amide bond forming reaction; oxalyl chloride in THF (see fig 3.3.2) was used. However, the molecule did not cyclize and the starting material was recovered. DMF and DMSO were used as solvents in order to reach higher temperatures, but still no reaction occurred (fig 3.3.4).

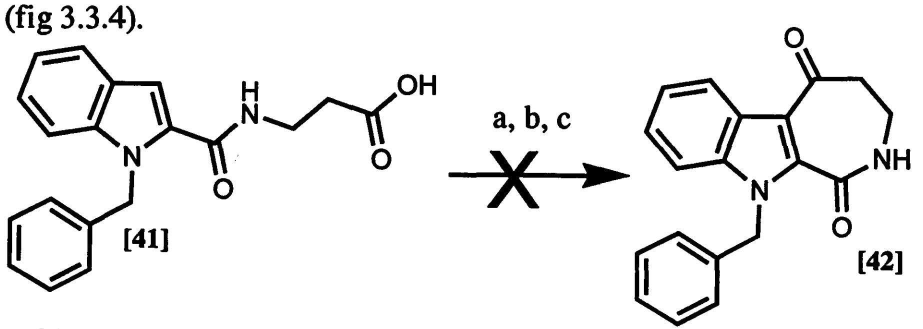

Fig 3.3.4: a: $SOCl_2$, $MeSO_3H$, DMF, 150 °C 20 h
b: i. Oxalyl chloride, TEA, DMF, 0 °C, ii. Δ
c: i. Oxalyl chloride, TEA, DMSO, 0 °C, ii. Δ

A literature method for acid chloride acylation of indoles using an $AlCl_3$-THF complex was attempted (fig 3.3.5).[111] The ^1H NMR was inconclusive although reaction had clearly occurred; the characteristic singlet peak that is seen at approximately δ 7.10 in the ^1H NMR, from the indole 3-H that is removed during cyclization, was no longer present. The NH peak was also absent. While exchangeable peaks are sometimes missing in ^1H NMR, the evidence was certainly not conclusive.

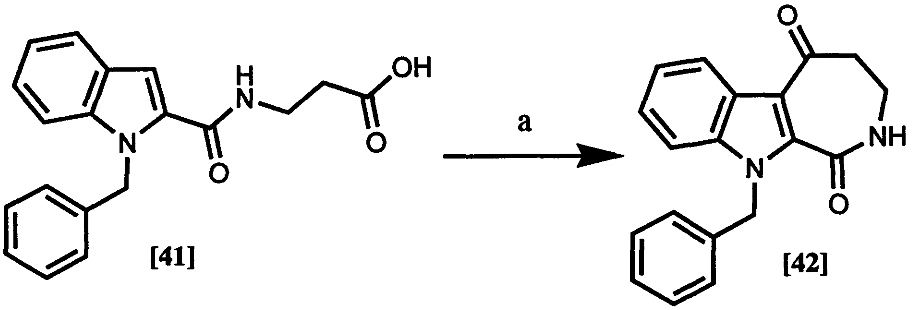

Fig 3.3.5: a: $AlCl_3$-THF, THF, 3 %

The yield was also extremely low (3 %), and high-resolution mass spectrometry (HRMS) did not give the expected peak. If the cyclized compound N-benzyl indoloazepinone **[42]** had been formed, a peak at 304 would be expected, but the HRMS gave a peak at 208. This is consistent with bond cleavage between the indole and the carbonyl, giving **[43]**. This structure has no NH, hence the absence of this peak, and the indole 3-H aromatic singlet is now a doublet. This would appear to fit with the ^1H NMR; rather than the expected pair of CH_2 peaks in the lactam ring (see fig 3.2.8 page 45), the NMR had two peaks much higher field than would be expected for N-benzyl indoloazepinone **[42]**. Although the splitting could not be identified, this would be appropriate for the 3-H and 2-H doublets of **[43]**.

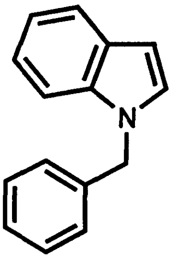

[43]

Cyclization of the precursor, **[40]**, was also attempted. This was heated in DMF with methane sulfonic acid. The reaction mixture was heated to 200 °C, so that the side product from the reaction, ethanol, would evaporate, driving the reaction to completion. As indole is usually substituted at the 3-posititon, this could lead to the desired product, the N-methylindoloazepinone **[42]**. While there was evidence of reaction, the product was **[41]** (fig 3.3.6).

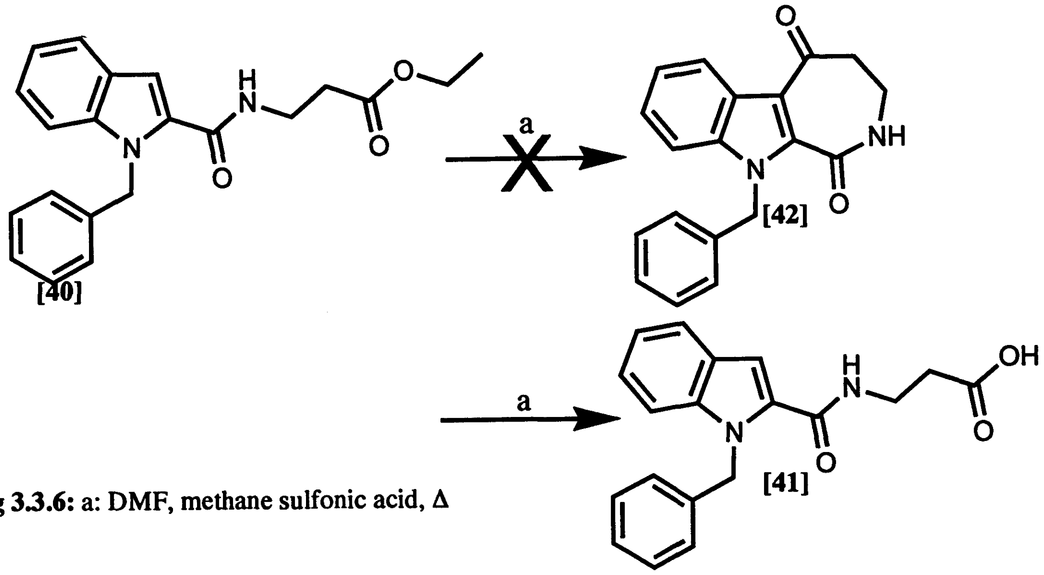

Fig 3.3.6: a: DMF, methane sulfonic acid, Δ

As the cyclization step was clearly a problem for the benzyl protected compounds, other protecting groups were investigated in order to try to successfully synthesize the lead compound **[25]**.

The tosyl-protected compound **[44]** was synthesized from the ester **[32]** (fig 3.3.7), and this reaction worked successfully.

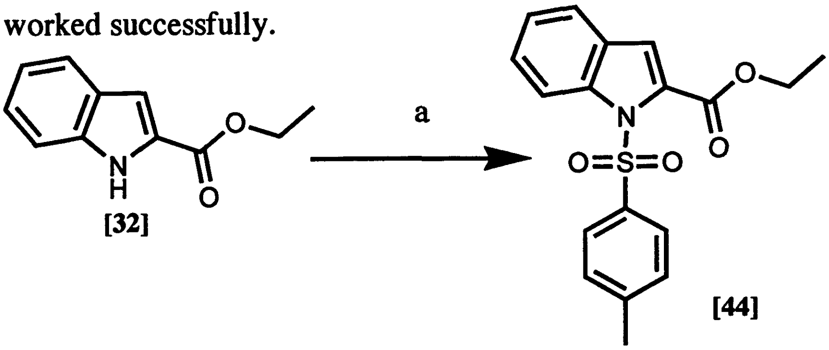

Fig 3.3.7: a: Potassium tert-butoxide, 18-crown-6, tosyl chloride, THF, 72 %

However, the removal of the ester protecting group proved extremely difficult compared to the previous experiments; the original conditions (NaOH (aq), MeOH fig 3.2.2) used for the methyl derivative cleaved the tosyl group. Therefore, the milder conditions, using $LiOH.H_2O$ in THF (see fig 3.2.8) were attempted. While it seemed possible to cleave the ester and not the tosyl group on small scale, the yield was poor (19 %), and the product impure. Also, the reaction did not scale up. As the tosyl group was clearly very labile, it was felt that it would not be suitable for the rest of the chemistry, even if this step could be improved due to the harsher conditions of the steps to follow.

An alternative protecting group, *tert*-butyl dimethyl silyl (TBDMS) **[45]** was considered, but multiple attempts were unable to successfully perform the reaction (fig 3.3.8), despite a literature procedure for protection of indole derivatives using this group.[112]

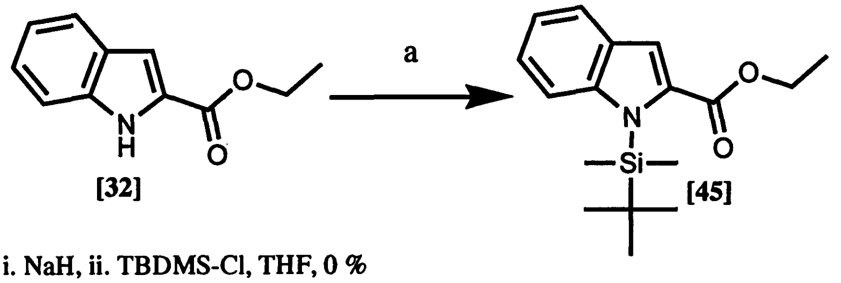

Fig 3.3.8: a: i. NaH, ii. TBDMS-Cl, THF, 0 %

Another protecting group, diphenyl-4-pyridylmethyl chloride hydrochloride **[50]**, was identified as a suitable protecting group due to it being "markedly more stable to acid than benzyl esters".[113] If the acidic conditions of the cyclization step had indeed cleaved the benzyl group, this reported increase in stability could lead to a more successful cyclization.

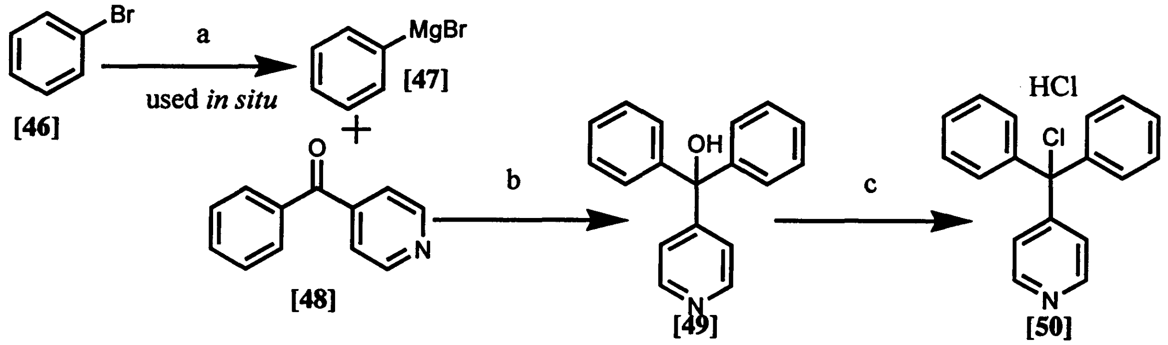

Fig 3.3.9: Synthesis of diphenyl-4-pyridylmethyl chloride hydrochloride. a: Mg, ether, b: Δ, ether, 81 %, c: $SOCl_2$, Δ, chloroform, 80 %

The literature method was successfully followed (fig 3.3.9), with yields only slightly lower than those reported (81 % and 80 % compared to 88 % and 86 % respectively). However, the reaction to attach this group to the indole (NH) ester **[32]** was not successful (fig 3.3.10). It had been felt that the bulkiness of the protecting group **[50]** might cause steric problems, and this would appear to have been a major factor in the reaction not occurring.

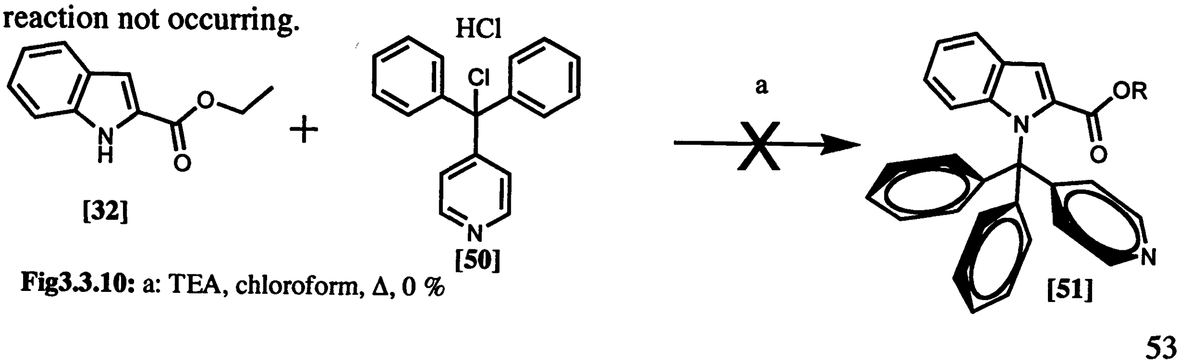

Fig3.3.10: a: TEA, chloroform, Δ, 0 %

The literature had evidence for the protection of imidazole based compounds,[113] but not indoles, and it is not surprising that the aromatic groups were not all accommodated. For both this protecting group and TBDMS, the steric bulk of the protecting group would appear problematic, and was analyzed further (see page 77).

As the protecting groups were proving to be a problem, it was decided to investigate alternative ways of synthesizing the lead compound **[25]** without the need for a protecting group and an alternative synthetic route to form the amide bond without the need to protect the indole nitrogen was identified (fig 3.3.11-a).[114]

The synthesis involved using 1-(3-dimethylaminopropyl)-3-ethylcarbodiimide hydrochloride (EDCI) as a coupling agent and 4-dimethylaminopyridine (DMAP) as a catalyst.

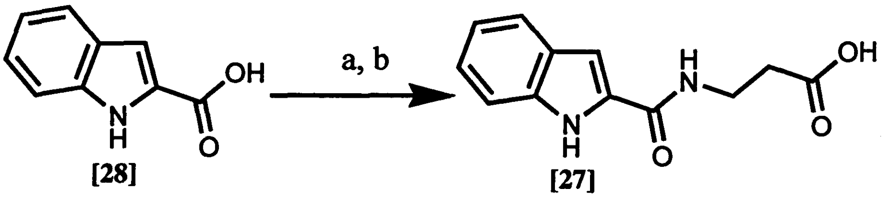

[28] [27]

Fig 3.3.11: a: EDCI, DMAP β-alanine ethyl ester hydrochloride, DCM, 85 %
b: $LiOH.H_2O$, THF, 97 %

The reaction was carried out in DCM, and when the reaction was finished the solvent was removed *in vaccuo* and water added. The pure product crashed out immediately and was collected by filtration with no further purification necessary. N,N'-dicyclohexylcarbodiimide (DCC) was tried as an alternative coupling reagent to EDCI, but the yield dropped dramatically from 85 % with EDCI to 24 % with DCC. This was probably due to steric crowding, as the DCC is much bulkier than EDCI. The DCC reaction was also much harder to purify, as the urea by-product did not dissolve in water.

Depropotection of the indole (NH) ester **[52]** with $LiOH.H_2O$, as seen with the indole (N-methyl) ester **[35]**, was successful (fig 3.3.11-b).

The cyclization step was then carried out using the same conditions as for the protected compound (fig 3.3.12).

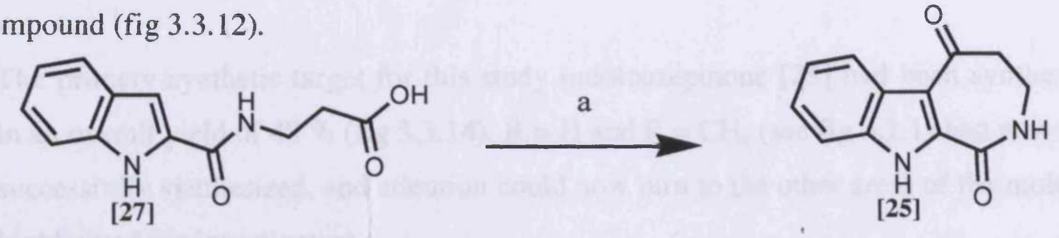

[27] [25]

Fig 3.3.12: cyclization a: Phosphorus pentoxide, methane sulfonic acid, 100 °C, 58 %

The reaction was not as effective as with the methyl analogue, and the ^{1}H NMR had a doubling of peaks, indicating two products. The major set of peaks was for the indoloazepinone **[25]** while the minor peaks showed evidence for cyclization, as it had the characteristic multiplet of the ε-lactam ring structure (see fig 3.2.9). The minor compound (obtained in about 20 %yield) was believed to be cyclized to the free NH **[53]**, although it was not fully characterized.

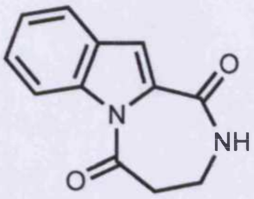

[53]

Recrystallization of indoloazepinone **[25]** gave an analytically pure sample, (fig 3.3.13) although the recovered yield was much reduced. The reaction was repeated and the temperature increased from 80 °C to 100 °C, and the problem of the unwanted production of **[53]** was reduced.

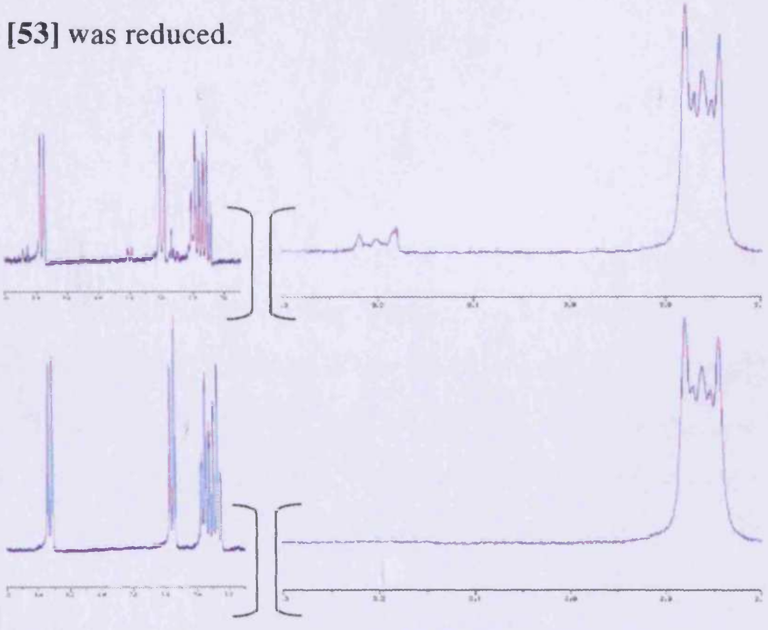

Fig 3.3.13: ^{1}H HMR signals before (*top*) and after (*bottom*) recrystalization. The regions 2.8 to 3.3 δ and 7.2 to 8.5 δ are shown. A second set of peaks can be seen in the aromatic region, and a second ε-lactam triplet at 3.2 δ can also be seen. These peaks are no longer present after recrystallization.

The primary synthetic target for this study indoloazepinone **[25]** had been synthesized in an overall yield of 48 % (fig 3.3.14). R = H and R = CH_3 (see fig 3.1.1) had now been successfully synthesized, and attention could now turn to the other areas of the molecule highlighted for investigation.

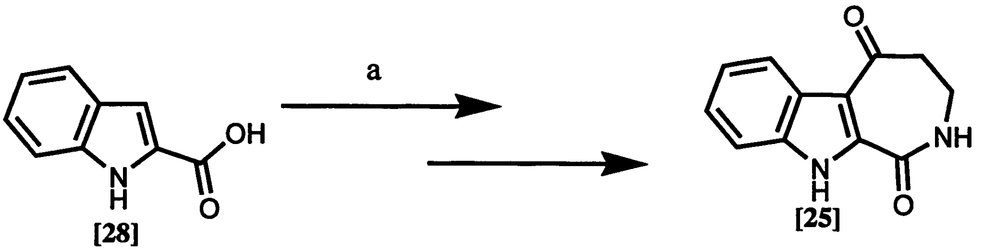

Fig 3.3.14: a: Overall synthesis of indoloazepinone **[25]** from indole-2-carboxylic acid **[28]**; 48 %

3.4 Alterations at the X-position

Interest in the X position (see fig 3.1.1) mainly revolved around the incorporation of bromine at the 7-position of indoloazepinone. As has been already seen (page 25-30), bromine plays an important role in the biological activity of both Kenpaullone and Hymenialdisine. The addition of bromine has also been shown to enhance the activity of other biologically active kinase inhibitors such as the Rebeccamycin analogue **[54]**.[115]

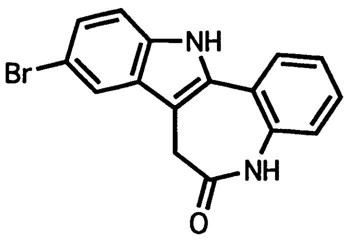

[14]

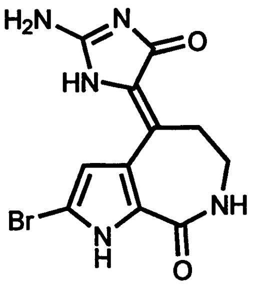

[17]

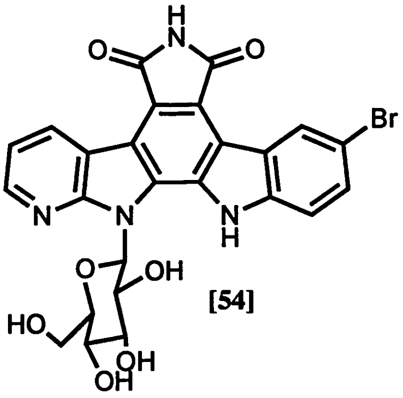

[54]

A bromine derivative could also be explored synthetically, displaced by various reagents to afford a series of derivatives to explore further beneficial interactions in the active site. This could be achieved using palladium[116] or copper[117] catalyzed coupling reactions.

It was felt that the best way to incorporate the bromine would be to use brominated indole (NH) carboxylic acid **[55]** in place of the standard indole (NH) carboxylic acid **[28]** in the reaction scheme.

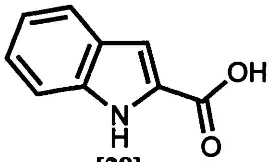

[28]

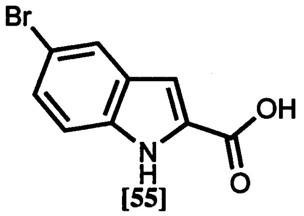

[55]

This compound was not available commercially, so it would need to be synthesized. A reported method of bromination using N-bromo succinimide (NBS) was attempted.[118] Indoles are preferentially brominated at the 3-position and it was found that bromination occurred exclusively at this position (fig 3.4.1). This bromination is still of interest, to synthesize an alternative precursor for the azepinone cyclization (see chapter 3.6 page 88).

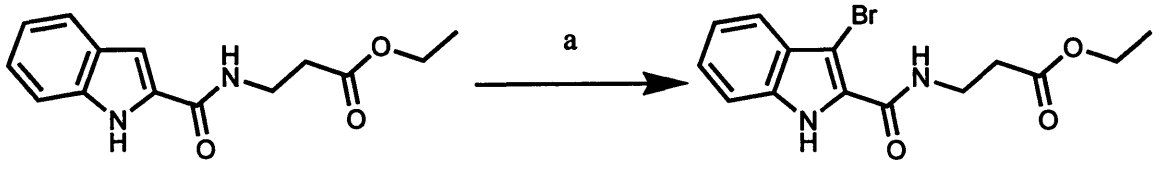

[52] [56]

Fig 3.4.1: bromination a: NBS, DMF, 51 %

However, this method also showed that a second highly regioselective bromination could be carried out if the 3-positon was blocked, i.e. after the cyclization step, and further literature supported this.[119] This bromination was successfully carried out (fig 3.4.2).

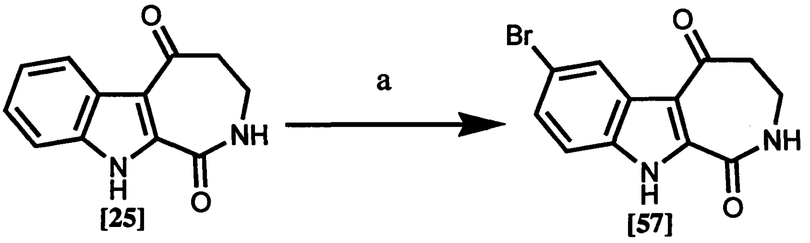

[25] [57]

Fig 3.4.2: a: NBS, DMF, 88 %

There were four possible bromination positions (fig 3.4.3), although the ^{1}H NMR had sharp peaks implying only one structure had been synthesized. The ^{1}H NMR showed a singlet and two overlapping doublets in the aromatic region. **[58]** and **[59]** would be expected to give two doublets and a double-doublet, whereas **[57]** and **[60]** would be expected to give a singlet and two doublets. This implies structures **[58]** and **[59]** were not formed.

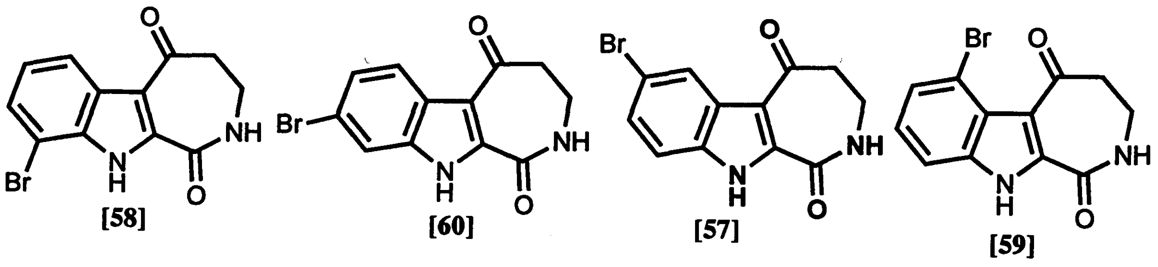

[58] [60] [57] [59]

Fig 3.4.3: The 4 possible bromination positions: 9-bromo **[58]**, 8-bromo **[60]**, 7-bromo **[57]** and 6-bromo **[59]**.

NOE interactions could be seen between the NH (H^{a}) and an aromatic doublet (H^{b}), but not between H^{a} and the singlet peak (H^{c}) (fig 3.4.4). Therefore the evidence points to the 7-bromo compound – structure **[57]**.

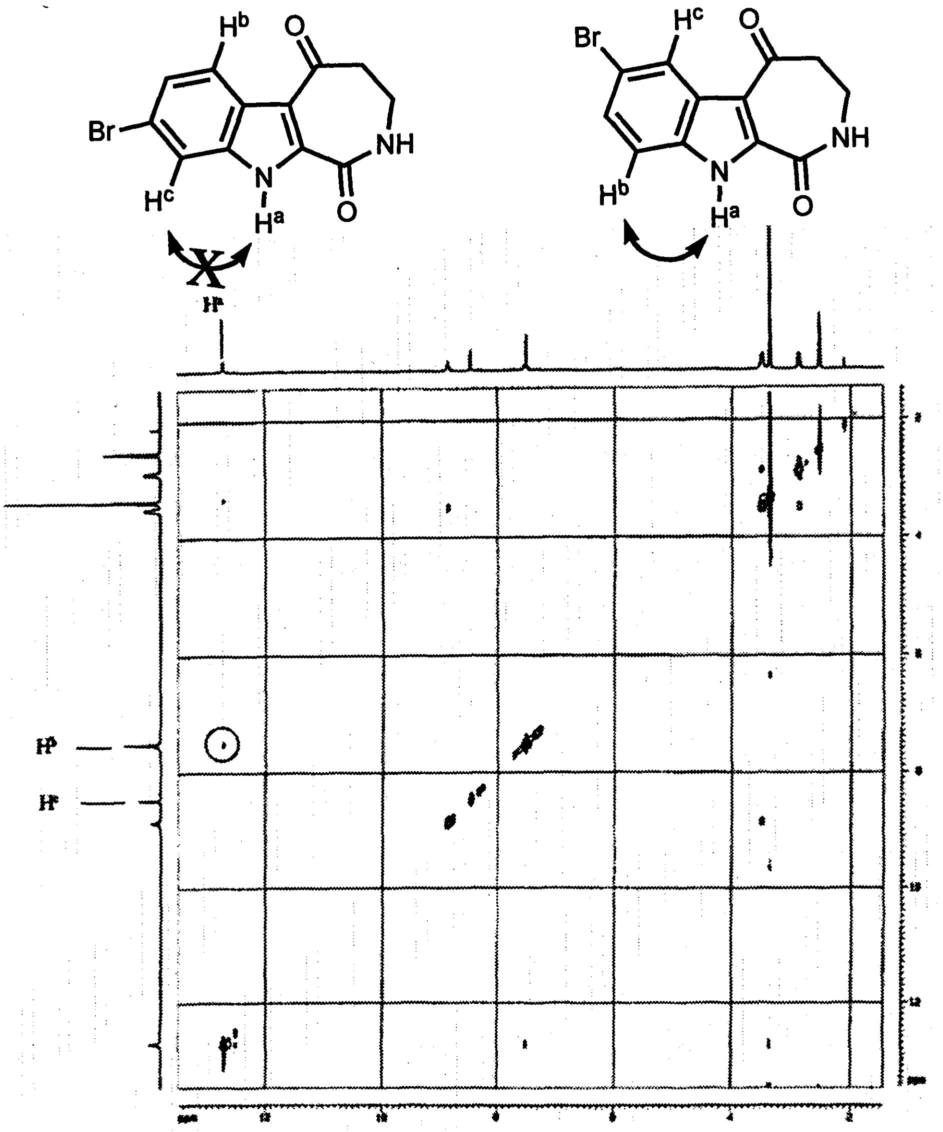

Fig 3.4.4: NOESY of [57] showing NOE interactions between H^a, the NH, and H^b, the multiplet, but not between H^a and H^c, the singlet.

Looking at the assumed mechanism of the reaction (fig 3.4.5), it is expected that the bromination by NBS [61] would occur in either in position 7 [57] or 9 [58].

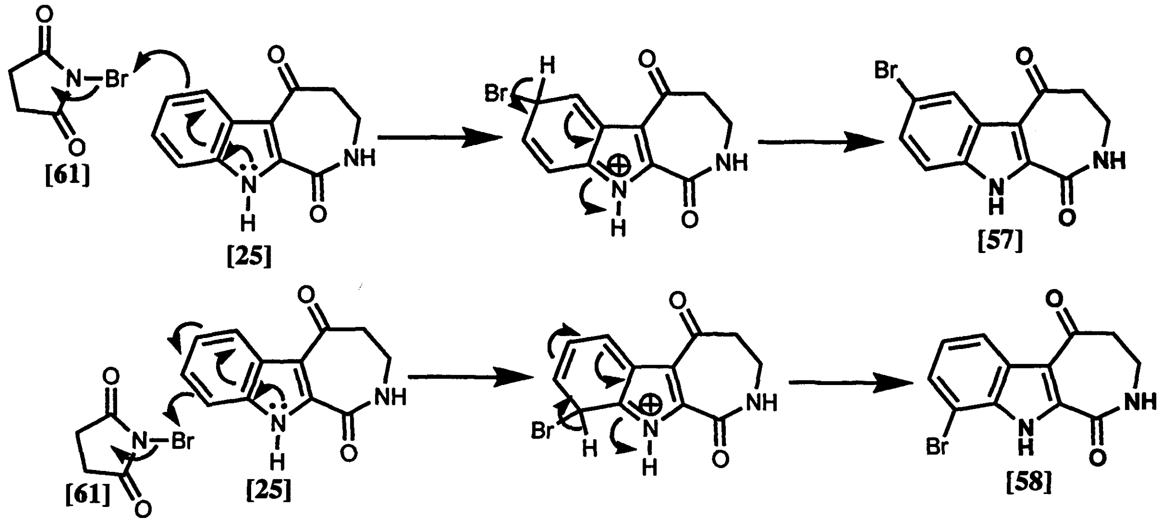

Fig 3.4.5: Proposed mechanism of bromination of [25] to give 7 [57] or 9 [58] brominated compound.

While X-ray crystallography is the most definitive way of confirming a structure, the NOESY backed up by the theoretical mechanism gave good evidence for the site of bromination. Further conformation would only be needed if the compound, or a derivative, proved to be an important inhibitor. If this were the case, the crystal structure of the compound in the active site would hopefully be generated, providing both evidence for its inhibition as well as the position of the bromine.

The equivalent reaction was attempted on the methyl analogue [31], but only the starting material was recovered. The reaction also did not work with the uncyclized methyl compound [35] (fig 3.4.6).

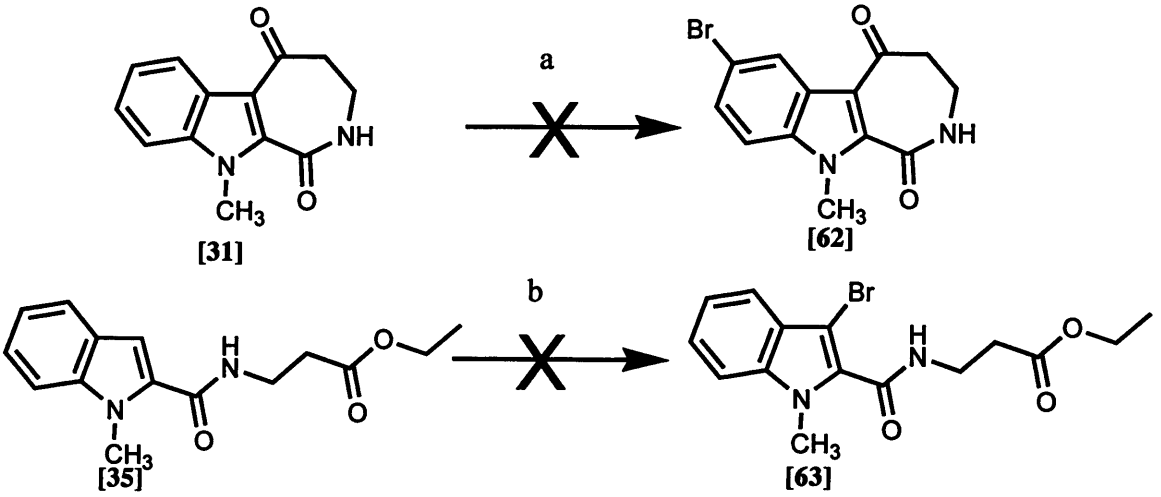

Fig 3.4.6: Non-bromination of N-methyl compounds. Both the cyclized, a: NBS, 0 %, and the uncyclized, b: NBS 0 %.

3.5 Alterations in the Y position

As seen previously (page 21), ATP forms two hydrogen bonds with the backbone residues of the active site, and the ability to form two or three hydrogen bonds was seen as a key feature when designing the molecules. Another key feature of the ATP molecule is the tri-phosphate group, which extends into a cleft in the active site making many favourable interactions.

Interest in the Y-position centred around extending the molecule from the ketone position in order to provide additional groups to interact with this cleft and improve the overall binding affinity of the compound in the active site. Recent work has demonstrated an important positive effect of bulky, lipophilic groups in this region,[120] so it was decided that hydrazones and oximes incorporating an aromatic or cyclohexyl ring would be used for these extensions. There was literature precedence for these extensions in other biologically active compounds,[121,122] so they would be expected to be biologically stable. It was important to consider the potential geometric implications of any extensions, and retaining the sp2 hybridisation of the ketone position removed the racemic complications introducing a chiral centre into the compound would bring. Molecular modelling studies had also shown that substituents with tetrahedral geometry would not fit in the active site.

3.5.1 Hydrazone Extension

At the outset of the study, to investigate whether the extended compounds could be accommodated in the active site of CDK2, indoloazepinone **[25]** and its hydrazone **[64]**, along with N-methylindoloazepinone hydrazone **[65]** were superimposed over Hymenialdisine in the crystal structure of CDK2 (PDB ID: 1DM2) using the SYBYL program. These initial dockings implied all three structures would be accommodated by the active site, with the hydrazone extension potentially capable of interaction with the cleft of the active site, potentially making it a more potent inhibitor.

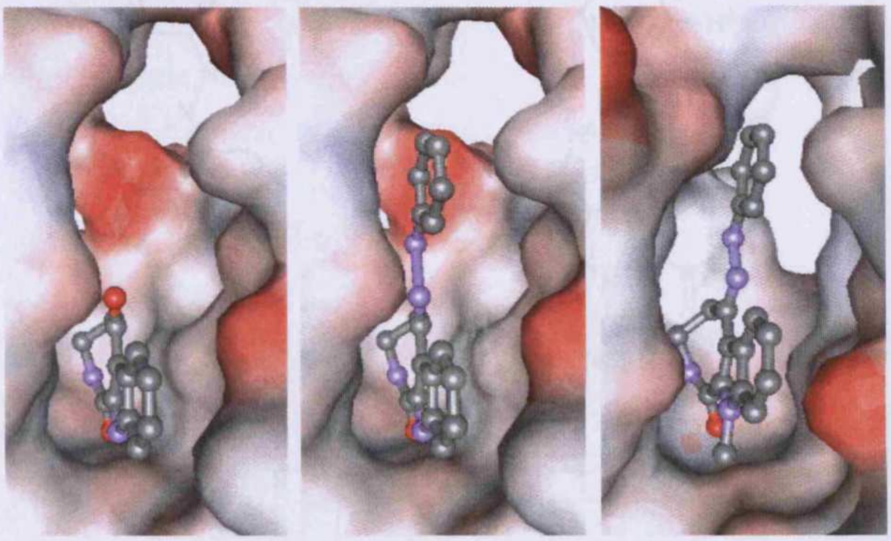

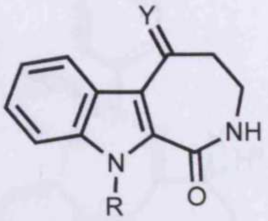

R=H, Y=H **[25]**
R=H, Y=NNHPh **[64]**
R=CH_3, Y=NNHPh **[65]**

Fig 3.5.1: Superimpositions of **[25]** (*left*), and **[64]** (*centre*), and **[65]** (*right*) superimposed in the active site of CDK2 using SYBYL.

Extension was attempted with phenyl hydrazine.HCl (fig 3.5.2). An analogous reaction using an Aldisin based starting material had been found[123,124] and the reaction proceeded straightforwardly with a 62 % yield after being purified by column chromatography.

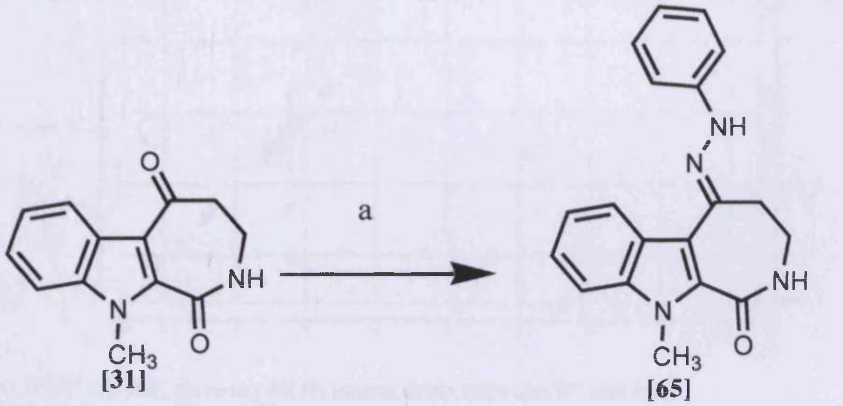

Fig 3.5.2: a: Phenylhydrazine hydrochloride, NaOAc, 50 °C, 62 %

This product had two possible E and Z isomers (fig 3.5.3). The two orientations would potentially interact very differently with the active site, which will be discussed later in this chapter (section 3.7). It was therefore important to ascertain which isomer had been formed, or if there was a mixture of the two. The ^{1}H, and ^{13}C NMR peaks were sharp and there was no doubling up of peaks, which indicated that only one of the two possible isomers had been formed, and NOESY spectrum shows NOE interactions between H^a and H^b, but not between H^a and H^c (fig 3.5.3) This would imply that only the E isomer was synthesized.

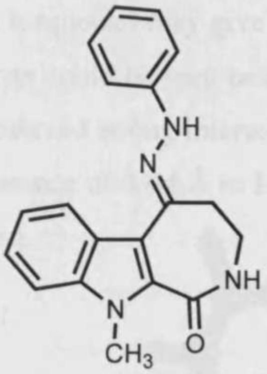

[65]

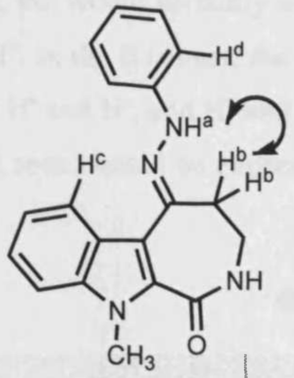

[65]-E

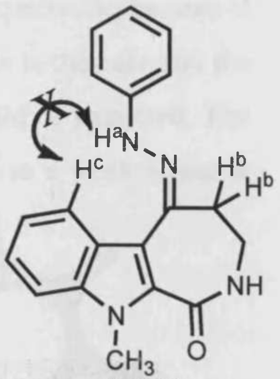

[66]-Z

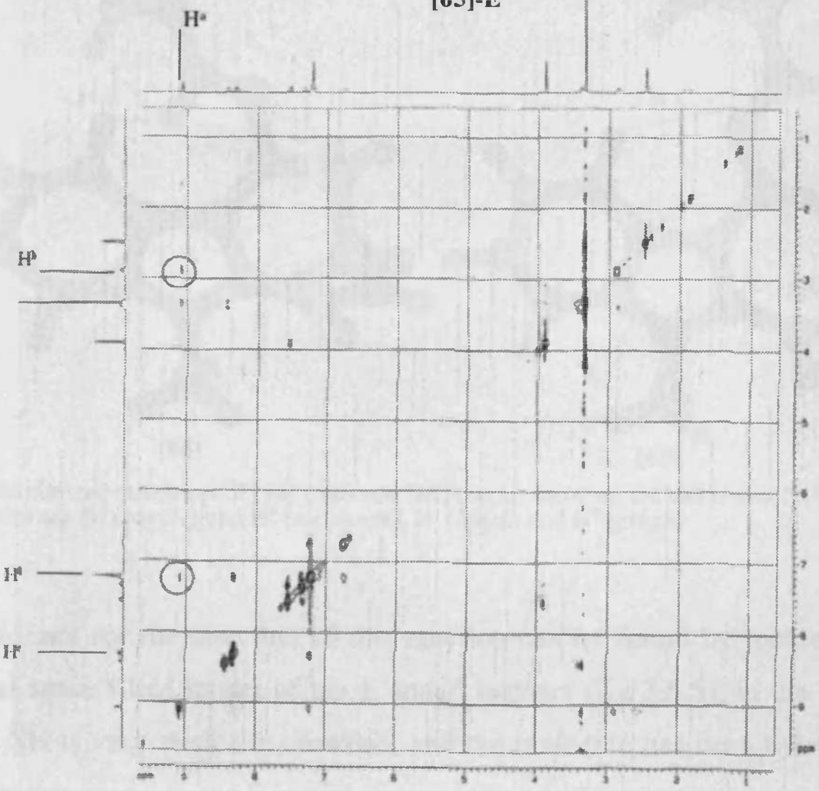

Fig 3.5.3: NOESY of **[65]**, showing NOE interactions between H^a and both H^b and H^d, but not between H^a and H^c.

By using loose approximate interproton distances restraints, strong NOE signals can be expected for protons 1.8-2.7 Å apart, medium signals for a distance of 1.8-3.3 Å, and a weak signal up to 5 Å may be seen.[125]

Looking at the models of the E **[65]** and Z **[66]** isomers minimized using Chemdraw3D, shows the distances of the potential NOE interactions (fig 3.5.4). It can clearly be seen that the Z isomer will show strong interactions between H^a (shown in purple) and H^b (shown in black), and H^a and H^d (shown in green). The distance of 4.31 Å to H^c (shown in turquoise) may give a weak signal, but would certainly not be expected to be seen if none could be seen between H^a and H^b. In the E isomer, the opposite is the case and the observed strong interactions between H^a and H^c, and H^a and H^d would be expected. The distance of 4.44 Å to H^c which is not seen, would be expected to give a weak signal at best.

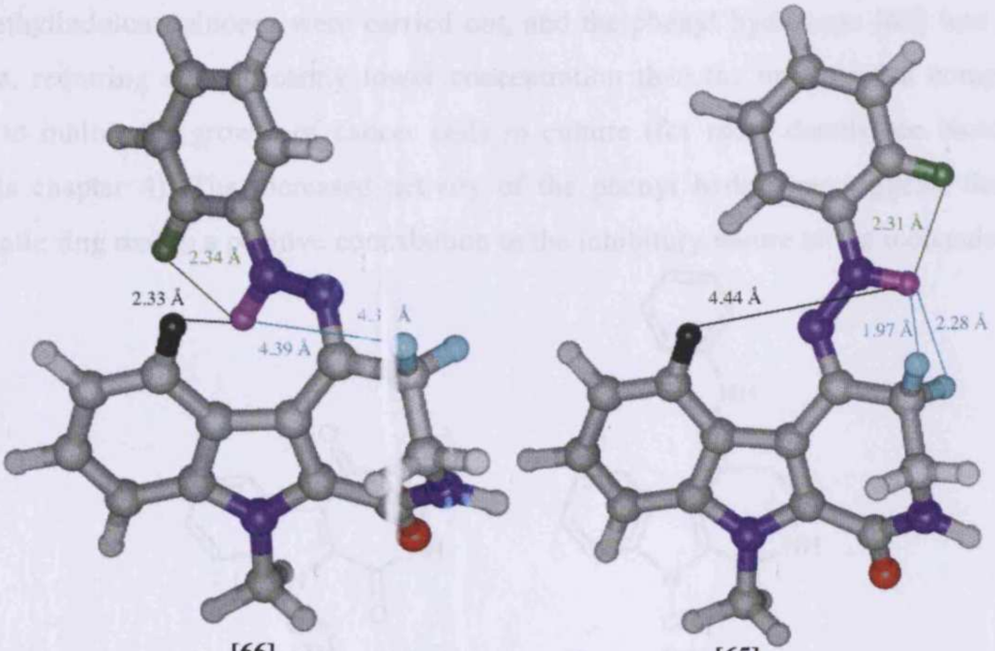

[66] **[65]**

Fig 3.5.4: Minimized structures of **[66]** (*left*) and **[65]** (*right*) showing the calculated NOE distances between H^a (*purple*) and H^b (*turquoise*), H^c (*black*) and H^d (*green*).

Further evidence for the direction of this reaction can be found by looking at a three-dimensional space filled model of the E and Z isomers (fig 3.5.5); in the Z model, the hydrazone NH is very sterically crowded, and the molecule has been twisted to satisfy both aromatic systems. In the E model, these steric problems are not seen, which would imply that it is the more likely conformation.

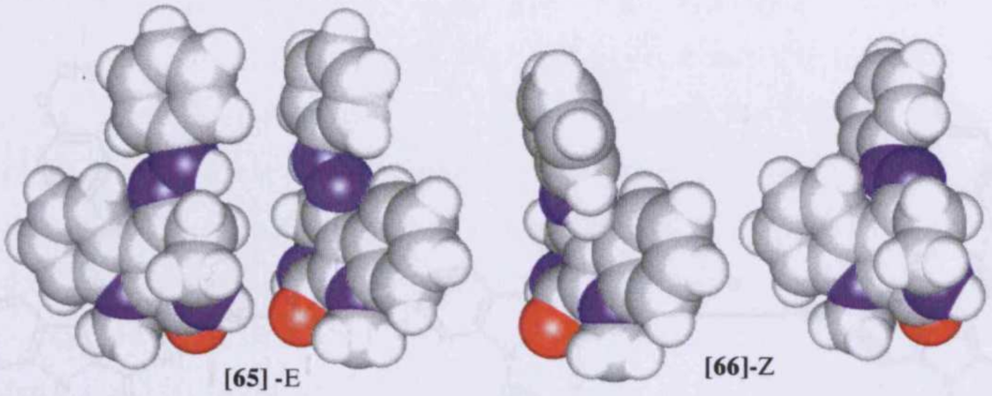

Fig3.5.5: Space filled representations of the E (*left*) and Z (*right*) isomers of **[65]**, showing steric problems for the Z orientation, but not for the E orientation.

Growth inhibition assays of the unextended **[31]** and phenyl hydrazone extended **[65]** N-methylindoloazepinones were carried out, and the phenyl hydrazone **[65]** was more active, requiring a significantly lower concentration than the un-extended compound **[31]** to inhibit the growth of cancer cells in culture (for more details see biological results chapter 4). The increased activity of the phenyl hydrazone suggests that the aromatic ring makes a positive contribution to the inhibitory nature of the molecule.

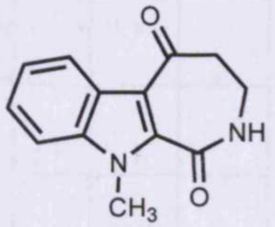
[31]

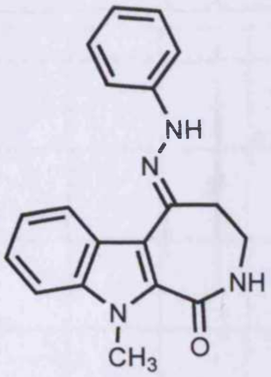
[65]

It was decided to investigate how the electron density of the ring affected its biological properties. It was decided that analogues with an electron rich hydrazone ring **[67]**, and an electron deficient hydrazone ring **[68]** would be prepared to investigate how this would affect the activity of the inhibitor.

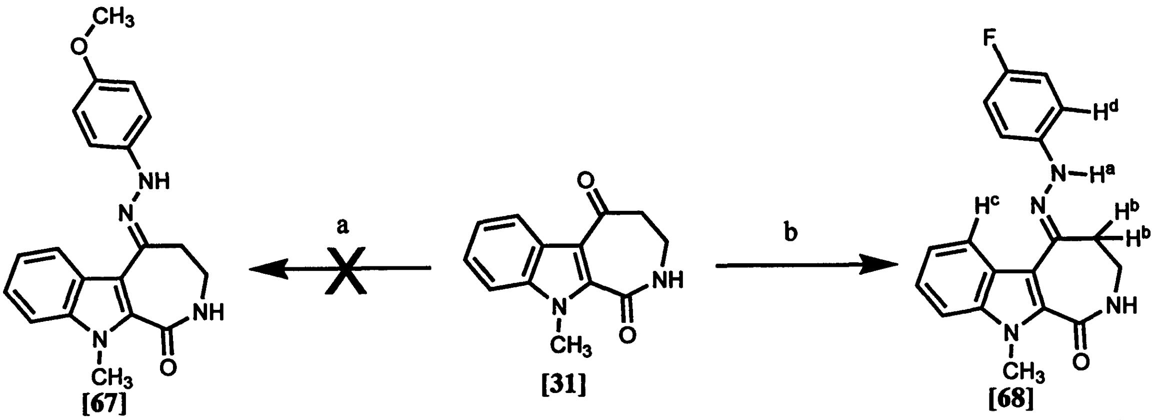

Fig 3.5.6: a: 4-Methoxy phenylhydrazine hydrochloride, NaOAc, 50 °C, 0 %
b: 4-Fluoro phenylhydrazine hydrochloride, NaOAc, 50 °C, 22 %

These were prepared from the N-methylindoloazepinone and para-substituted phenyl hydrazine (fig 3.5.6). The 4-fluoro phenylhydrazone **[68]** was readily prepared and analysed. Again, the NOESY spectrum (fig 3.5.6) suggests that only the E isomer (as shown) is formed.

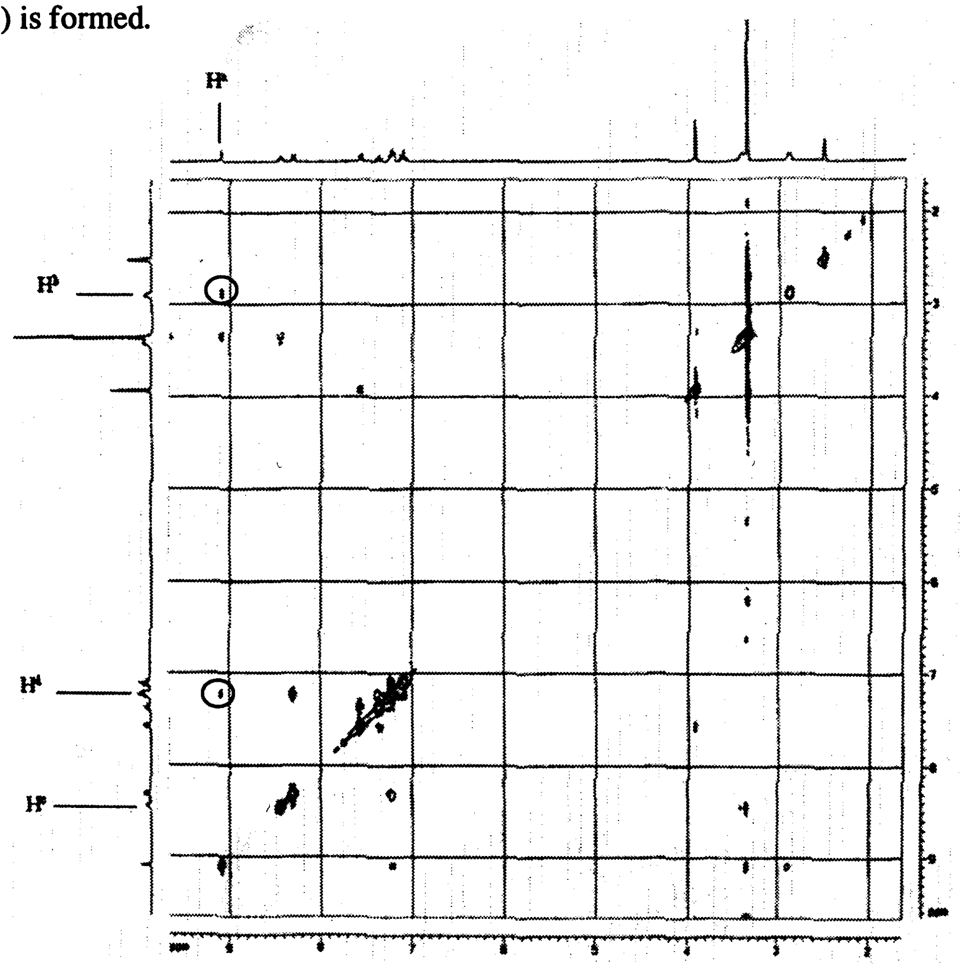

Fig 3.5.7: NOESY of **[68]**, showing NOE interactions between H^a and both H^b and H^d, but not between H^a and H^c.

The R_f of the N-methylindoloazepinone [31] and the hydrazones were too similar to allow the reaction to be monitored by TLC, and the crude methoxy-hydrazone [67] was not pure enough to be characterized by ^1H NMR, although the characteristic hydrazone NH peak at approximately δ 9.10 (shown as H^a with both [65] and [68]) did appear to be present. However, after purification by column chromatography, ^1H NMR indicated that only the starting material [31] was left. It was thought that the acidic environment of the silica column might have catalysed the breakdown of the hydrazone to the original hydrazine, and the ketone of the starting material [31], so the reaction was repeated and purified on a neutral column,[126] but again only the starting materials were isolated. The crude ^1H NMR would appear to have been misleading, and the methoxy-hydrazone [67] was not synthesized.

Attempts were made to synthesize the 4-carboxylic acid-hydrazone, [71]. The same conditions were again used, but no reaction occurred. The carboxylic acid functional group was protected as a methyl ester, and the carboxylic acid ester-hydrazone [72] was synthesized (fig 3.5.8). Ester hydrolysis was attempted with both methods previously used, but the carboxylic acid was not isolated.

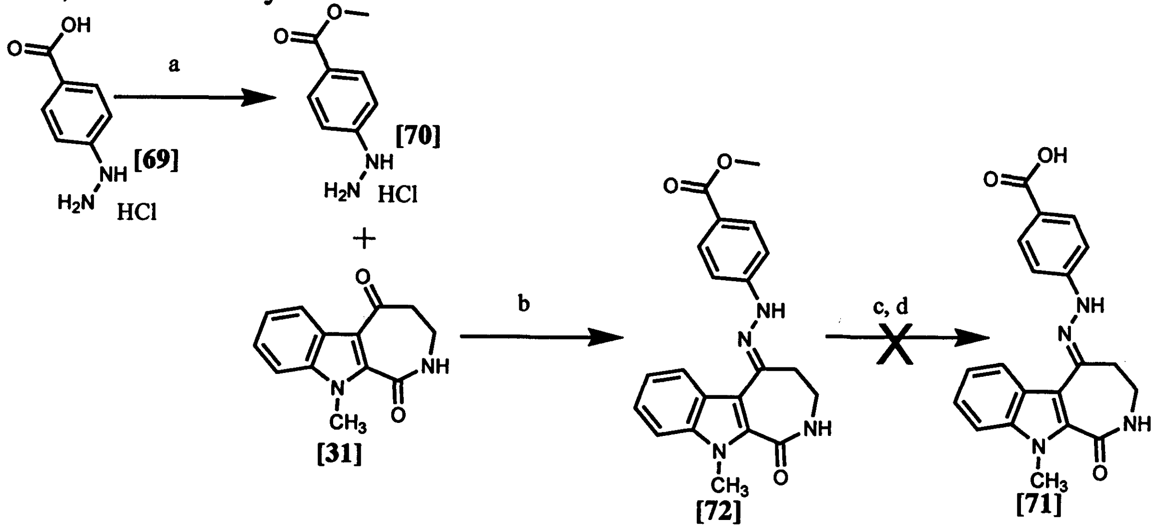

Fig 3.5.8: a: $SOCl_2$, MeOH, Δ, 96%, b: sodium acetate, Δ, 43 %
c: $LiOH..H_2O$, THF 0 %, d: MeOH, 4M NaOH, Δ, 0 %

3.5.2 Oxime Extension

In addition to the hydrazone extension, oximes were investigated as alternative extensions from the ketone position.

The unsubstituted oxime [73] was synthesized utilizing the same method (fig 3.5.9). It was found that heating the reaction to a higher temperature gave the product pure and in higher yields.

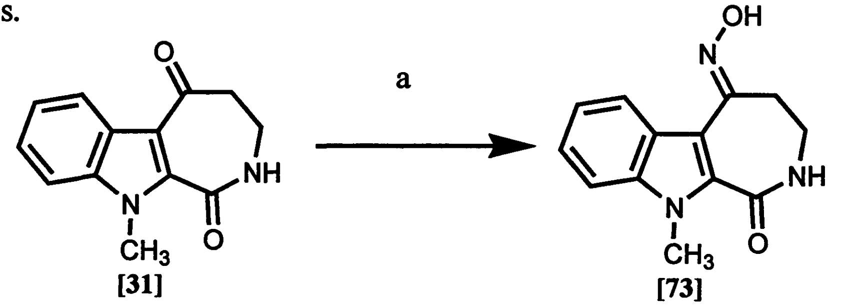

Fig 3.5.9: a: $HONH_2.HCl$, NaOAc, 80 °C, 21 h, 82 %

The ^1H NMR only had one set of sharp peaks, which indicated only one isomer had been formed. The NOESY (fig 3.5.9), however, was inconclusive as a strong NOE interaction can be seen between H^a and H^b, and a weaker NOE interaction between H^a and H^c. this implied that the product might be a mixture of the E [73] and Z [74] isomers.

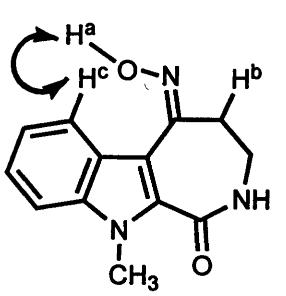

[74]

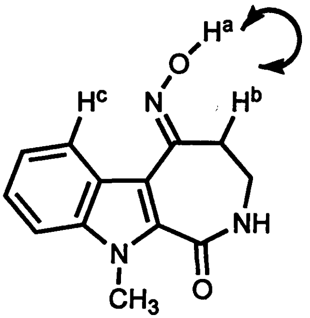

[73]

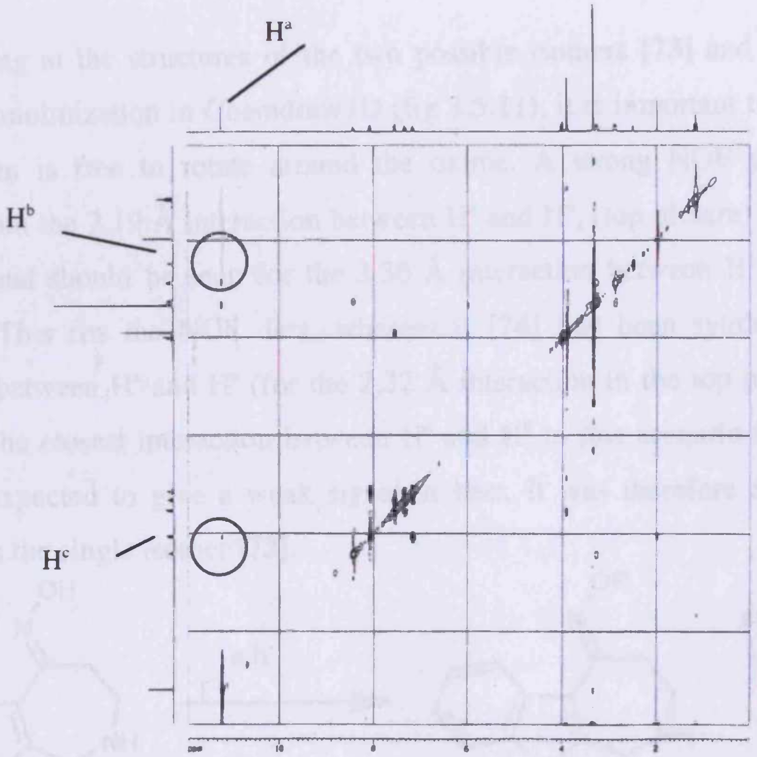

Fig 3.5.10: NOESY spectrum showing interactions between H^a and H^b, as well as between H^a and H^c.

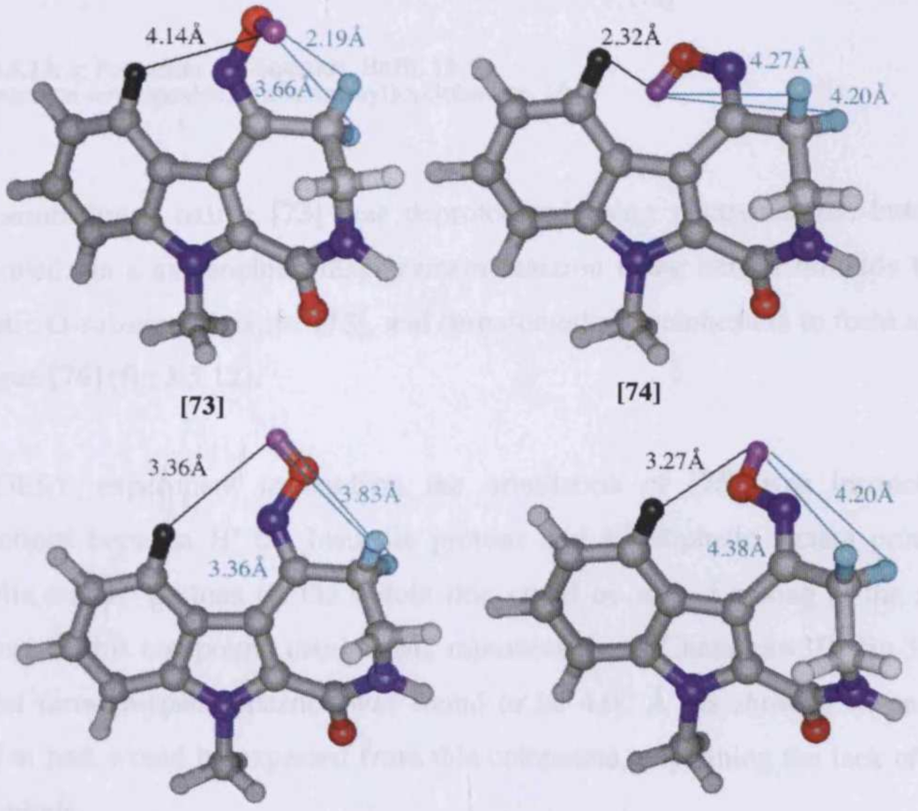
4.14Å
2.19Å
3.66Å
2.32Å
4.27Å
4.20Å
[73]
[74]
3.36Å
3.83Å
3.36Å
3.27Å
4.20Å
4.38Å

Fig 3.5.11: Pictures showing the NOE distances of **[73]** (*left*) and **[74]** (*right*) between H^a (*purple*) and H^b (*turquoise*), and between H^a and H^c (*black*). Two minimized structures with H^a at the extremes of its rotation are shown.

When looking at the structures of the two possible isomers [73] and [74] minimized with MM2 minimization in Chemdraw3D (fig 3.5.11), it is important to remember that the hydrogen is free to rotate around the oxime. A strong NOE signal would be expected from the 2.19 Å interaction between H^a and H^b, (top picture) while a medium strength signal should be seen for the 3.36 Å interaction between H^a and H^c (bottom picture).[125] This fits the NOE data, whereas if [74] had been synthesized, a strong interaction between H^a and H^c (for the 2.32 Å interaction in the top picture) would be expected. The closest interaction between H^a and H^b in this scenario is 4.20 Å, which would be expected to give a weak signal at best. It was therefore assumed that the product was the single isomer [73].

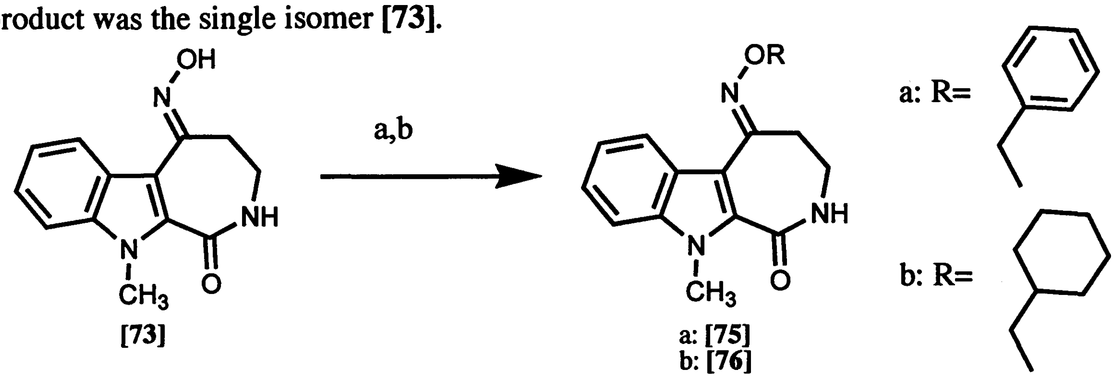

Fig 3.5.12: a: Potassium *tert*-butoxide, BnBr, 15 %
b: Potassium *tert*-butoxide, (bromomethyl)cyclohexane, 16 %

The unsubstituted oxime [73] was deprotonated using potassium *tert*-butoxide, and substituted via a nucleophilic displacement reaction using benzyl bromide to form an aromatic O-substituted oxime [75], and (bromomethyl)cyclohexane to form an aliphatic analogue [76] (fig 3.5.12).

A NOESY experiment to confirm the orientation of [75] was inconclusive; no interactions between H^a the benzylic protons and H^b aliphatic lactam protons or H^a benzylic and H^c protons on the indole ring could be seen. Looking at the minimized structure of this compound using MM2 minimisation in Chemdraw3D (fig 3.5.13), the shortest through-space distance was found to be 4.00 Å (as shown), so only a weak signal at best would be expected from this compound, explaining the lack of any NOE interactions.

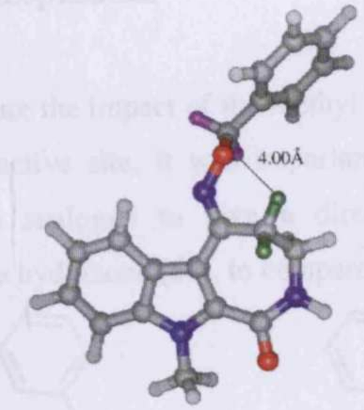

Fig 3.5.13: Minimized structure of **[75]**. The shortest NOE distance between H^a (*purple*) and H^b (*green*) is shown.

When the aromatic oxime **[75]** was synthesized, the sample was left in the NMR tube awaiting further analysis in a DMSO solution at room temperature for approximately two weeks. When these later NMR experiments were performed on this sample, there were clear signs of breakdown back to the simple oxime (fig 3.5.14). As the compound was not stable in the d6-DMSO at room temperature, it was important to ascertain if it would be stable in the growth medium used for the biological analysis at 37 °C, as if it broke down under these conditions also, then it would give false results in the assay.

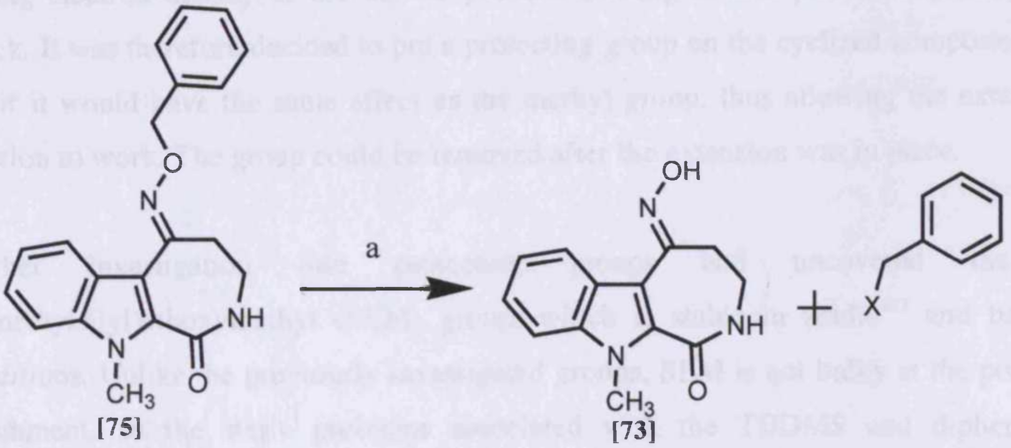

Fig 3.5.14: The breakdown of **[75]** to **[73]** and a benzyl derivative.
a: d6-DMSO, 50 %

A 100 mmol and a 10 mmol solution of the compound in the growth medium were placed in sealed containers at 37 °C in a water bath for 7 days. The experiment was monitored after 2, 4, 6, 8, 24 and 48 hours by TLC and again after the 7 days. The TLC analysis showed evidence only for **[75]**, but ^1H NMR showed almost 50 % breakdown. Due to this result, the stability of **[76]** was also tested in the same manner, with no sign of breakdown. The aromatic benzyl group formed by cleavage of the O-C bond would be a more stable leaving group than the aliphatic counterpart.

3.5.3 Extended Indoloazepinones

In order to accurately measure the impact of the methyl substituent on the ability of the compound to bind in the active site, it was important to synthesize a Y extended, unsubstituted indole (NH) analogue to give a direct comparison to the methyl compounds. Synthesis of the hydrazone **[64]**, to compare with **[65]** was attempted first.

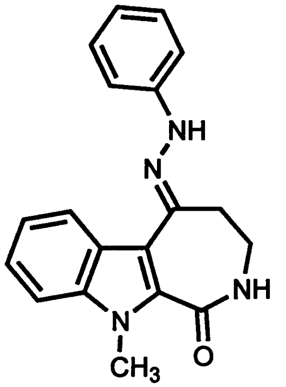

[65]

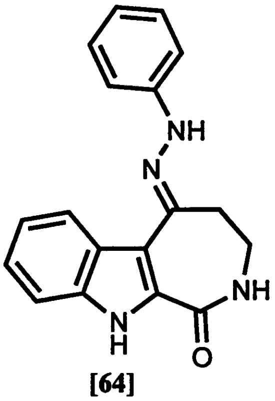

[64]

However no reaction occurred with the indole (NH) analogue, and **[64]** was not isolated using this method. It was thought that the lone pair of electrons on the indole (NH) was adding electron density at the ketone position making is less prone to nucleophilic attack. It was therefore decided to put a protecting group on the cyclized compound and see if it would have the same effect as the methyl group, thus allowing the extension reaction to work. The group could be removed after the extension was in place.

Further investigation into protecting groups had uncovered the 2-(trimethylsilyl)ethoxymethyl (SEM) group, which is stable in acidic[127] and basic[128] conditions. Unlike the previously investigated groups, SEM is not bulky at the point of attachment, so the steric problems associated with the TBDMS and diphenyl-4-pyridylmethyl groups would not be a problem. The group was attached to **[25]** using the same method used for the methyl and benzyl groups. The SEM group was found to react equally well with both the indole and amide NH groups, resulting in mixtures when less than two equivalents of the reagent were used. Therefore two equivalents were used to fully protect both positions and **[77]** was isolated as a dark oil (fig 3.5.15).

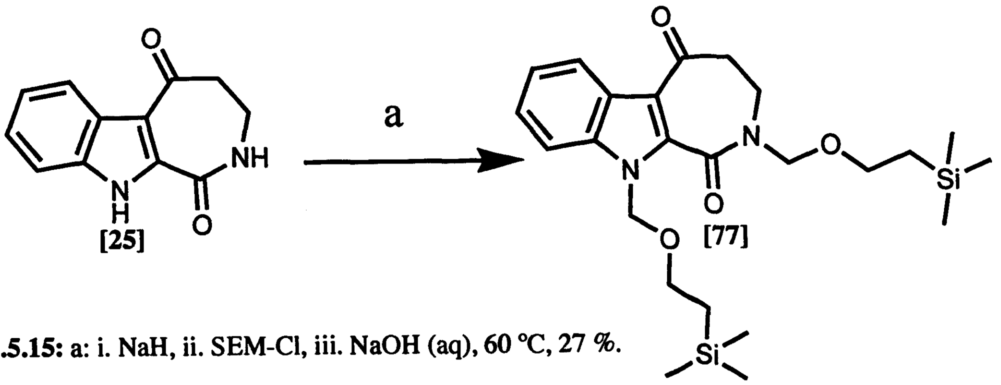

Fig 3.5.15: a: i. NaH, ii. SEM-Cl, iii. NaOH (aq), 60 °C, 27 %.

The hydrazone extension was attempted on this molecule, but purification was a major problem. The SEM protected compound [77] and the product, if it was made, had the same R_f as the phenyl-hydrazine, and, due to its oily nature, there was no precipitate formed during the workup. If the extended product could be deprotected, then it would be much easier to isolate from this mixture.

Standard SEM-deprotection of pyrrole and indole derivatives is with concentrated anhydrous tetrabutylammonium fluoride (TBAF).[129,130] This was carried out on the mixture, but there was no evidence for the formation of the deprotected product, even after heating at reflux for 20 hours. Hydrochloric acid had also been reported to remove SEM from imidazole derivatives[131] and indoles,[132] but when attempted nothing could be isolated from the mixture (fig 3.5.16).

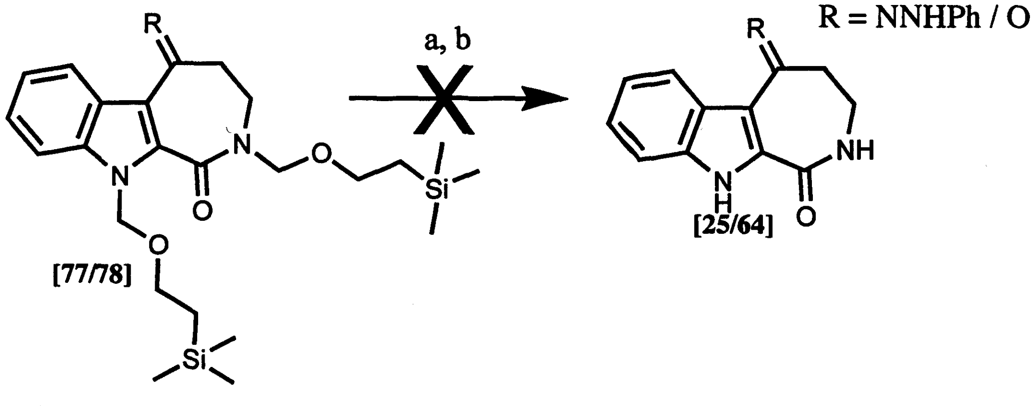

Fig 3.5.16: a:TBAF, Δ, 0 % b: 4M HCl, EtOH, Δ, 0 %

It was difficult to ascertain if either the extension or the deprotection reactions had worked or not as the mixture was very impure and phenyl hydrazine was the main component. Therefore the deprotection chemistry was carried out on the pure un-extended compound to establish a reliable method for the SEM removal, and this would be attempted on the crude product from the extension reaction. Again, there was no evidence of SEM removal with either the TBAF or acidic conditions so further methods were investigated.

Two further methods for SEM removal were found (fig 3.5.17); the first used boron trifluoride dietherate,[128] and the second lithium tetrafluoroborate, followed by 2M sodium hydroxide.[133] Unfortunately, both reactions again left pure starting material.

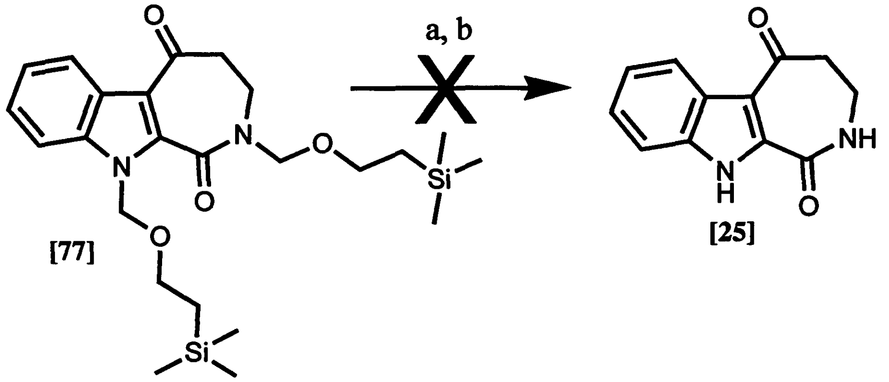

Fig 3.5.17: a: $BF_3(Et_2O)_2$, 0 %. b: $LiBF_4$, 2M NaOH (aq), 0 %

As it did not appear possible to remove the SEM group, the previously used protecting groups were reviewed.

The tosyl group had proved to be labile in earlier reactions (page 52), so this could be the ideal group for this reaction. The reaction was repeated with two equivalents of tosyl-chloride and sodium hydride, with the aim of tosylating the indole and amide NH, as achieved with SEM (fig 3.5.15) to remove the possibility of mixtures of the three possible tosyl derivatives. However, only **[25]** was isolated (fig 3.5.18).

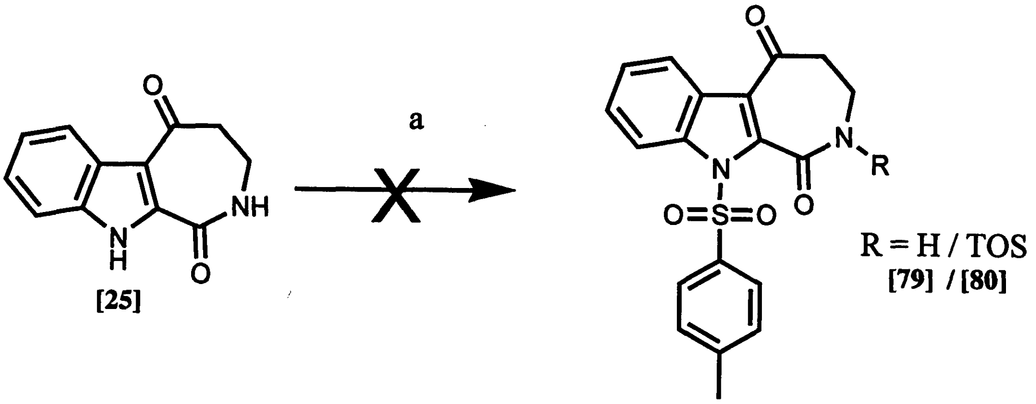

Fig 3.5.18: a: Potassium *tert*-butoxide, 18-crown-6, tosyl chloride 0 %

The benzyl derivative had been synthesized with relative simplicity, so would be ideal if it could be removed. The standard benzyl removal conditions are hydrogenation,[107] so this was carried out on N-benzyl protected carboxylic acid [41]. However, even with high pressure (45 psi), using Pd/C or PdOH/C catalysts had no impact on this group (fig 3.5.19).

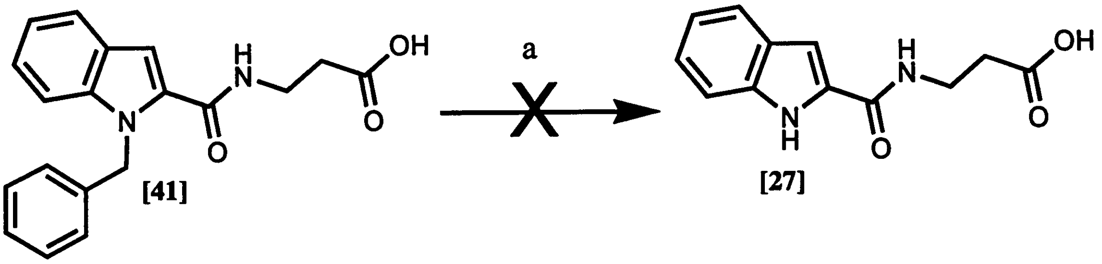

Fig 3.5.19: a: Pd/C, 45 PSI 0 %. b: PdOH/C, 45 PSI, 0 %.

4-methoxybenzyl is more labile than the unsubstituted benzyl group, as it forms a better leaving group. It was decided to attach this protecting group to [32] as a model compound, in order to study the removal of the protecting group before applying it to the cyclized compound [77].

The protection procedure was not as effective as the previous benzylation, and [81] was not isolated pure. The ^1H NMR of the mixture did give strong evidence of the benzylated compound however, as there were two separate peaks for the benzyl CH_2.

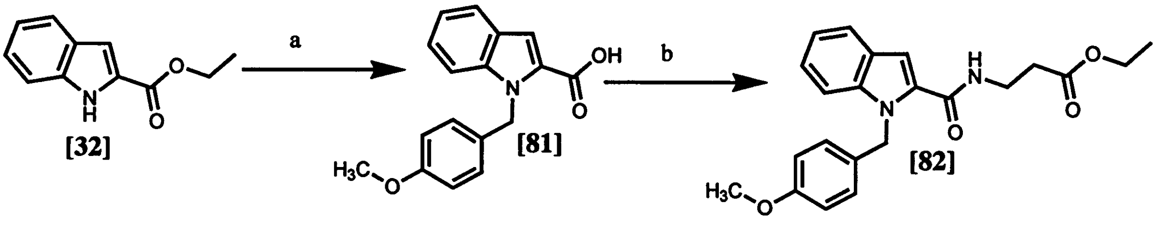

Fig 3.5.20: a: i. NaH, THF ii. 4-methoxy benzyl chloride, KI, THF. b: EDCI, DMAP, β-alanine ethyl ester hydrochloride, DCM, 2 %.

The EDCI method was used to synthesize the amide derivative of 4-methoxybenzyl-protected indole, as this compound should be a lot easier to purify. Although a low overall yield of 2 % of [82] was obtained, (fig 3.5.20), sufficient material was isolated pure from the column allowing the deprotection to be attempted on this sample. As with the benzyl group though, there was no evidence of any deprotection (fig 3.5.21).

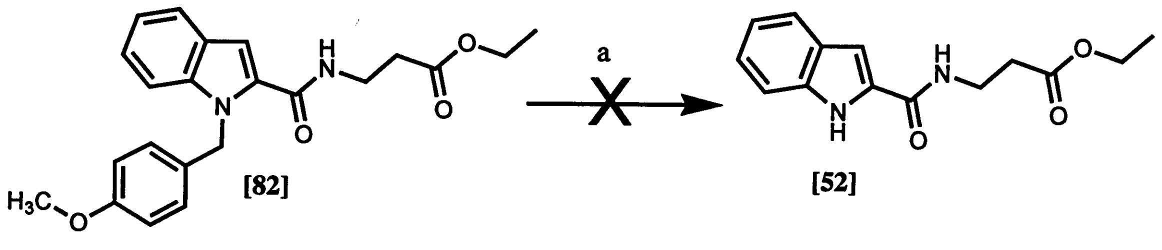

Fig 3.5.21: a: PdOH/C, 45 PSI, 0 %

Further scrutiny showed that this problem was not uncommon, and N-benzyl removal by hydrogenation was "usually unsuccessful".[134] There are many reported cases of O-debenzylation by hydrogenation (e.g.[135,136]), but very few incidence of N-debenzylation using this method, and none were found with an equivalent indole molecule. Two further methods of N-debenzylation were uncovered: $AlCl_3$ in benzene has been successfully employed for this purpose,[137] and lithium diisopropylamide (LDA) in THF has also recently been used.[134] These methods was not attempted due to time restraint at the end of the project, although the effect of $AlCl_3$ on the molecule (fig 3.3.5) would suggest that this method would be unlikely to work in this case.

A number of protecting groups had proved unsuccessful, so further analysis of these compounds was carried out. The compounds were minimized using MM2 minimization on Chemdraw3D, and Molecular Operating Environment (MOE). The MM2 atom type parameters and MM2 constants were unchanged for the MM2 minimization, while forcefield charges were used for MOE minimization.

The successfully protected compounds were used as a reference. The features of interest were the bond length from the indole nitrogen, and the angle of this bond. The angle of the carbonyl group was also recorded. Molecular Orbital theory predicts that both bonds should be in plane with the indole, (i.e. 180°) for uncyclized compounds. The carbonyl group in cyclized compounds is out of the plane in order to accommodate the ε-lactam ring.

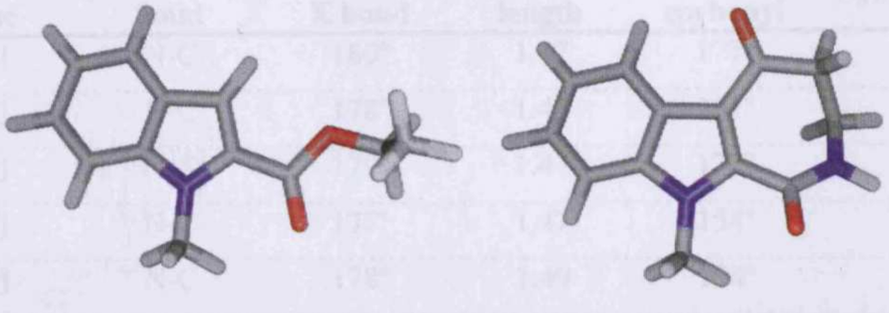

Fig 3.5.22: Structures of **[33]** and **[31]** minimized using MOE. The N-methyl bond is at 180° in respect to the plane of the indole. The carbonyl function of **[33]** is almost at 180°, while in **[31]** the ε-lactam ring forces it to adopt an angled orientation.

Minimization of the indole (N-methyl) carboxylic acid ester **[33]** confirmed the theory (fig 3.5.22), with both bond angles recorded within 3° of 180° with both methods of minimization.

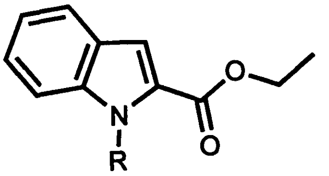

[33] R=CH$_3$
[83] R=Bn
[51] R= diphenyl-4-pyridylmethyl
[45] R=TBDMS
[44] R=tosyl

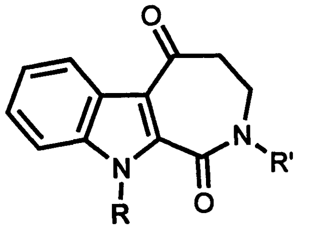

[31] R=R'=H
[77] R=R'=SEM
[79] R=R'=tosyl
[80] R=tosyl, R'=H

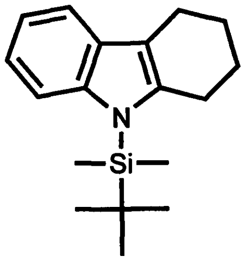

[84]

Compound number	Indole N-X bond	Angle of N-X bond	Bond length	Angle of carbonyl	Synthesized
[33]	N-C	180°	1.45	178°	Yes
[31]	N-C	180°	1.45	144°	Yes
[83]	N-C	180°	1.45	177°	Yes
[77]	N-C	180°	1.45	122°	Yes
[51]	N-C	180°	1.51	119°	NO
[45]	N-S	169°	1.73	151°	NO
[84]	N-S	180°	1.72	No carbonyl	Reported
[44]	N-Si	171°	1.73	139°	Yes
[79]	N-Si	170°	1.74	148°	NO
[80]	N-Si	170°	1.74	148°	NO

Table3.6.1: Data for compounds minimized using MOE.

Compound name	Indole N-X bond	Angle of N-X bond	Bond length	Angle of carbonyl	Synthesized
[33]	N-C	180°	1.47	177°	Yes
[31]	N-C	178°	1.47	151°	Yes
[83]	N-C	179°	1.47	178°	Yes
[77]	N-C	177°	1.47	154°	Yes
[51]	N-C	178°	1.49	154°	NO
[45]	N-S	114°	1.82	174°	NO
[84]	N-S	173°	1.80	No carbonyl	Reported
[44]	N-Si	179°	1.69	178°	Yes
[79]	N-Si	126°	1.71	140°	NO
[80]	N-Si	118°	1.71	126°	NO

Table3.6.2: Data for compounds minimized using Chemdraw 3D.

Four compounds were synthesized incorporating a C in the α-position of the protecting group, while one was attempted which was not synthesized. Comparison of these N-C bonds showed that all the compounds synthesized had identical N-C bonds. Both minimization techniques predicted a longer bond for **[51]** (by 0.06 Å for MOE and by 0.02 Å according to Chemdraw 3D), with the carbonyl group significantly out of the plane (61° according to MOE, 26° for Chemdraw 3D). The analogous compounds, **[33]** and **[83]** both minimized with this group within 3° of the predicted 180°.

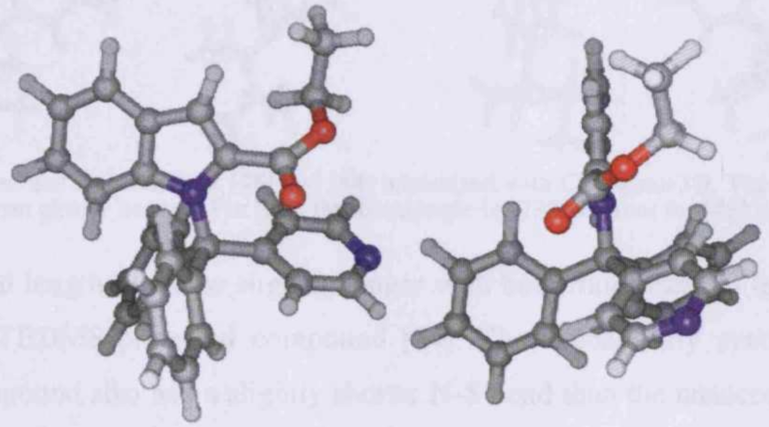

Fig 3.5.23: Two views of the MOE minimized structure of **[51]**, showing the angle that the carbonyl group is now at.

Both minimization techniques imply undesirable alteration to the molecule in order to accomodate the steric bulk of the protecting group (fig 3.5.23). This could account for the protected compound not being successfully synthesized.

While the TBDMS group had been reported in indoles, closer analysis of the literature showed that all the indoles in the reference had an α-CH_2 group, whereas the indole carboxylic acid ester **[32]** has a carbonyl group in the α position.

For all the reported compounds, the N-Si bond was within a few degrees of 180° as would be expected (an example from the literature being **[84]**). However, the minimization of carboxylic acid ester **[45]** had this bond at an angle of 66° out of the plane when minimized with Chemdraw 3D (fig 3.5.24). MOE clearly took an alternative approach to minimizing this compound, with this angle only distorted by 11°. However, to accommodate this, the carbonyl function was forced out of position by 29°.

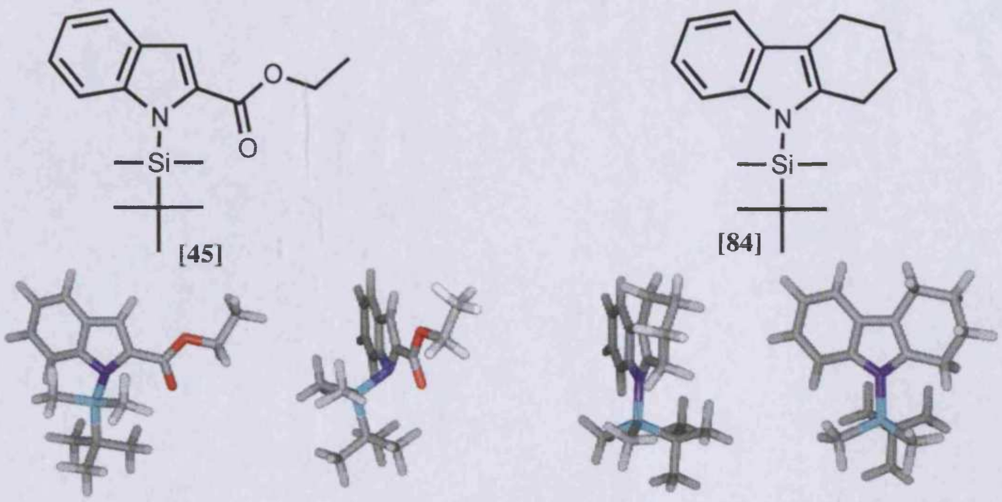

[45]

[84]

Fig 3.5.24: front and side views of **[45]** and **[84]** minimized with Chemdraw3D. The angle of the N-Si bond can clearly be seen. For **[84]**, this bond angle is 173°, whereas for **[45]** it is 114°.

The N-Si bond length was also slightly longer with both minimization techniques than the reported TBDMS-protected compound **[84]**. The successfully synthesized tosyl-protected compound also had a slightly shorter N-S bond than the unsuccessful cyclized analogues. However, the discrepancies in bond length were not conclusive for either compound.

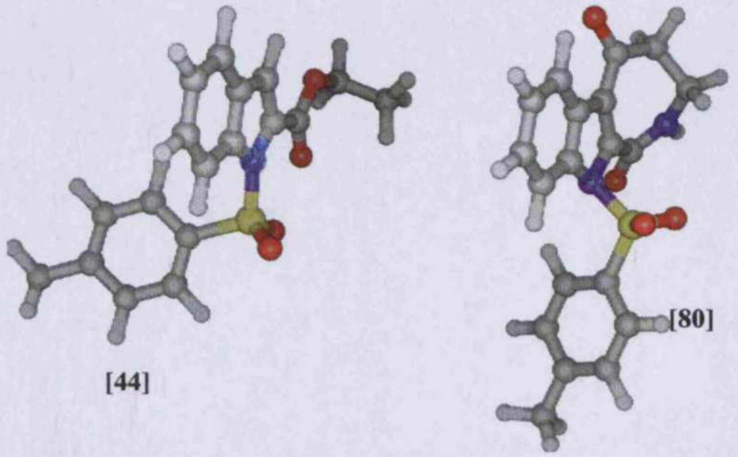

[44]

[80]

Fig 3.5.25: Structures of **[44]** (*left*) and **[80]** (*right*) minimized with Chemdraw3D, showing poor N-S bonding in the cyclized structure compared to the successfully made uncyclized compound.

Interestingly, there was no real difference in the tosyl compounds when minimized with MOE, with the N-S bond consistently skewed by 10°, while the carbonyl functional group of **[44]** was also considerably offset (41°) in the MOE minimization to accommodate the tosyl group. However, Chemdraw 3D gave a very different result (fig 3.5.25). The successfully synthesized compound **[44]** showed a good bonding angle, whilst the cyclized compound forced the N-S bond over 50° out of the plane. These observations indicate that tosylation of indoloazepinone **[25]** would be dis-favoured, while the conflicting results for tosylation of the indole carboxylic acid ester **[32]** imply that the N-S bond may be easily cleaved. This view was backed up by the chemistry as the tosyl group in **[44]** was found to be extremely labile.

Whilst not being definitive, the evidence of these minimizations supported the results found when synthesis was attempted. The protecting groups predicted to form bonds from the indole nitrogen out of the plane, or where their incorporation would be predicted to alter the angle of the carbonyl in respect to the indole were not successfully synthesized. Conversely, the minimizations showing good bond angles also proved to be synthetically achievable. Successfully synthesized molecules also consistently had shorter N-X bonds than compounds where synthesis failed.

It would therefore appear that bulky protecting groups are not a viable option for the protection of indole-2-carboxylic acid esters. The four groups that had been successfully incorporated (methyl, benzyl, methoxybenzyl and SEM) had all proved too robust to be removed. The indole nitrogen position would appear very crowded, which may play a role in the stability of the successful protecting groups to conditions that have been reported to remove them. Therefore, alternative reactions to generate the extensions from the unprotected indole (NH) molecule were investigated.

It had been reported that the hydrazone extension could be achieved on similar molecules using acidic conditions, but after 23 hours of reflux with isopropanol there was no sign of reaction. Potassium carbonate was used as a stronger base than the usual sodium acetate, but again only the starting material was isolated. Further literature research yielded a method using titanium (IV) chloride ($TiCl_4$) to activate the carbonyl functional group,[138,139] and the product from this reaction showed good evidence for containing **[64]**, although it was very impure and in low yield.

As an alternative to $TiCl_4$, boron trifluoride dietherate [$BF_3.(Et_2O)_2$] was used, as it is a stronger Lewis acid. After a column, ^1H NMR showed good evidence for the hydrazone **[64]** as the only product, although there was still a lot of solvent present. Unfortunately, once the compound had been dried, there was evidence of decomposition back to the starting material and this compound was not isolated pure from the mixture (fig 3.5.26).

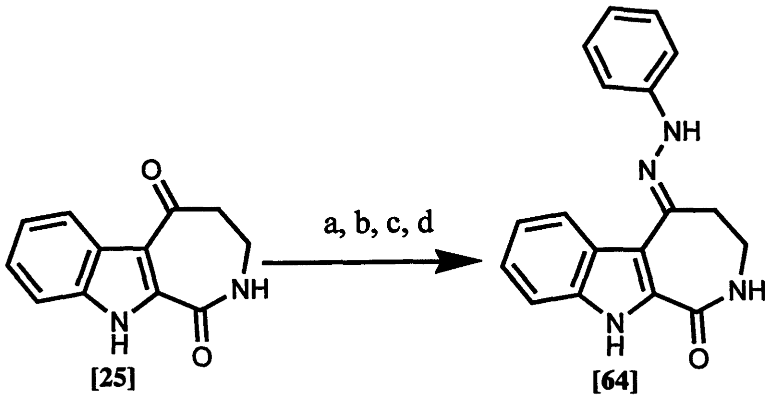

Fig 3.5.26: a: 6M HCl in isopropanol, Phenylhydrazine hydrochloride, Δ, 0 %
b: Potassium carbonate, Phenylhydrazine hydrochloride, Δ, 0 %
c: $TiCl_4$, pyridine, Phenylhydrazine hydrochloride, -10 °C
d: $BF_3(Et_2O)_2$, pyridine, Phenylhydrazine hydrochloride, -10 °C

While the product had not successfully been isolated, the chemistry had worked so this method was also attempted with the brominated compound **[57]**. After 21 hours at reflux, the product was purified to yield a 4:1 mixture of starting material to product, and **[85]** was also not isolated pure (fig 3.5.27).

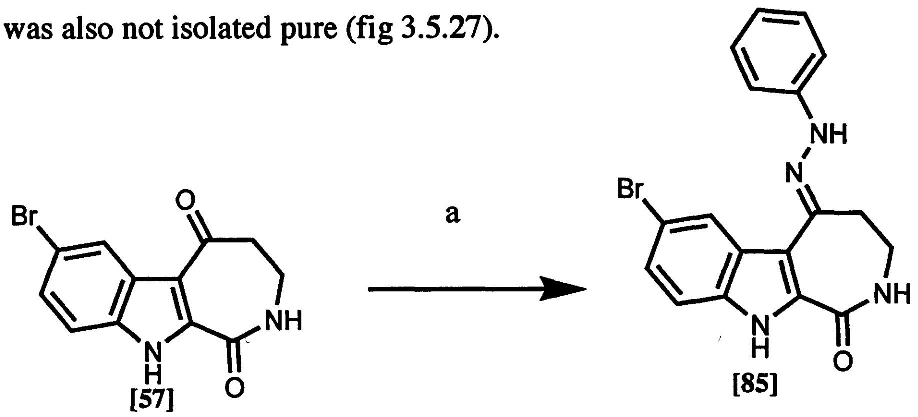

Fig 3.5.27: a: Phenylhydrazine hydrochloride, $BF_3(Et_2O)_2$, pyridine, -10 °C, 30 % of 4 : 1 **[57]** : **[85]**.

The reaction was a lot more successful with the oximes however, and both the brominated **[86]** and the unbrominated indoloazepinone **[87]** oximes were synthesized using this method to compare to N-methylindoloazepinone oxime **[73]**. *O*-Benzylhydroxylamine was used in place of hydroxylamine hydrochloride, and with the unbrominated compound, the O-substituted oxime **[88]** was successfully synthesized (fig 3.5.28).

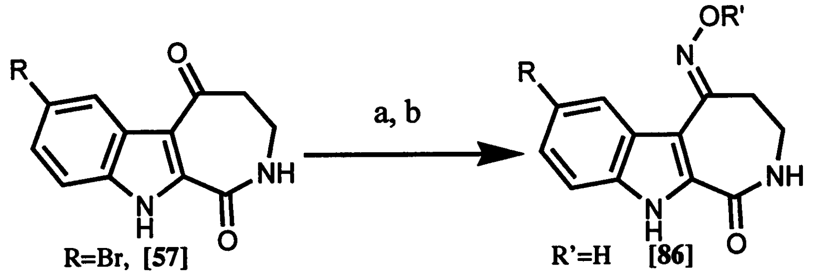

R=Br, [57]
R=H, [25]
R=H, [25]
R=Br [57]

R'=H [86]
R'=H [87]
R'=Bn [88]
R'=Bn [89]

Fig 3.5.28: a: hydroxylamine hydrochloride, pyridine, $BF_3(Et_2O)_2$. R=H R'=H 43 %, R=Br R'=H 57 %, b: *O*-benzylhydroxylamine, pyridine, $BF_3(Et_2O)_2$. R=H R'=Bn 27 %, R=Br R'=Bn 0 %.

This was a direct comparison to the indole N-methylindoloazepinone benzyl-substituted oxime [75], which had been shown to be unstable (see fig 3.5.12). Therefore the same stability test was carried out on this compound. Interestingly, this new derivative was found to be stable in the cell culture medium, and was therefore suitable for biological evaluation. Presumably the indole (NH) pushes electrons towards the oxime making it more electron rich, thus disfavouring cleavage.

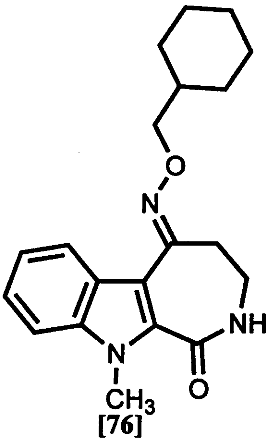

[76]

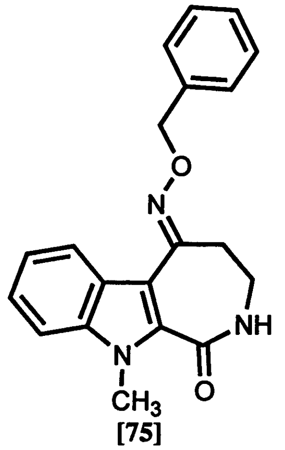

[75]

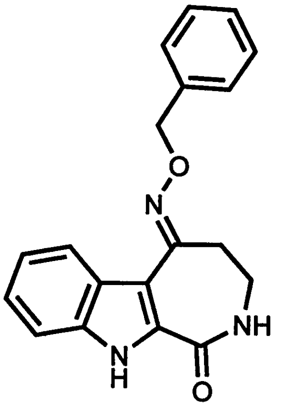

[88]

O-Substitution of the indoloazepinone unsubstituted oximes [86] and [87] with (bromomethyl)cyclohexane to make comparisons to [76] were also attempted, but only starting material was isolated (fig 3.5.29).

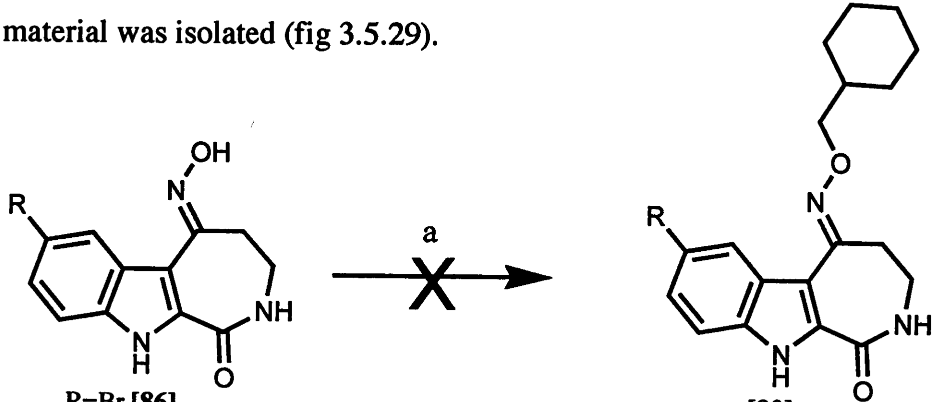

R=Br [86]
R=H [87]

[90]
[91]

Fig 3.5.29: a: (bromomethyl)cyclohexane, R=H 0 %, R=Br 0 %.

3.6 Alterations at the Z position

The Z-position is the region of the lactam ring between the amide group and the ketone: CH_2CH_2 in the compounds with a 7-membered ε-lactam ring. This ring is a feature of both Hymenialdisine and the Paullone series, as well as all the cyclized compounds so far reported.

In order to investigate the importance of the size of the lactam ring, it was decided Z=Ph **[92]**/**[93]**, Z=CH_2 **[94]**/**[95]** and Z=$CH_2CH_2CH_2$ **[96]**/**[97]** would be synthesized to see the effect on biological activity of increasing and decreasing the size of the lactam ring, and incorporating a fused benzene ring, to give derivatives of the "inverted Paullone" structure discussed earlier (page 34).

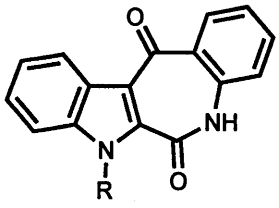

R=H; **[92]**
R=CH_3; **[93]**

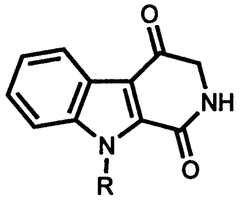

[94]
[95]

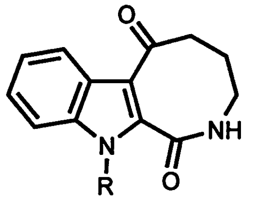

[96]
[97]

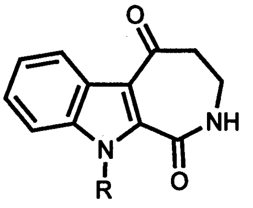

[25]
[31]

The EDCI coupling reaction (see Fig 3.3.11) was used to try to synthesize the unsubstituted indole (NH) forms of the three compounds. The aromatic compound **[98]** was not formed; the steric effects of the bulky aromatic group would appear to disfavour the use of DMAP as a catalyst for this reaction (fig 3.6.1).

The other two esters were synthesized using these conditions, and successfully hydrolysed using $LiOH.H_2O$ to give the carboxylic acids **[99]** and **[100]**.

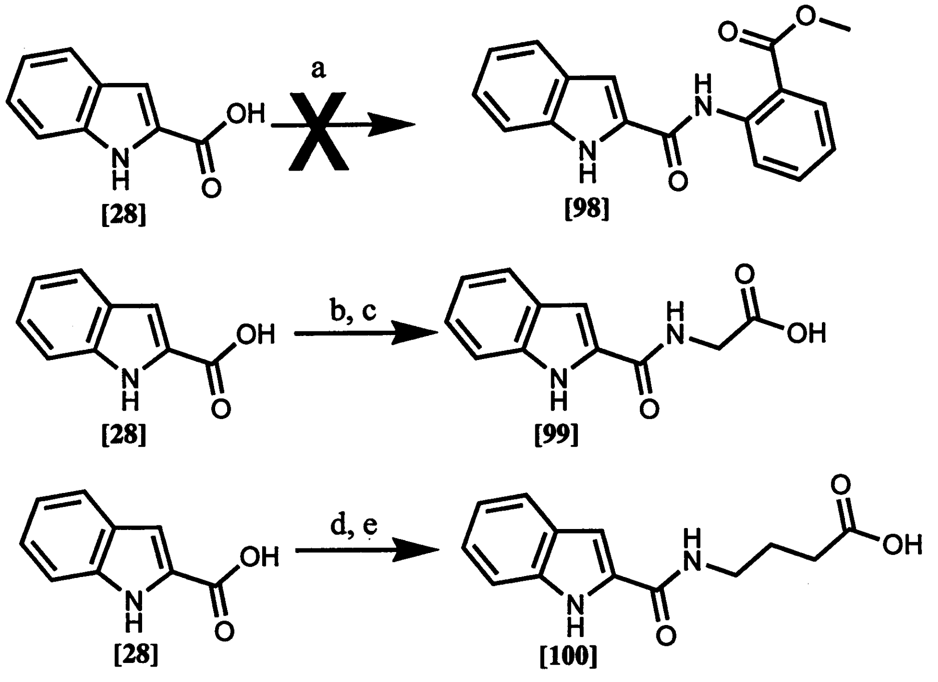

Fig 3.6.1: a: EDCI, DMAP, methyl anthranilate, DCM, 0 %. b: EDCI, DMAP, glycine ethyl ester hydrochloride, DCM, 95 %. c: $LiOH.H_2O$, THF, 70 %. d: EDCI, DMAP, 4-amino-butyrate ethyl ester hydrochloride, DCM, 95 %. e: $LiOH.H_2O$, THF, 68 %.

Attempts to cyclize **[100]** to form the ζ-lactam **[96]** were not successful, and nothing could be identified from the reaction residue. As an 8-exo trig reaction, this is predicted by Baldwin's rules to be disfavoured,[140] which could account for the lack of reaction (fig 3.6.2).

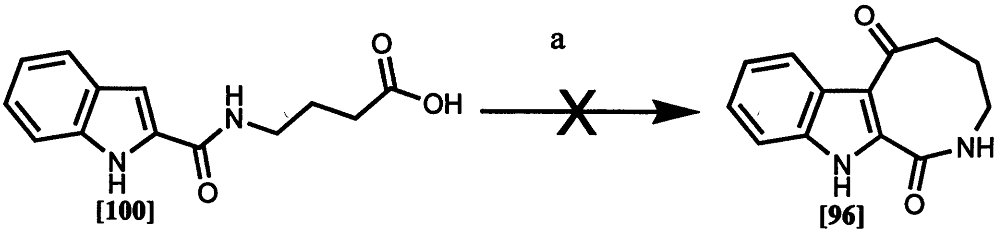

Fig 3.6.2: a: Phosphorus pentoxide, methane sulfonic acid, Δ, 0 %

When **[99]** was cyclized, it was found that unlike the ε-lactam equivalent **[25]**, where the cyclization to the indole NH was the minor product, the pyrazine derivative **[101]** was the sole product, and the desired pyridine derivative **[94]** was not detected (fig 3.6.3).

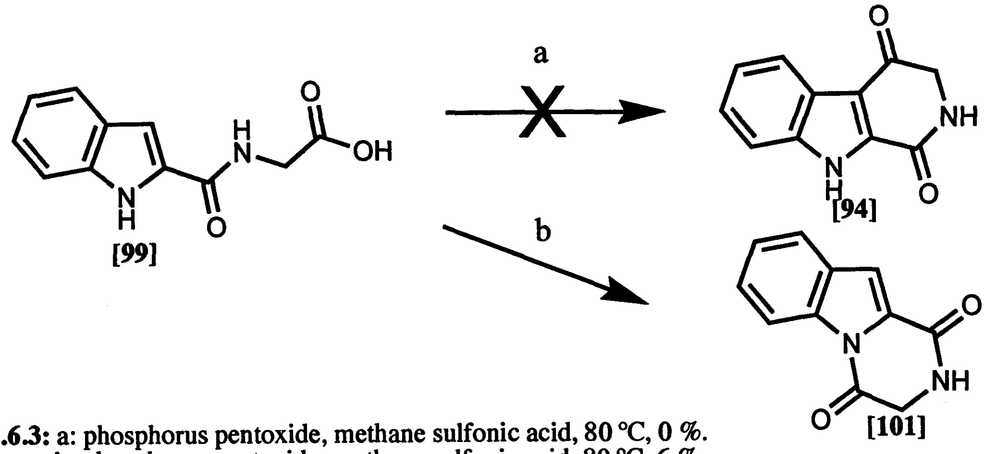

Fig 3.6.3: a: phosphorus pentoxide, methane sulfonic acid, 80 °C, 0 %.
b: phosphorus pentoxide, methane sulfonic acid, 80 °C, 6 %.

Interestingly, [94] has been reported as the product of this cyclization,[141] although more recent literature concurs with the findings of this study, with [101] being the sole product.[142]

In order to block the production of this product, the indole NH needed to be protected again. As the protecting groups, other than the methyl group, had been so ineffective, it was decided to synthesize N-methyl pyridine [95]. The amide extension and hydrolysis of the carboxylic acid ester proceeded as usual (fig 3.6.4).

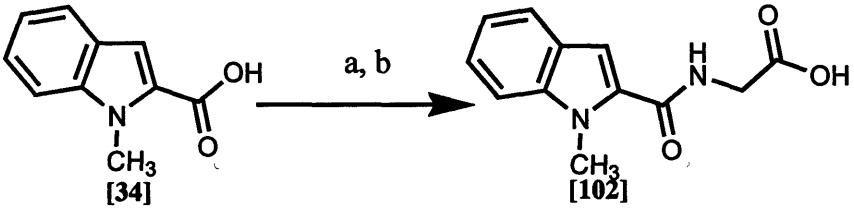

Fig 3.6.4: a: EDCI, DMAP, glycine ethyl ester hydrochloride, DCM, 88 %.
b: $LiOH.H_2O$, THF, 95 %.

Again, the cyclization step to synthesize the pyridine [95] proved to be problematic, and [95] was not isolated (fig 3.6.5). With the alkyl chain reduced by a CH_2 group, the degree of freedom for rotation of the chain is lessened, possibly inhibiting the chain reaching the required angle for attack to occur.

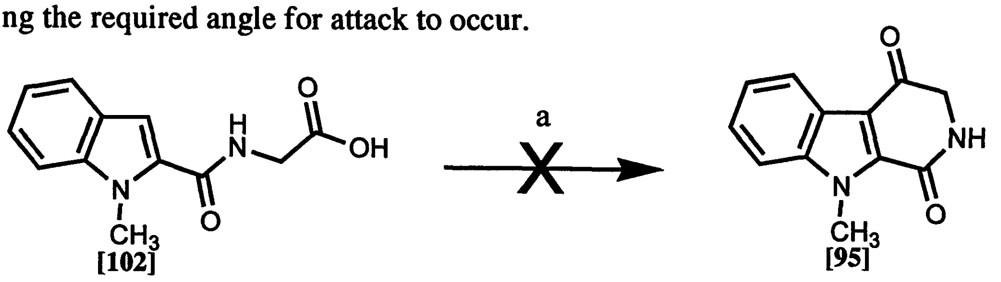

Fig 3.6.5: a: Phosphorus pentoxide, methane sulfonic acid, 80 °C, 0 %

As the EDCI reaction had not worked with the aromatic derivative, it was decided to use the acid chloride route originally used to form the methyl protected compounds (fig 3.6.6).

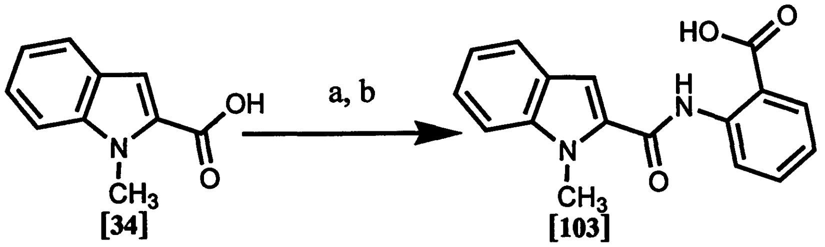

Fig 3.6.6: a: i. TEA, oxalyl chloride, DMF, THF. ii. Methyl anthranilate, THF, 11 %
b: $LiOH.H_2O$, THF, 75 %.

Unlike the β-alanine reaction, the yields were very poor – 11 % was the highest obtained. This was presumably because of the reduced nucleophilicity of methyl anthranilate **[104]** compared to the amino group of β-alanine ethyl ester hydrochloride **[36]**, and this presumably played a role in the failure to synthesize the indole (NH) equivalent.

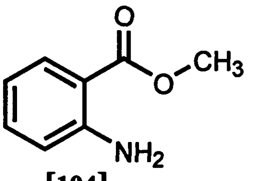

[104]

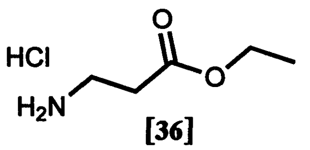

[36]

When the cyclization reaction was attempted, a surprising product was obtained. Rather than cyclizing to the 3-position of the indole as the β-alanine equivalent had done, it was found that a cyclodehydration between the carboxylic acid and amide nitrogen had occurred, forming a 4-membered β-lactam ring (fig 3.6.7).

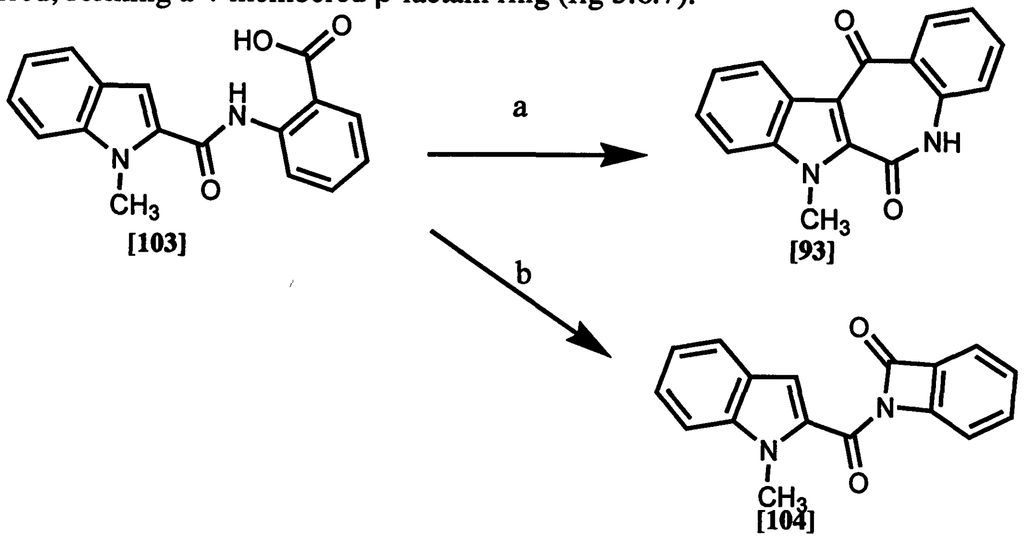

Fig 3.6.7: a: Phosphorus pentoxide, methane sulfonic acid, 80 °C, 0 %, b: 21 %.

The high resolution mass spectrometry analysis was accurate for the expected compound. The ^1H NMR showed an aromatic singlet consistent with the indole C-3 proton, which would not be present if cyclization to the indole had occurred (see fig 3.2.8). There was also no signal for the NH peak. Infrared spectroscopy indicated no NH, as the broad peak expected and seen with the other cyclized compounds at around 3200 cm^{-1} was absent. This evidence pointed to cyclization to the N rather than to the aromatic indole C3, and all the data fitted with the reported compound.

This type of β-lactam ring, trivially called benzoazetones **[105]**, have been reported and are known to be stable and isolatable when R is a bulky substituent.[143] β-lactam rings are also seen in the penicillin family **[106]**. These are less stable β-lactams as the nitrogen lone pair must remain localized on the nitrogen to avoid an impossibly strained flat system.[144]

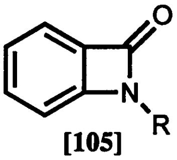

[105]

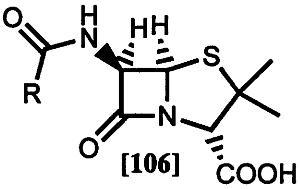

[106]

While it was not the desired compound, it was still an interesting molecule, and further investigations in to the chemistry of this system were performed. Oxime extension was carried out on it so that comparisons in biological behaviour could be carried out between this compound and the ε-lactam series. It was found that on reaction with *O*-benzylhydroxylamine the, β-lactam ring had been opened to give **[107]** (fig 3.6.8).

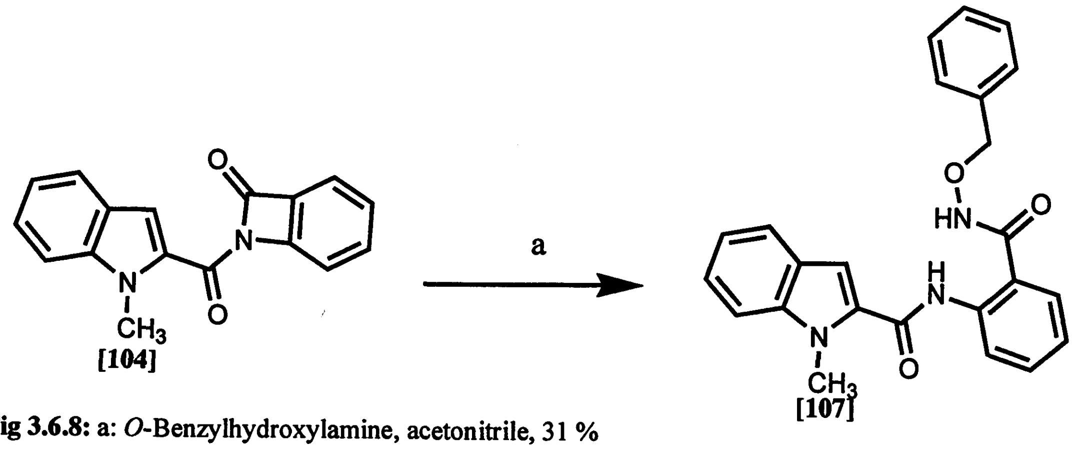

Fig 3.6.8: a: *O*-Benzylhydroxylamine, acetonitrile, 31 %

It was becoming increasingly obvious that alterations in the lactam ring would not be achieved straightforwardly, so alternative methods for cyclization were investigated.

Literature was found surrounding the substitution of a bromine for a carbonyl based group on an aromatic scaffold.[108,145] As it had been seen earlier (fig 3.4.1) that bromination of uncyclized compounds was selective for this position, this could be a good way to induce the cyclization to the 3-position, improving the synthesis of the desired compounds (fig 3.6.9).

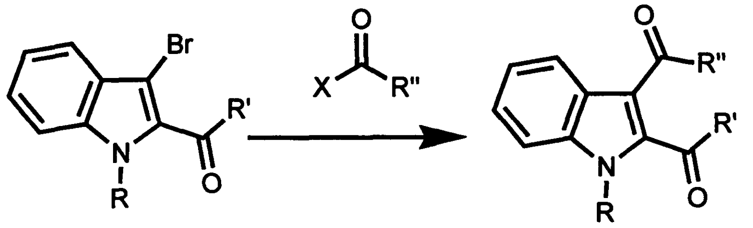

R = H, CH_3
X = leaving group

Fig 3.6.9: Generic reaction for alkylation of brominated indole derivatives.

A procedure for synthesis of the target compounds via intramolecular cyclization of R' substituents bearing a terminal carbonyl group to a 3-bromoindole was proposed. This could be a powerful new route to cyclized products. There was precedence for intramolecular cyclization of this kind, with a not dissimilar series (fig 3.6.10).[146]

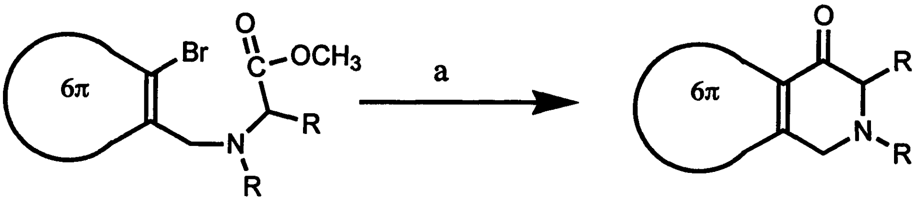

Fig 3.6.10: *n*-BuLi, -100 °C, 10-81 %

As the ε-lactam ring seen in [31] and [25] had been successfully synthesized, the method was attempted for indoloazepinone first to gauge their effectiveness. This method was attempted (fig 3.6.11), but was unsuccessful and just gave pure starting material [56].

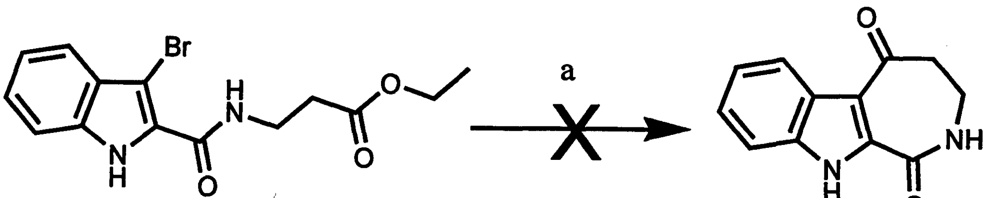

[56] **[25]**

Fig 3.6.11: a: *n*-BuLi, -100 °C, 0 %.

All the indole compounds in the reference had the indole (NH) blocked. It was possible that the free indole (NH) was influencing the chemistry. The leaving group could also potentially be improved to encourage reaction. A literature reaction was found using a Weinreb amide as an alternative leaving group, with the more potent *tert*-BuLi.[147] The literature reaction had a bulky group in the 2-position (fig 3.6.12), which was felt to be a good mimic for the attacking group being part of the chain from the 2-position.

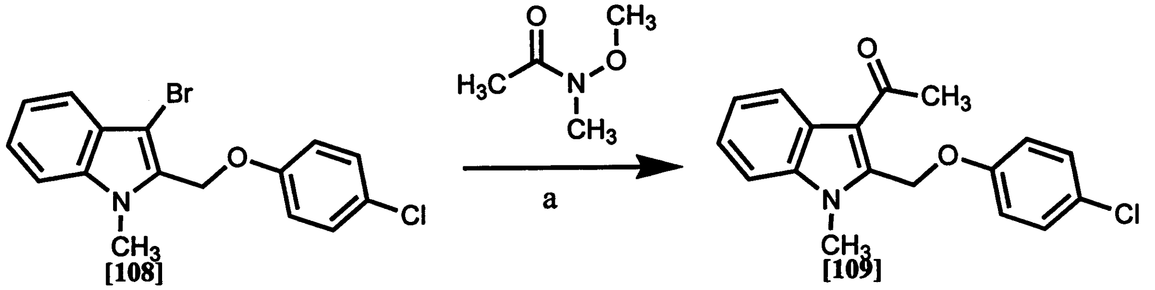

[108] [109]

Fig 3.6.12: a: *t*-BuLi, -78 °C, 43 %

It was decided to attempt this chemistry with the N-methyl indole β-alanine amide to form N-methylindoloazepinone **[31]** first. The reported reaction used an N-methyl indole scaffold, so blocking the indole (NH) might be important.

Literature indicated that the Weinreb amide could be formed from an acid chloride and N,O-dimethylhydroxylamine,[148] so β-alanine **[29]** was reacted with thionyl chloride and N,O-dimethylhydroxylamine added to form the desired precursor **[110]** to couple to the 3-bromo indole carboxylic acid. No reaction appeared to have occurred (fig 3.6.13). 3-Nitropropanoic acid **[111]** was proposed as an alternative starting material, to eliminate any possibility of the amine group affecting the reaction. This could then be hydrogenated to form the desired product.

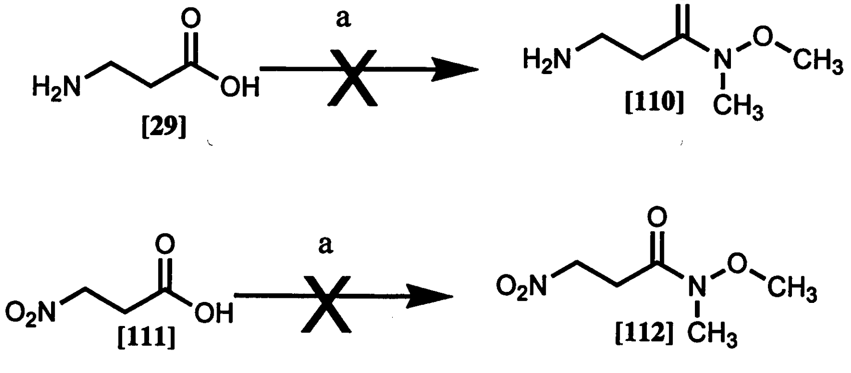

[29] [110] [111] [112]

Fig 3.6.13: a: $SOCl_2$, N,O-dimethylhydroxylamine,

Thionyl chloride activation of the carboxylic acid was not successful in forming the Weinreb amide, therefore an alternative method was sought. Peptide coupling reagents such as DCC have been used for direct conversion of carboxylic acids into Weinreb amides.[149] As EDCI had been used earlier in preference to DCC, it was proposed as an alternative activating reagent. This reaction was attempted on **[111]**. The ^1H NMR showed that the reaction had been successful, but had not gone to completion. The mixture was going to be difficult to separate, so it was decided to incorporate the Weinreb amide after the β-alanine had been reacted with the brominated indole.

As it had been shown that bromination only occurred with the free NH compounds, the ester **[32]** was brominated using the procedure seen previously (fig 3.4.1 page 57). The reaction was successful and went in high yield.

Methylation of this compound was done in the same way as for the non-brominated equivalent. The product was isolated pure, but the crude yield was much lower than with the non-brominated molecule (fig 3.6.14).

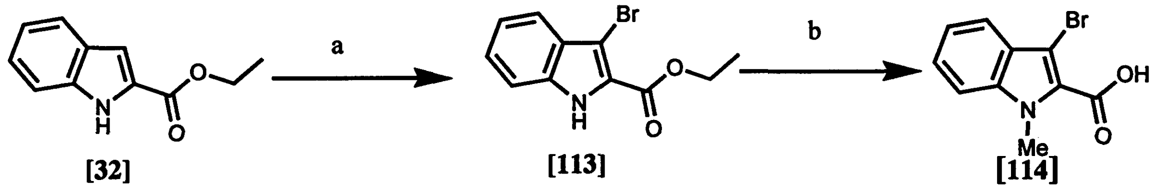

Fig 3.6.14: a: NBS, 87 %, b: i. NaH, ii. MeI, iii. NaOH (aq), 60 °C, 52 %

The amide bond forming reaction and subsequent de-protection of the carboxylic acid proceeded in comparative yields to the subsequent reactions, and gave pure products (fig 3.6.15).

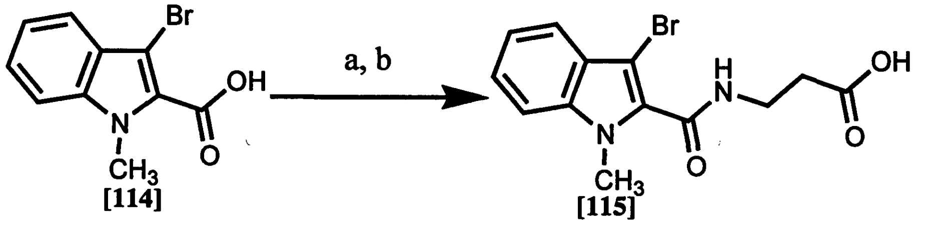

Fig 3.6.15: a: EDCI, DMAP, β-alanine ethyl ester hydrochloride, 89 %. b: LiOH.H_2O, 74 %

The EDCI promoted reaction to form the Weinreb amide gave a sticky viscous oil which was difficult to transfer and handle, but was shown to be analytically pure Weinreb amide **[116]** (fig 3.6.16).

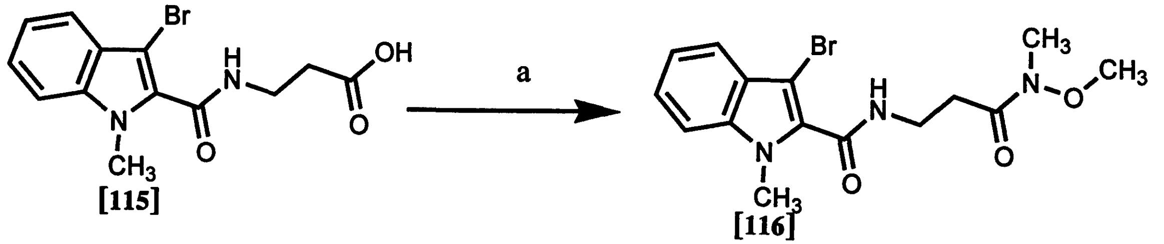

Fig 3.6.16: a: EDCI, DMAP, N,O-dimethylhydroxylamine hydrochloride, 47 %

Amide **[116]** was dissolved in dry THF in a nitrogen atmosphere at –78 °C and *tert*-BuLi was added. The mixture was allowed to return to room temperature after two hours, but there was no evidence of reaction after being left at room temperature for two hours (fig 3.6.17).

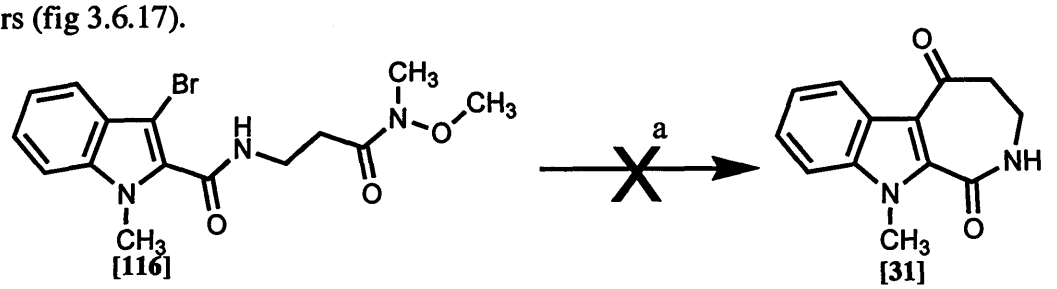

[116] [31]

Fig 3.6.17: a: t-BuLi, -78 °C, 0 %

While the Weinreb amide **[116]** had been successfully synthesized, the overall yield had been quite low (15 %) and the compound had all been used in the attempted cyclization. The indole (NH) Weinreb amide analogues with Z=CH_2, CH_2CH_2 and $CH_2CH_2CH_2$, had been synthesized in parallel, with the reactions proceeding with similar yields to those seen previously (fig 3.6.18).

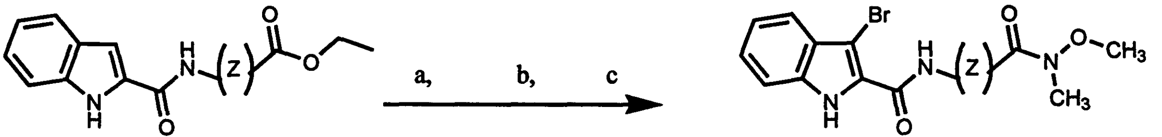

		a	b	c		
[117]	Z = CH_2	78 %	99 %	86 %	[118]	Z = CH_2
[52]	Z = CH_2CH_2	51 %	98 %	64 %	[119]	Z = CH_2CH_2
[120]	Z = $CH_2CH_2CH_2$	58 %	85 %	54 %	[121]	Z = $CH_2CH_2CH_2$

Fig 3.6.18: a: NBS, DMF. b: LiOH.H_2O. c: EDCI, DMAP, N,O-dimethylhydroxylamine hydrochloride.

Unlike the N-methyl indole analogue, the unsubstituted NH indoles were all solids. Despite the lack of reaction for the first Weinreb amide cyclization attempted **[116]**, the three cyclization reactions on the indole (NH) compounds **[118]**, **[119]** and **[121]** were carried out. It was clear by TLC that reaction had taken place, so the reactions were worked up. With the reaction to form the pyridine derivative, the only major product was **[122]**, where the N-methoxy group had been cleaved from the Weinreb amide (fig 3.6.19).

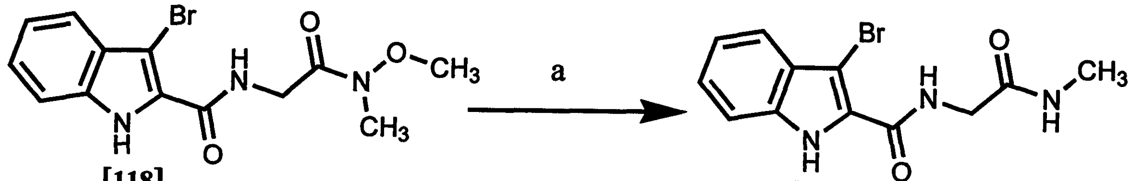

[118] [122]

Fig 3.6.19: a: *t*-BuLi, 22 %

In the reaction to form the ζ-lactam, the main compound in the mixture appeared by TLC to be the starting material, but two other compounds were isolated. The same N-methoxy cleavage had occurred **[123]**, and the *tert*-butyl group had displaced the Weinreb amide to give **[124]** (fig 3.6.20). This unusual result was confirmed by NMR and HRMS.

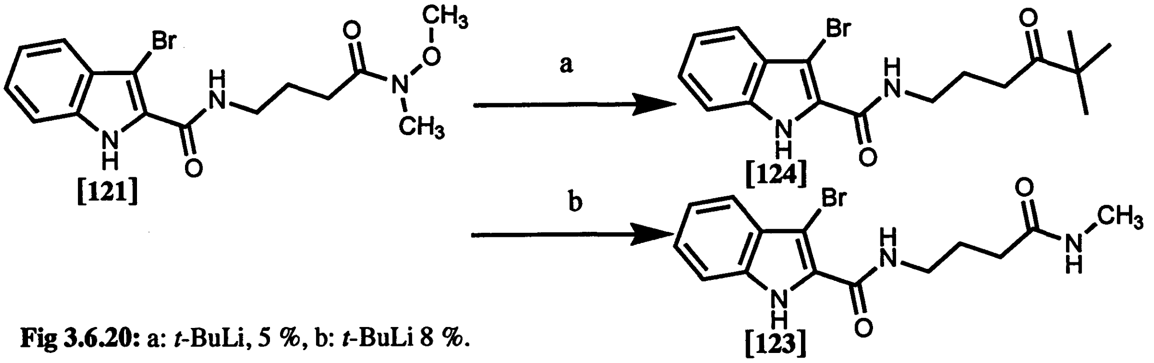

Fig 3.6.20: a: *t*-BuLi, 5 %, b: *t*-BuLi 8 %.

The TLC of the reaction to form the ε-lactam showed spots consistent with the products seen for the ζ-lactam, but the starting material was in such excess that the two products were not isolated.

No reports were uncovered of any other attempts of intramolecular reactions of this sort using Weinreb amides, but literature was found that could explain the result. The reduced amine seen in **[122]** and **[123]** was reported as the unwanted product of attempted condensation of an aldehyde with a Weinreb amide.[148] During the synthesis of substituted pyrroles[150] excess organometallic agent was shown to cause displacement of the Weinreb amide by the organo substituent (R'), giving the same result as seen with **[124]** (fig 3.6.21).

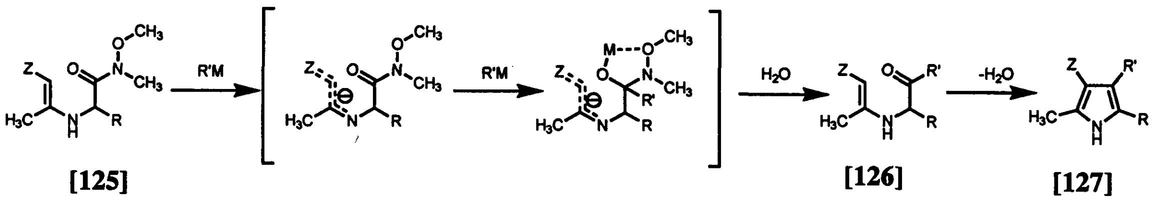

Fig 3.6.21: Reported Weinreb displacement by R' with excess R'M

N-Methoxy-N-methylacetamide **[128]** was also used for acylation of lithium enolates (fig 3.6.22).[151]

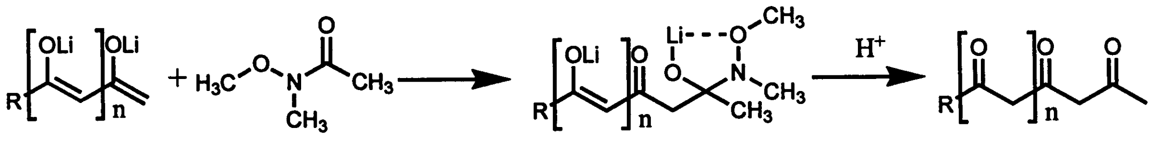
[129] **[128]** **[130]** **[131]**

Fig 3.6.22: Reported acylation of lithium enolates with Weinreb

It would seem likely that rather than displacing the Br, the Li was coordinating to the carbonyl function making this more prone to attack. The *tert*-butyl group could then attack the carbonyl either displacing the Weinreb amide to form **[124]**, or removing the methoxy group resulting in **[122]** and **[123]**. In the literature,[147] the Weinreb amide was added after the *tert*-BuLi. Presumably displacement of Br by *tert*-BuLi prior to addition of the Weinreb amide is important. Unfortunately as the attempted cyclization is an intramolecular reaction, it was not possible to incorporate the Weinreb amide after addition of BuLi.

While the Z = CH_2 and $CH_2CH_2CH_2$ structures had not been synthesized to compare with the Z = CH_2CH_2 series in the biological assay, this work did show that the ε-lactam ring is by far the easiest of the three to synthesize, which could be one explanation as to why the Paullone and the natural compound Hymenialdisine contain this ring rather than the larger ζ-lactam or smaller pyridine derivative.

3.7 Molecular modelling

Molecular modelling is a powerful tool to aid rational drug design. In addition to the SYBYL program discussed earlier, Chimera[152,153] was also utilized during this project. This is a viewing program that also allowed manual superimposition. Also a new, more advanced molecular modelling program Molecular Operating Environment (MOE™) had recently become available. This program can be used to dock molecules in the active site, predicting if and how a molecule can interact with an active site. The results could be then viewed using Chimera. This technology could give further insight into whether the compounds could be accommodated in the active site of CDK2, and what alterations to the molecule might improve inhibition.

The SYBYL superimposition (see fig 3.5.1) had given evidence that the hydrazones extension of **[65]** should be accommodated in the active site. Manual docking using Chimera was less clear. The compound was minimized using Chemdraw 3D, then imported into Chimera and manoeuvred to overlap the Aldisin motif of Hymenialdisine in the crystal structure of this compound with CDK2 (PDB ID: 1DM2). However, as can clearly be seen (fig 3.7.1), this method predicted that the hydrazone **[65]** would not be accommodated without alterations either to the position of the inhibitor, its structure or the structure of the active site itself.

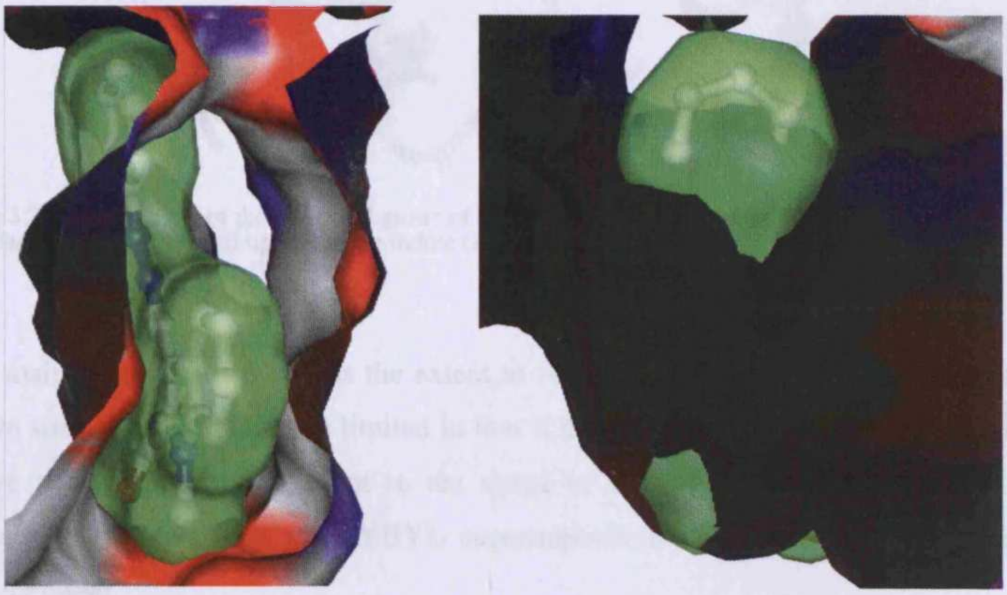

Fig 3.7.1: [65] manually docked in the active site of CDK2. The surface only of the active site is shown, with **[65]** shown as ball and stick, and the compounds surface is also shown (*green*). Views through the entrance to the active site (*left*) and a side view of the active site (*right*) are shown.

Interestingly, there was a clear disparity between these two methods of minimization (table 3.7.1), with the SYBYL minimization significantly shorter than with Chemdraw, while MOE minimization gave good correlation to Chemdraw 3D. This could explain the difference in results between the SYBYL and Chemdraw 3D methods.

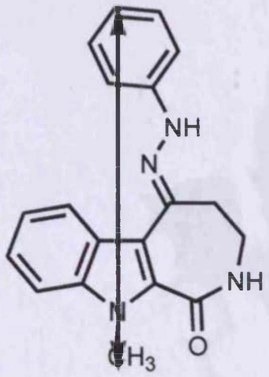

Technique	Distance between N-methyl and tip of hydrazone
SYBYL	10.66 Å
Chemdraw 3D	11.04 Å
MOE	11.05 Å

Table 3.7.1: Intramolecular distance recorded with three different minimization techniques.

Not surprisingly as the Aldisin motif was used as a reference for the manual docking, the N-methyl group broke through the surface of the active site (fig 3.7.2).

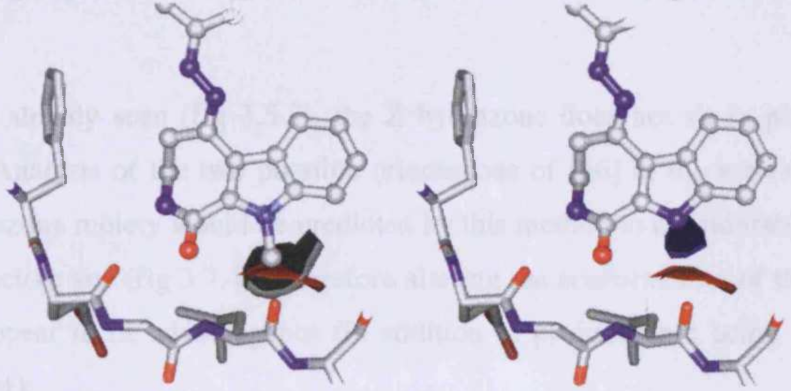

Fig 3.7.2: The surface of the N-methyl group of **[65]** and its interaction with the carbonyl surface of Leu83 (*left*), compared to the indole (NH) analogue **[64]** (*right*).

The main concern however was the extent to which the hydrazone extended out of the active site. Manual docking is limited in that it takes no account of the potential of the active site to modify and adapt to the shape of the inhibitor. Nevertheless, it was persuasive evidence that the SYBYL superimposition could not be assumed to be correct either.

Reviewing the structure compared to the ATP binding it is attempting to mimic implies

CARDIFF UNIVERSITY * PRIFYSGOL CAERDYDD *

that the orientation of the hydrazone extension is detrimental to the molecules ability to occupy the active site. It had been noted during synthesis that all the hydrazones and, probably (although not conclusively) the oximes, were E isomers. It would appear that the Z isomer might be advantageous, as it may be more likely to be able to interact with the cleft used by the tri-phosphate group of ATP (fig 3.7.3).

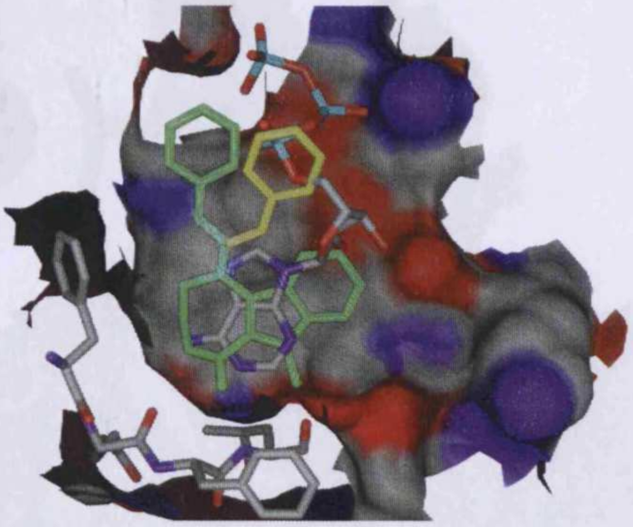

Fig 3.7.3: Manually docked **[65]***(Green)*, with superimposed ATP. The C=N bond is rotated 180° to give the potential hydrazone position in the Z isomer *(yellow)*.

However, as already seen (fig 3.5.5), the Z hydrazone does not sit in plane with the indole ring. Analysis of the two possible orientations of **[66]** in the active site showed that the hydrazone moiety would be predicted by this method to considerably breach the sides of the active site (fig 3.7.4). Therefore altering the conformation of the hydrazone would not appear to be advantageous (in addition to probably not being synthetically possible either).

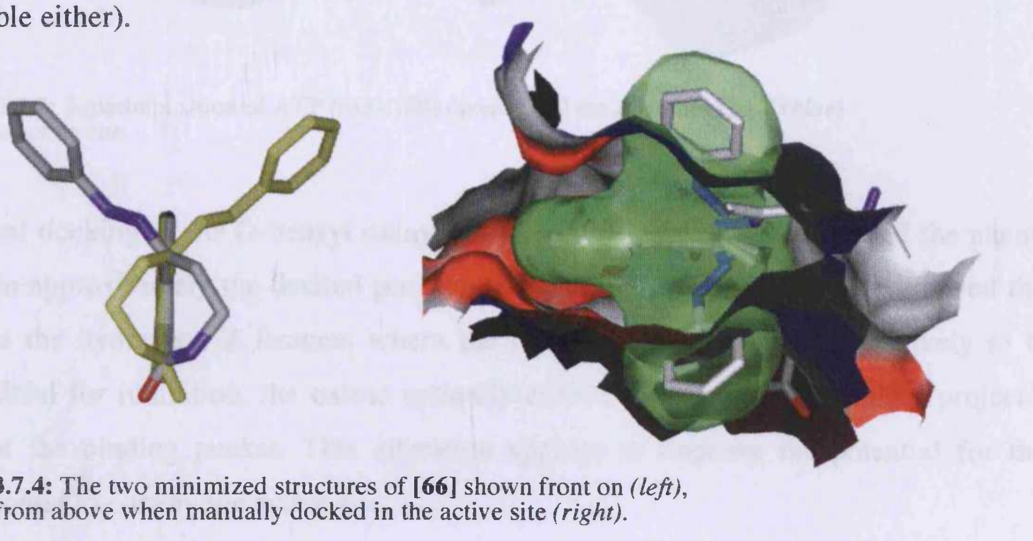

Fig 3.7.4: The two minimized structures of **[66]** shown front on *(left)*, and from above when manually docked in the active site *(right)*.

The O-substituted oximes have an extra atom in the chain between the lactam ring and the ring of the extension. This might allow a more beneficial orientation to be achieved.

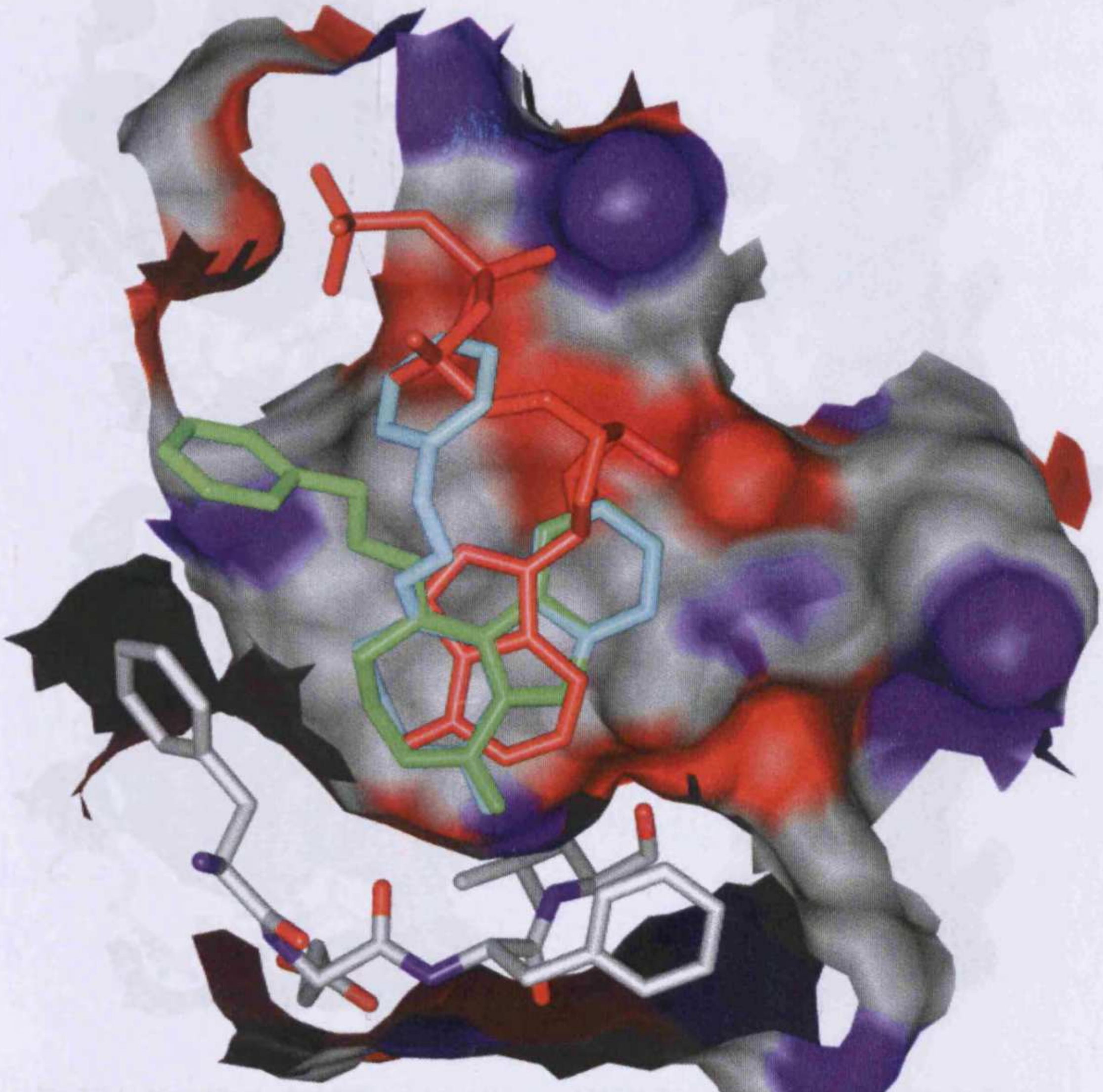

Fig 3.7.5: Superimposition of ATP *(red)*, **[88]** *(green)* and the Z isomer **[132]** *(blue)* in the active site.

Manual docking of the O-benzyl oxime **[88]** and its Z isomer **[132]** showed the phenyl ring in approximately the desired position (fig 3.7.5). Further examination showed that unlike the hydrazone Z isomers where the ring protruded at an angle unlikely to be beneficial for inhibition, the oxime naturally curved round and only slightly projected out of the binding pocket. This alteration appears to improve the potential for this compound to occupy the active site.

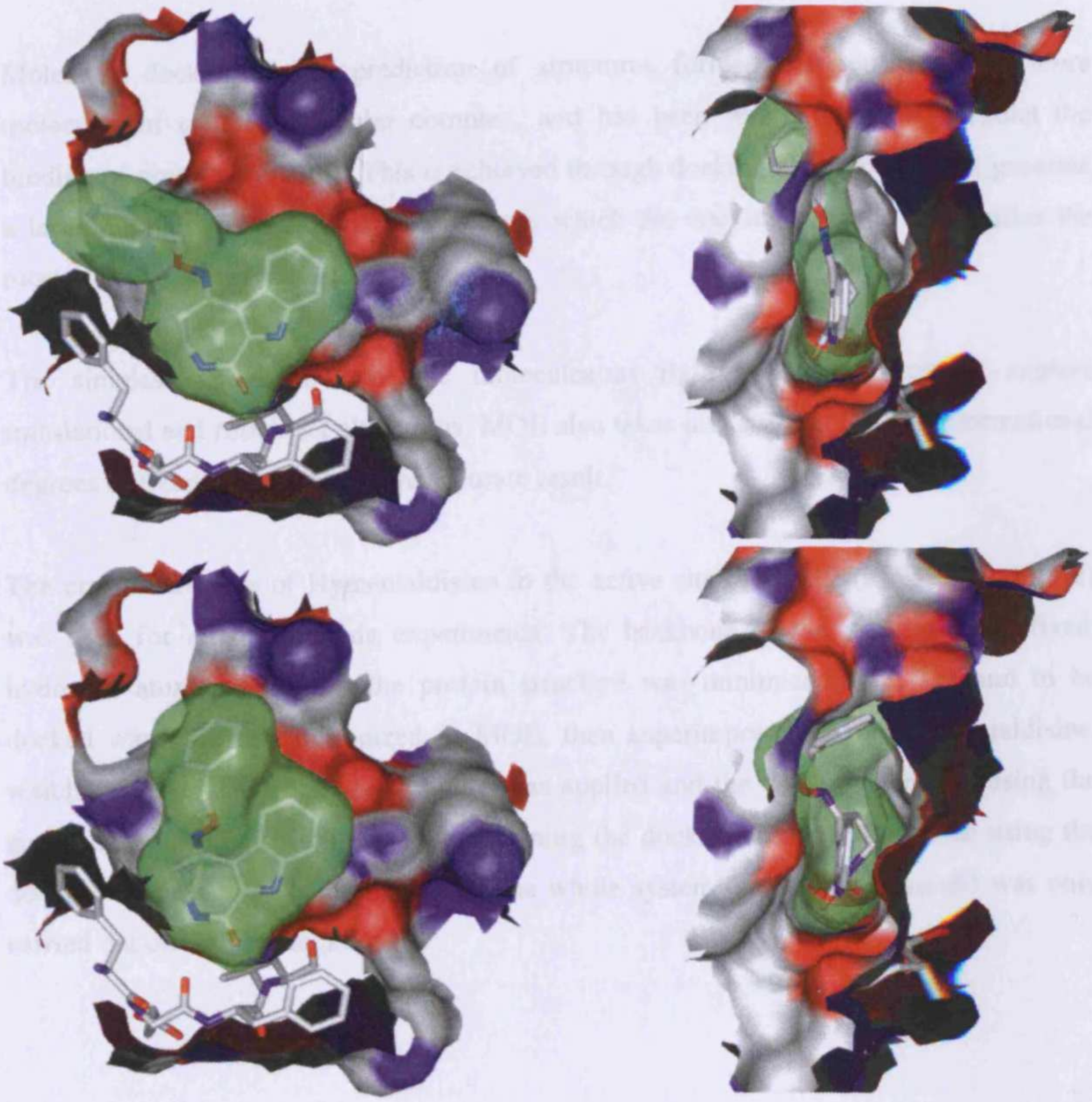

Fig 3.7.6: Manually docked **[88]** E isomer (*top*), and **[132]** Z isomer (*bottom*). Cut away side view (*left*) and view from the entrance to the binding pocket (*right*) are shown.

3.8. Molecular Docking with MOE

Molecular docking is the prediction of structures formed between two or more molecules in an intermolecular complex, and has been widely used to predict the binding of protein inhibitors. This is achieved through docking algorithms that generate a large number of possible structures from which the docking program identifies the most plausible structures.

The simplest algorithms treat the molecules as rigid bodies, and only explore translational and rotational alterations. MOE also takes into account the conformational degrees of freedom, giving a more accurate result.

The crystal structure of Hymenialdisine in the active site of CDK2 (PDB ID: 1DM2) was used for all the docking experiments. The backbone of the protein was fixed, hydrogen atoms added and the protein structure was minimized. The ligand to be docked was built and minimized in MOE, then superimposed onto Hymenialdisine, which was then deleted. The forcefield was applied and the docking started using the simulated annealing search protocol, confining the docking to the active site using the docking box function. Minimization of the whole system (enzyme + ligand) was only carried out on the best dockings.

3.8.1 Control Experiment

In order to verify the method, Hymenialdisine **[17]** itself was docked using MOE-dock, and the minimized structures compared to the original crystal structure.

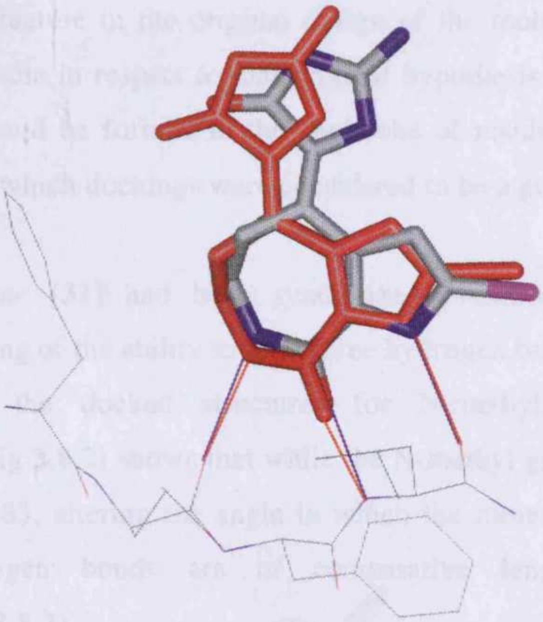

Fig 3.8.1: Superimposition of Hymenialdisine **[17]** docked molecule (*coloured by element*) over the published data (*red*), both displayed in stick form. The CDK2 backbone residues Phe80 to Leu83 are shown, as are the hydrogen bonds from both molecules to these residues.

	Glu 81 CO	Leu 83 NH	Leu 83 CO
Original Hymenialdisine	2.8	2.7	3.2
Docked Hymenialdisine	3.2	2.7	3.0

Table 3.8.1: Hydrogen bond lengths in Å calculated from Hymenialdisine docking in CDK2, compared to the published data.

As can be seen from the docking (fig 3.8.1) and the hydrogen bond lengths (table 3.8.1), the docking gave an accurate result, justifying the method used. Molecules were therefore docked within the CDK2 active site using this method in order to establish the theoretical potential of the compounds to act as CDK2 inhibitors, and the impact on binding that the key alterations would have.

3.8.2 Docking Results

The ability to form two or three hydrogen bonds to Glu81 and Leu83 was of great importance to all the inhibitors whose crystal structure in CDK2 has been published, and had been a major feature in the original design of the molecules. Therefore, the orientation of the molecule in respect to that original hypothesis and the length of the hydrogen bonds that could be formed to the backbone of residues Glu81 and Leu83 were used to determine which dockings were considered to be a good representation.

N-Methylindoloazepinone **[31]** had been synthesized primarily to investigate the importance to the bonding of the ability to form three hydrogen bonds as apposed to just two. Comparison of the docked structures for N-methylindoloazepinone and indoloazepinone **[25]** (fig 3.8.2) shows that while the N-methyl group forces the indole away from residue Leu83, altering the angle in which the molecule is orientated, the two remaining hydrogen bonds are of comparative length to the docked indoloazepinone (table 3.8.2).

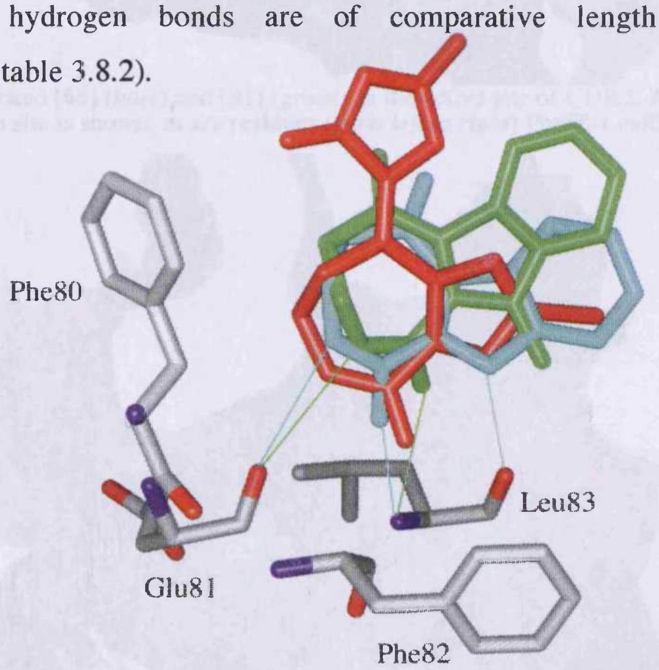

Fig 3.8.2: Superimposition of dockings of **[31]** (*green*) and **[25]** (*blue*) over the Hymenialdisine (*red*) crystal structure showing the residues Phe80-Leu83. The hydrogen bond interactions for **[31]** and **[25]** are shown.

When the hydrazones of N-methylindoloazepinone **[65]** and indoloazepinone **[64]** were docked, the alteration in orientation became more pronounced (fig 3.8.3 and fig 3.8.4).

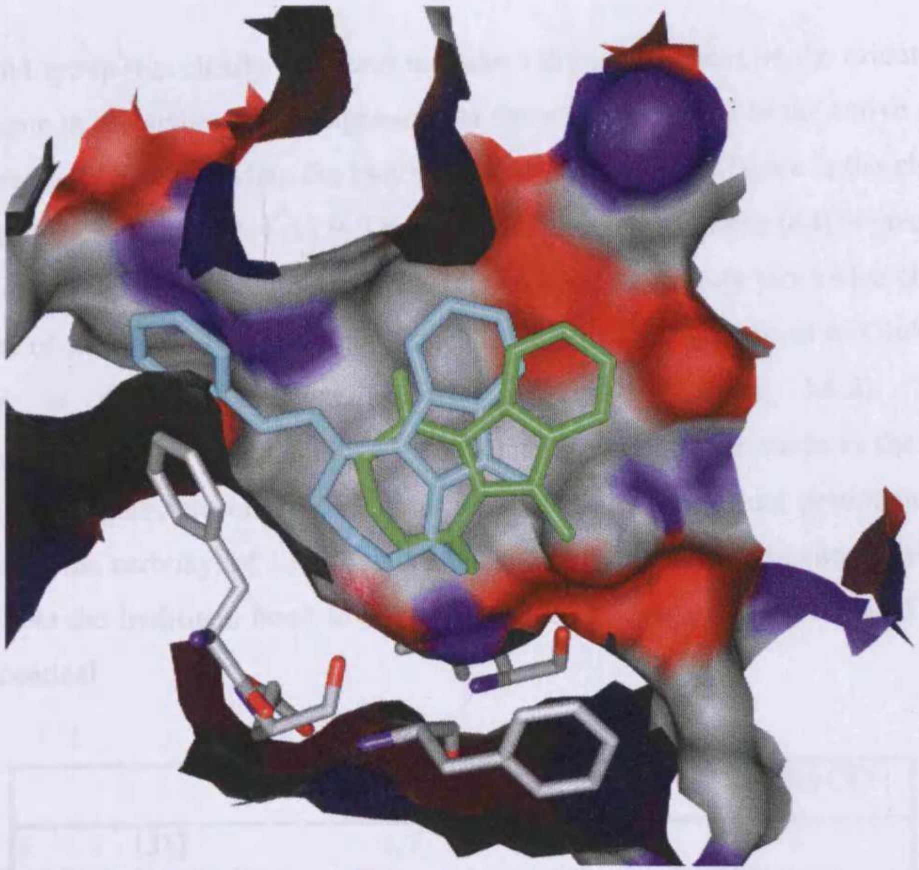

Fig 3.8.3: MOE-docked **[65]** (*blue*) and **[31]** (*green*) in the active site of CDK2. A cut-away of the surface of the active site is shown, as are residues (*from left to right*) Phe80-Leu83.

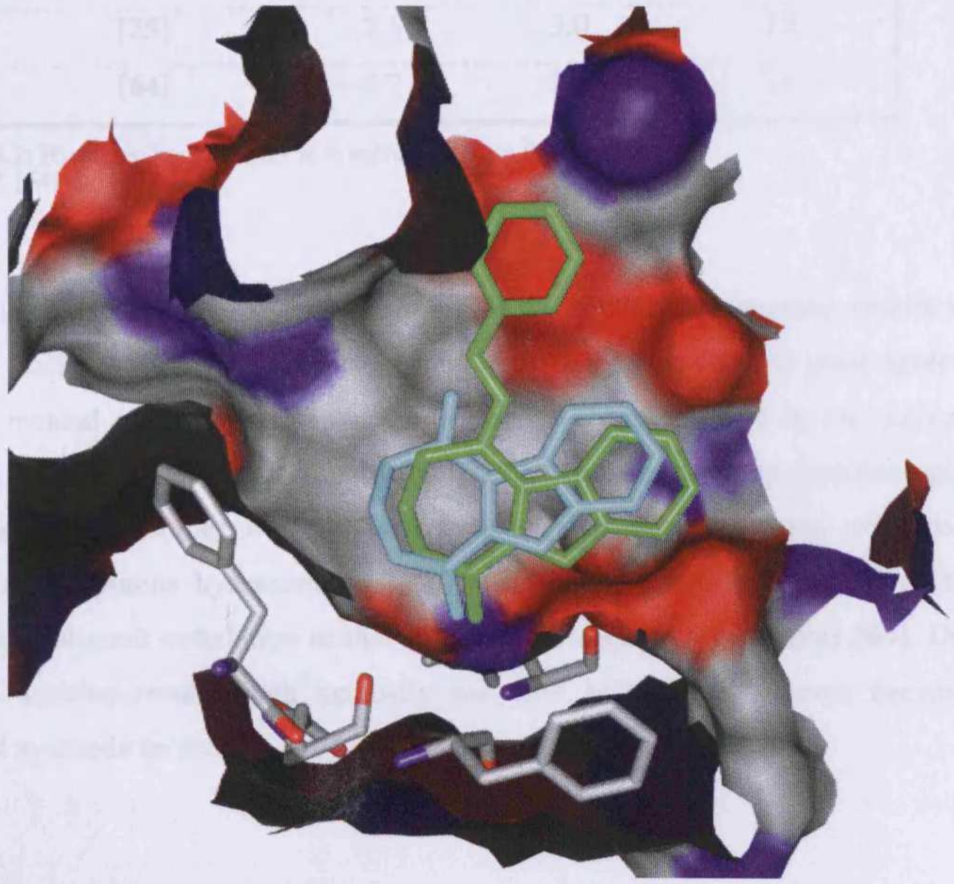

Fig 3.8.4: MOE-docked **[64]** (*green*) and **[25]** (*blue*) in the active site of CDK2. A cut-away of the surface of the active site is shown, as are residues (*from left to right*) Phe80-Leu83.

The methyl group was clearly predicted to make a dramatic impact on the orientation of the molecule in the active site. It appears that there are two clefts in the active site that could potentially accommodate the hydrazone. At the top of the figure is the cleft used by the tri-phosphate moiety of ATP. The indoloazepinone hydrazone **[64]** is predicted to use this cleft, which rotates the indoloazepinone scaffold further clockwise (from the viewpoint of fig 3.8.4), leading to an elongation of the hydrogen bond to Glu81 and a reduction in the two hydrogen bonds to Leu83 (table 3.8.2). The N-methylindoloazepinone hydrazone **[65]** is predicted to orientate towards to the cleft on the left of the figure, presumably because the methyl group does not permit such close proximity to the carbonyl of Leu83 as is achieved with the indoloazepinone hydrazone. This reduces the hydrogen bond to Glu81, while the hydrogen bond to Leu83 remains almost identical.

	Glu 81 O	**Leu 83 NH**	**Leu 83 CO**
[31]	3.7	3.3	-
[65]	3.2	3.4	-
[25]	3.5	3.0	3.2
[64]	3.7	2.6	2.6

Table 3.8.2: Hydrogen bond lengths in Å calculated from the dockings of **[25]**, **[31]**, **[64]** and **[65]**.

The E/Z isomerism of the O-benzyl oxime **[88]** has produced interesting results when manually docked. MOE-dock of these compounds (fig 3.8.5) showed good agreement with the manual results, with the Z isomer being accommodated in the active site preferentially to the E isomer. Interestingly, the orientation of the indoloazepinone scaffold of the E isomer was almost exactly the same as that seen with the N-methylindoloazepinone hydrazone **[65]**, while the indoloazepinone scaffold of the Z isomer showed good correlation to that of the indoloazepinone hydrazone **[64]**. Due to the good docking results, both manually and with MOE, the Z isomer became an additional synthetic target.

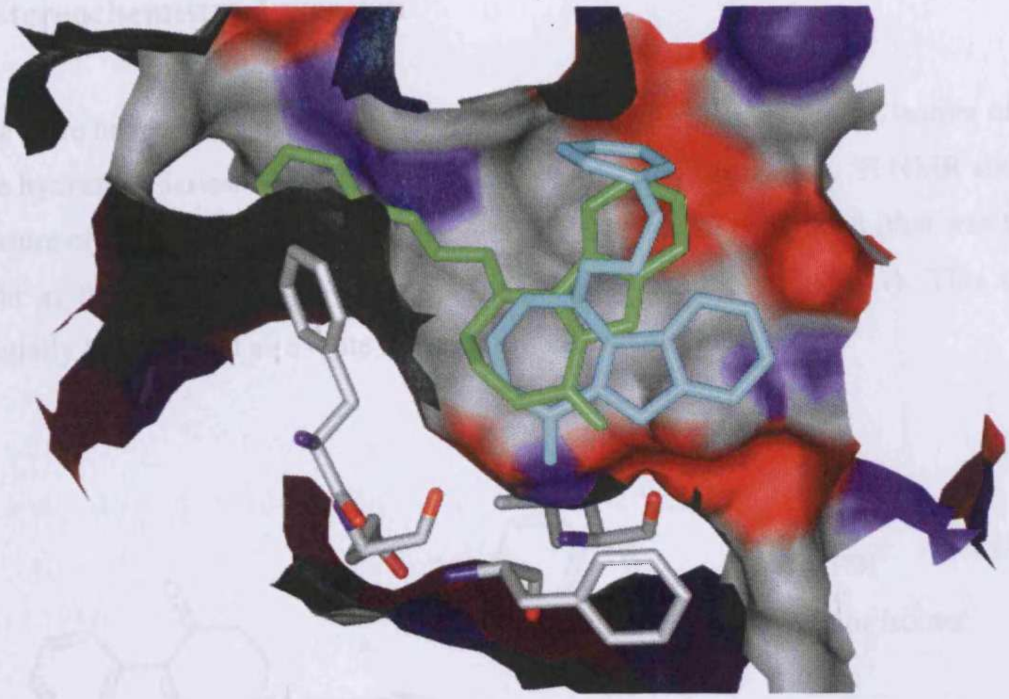

Fig 3.8.5: MOE-docked **[88]** (*green*) and **[132]** (*blue*) in the active site of CDK2.

It was interesting to note that despite the very different orientations of the two molecules, the hydrogen bonds Glu81 and Leu83 (NH) remained comparable (table 3.8.3).

	Glu 81 O	Leu 83 NH	Leu 83 CO
[88]	3.6	3.8	5.0
[132]	3.5	3.6	2.5

Table 3.8.3: Hydrogen bond lengths in Å calculated from the dockings of **[88]** and **[132]**.

The dockings predicted that **[31]** and **[25]** should be able to form two and three hydrogen bonds respectively to the backbone of residues Glu81 and Leu83. The dockings also predicted that extended N-methylindoloazepinone compounds would not interact with the cleft used by the triphosphate moiety of ATP. The extensions of these compounds and the (E) O-benzyl oximes would interact with an alternative cleft according to the docking results. This observation casts doubt over the ability of the extended compounds to interact with the active site of CDK2 in the desired manner, implying that the improved growth inhibition of **[65]** compared to **[31]** may not be due to the ability to inhibit CDK2. Assays against the target protein were used to assess the accuracy of this observation, and the biological results are discussed in chapter 4.

3.9 Stereochemistry Inversion

While there had been no experimental evidence for the formation of the Z isomer of any of the hydrazone series, when the oxime reaction was first carried out, ^{1}H NMR showed a mixture of two products which appeared to be mainly the E compound (that was being sought at the time) with the Z oxime as a minor impurity (fig 3.9.1). This could potentially be exploited as a route to the desired Z isomer [132].

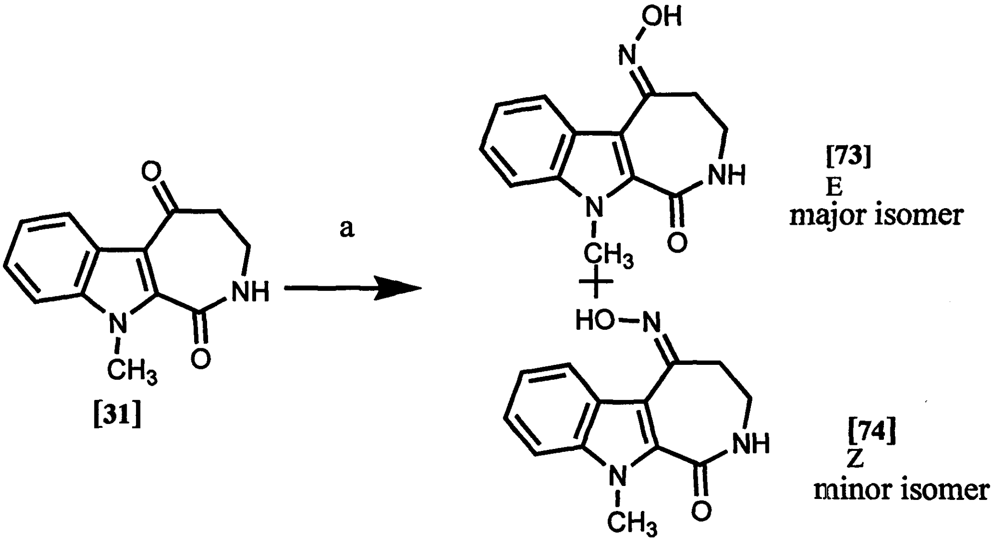

[31]

[73]
E
major isomer

[74]
Z
minor isomer

Fig 3.9.1: a: Hydroxylamine hydrochloride, sodium acetate, 50 °C, 35 %

Recrystallization was used to purify the major isomer, it was hoped to recover the minor isomer from the mother liquid, but it was not isolated. The synthetic procedure was modified to give only one product [73] (fig 3.5.9) by increasing the temperature of the reaction.

It was predicted from the fact that increasing the temperature gave [73] as the sole product that reducing the temperature would give a greater proportion of [74]. The reaction was carried out and kept in the fridge or ice bath (i.e. between 0 and 5 °C) for a period of two weeks. ^{1}H NMR of the crude product showed evidence for three compounds; [31], [73] and [74]. The reduction in temperature had clearly given the desired result although [74] was very much a minor isomer.

This mixture was purified by column chromatography, but this revealed that the R_f of the E and Z isomers were the same.

The reaction was repeated on a larger scale giving a ratio of 1 : 2.6 : 9.3 (**[74]** : **[31]** : **[73]**).

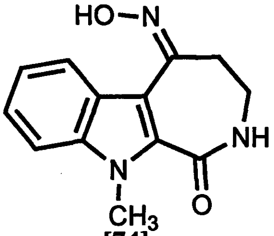

[74]

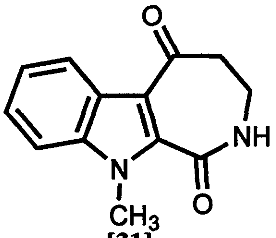

[31]

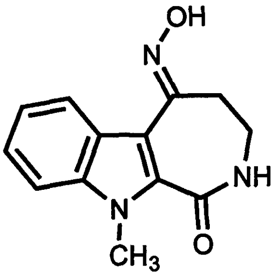

[73]

Recrsytallization from acetone and petrol was found to give a much purer sample of **[73]**, leaving a better proportion of **[74]** in the remaining mixture. Two recrsytallizations were performed (table 3.9.1), improving the ratio of **[74]**, although it was still the minor product.

	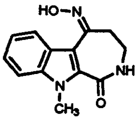 [74]	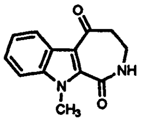 [31]	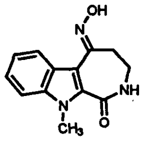 [73]
Starting mixture	1	2.6	9.3
1st Recrystalization	1	0.6	22.5
2nd Recrystalization	1	1.2	15.6
Final mixture	1	3	4.6

Table 3.9.1: The ratios of the three components before and after the recystalizations.

As the use of a Lewis acid had been more successful for the oxime synthesis on the R=H compounds **[86]** and **[87]**, it was thought that this might catalyze this reaction at low temperature to form **[74]**. The mixture was kept in the fridge for one week, but ^{1}H NMR of the crude mixture showed only starting material and **[73]** were present (fig 3.9.2).

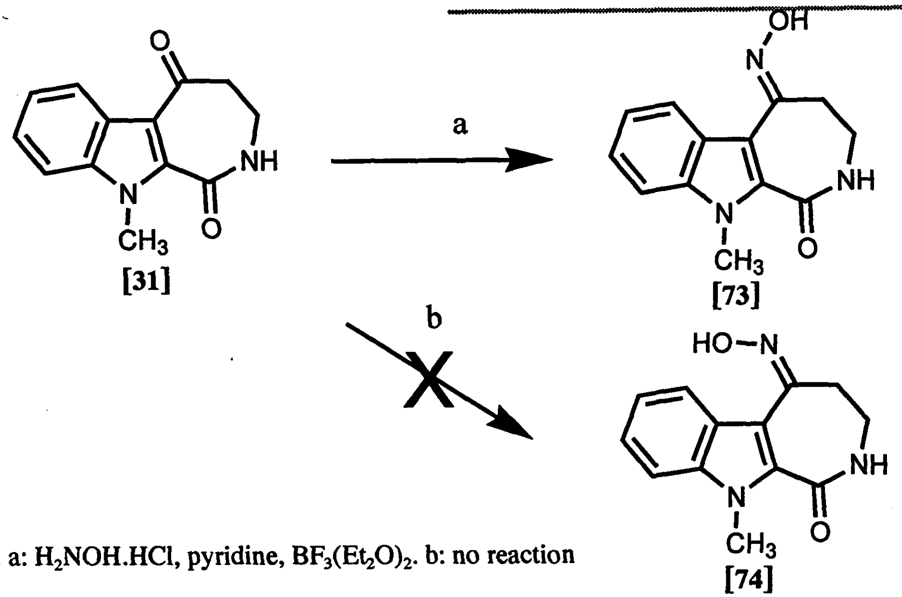

[31] [73] [74]

Fig 3.9.2: a: $H_2NOH.HCl$, pyridine, $BF_3(Et_2O)_2$. b: no reaction

In order to isolate the Z isomer **[74]**, an alternative separation method would be required. Column chromatography had been unsuccessful as the two compounds share the same R_f, and while recrystalization had been successfully used to improve the ratio, there was still an excess of the E product **[73]**. One possible route would be via a polymer-based molecularly imprinted resin that could be used as a stationary phase and retard elution of **[73]** down a column. Tentative steps were made in a collaboration to attempt this, and it would make interesting further research.

As it was clear that inversion of stereochemistry would not be possible at this time, smaller oxime extensions were investigated. The appropriate molecules needed to synthesize a series of oximes direct from the ketone were not commercially available and would need to be synthesized. A method for this was found and followed.[154,155]

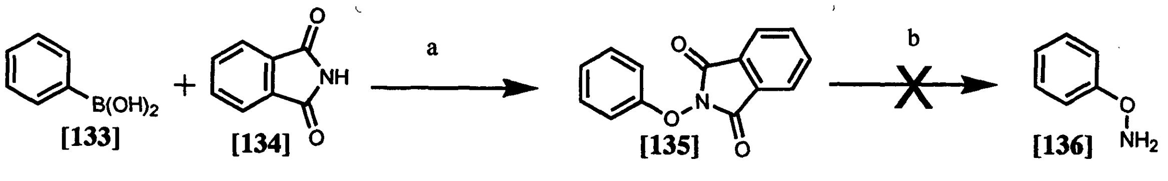

[133] [134] [135] [136]

Fig 3.9.3: a: CuI, pyridine, 3 Å molecular sieves, DCM, 36 %
b: $NH_2NH_2.H_2O$, $CHCl_3$, MeOH, 0%

N-Phenoxy phthalimide **[135]** was successfully synthesized from hydroxyphthalimide **[134]**, but the aryloxyamine **[136]** was not isolated (fig 3.9.3). In the workup procedure, the entire reaction mixture is placed on a column, and nothing was isolated from any of the column fractions. The significant safety issues surrounding the use of hydrazine monohydrate,[156,157] as well as time restraint resulted in this area of study being discontinued.

3.10 Kenpaullone Synthesis

In order to make direct comparisons between the biological results from the synthesized compounds, and published data from existing inhibitors, it was important to synthesize a known inhibitor and test this in the same conditions as used for the synthesized compounds. These results could also be used as a control to confirm the validity of the results.

It was decided that Kenpaullone **[14]** would be synthesized. Literature was found reporting the synthesis of Kenpaullone analogues, and was followed to synthesize Kenpaullone (fig 3.10.1).[87,158,159]

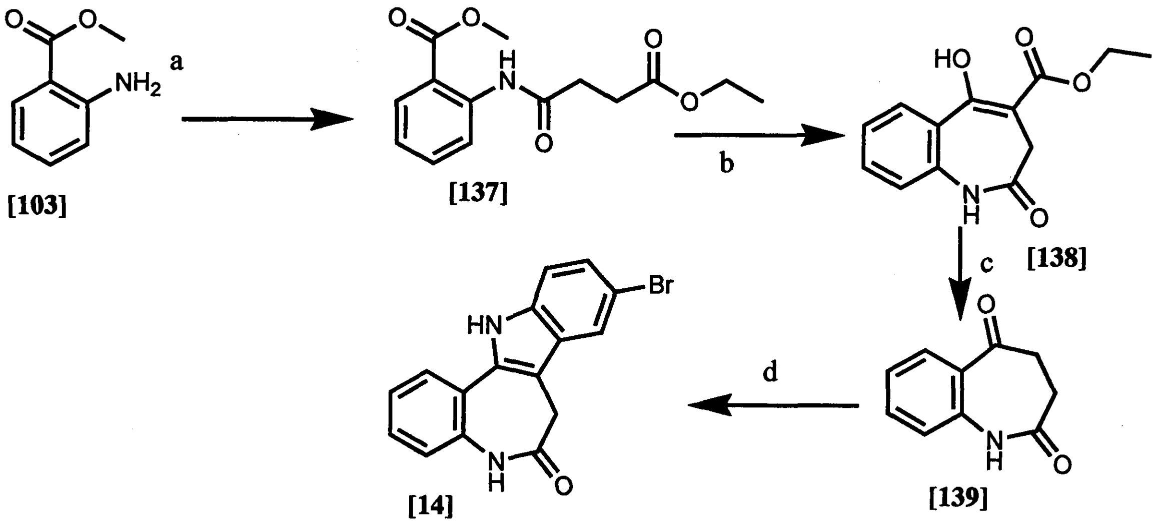

Fig 3.10.1: a: Ethyl succinyl chloride, pyridine, Δ, 52 %, b: NaH, Δ, 0%, c; DMF, Δ, d:, 4-bromo-phenyl hydrazine hydrochloride, sodium acetate.

Amide **[137]** was successfully synthesized, but the literature procedure for the next step was unsuccessful.

Further literature research suggested an alternative method for the synthesis of the key intermediate **[139]** from commercially available tetralone **[140]** via ring expansion **[141]** and oxidation (fig 3.9.2).[160]

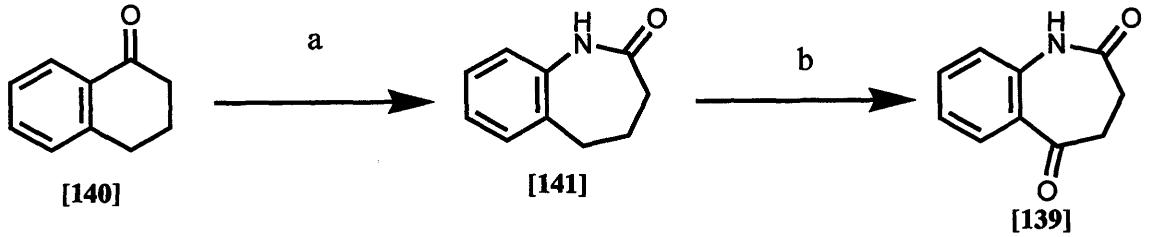

Fig 3.10.2: a: Trichloroacetic acid, sodium azide, Δ, 30 %,
b: Potassium permanaganate, magnesium nitrate hexahydrate, 11 %

This method was successful, although the yields for the two steps were quite low; 30 % (lit 57 %) for the first step and 11 % (Lit 26 %) for the second step. Intermidiate **[139]** was produced pure after two recrsytallizations.

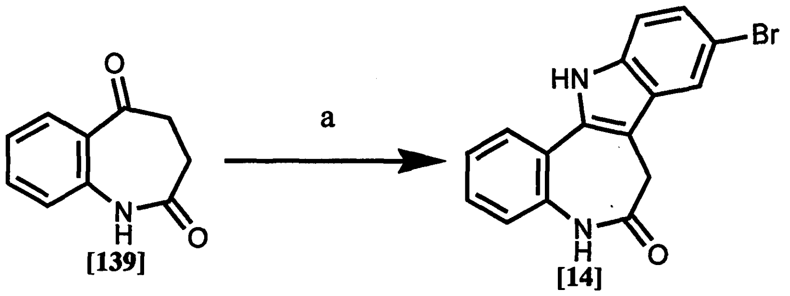

Fig 3.10.3: a: 4-bromo-phenyl hydrazine hydrochloride, sodium acetate, Δ, 37 %

The original literature was returned to for the final step to synthesize Kenpaullone **[14]**,[158] and the known inhibitor was successfully synthesized. This could now be used as comparison between literature reported biological results and those for the compounds synthesized during this study.

3.11 Synthesis Conclusions

In conclusion, a series of potential inhibitors have been designed and synthesized based on the ε-lactam ring fused to an indole as described in chapter 2. Both NH and N-methylindoloazepinones were successfully synthesized and a number of oxime and hydrazone extensions from the ketone position were achieved. Bromination of the indole ring of indoloazepinone, and an extension from its ketone position were also successful. Ultimately, suitable indole (NH) protection was not achieved, and this impacted on the number of analogues that were produced in the study.

Alterations to the lactam ring were also not achieved, with unexpected cyclization products or no reaction resulting from cyclization reactions.

The potential for improvement of activity of Z isomers was demonstrated, and synthesis of an unsubstituted Z oxime was shown to be plausible. Although the product was not isolated, this would be an exciting target for future synthetic work.

The known inhibitor Kenpaullone was also synthesized by a modified procedure to complement the series and provide a reference to published data.

4. BIOLOGICAL RESULTS 112

4.1 GROWTH INHIBITION ASSAYS 112

4.1.1 Reference compounds 113

4.1.2 Alterations in the X and R Positions 114

4.1.3 N-Methylindoloazepinone Analogues 117

4.1.4 Miscellaneous Compounds 120

4.1.5 Comparisons to Pyrrole Derivatives 121

4.2 CELL CYCLE ANALYSIS 122

4.3 CDK2/CYCLIN A INHIBITION 123

4.3.1 Reference Compounds 124

4.3.2 Synthesized Compounds 125

4.3.3 Comparisons to Pyrrole Derivatives 128

4.4 CHK2 INHIBITION 129

4.5 BIOLOGICAL CONCLUSIONS 132

4. Biological Results

The biological activity of the molecules synthesized in this project were assessed by a number of biological assays. These were conducted by the Tenovus Centre for Cancer Research in the Welsh School of Pharmacy, Cardiff University. The growth inhibition of the series of compound was determined against two cancer cell lines. Selected compounds were also tested for inhibition against the CDK2/cyclin A complex, while cell cycle analysis was carried out on one compound. KuDOS Pharmaceuticals Ltd, Cambridge, UK. also conducted assays against Chk2, a new protein kinase implicated in cell cycle control,

4.1 Growth Inhibition Assays

Growth inhibition assays were carried out against the MCF-7 human breast cancer cell line, as well as the A549 small cell lung cancer cell line. MCF-7 is derived from epithelial cells in breast carcinoma and in widely used for testing of this nature. There are no major aberrations apparent in the cell line, and they are easy to grow in culture.[161] A549 meanwhile, which has been largely studied in recent years, is a cell line derived from type II alveolar epithelial cells in lung carcinoma, and is similarly easy to work with in culture.[162]

Results are quoted as 50 % Growth Inhibition (GI_{50}) values. GI_{50} is the concentration required to inhibit 50 % of cell growth compared to a control, and results with a GI_{50} value in excess of 100 μM were considered to be inactive.

4.1.1 Reference Compounds

Two known inhibitors, Kenpaullone **[14]** (the synthesis of which is described in chapter 3.10) and NU2058 **[6]**, which was synthesized by another research team,[163] were used as reference compounds in order to gauge the synthesized compounds' potency compared to known inhibitors (table 4.1.1).

Compound Number	Structure	MCF-7 GI_{50} (μM)	A549 GI_{50} (μM)	ClogP[a]
14	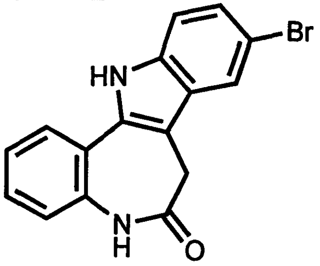	4	NT	3.8
6	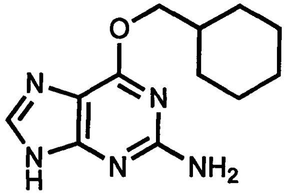	72	NT	3.5

Table 4.1.1: Known inhibitors. NT: Not Tested.[a] ClogP calculated using Chemdraw Ultra.

Kenpaullone **[14]** showed good activity against the MCF-7 cell line, while interestingly NU2058 **[6]** was only modestly active against this cell line.

4.1.2 Alterations in the X and R Positions

Analysis of the compounds displayed in table 4.1.2 was used to evaluate the impact of the incorporation of a methyl group in the R position, or a bromine atom in the X position.

The lead compound indoloazepinone **[25]** was essentially inactive against the MCF-7 cell line. Due to it being the lead compound of the study, higher concentration assays were conducted. These showed that the compound did have some limited inhibition. The unsubstituted oxime **[87]** was also inactive against MCF-7, although it did show modest activity again the A549 cell line.

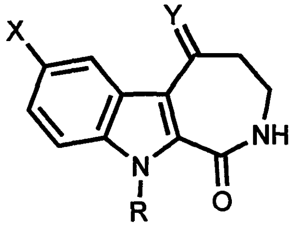

Compound Number	R	X	Y	MCF-7 GI$_{50}$ (μM)	A549 GI$_{50}$ (μM)	ClogP[a]
31	CH_3	H	O	61	NT	1.3
25	H			223	NT	0.9
57	H	Br		ND[b]	NT	1.8
73	CH_3	H	NOH	69	NT	1.8
87	H			> 100	89	1.2
86	H	Br		46	7	2.2
75	CH_3	H	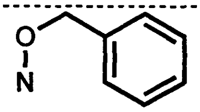	NT[c]	NT[c]	4.3
88	H			10	47	3.8
76	CH_3	H	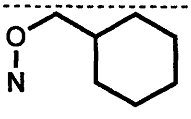	7	> 100	5.1

Table 4.1.2:. NT: Not Tested. ND: Not Determined. [a] ClogP calculated using Chemdraw Ultra. [b] bacterial growth promotion. [c] Not stable in the culture medium.

Blocking the indole (NH) with a methyl group had been expected to decrease the activity of the compound, as it would only be able to form two hydrogen bonds to the backbone residues in the active site of CDK2 as seen in chapter 3. However, the opposite effect was the case. Blocking the indole (NH) resulted in a 3.5 fold increase in the growth inhibitory activity of the ketone **[31]**, and this compound, along with the unsubstituted oxime **[73]** showed modest growth inhibition against MCF-7. These results were comparable to the known inhibitor NU2058.

Evidently the loss of the hydrogen bond is well compensated by the presence of the methyl group. The presence of the methyl group does slightly enhance the lipophilicity of the compound, possibly improving its ability to traverse the cell membrane. However, indoloazepinone **[25]** is still inside the ideal ClogP range of 0-5 (as described in Lipinski's "rule of five"),[164] and there is only a slight improvement in lipophilicity when the methyl group is added. It is also possible that the methyl group can form favourable interactions in the active site of CDK2, possibly a hydrophobic interaction with phenyl ring of Phe82. Alternatively, the N-methylindoloazepinone motif could be favourable for interaction with an alternative cell cycle anti-proliferative target.

The incorporation of bromine had been seen to have a positive effect on inhibition for both Hymenialdisine and Kenpaullone, as discussed earlier. This desired effect was evident with the unsubstituted oxime **[86]**, which showed good inhibition of A549 cells, and modest activity against MCF-7 cells. Intriguingly, the assay of the ketone analogue **[57]** resulted in significant bacterial growth in the cell culture medium. This strange outcome affected the cell growth and invalidated the measurement of cell numbers. This contamination was not seen in the control sample, or in any other experiments attempted with other compounds. However, it occurred consistently with **[57]** when the assay was repeated twice more with samples synthesized and stored independently implying that **[57]** in some way acts to promote bacterial growth, although how this occurs is unclear.

The unsubstituted oxime held no significant advantage over the ketone in the unbrominated compounds. Indeed, the N-methyl unsubstituted oxime **[73]** was, if anything, slightly less active than the ketone pre-cursor **[31]**. Unfortunately due to the bacterial anomaly, comparisons could not be drawn between the brominated compounds.

While it was not possible to have a direct comparison of substituted oximes due to the instability in the culture medium of **[75]**, both extended oximes that were tested showed good activity against the MCF-7 cell line, although their activity was markedly reduced against A549, with **[76]** being inactive.

This compound was noticeable as it had by far the highest ClogP out of all the synthesized compounds, and was actually slightly outside the ideal range of 0-5. This high lipophilicity does not appear to have a negative effect in the MCF-7 cell line, although it could play a part in the disappointing inactivity against A549.

4.1.3 N-Methylindoloazepinone Analogues

The majority of compounds successfully extended in the Y position were of the N-methylindoloazepinone series. Comparisons of these compounds could be used to compare the benefits of these extensions, and reveal the most advantageous features (table 4.1.3).

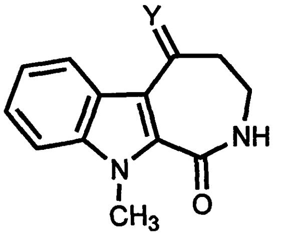

Compound Number	Y	MCF-7 GI_{50} (μM)	A549 GI_{50} (μM)	ClogP[a]
31	O	61	NT	1.3
73	NOH	69	NT	1.8
65	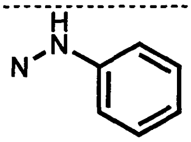	3	27	3.2
68	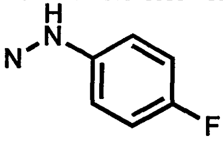	5	46	3.5
72	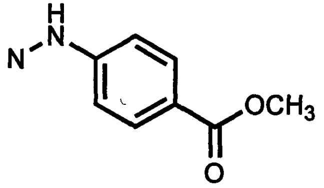	6	5	3.4
76	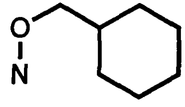	7	> 100	5.1

Table 4.1.3:. NT: Not Tested. [a] ClogP calculated using Chemdraw Ultra.

As seen with the oxime extensions (table 4.1.2), the incorporation of the bulky lipophilic extension vastly increased the inhibitory effect of the molecule. This good activity was present throughout the hydrazone series, with all extended N-methylindoloazepinones exhibiting GI_{50} activity at concentrations below 10 μM when assayed against the MCF-7 cell line. The beneficial effects of a bulky ring suggest that this portion of the molecule can interact with a lipophilic pocket in the target binding site. However, the lack of disparity in activity between the five extended compounds suggests that the pocket lacks the ability to form any explicitly favourable interactions with any of the different groups. Hydrazones **[68]** and **[72]** have additional substituents with the capacity to accept hydrogen bonds via the 4-substituent. There is no marked improvement compared to **[65]**, which does not have this feature, implying that no additional hydrogen bonding occurs. Additionally, the putative pocket could also accommodate extra chain length prior to the bulky group. This was displayed by the oximes, and again the activity against MCF-7 was not altered.

The only compound to couple an indole NH with a sizable extension from the ketone position (i.e., hydrazone or O-substituted oxime) was **[88]**. This compound has the potential to form three hydrogen bonds in the active site, as well as having an extension with the potential to make positive interactions with the ATP cleft of the active site. Therefore, this compound was predicted to be the most active compound of the series.

The extension was clearly important, with all compounds containing a bulky substituent having good activity against MCF-7, while none of the compounds without this feature showed anything more than modest activity against this cell line. However, it would appear from these results that the ability to form three hydrogen bonds in the active site considered so crucial in the design of the molecules was fairly irrelevant to their activity. Indeed, if anything, the N-methyl group improved activity, despite the compounds only having the ability to form two hydrogen bonds to the backbone residues of the active site.

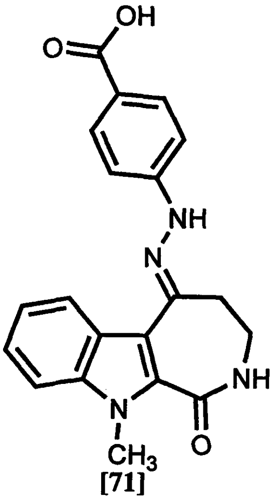

[71]

In contrast to the MCF-7 cell line, there were only two compounds that showed good activity against A549 cells. Carboxylic acid methyl ester **[72]** retained sub 10 μM activity against both cell lines, but it is important to consider the possibility that **[72]** acts as a pro-drug with cellular hydrolysis releasing the carboxylic acid **[71]**. Also the brominated compound **[86]** showed good activity against this cell line, compared to only modest activity against MCF-7 cells. Clearly the two cell lines possess differences, for instance there is hormonal regulation in breast cancer, which is not the case for lung cancer. While the reason for the inconsistent activity of **[86]** compared to the other compounds cannot be rationalised at this point, it does highlight the importance of screening compounds against multiple cell lines to avoid missing potentially important results.

4.1.4 Miscellaneous Compounds

Compound Number	Structure	MCF-7 GI_{50} (μM)	A549 GI_{50} (μM)	ClogP[a]
101	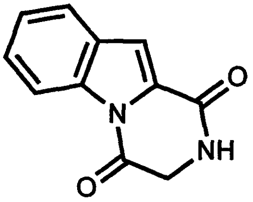	100	100	0.9
104	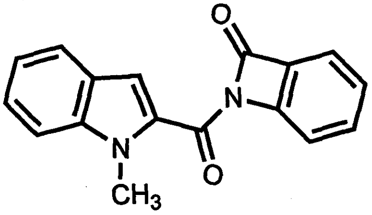	52	81	2.8
107	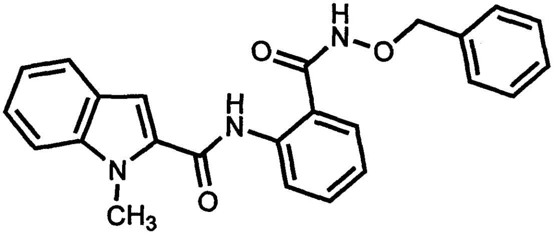	5	NT	4.2

Table 4.1.4:. Miscellaneous compounds. NT: Not Tested. [a] ClogP calculated using Chemdraw Ultra.

The alternative cyclization compound **[101]** showed weak inhibiting effect against both cell lines, with both results right on the self-imposed activity borderline of 100 μM. The benzoazetone **[104]** showed modest activity against both cell lines, while the ring-opened extension **[107]** showed good activity comparable to both Kenpaullone and the extended indoloazepinones. Unfortunately this compound was not assayed against the A549 cell line, but this family of compounds certainly warrants further study.

4.1.5 Comparisons to Pyrrole Derivatives

The known inhibitor Hymenialdisine was based on a pyrroloazepinone scaffold. It would be interesting to compare the indoloazepinone series with their pyrrolo counterparts to reveal the influence of this additional fused benzene ring. A parallel study in the research group had produced some compounds from which direct comparisons could be drawn (table 4.1.5).[165]

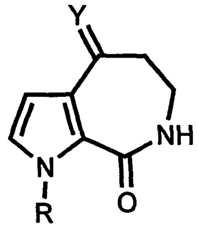

Compound Number	R	Y	MCF-7 GI$_{50}$ (μM)
142	H	O	> 100
143	CH_3	O	> 100
144	CH_3	NOH	> 100
145	CH_3	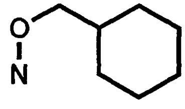	46
146	H	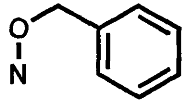	> 100
147	H	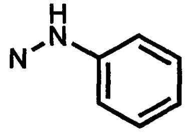	6

Table 4.1.5:. Pyrrolo compounds.

The hydrazone, (while not a direct comparison due to the absence of the N-methyl blocking group) was the only one of the pyrrolo series to show good activity. The aliphatic oxime showed modest activity, while all other comparative compounds were inactive. This data clearly demonstrates that the fused benzene ring of the indolo series greatly enhances the activity of the compounds.

4.2 Cell Cycle Analysis

Cell cycle analysis provides evidence for where in the cell cycle an inhibitor is acting. This series of compounds were intended as CDK2/cyclin A inhibitors. If this were indeed their mode of action, then the cell cycle would be arrested at the G_1/S transition. This would lead to an accumulation of cells in the G_1 phase, and a decrease in the concentration of cells in the S and G_2/M phases compared with a control sample of cells with no inhibitor.

	Percentage of Cells – 48 h			**Percentage of Cells – 7 days**		
	G_0/G_1	**S**	**G_2/M**	**G_0/G_1**	**S**	**G_2/M**
Control	53.7	32.5	13.8	78.9	12.8	8.3
65	61.1	27.3	11.6	84.3	10.7	5

Table 4.2.1:. Cell cycle analysis. **[65]** at 10 μM with MCF-7 cells against a control of MCF-7 cells with no drug.

The most active compound against the MCF-7 cell line assay was the hydrazone **[65]**, and this compound was used for the cell cycle analysis. The assay was consistent with hypothesis of **[65]** as a CDK2 inhibitor, with an increase in the concentration of cells in the G_0/G_1 phase and a decrease across the rest of the cell cycle. However, the effect was moderate indicating that while some CDK2/cyclin A inhibition may be occurring, it would not account for the good *in vitro* results of this and related compounds, implying that another biological target or mechanism is also involved.

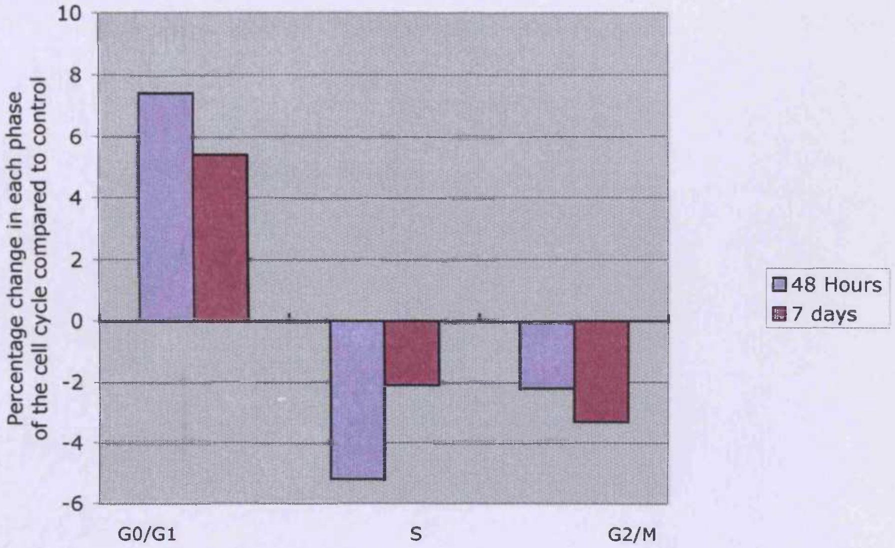

Fig 4.2.1: Cell cycle analysis of **[65]** at 10 μM with MCF-7 cells against a control of MCF-7 cells with no drug.

4.3 CDK2/Cyclin A Inhibition

The theoretical target for the compounds was the CDK2/cyclin A complex. A number of the compounds had shown good inhibitory effects when assayed against cell lines, and cell cycle analysis had indicated that the series was acting to stop cells passing through the G_1/S phase transition. Selected compounds were therefore tested against this CDK2/cyclin A complex to establish if it was indeed their site of action.

Radiolabelled ATP (^{32}P on the γ-phosphate) was used as the substrate for the CDK2/cyclin A complex, and the assay measured the phosphorylation of Histone 1. The percentage of phosphorylation of the Histone protein at various concentrations of inhibitor was then calculated.

The concentration required to inhibit 50 % of Histone phosphorylation (IC_{50}) was recorded where it was less than 100 μM. The assay was carried out at concentrations of 1, 10 and 100 μM. Therefore, as with the GI_{50} values, IC_{50} values above 100 μM could not be accurately calculated.

Percentage inhibition at 10 μM is also displayed, as a means to compare compounds with lower activities than 100 μM.

4.3.1 Reference Compounds

Compound Number	Structure	% Inhibition at 10 μM	Observed CDK2/CyclinA IC_{50} (μM)	Reported CDK2/CyclinA IC_{50} (μM)
14	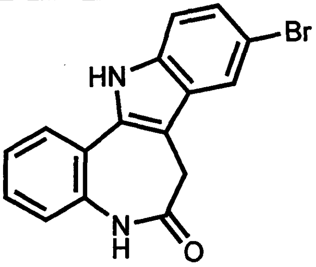	28 %	53	0.68
6	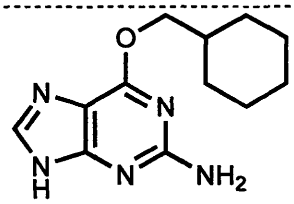	55 %	6	17

Table 4.3.1:. CDK2 activity represented as percentage of non-phosphorylated histone 1 compared to control.

Both of the reference inhibitors were assayed, and they showed clear discrepancies when compared with the published results for these compounds. NU2058 [6] was twice as active as reported, while conversely [14] was over 70-fold less active than published results indicate. This could be due to a number of factors including human error, subtle differences in technique, purity of samples or partial degradation of the radiolabelled ATP. This is an important observation, indicating that direct comparison to data collected from different sources may lead to incorrect conclusions being drawn. Ideally, all the inhibitors displayed in chapter 1 would be assayed at the same time and place, although of course this is impractical.

4.3.2 Synthesized Compounds

Due to restraints of available assay material, only selected compounds were assayed against the CDK2/cyclin A complex. Good cellular activity was used as a selection criteria for the kinase assay. The three hydrazones and the two extended oximes had shown good activity *in vitro*, and were assayed. This would enable comparisons to be drawn based on the extensions from the ketone position, and also the effect of blocking the potential third hydrogen bond with the N-methyl compounds compared to the indole (NH) oxime **[88]**. The brominated unsubstituted oxime had also shown good activity *in vitro*, and was assayed along with its non-brominated equivalent **[87]**.

Unfortunately, the assay of **[72]** failed, but there was no activity at all for the other hydrazones, presumably either due to the presence of the N-methyl blockage and, or, because of the influence of the hydrazone extension. As **[72]** contains both of these features, it is reasonable to assume that it too would have displayed no activity had the assay been successfully completed. This is consistent with the molecular modelling studies presented in the previous chapter, which predicted that the N-methyl Indoloazepinones with a hydrazone extension might not be accommodated within the active site of this protein.

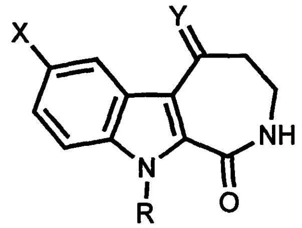

Compound Number	R	X	Y	% Inhibition at 10 μM
65	CH_3	H	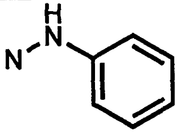	0 %
68	CH_3	H	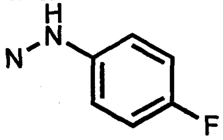	0 %
72	CH_3	H	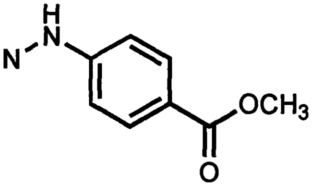	NT[a]
76	CH_3	H	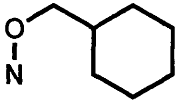	12 %
88	H	H	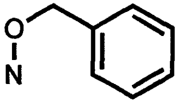	32 %
87	H	H	NOH	0 %
86	H	Br	NOH	45 %

Table 4.3.2:. CDK activity represented as percentage of non-phosphorylated histone 1 compared to control. [a]Assay failed.

In contrast, despite being a larger extension, moderate inhibition was seen for both O-substituted oxime compounds. The oximes therefore appear to be better CDK ligands than the hydrazones, possibly the extra chain length allows more flexibility of the extension allowing it to fit into the binding pocket more effectively.

Oxime [88] has the capacity to form three hydrogen bonds, so this would be the logical reason for the improvement in activity compared to **[76]**. However, the oxime extensions of the two compounds were different. The methyl-cyclohexyl ring of **[76]** could be an advantageous feature, as it is more flexible, and therefore more able to achieve a good fit in the active site. However, it could also be detrimental, being more bulky, and that could be the reason for the lower activity compared to **[88]**. Again, the instability of **[75]** proved to be a major disappointment, as this compound would have allowed a direct comparison between the two oxime extensions.

Incorporation of bromine had a considerable effect *in vitro*, and **[86]** again showed good results in the CDK2/cyclin A assay, whereas the unbrominated compound **[87]** was inactive. Both compounds are examples of the ideal hydrogen bonding pattern, and have an unsubstituted oxime extension. The lack of any activity for **[87]** implies that this hydrogen bonding motif alone is not sufficient for inhibition. In stark contrast, the brominated compound gave the best results with an IC_{50} value calculated at 25 μM, which is comparable to known CDK inhibitors. The second most active compound in this series, **[88]** gave a % inhibition value less than 50 %, not permitting an accurate IC_{50} measurement.

Clearly inhibition of CDK2 does not account for the excellent *in vitro* activity of the compounds, with only one compound **[86]** showing good activity against the protein complex. Even this compound was more active in the cell lines than against the protein it was designed to target. This suggests that the compounds are targeting another biological target associated with proliferation or a cell cycle associated protein.

4.3.3 Comparisons to Pyrrole Derivatives

The pyrroloazepinone series discussed previously was drawn on in an attempt to clarify the situation concerning the O-substituted oximes. Unlike the indoloazepinones, in the di-bromo pyrroloazepinone series, both the NH and N-methyl compounds formed stable benzyl oximes.[165] This allowed a direct comparison that was not possible in the indoloazepinone series.

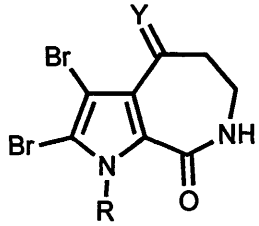

Compound Number	R	Y	% Inhibition at 10 μM
148	Me	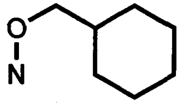	13 %
149	Me	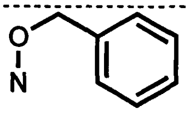	22 %
150	H		Inactive

Table 4.3.3: CDK activity represented as percentage of non-phosphorylated histone 1 compared to control.

Interestingly, the removal of the methyl group allowing the compound to form the full complement of hydrogen bonds resulted in an inactive compound, rather than the predicted increase in activity. Also incorporation of the methyl-cyclohexyl ring produced a decrease in activity compared to the benzyl compound. This change was not as great as seen with the indoloazepinone oximes, and the data is far from conclusive. However, these results do indicate that it could be the alteration in oxime extension that is causing the change in activity between **[76]** and **[88]**, rather than the free indole NH that had been predicted to play such a crucial role in the binding of the compounds in the active site.

4.4 Chk2 Inhibition

The series of compounds had been synthesized with the objective of inhibiting the CDK2/cyclin A complex. While good activity had been seen in *in vitro* cellular growth assays, the target complex was clearly not the site of action. An alternative target was sought, and the Chk2 protein introduced in chapter 1 was proposed as a possible target. A number of CDK2 inhibitors have been shown to also be active against this enzyme, significantly including debromohymenialdisine **[151]**.[31]

Cancer cells usually, if not always have checkpoint defects. This distinguishes them from other cells, providing a potential therapeutic target. Inhibition of remaining checkpoints, such as Chk2, could enhance the impact of DNA-damaging drugs or radiation. Normal cells could still activate other checkpoints and recover from the temporary cell cycle arrest resulting from the treatment. Tumours with one or more defective checkpoints however, could be deprived of their remaining checkpoint pathways and ultimately cell death may result from the excessive DNA damage.[166]

Compound Number	**Structure**	**Observed Chk 2 IC_{50} (μM)**	**Reported Chk 2 IC_{50} (μM)**
151	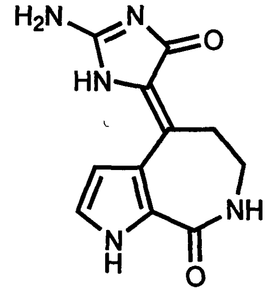	-	3
14	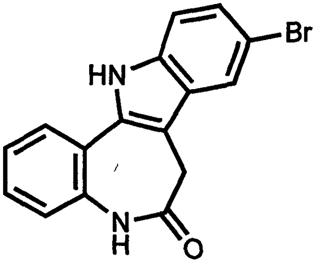	0.84	-
6	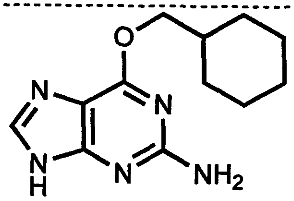	> 100	-

Table 4.4.1:. Chk2 inhibition by known inhibitors.

The two control compounds were assayed (table 4.4.1), with Kenpaullone showing good activity. Interestingly, this feature of Kenpaullone does not appear to have been reported previously. However, all the synthesized compounds that were assayed were found to be inactive as Chk2 inhibitors, with IC_{50} values in excess of 100 μM (Table 4.4.2).

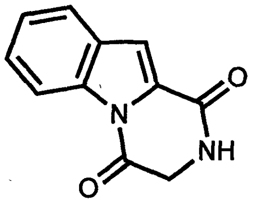

[101]

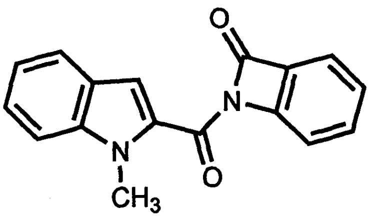

[104]

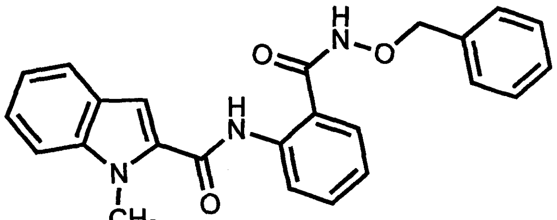

[107]

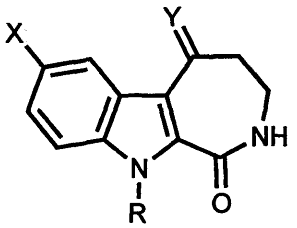

Compound Number	R	X	Y	Chk 2 IC_{50} (μM)
101	-	-	-	> 100
104	-	-	-	> 100
107	-	-	-	> 100
31	CH_3	H	O	> 100
73	CH_3	H	NOH	> 100
76	CH_3	H	$NOCH_2C_6H_{11}$	> 100
65	CH_3	H	$NNHC_6H_5$	> 100
68	CH_3	H	$NNHC_6H_4F$	> 100
72	CH_3	H	$NNHC_6H_4COOCH_3$	> 100
25	H	H	O	> 100
57	H	Br	O	> 100
88	H	H	$NOCH_2C_6H_5$	> 100

Table 4.4.2: Chk2 Activity of the synthesized compounds

The pyrrole series also exhibited no activity when assayed against Chk2. In some cases, such as **[142]**, **[147]** and **[152]**, the only variation between their structure and that of debromohymenialdisine was the aminoimidazolidinone moiety of debromohymenialdisine. This feature would therefore appear to play a major role in the ability of debromohymenialdisine to inhibit Chk2.

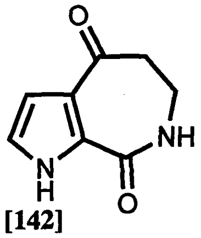

[142]

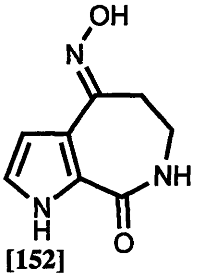

[152]

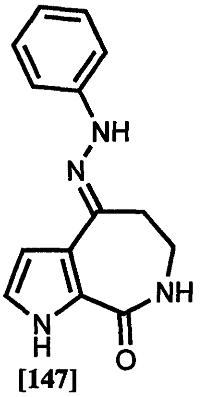

[147]

The only compound to show sub 100 μM activity against the CDK2/cyclin A complex was **[86]**, so it was unfortunate that this compound was not tested against Chk2. As none of the other compounds displayed sub 100 μM activity in either assay, and percentage inhibition at 10 μM was not recorded for the Chk2 assay, comparison of activity against the two proteins was not possible.

Nevertheless, it was clear that neither CDK2, nor Chk2 was responsible for the good *in vitro* growth inhibition results for this series of compounds. No further assays have been carried out against other cell cycle proteins, so the site of action remains unidentified. The results do indicate that the target protein (or proteins) has some regulatory effect on the transition through the G_1 to S phase, and would appear to play a significant role in cell cycle control.

4.5 Biological Conclusions

In conclusion, a series of compounds have been synthesized with good *in vitro* growth inhibition against the MCF-7 breast cancer cell line, and moderate activity against the A549 lung cancer cell line. Notable compounds were the hydrazone **[72]**, which showed good activity against both cell lines and the brominated compound **[86]** which showed considerable improvement compared with the unbrominated analogue, particularly against the A549 cell line.

Cell cycle analysis of **[65]** showed cell accumulation in the G_0/G_1 phase, consistent with CDK2 inhibition. The CDK2/cyclin A inhibition assay however showed only moderate inhibition. It would therefore appear that CDK2 inhibition is not the main mechanism of action of these compounds, but they are active against another, as yet unidentified target within the cell. The one exception to the CDK2/cyclin A activity was **[86]**. This novel compound showed promising inhibition with an IC_{50} of 25 μM, and has excellent potential for further development.

The novel and unexpected β-lactam compound **[104]** showed modest activity, while its ring-opened oxime **[107]** showed good activity against the MCF-7 cell line. This interesting class of compounds will also need further future investigation.

5. Conclusion

The syntheses of indoloazepinone **[25]** and N-methylindoloazepinone **[31]** were successfully achieved, and derivatives were generated from these molecules providing the anti-proliferative structure activity relationships proposed in this thesis (fig 5.1).

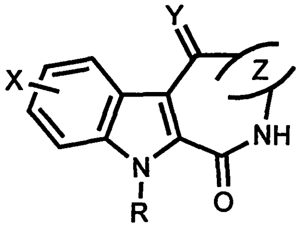

Fig 5.1: Proposed modifications of the molecule. Indoloazepinone **[25]** R=H, X=H, Y=O, Z=CH_2CH_2. N-methyl indoloazepinone **[31]** R=CH_3, X=H, Y=O, Z=CH_2CH_2.

Extension from the ketone functional group (Y position) was achieved with 3 hydrazone and 3 oxime extensions of the N-methyl series, although attempts to synthesize further derivatives in this position were unsuccessful.

Bromination of the indole in the X position was achieved for indoloazepinone **[25]**, but extension from the Y position with these indole (NH) compounds proved very challenging. Whilst the unsubstituted oxime of both indoloazepinone and bromo-indoloazepinone were generated, only one O-substituted indoloazepinone oxime, and no hydrazones, was successfully synthesized. Despite extensive attempts, the required protecting group could not be found to facilitate the synthesis of further compounds based on the indoloazepinone scaffold.

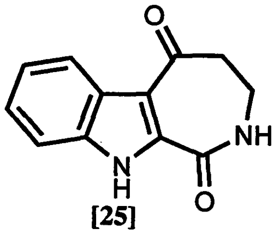

[25]

All extensions from the ketone position were found to be E isomers. Molecular modelling suggested that the Z isomers might be a more suitable fit in the active site of the intended biological target CDK2, but purification of a Z isomer formed was not achieved.

Alteration of the size of the lactam ring was not achieved, with cyclization unsuccessful with both reduced and increased ring size. However the cyclization of the reduced ring size with the indole (NH) compound resulted in an alternative cyclization to the indole NH. Attempts to synthesize an indoloazepinone with a phenyl ring fused to the lactam resulted in another unexpected cyclization; forming benzoazetone **[104]**, which yielded the ring opened derivative **[107]** when oxime extension was attempted.

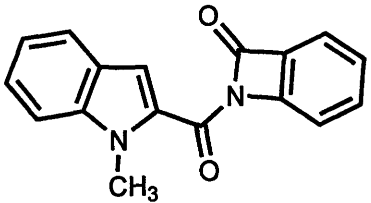

[104]

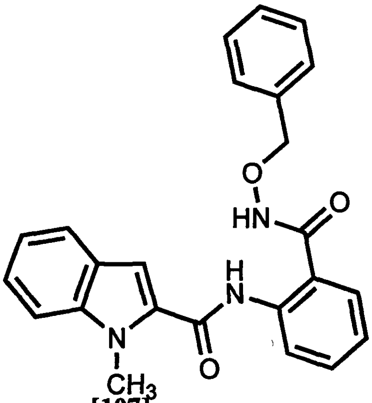

[107]

The known CDK inhibitor Kenpaullone was successfully synthesized by a modified procedure, as a reference compound, and the series was assayed for biological activity.

Good results were seen in anti-proliferative *in vitro* cellular assays, with all hydrazones and O-substituted oximes having a GI_{50} of 10 μM or less against the MCF-7 cell line. The compounds were generally less active against the A549 cell line with only **[72]** retaining sub 10 μM activity. However, the bromo indoloazepinone unsubstituted oxime **[86]** had the opposite activity, and displayed good inhibition against A549 compared with only moderate inhibition of MCF-7.

Cell cycle analysis implied inhibition was occurring in the G_1/S phase transition, although only moderate activity was seen against the proposed target protein complex with O-substituted oximes, while hydrazones were completely inactive. The exception again was **[86]** with an IC_{50} of 25 μM against the CDK2/cyclin A complex.

The three most interesting outcomes of this project were the brominated compound **[86]**, the carboxylic acid ester hydrazone **[72]** and the β-lactam compound synthesized while attempting to form benzo-fused lactam analogue. Compound **[86]** showed good activity against the CDK2/cyclin A complex, as well as good activity against the A549 cell line, and has scope for further investigation. Hydrazone **[72]** showed good activity against both cell lines, and was clearly the best compound *in vitro*. Meanwhile, the ring opened β-lactam **[107]** showed good activity against MCF-7, and also warrants further study.

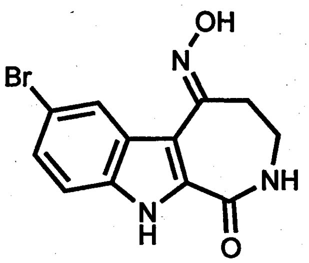

[86]

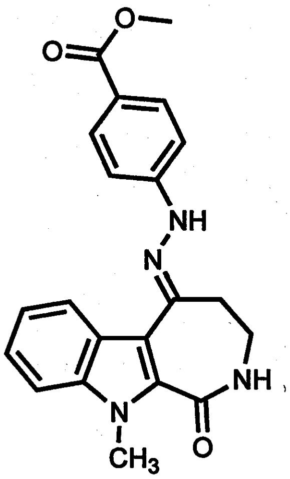

[72]

In conclusion, small molecules based on the interesting indoloazepinone pharmacophore displaying good tumour growth inhibition have been synthesized. Two novel pharmacophores have been produced which also warrant further study. The site of action of this series of compounds remains unclear, and further experimentation to establish the intracellular target would be of great interest.

6. EXPERIMENTAL **140**

6.1 GENERAL METHODS 140

6.1.1 Thin Layer Chromatography *140*

6.1.2 Column Chromatography *140*

6.1.3 NMR Spectroscopy *140*

6.1.4 Mass Spectrometry *140*

6.1.5 Infrared Spectroscopy *141*

6.1.6 Melting point *141*

6.1.7 Cooling Baths *141*

6.2 GENERAL PROCEDURES 142

Method A – Indole N protection *142*

Method B – Amide bond formation (i) *142*

Method C – Amide bond formation (ii) *143*

Method D –Hydrolysis *143*

Method E – Cyclization *143*

Method F – Extension from ketone position (i) *144*

Method G – Extension from ketone position (ii) *144*

Method H – Extension from oxime *144*

Method I - Bromination *145*

Method J Cyclization (ii) *145*

Method K Esterification *145*

Ethyl 1H-indole-2-carboxylate [32] *146*

1-Methyl-1H-indole-2-carboxylic acid [34] *146*

1-Benzyl-1H-indole-2-carboxylic acid [39] *147*

2,10-bis((2-(Trimethylsilyl)ethoxy)methyl)-3,4-dihydroazepino [3,4-b]indole-1,5(2H,10H)-dione [77] *147*

3-Bromo-1-methyl-1H-indole-2-carboxylic acid [114] *148*

1-(4-Methoxybenzyl)-1H-indole-2-carboxylic acid [80] *148*

Ethyl 3-(1-methyl-1H-indole-2-carboxamido)propanoate [35] *148*

Methyl 2-(1-methyl-1H-indole-2-carboxamido)benzoate [153] *149*

Ethyl 3-(1-benzyl-1H-indole-2-carboxamido)propanoate [40] *149*

Ethyl 3-(1H-indole-2-carboxamido)propanoate [52] *150*

Ethyl 2-(1H-indole-2-carboxamido)acetate [117] *150*

Ethyl 2-(1-methyl-1H-indole-2-carboxamido)acetate [154] *151*

Ethyl 3-(3-bromo-1-methyl-1H-indole-2-carboxamido)propanoate [63] *151*

Ethyl 3-(1-(4-methoxybenzyl)-1H-indole-2-carboxamido) propanoate [82] *152*

Ethyl 4-(1H-indole-2-carboxamido)butanoate [120] *152*

N-(2-(N-Methoxy-N-methylcarbamoyl)ethyl)-3-bromo-1-methyl-1H-indole-2-carboxamide [116] *153*

N-(3-(N-Methoxy-N-methylcarbamoyl)propyl)-3-bromo-1H-indole-2-carboxamide [121] *153*

N-((N-Methoxy-N-methylcarbamoyl)methyl)-3-bromo-1H-indole-2-carboxamide [118] *154*

N-(2-(N-Methoxy-N-methylcarbamoyl)ethyl)-3-bromo-1H-indole-2-carboxamide [119] *154*

3-(1-Methyl-1H-indole-2-carboxamido)propanoic acid [37] *155*

2-(1-Methyl-1H-indole-2-carboxamido)acetic acid [102] *155*

2-(1-Methyl-1H-indole-2-carboxamido)benzoic acid [103] *156*

3-(1H-Indole-2-carboxamido)propanoic acid [27] *156*

2-(1H-Indole-2-carboxamido)acetic acid [99] *156*

3-(3-Bromo-1H-indole-2-carboxamido)propanoic acid) [157] *157*

3-(3-Bromo-1-methyl-1H-indole-2-carboxamido)propanoic acid [115] *157*

4-(3-Bromo-1H-indole-2-carboxamido)butanoic acid [155] *158*

2-(3-Bromo-1H-indole-2-carboxamido)acetic acid [156] *158*

4-(1H-Indole-2-carboxamido)butanoic acid [100] *159*

3-(1-Benzyl-1H-indole-2-carboxamido)propanoic acid [41] *159*

3,4-Dihydro-10-methylazepino[3,4-b]indole-1,5(2H,10H)-dione [31] *160*

3,4-Dihydroazepino[3,4-b]indole-1,5(2H,10H)-dione [25] *160*

2,3-Dihydro-pyrazino[1,2-a]indole-1,4-dione [101] *161*

1-(1-methyl-1H-indole-2-carbonyl)benzo[b]azet-2(1H)-one [104] *161*

(E)-5-(2-Phenylhydrazono)-2,3,4,5-tetrahydro-10-methylazepino[3,4-b]indol-1(10H)-one [65] *162*

(E)-5-(2-(4-Fluorophenyl)hydrazono)-2,3,4,5-tetrahydro-10-methylazepino[3,4-b]indol-1(10H)-one [68] *162*

(E)-5-(2-(4-Carboxylic acid methyl ester)hydrazono)-2,3,4,5-tetrahydro-10-methylazepino[3,4-b]indol-1(10H)-one [72] *163*

(E)-2,3,4,5-Tetrahydro-5-(hydroxyimino)-10-methylazepino[3,4-b]indol-1(10H)-one [73]. *164*

(E)-5-(2-Phenylhydrazono)-2,3,4,5-tetrahydroazepino[3,4-b]indol-1(10H)-one [64] *164*

(E)-2,3,4,5-Tetrahydro-5-(hydroxyimino)azepino[3,4-b]indol-1(10H)-one [87] *165*

(E)-7-Bromo-2,3,4,5-tetrahydro-5-(hydroxyimino)azepino[3,4-b]indol-1(10H)-one [86] *165*

(E)-5-(Benzyloxy)imino-2,3,4,5-tetrahydroazepino[3,4-b]indol-1(10H)-one [88] *166*

N-(2-(Benzyloxycarbamoyl)phenyl)-1-methyl-1H-indole-2-carboxamide [107] *167*

(E)-5-(benzyloxy)imino-2,3,4,5-tetrahydro-10-methylazepino[3,4-b]indol-1(10H)-one [75] *167*

(E)-5-(Cyclohexylmethoxy)imino-2,3,4,5-tetrahydroazepino[3,4-b]indol-1(10H)-one [76]. *168*

Ethyl 3-(3-bromo-1H-indole-2-carboxamido)propanoate [56] *169*

7-Bromo-3,4-dihydro-2H,10H-azepino[3,4-b]indole-1,5-dione [57] *169*

Ethyl 3-bromo-1H-indole-2-carboxylate [113] *169*

Ethyl 4-(3-bromo-1H-indole-2-carboxamido)butanoate [158] *170*

Ethyl 2-(3-bromo-1H-indole-2-carboxamido)acetate [159] *170*

N-((Methoxycarbamoyl)methyl)-3-bromo-1H-indole-2-carboxamide [122] *171*

N-(3-(Methoxycarbamoyl)propyl)-3-bromo-1H-indole-2-carboxamide) [123] and 3-Bromo-N-(5,5-dimethyl-4-oxohexyl)-1H-indole-2-carboxamide [124] *171*

β-Alanine ethyl ester hydrochloride [36] *172*

Methyl 4-hydrazinylbenzoate hydrochloride [70] *172*

Ethyl 1-tosyl-1H-indole-2-carboxylate [44] *173*

Phenylmagnesium bromide [47] *173*

Diphenyl-4-pyridylmethanol [49] *174*

Diphenyl-4-pyridylmethyl Chloride Hydrochloride [50] *174*

2-(3-Ethoxycarbonyl-propionylamino)-benzoic acid methyl ester [137] *175*

4,5-Dihydro-1H-benzo[b]azepin-2(3H)-one [141] *175*

3,4-Dihydro-1H-benzo[b]azepine-2,5-dione [139] *176*

Kenpaullone [14] *176*

2-Phenoxyisoindoline-1,3-dione [135] *177*

Cellular Proliferation Assays *177*

CDK2/Cyclin A Assay *178*

Chk2 Assay *178*

Molecular Modelling *179*

6. Experimental

6.1 General Methods

Where required, all glassware was dried overnight in an oven, and all reactions were carried out in a nitrogen or argon atmosphere. Water refers to de-ionized water. All anhydrous solvents were purchased from Lancaster or Sigma-Aldrich in sure-seal bottles.

6.1.1 Thin Layer Chromatography

Thin layer chromatography (TLC) was performed on commercially available Merck Kieselgel 60F254 plates and separated components were visualized using ultraviolet light (l=254 nm or 366 nm), or by treatment with iodine or permanganate dip.

6.1.2 Column Chromatography

Glass columns were slurry packed in the appropriate eluent under gravity, with silica gel (C-gel 60 A, 40-60 µm, Phase Sep, UK). Samples were applied as a concentrated solution in the same eluent, or pre-absorbed onto silica gel. Fractions containing product were identified by TLC, collected and the solvent removed *in vaccuo.*

6.1.3 NMR Spectroscopy

^{1}H and ^{13}C-NMR were recorded on a Bruker Avance DPX300 spectrometer with operating frequencies of 300 MHz and 75 MHz respectively.

The following abbreviations are used in the assignment of NMR signals: δ (chemical shift), s (singlet), d (doublet), t (triplet), q (quartet), m (multiplet), br (broad signal), dd (doublet of doublet), dt (doublet of triplet), J (coupling constant in Hz).

6.1.4 Mass Spectrometry

Low resolution mass spectra were run on a VG platform II Fisons instrument (Fisons, Altrincham, UK) (atmospheric pressure ionisation, electrospray mass spectrometry) in either positive or negative mode using a mobile phase of methanol.

High resolution mass spectrometry was performed by EPRSC National Mass Spectrometry Service Centre, University of Wales Swansea, using electron impact/chemical ionization (EI/CI)

6.1.5 Infrared Spectroscopy

Infrared spectroscopy were recorded on a Perkin Elmer 1600 series FTIR spectrometer as solids via a diffuse reflectance accessory using a dry potassium bromide matrix.

6.1.6 Melting point

Melting points (mp) were determined on an electric variable heater (Gallenkamp) and were not corrected.

6.1.7 Cooling Baths

Cooling baths were used as necessary. An acetone/dry ice slurry was used for –78 °C, saturated brine/ice for –10 °C and thawing ice for 0 °C, while liquid nitrogen/dry ice was used for –100 °C.

6.2 General Procedures

Method A – Indole N protection

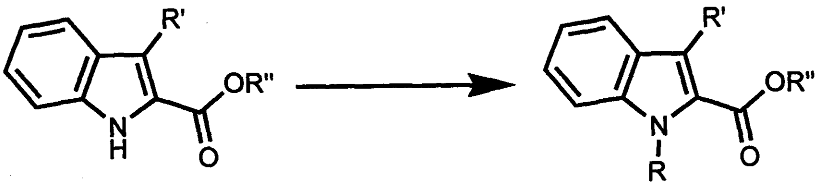

The ester was dissolved in THF (approx. 1g/10 mL) under nitrogen and cooled to 0 °C. Sodium hydride (3.4 equiv.) was washed with petrol 60/80 and then dissolved/suspended in THF. This was added in small amounts (with caution) to the cooled solution, which was allowed to return to room temperature and stirred for 3 hours. The appropriate alkyl halide (1.2 equiv.) was added dropwise to the mixture, which was then left to stir for a further 3h. Distilled water (approx. 10 mL/g) was added (with caution), and the solvents were evaporated. The residue was dissolved in MeOH (approx. 15 mL/g) and NaOH (4M) (10.8 equiv.). The mixture was stirred at 60 °C for 5 h. After the mixture had cooled to room temperature the solvents were evaporated and water was added to dissolve/suspend the remaining mixture. This was followed by dropwise addition of concentrated HCl to pH2, and the resultant solution was extracted with EtOAc, and dried over magnesium sulphate. The solvent was evaporated to recover the product.

Method B – Amide bond formation (i)[91,167]

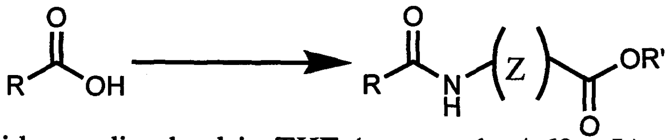

The carboxylic acid was dissolved in THF (approx. 1 g/ 60 mL) under nitrogen and TEA (5 equiv.) was added. The mixture was stirred and cooled to 0 °C before adding oxalyl chloride (2.2 equiv.) and a drop of DMF. After 5 minutes, the mixture was allowed to return to room temperature and was stirred under nitrogen for a further 24 h. The solvents were then evaporated and the remaining mixture was suspended in THF (approx. 1 g/ 20 mL). This was added to a solution of the appropriate amide ester (5 equiv.) and TEA (50 equiv.) in THF (approx. 1 g/40 mL) cooled at 0 °C. The mixture was stirred at room temperature for 24 h, and the solvents evaporated. Saturated sodium bicarbonate was added and the mixture was stirred for 15 minutes, and the organic layer was extracted with EtOAc. The organic phase was washed with 1M HCl and dried over magnesium sulphate, then the solvent was evaporated to recover the product.

Method C – Amide bond formation (ii)[114,138]

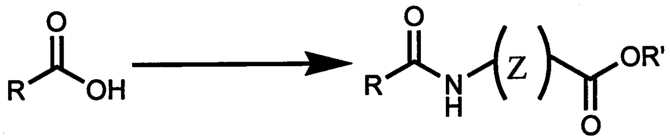

The amine ester (1.1 equiv.) and 4-dimethylaminopyridine (DMAP) (0.8 equiv.) were dissolved in DCM (approx. 1 g/15 mL) at 0 °C. To this was added the carboxylic acid in DCM (approx. 1 g/15 mL), then 1-(3-dimethylaminopropyl)-3-ethyl carbodiimide.HCl (EDCI) (1.1 equiv.) in DCM (approx. 1 g/15 mL) was added. The mixture was stirred for 4 h at 0 °C, then allowed to return to room temperature, and stirred for a further 24 h. The solvent was evaporated and water was added. The precipitate was filtered and washed with water to recover the product.

Method D –Hydrolysis[138]

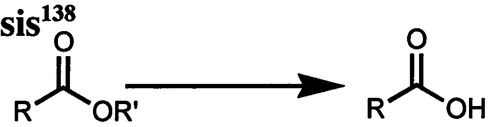

The ester was dissolved in wet THF (approx. 1 g/25 mL) and $LiOH.H_2O$ (3 equiv.) was added. The mixture was stirred at room temperature overnight, and the solvents were evaporated. Water was added, followed by dropwise addition of concentrated HCl to pH 2. The precipitate was filtered to recover the product.

Method E – Cyclization[104]

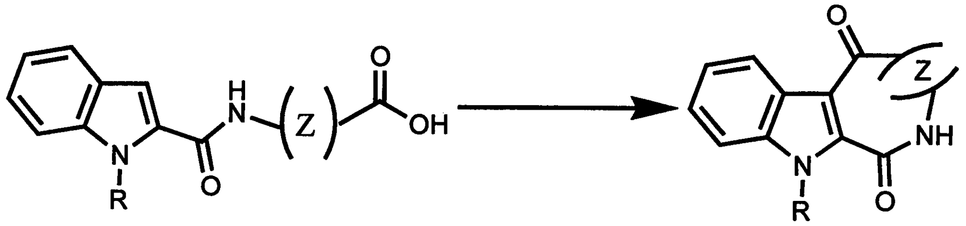

Phosphorus pentoxide (1 equiv.) was added to methane sulphonic acid (14 equiv.) and the mixture was vigorously stirred at 80 °C for 0.5 h under reflux. The carboxylic acid was added and the solution was stirred at 80 °C for 10 minutes, then removed from the heat and ice was added. The solution was extracted with EtOAc, and washed with saturated sodium bicarbonate, then dried over magnesium sulphate and the solvent evaporated to recover the product.

Method F – Extension from ketone position (i)[123,168]

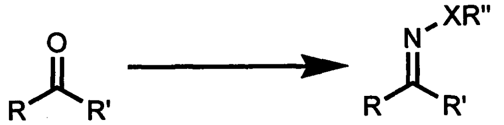

To a solution of appropriate hydrazine hydrochloride or amine hydrochloride (50 equiv.) and sodium acetate (79 equiv.) in distilled water (approx. 1 g/60 mL) was added the ketone (0.071 g; 0.3 mmol) in EtOH (approx. 1 g/100 mL), and the resultant stirring mixture was gently heated at 50 °C for 3 h, then left to stir overnight (16 h). The solvent was evaporated and the residue dissolved in EtOAc. This was washed with distilled water and sodium bicarbonate. The solvents were evaporated to recover the product.

Method G – Extension from ketone position (ii)[138]

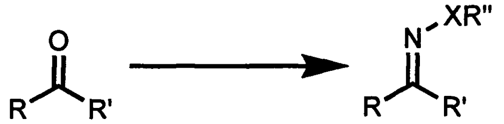

The ketone and the appropriate hydrazine hydrochloride or amine hydrochloride (10 equiv.) were dissolved in THF (approx. 1 g/75 mL) under nitrogen at –10 °C. Boron trifluoride diethyletherate (3.4 equiv.) was added, followed by pyridine (8 equiv.). The mixture was stirred at –10 °C for 1 h, then allowed to warm to room temperature and left stirring for 2 days. The solvents were evaporated, and the mixture dissolved in MeOH. Water was added, and this was left overnight in a beaker. The product was recovered as a precipitate.

Method H – Extension from oxime

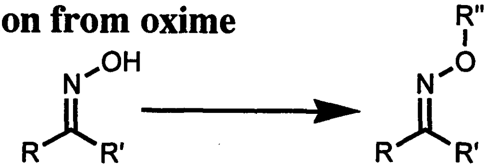

The unsubstituted oxime was dissolved in THF (approx. 1 g/100 mL) at 0 °C under argon. Potassium *tert*-butoxide (1 equiv.) was then added. After 30 minutes stirring, the appropriate bromo-compound (1.1 equiv) was added, and the mixture was allowed to return to room temperature. This was left for 2 days, and the solvents were evaporated to recover the product.

Method I - Bromination[115,118]

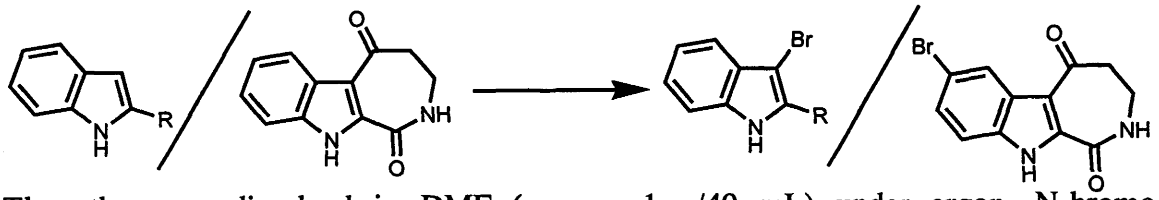

The ether was dissolved in DMF (approx. 1 g/40 mL) under argon. N-bromo succinimide (NBS) (1 equiv.) dissolved in DMF (approx 1 g/20 mL) was added and the reaction was left stirring overnight. Ice was added, and the resulting precipitate was filtered and washed with water to recover the product.

Method J Cyclization (ii)[147]

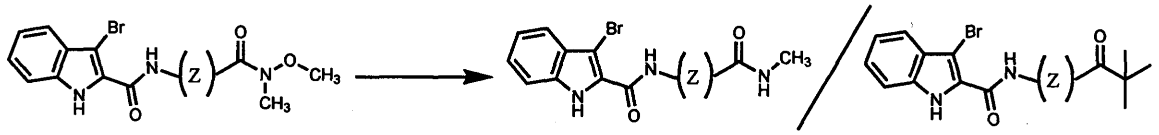

The Weinreb amide was dissolved in THF (approx. 1 g/45 mL) at –78 °C under nitrogen. *tert*-Butyllithium (2 equiv.) was added and the mixture stirred at –78 °C for 3 h and allowed to return to room temperature for 3 days, then heated to reflux for 20 h. EtOAc was added and the mixture washed with saturated sodium bicarbonate and brine, dried with magnesium sulphate and the solvents evaporated to recover the product.

Method K Esterification[103]

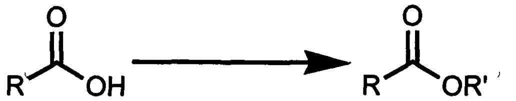

Thionyl chloride (2 equiv.) was slowly added dropwise to a stirred solution of freshly distilled alcohol (15 equiv.) at 0 °C. After 0.5 h of stirring, the mixture was left to warm up to room temp. Carboxylic acid was then added and the mixture was refluxed for 10 h, and the solvent was evaporated to recover the product.

Ethyl 1*H*-indole-2-carboxylate [32]

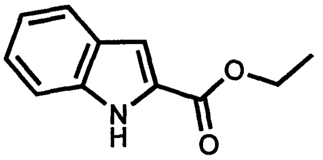

Indole-2-carboxylic acid **[28]** (2.00 g; 12.4 mmol) was dissolved in EtOH (50 mL; 856 mmol; 59 equiv.). Concentrated sulphuric acid (4 mL; 75 mmol; 6 equiv.) was added, and the solution was refluxed until reaction was complete (24 h). The mixture was allowed to cool, and then the solvents were evaporated. Saturated sodium bicarbonate solution was added to the residue until fizzing stopped. The aqueous phase was extracted with EtOAc, and dried over magnesium sulphate. The solvents were evaporated to afford an off yellow solid. Yield 2.188 g (94 %).

R_f 0.70 (4 : 3 Pet 60/80 : EtOAc); mp: 121-124 °C (Lit 122-123 °C^{169}); ^{1}H NMR (d6-DMSO) δ 1.32-1.37 (t, 3H, CH_3), 4.31-4.38 (q, 2H, CH_2), 7.05-7.16 (t, 1H), 7.15 (s, 1H), 7.24-7.29 (t, 1H), 7.45-7.48 (d, 1H), 7.65-7.67 (d, 1H), 11.89 (s, 1H); ^{13}C NMR (d6-DMSO) δ 14.7, 60.8, 108.0, 112.9, 120.5, 122.4, 125.0, 127.1, 127.7, 137.7, 161.7; MS (ES+) *mz* = 212.1 (M+Na).

1-Methyl-1*H*-indole-2-carboxylic acid [34]

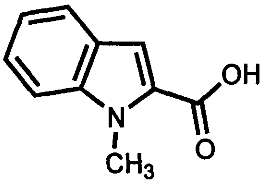

Method A. **[32]** (10.50 g; 55.5 mmol), Sodium hydride (4.59 g; 191.4 mmol; 3.4 equiv.), methyl iodide (4.00 mL; 64.2 mmol; 1.2 equiv.) produced a brown solid (8.6 g, 88 %).

R_f 0.29 (2 : 1 Pet 60/80 : EtOAc); mp: 214-126 °C (Lit 209-210 °C^{170}); ^{1}H NMR (d6-DMSO) δ 3.98 (S, 3H, CH_3), 7.05-7.10 (t, 1H), 7.18 (s, 1H), 7.26-7.31 (t, 1H), 7.51-7.54 (d, 1H), 7.61-7.64 (d, 1H) 12.9 (br s, 1H, OH, exchanges with D_2O); ^{13}C NMR (d6-DMSO) δ 31.8, 109.7, 111.2, 120.7, 122.5, 124.9, 125.7, 128.9, 139.6, 163.4; MS (ES-) *mz* = 173.8 (M-1).

1-Benzyl-1*H*-indole-2-carboxylic acid [39]

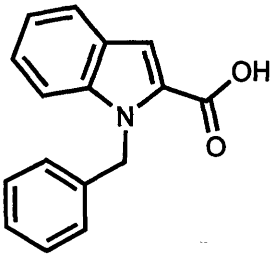

Method A. [32] (3.15 g; 16.6 mmol), Sodium hydride (0.80 g; 33.5 mmol; 2.0 equiv.), benzyl bromide (3.00 mL; 26.3 mmol; 1.6 equiv.) produced a red-brown solid, which was used crude (3.4 g, 81 %).

R_f 0.14 (2 : 1 Pet 60/80 : EtOAc); mp: 124-150 °C; ^{1}H NMR (d6-DMSO) δ 5.89 (s, 2H, CH_2), 7.02-7.73 (m, 10H, 10), 13.03 (br s, 1H ,COOH, exchanges with D_2O); ^{13}C NMR (d6-DMSO) δ 47.2, 110.8, 111.6, 121.0, 122.7, 125.3, 125.9, 126.6, 127.3, 128.5, 128.8, 139.0, 139.3, 163.3; MS (ES-) *mz* = 249.8 (M-1).

2,10-bis((2-(Trimethylsilyl)ethoxy)methyl)-3,4-dihydroazepino [3,4-*b*]indole-1,5(2*H*,10*H*)-dione [77]

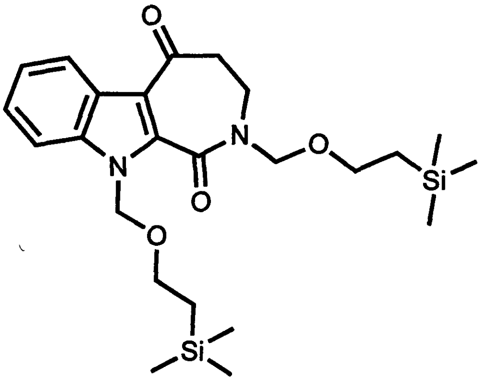

Method A. [25] (0.35 g; 1.6 mmol), NaH (0.17 g; 7.0 mmol; 4.3 equiv.), SEM-Cl (4.20 mL; 23.7 mmol; 14.5 equiv.). Column chromatography (eluent 4 : 1 Pet 60/80 : EtOAc); produced a dark yellow oil (0.2 g, 27 %).

R_f 0.83 (1 : 1 Pet 60/80 : EtOAc); ^{1}H NMR (d6-DMSO) δ $^-$0.13 (s, 9H, 3xCH_3), 0.00 (s, 9H, 3xCH_3), 0.74-0.80 (t, 2H, J 7.9, SiCH_2), 0.87-0.92 (t, 2H, J 8.2, SiCH_2), 2.90-2.93 (t, 2H, J 4.6, NCH_2C$\underline{H}_2$), 3.42-3.48 (t, 2H, J 7.9, OC$\underline{H}_2$), 3.56-3.62 (t, 2H, J 8.2, OC$\underline{H}_2$), 3.75-3.78 (t, 2H, J 4.6, NC$\underline{H}_2$$CH_2$), 5.03 (s, 2H, CH_2), 5.98 (s, 2H, CH_2), 7.31-7.36 (dd, 1H, J 7.1 7.9), 7.41-7.46 (dd, 1H, J 8.3 7.1), 7.75-7.78 (d, 1H, J 8.3), 8.20-8.26 (d, 1H, J 7.9); ^{13}C NMR (d6-DMSO) δ -0.2, 0.0, 18.5, 18.8, 44.3, 45.1, 66.4, 66.7, 74.6, 76.2, 113.1, 117.6, 123.9, 124.8, 125.6, 135.1, 139.3, 162.9, 197.6; MS (ES+) *mz* = 475.3 (M+H).

3-Bromo-1-methyl-1*H*-indole-2-carboxylic acid [114]

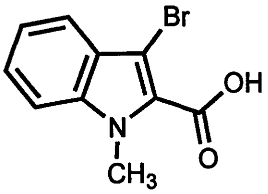

Method A. **[113]** (1.17 g; 4.4 mmol), NaH (0.22 g; 9.3 mmol; 2.1 equiv.), MeI (0.30 mL; 4.8 mmol; 1.1 equiv.) produced a light brown solid (0.57 g, 52 %).

R_f 0.74 (100 % EtOAc); mp: 202-204 °C (Lit 180 °C[170]); ^{1}H NMR (d6-DMSO) δ 4.05 (s, 3H, CH_3), 7.24-7.31 (dd, 1H), 7.43-7.49 (dd, 1H), 7.48-7.62 (d, 1H), 7.67-7.70 (d, 1H), 13.62 (bs, 1H, OH – exchange with D_2O).

1-(4-Methoxybenzyl)-1*H*-indole-2-carboxylic acid [80]

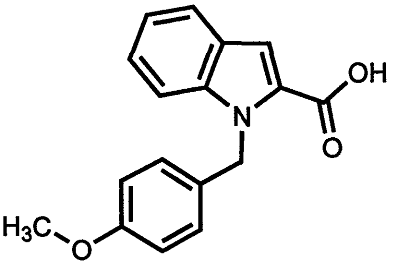

Method A. **[32]** (2.00 g; 10.6 mmol), NaH (0.51 g; 21.3 mmol; 2.0 equiv.), 4-methoxy benzyl chloride (1.40 mL; 10.3 mmol; 1.0 equiv.), KI (1.70 g; 10.2 mmol; 1.0 equiv.) produced a light brown solid, which was mainly starting material with a small amount of product. This was not purified, and used crude in the next step.

Ethyl 3-(1-methyl-1*H*-indole-2-carboxamido)propanoate[138] [35]

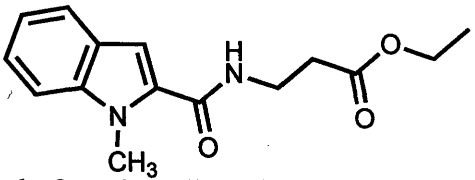

Method B. N-Methyl-indole-2-carboxylic acid **[34]** (2.61 g; 14.9 mmol), TEA (6.30 mL; 77.4 mmol; 5.2 equiv.), oxalyl chloride (2.90 mL; 33.2 mmol; 2.2 equiv.), β-alanine ethyl ester hydrochloride (11.40 g; 74.2 mmol; 5.0 equiv.), TEA (59.00 mL; 724.6 mmol; 48.7 equiv.) produced a dark oil (3.28 g, 80 %).

R_f 0.21 (2 : 1 Pet 60/80 : EtOAc); ^{1}H NMR ($CDCl_3$) δ 1.32-1.37 (t, 3H, CH_3), 2.70-2.74 (t, 2H, CH_2), 3.76-3.79 (q, 2H, CH_2), 4.11 (s, 3H, CH_3), 4.21-4.26(q, 2H, CH_2), 6.90-7.67 (m,6H); ^{13}C NMR (d6-DMSO) δ 0.0, 13.2, 29.3, 33.0, 59.9, 102.8, 109.1, 119.4, 120.8, 123.0, 125.0, 130.8, 138.0, 161.5, 171.8; MS (ES+) *mz*= 275.0 (M+1).

Methyl 2-(1-methyl-1*H*-indole-2-carboxamido)benzoate [153]

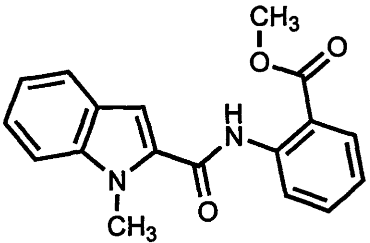

Method B. **[34]** (0.72 g; 4.1 mmol), Oxalyl Chloride (0.80 mL; 9.2 mmol; 2.2 equiv.), triethylamine (0.30 mL; 3.7 mmol; 0.9 equiv.) and (1.70 mL; 20.9 mmol; 5.1 equiv.), and methyl anthranilate (3.50 mL; 26.3 mmol; 6.4 equiv.). The residue produced was crystallised from methanol to yield a yellow solid (0.14 g, 11 %).

Rf 0.78 (1 : 1 Pet 60/80 : EtOAc); mp:176-178 °C; ^{1}H NMR ($CDCl_3$) δ 4.12 (s, 3H, CH_3), 4.27 (s, 3H, CH_3), 7.22-7.33 (m, 2H), 7.42 (s, 1H), 7.46-7.51 (t, 1H), 7.54-7.56 (d, 1H), 7.70-7.76 (t, 1H), 7.85-7.88 (d, 1H,), 8.21-8.24 (d, 1H), 8.97-9.00 (d, 1H), 12.16 (s, NH); ^{13}C NMR ($CDCl_3$) δ 30.8, 51.5, 104.6, 109.1, 114.0, 119.2, 119.6, 121.4, 121.4, 123.5, 125.1, 130.0, 131.0, 133.7, 138.6, 140.8, 160.0, 168.0; MS *mz* (EI+) 308.2.

Ethyl 3-(1-benzyl-1*H*-indole-2-carboxamido)propanoate [40]

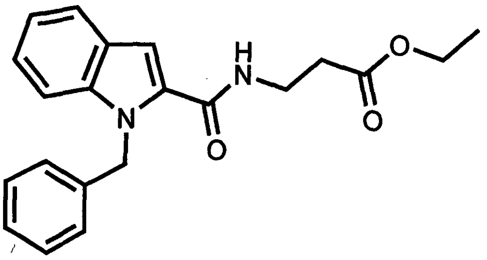

Method B. **[39]** (4.24 g; 16.9 mmol), oxalyl chloride (4.24 mL; 48.6 mmol; 2.9 equiv.), β-alanine ethyl ester hydrochloride (6.61 g; 43.0 mmol; 2.5 equiv.), triethylamine (1.00 mL; 12.3 mmol; 0.7 equiv.) and (24.00 mL; 294.8 mmol; 17.5 equiv.) produced a light yellow solid (5.40 g, 91 %).

R_f 0.62 (1 : 1 Pet 60/80 : EtOAc); mp: 74-80 °C; ^{1}H NMR (DMSO) δ 1.15-1.20 (t, 3H, J 7.1, CH_3), 2.55-2.59 (t, 2H, J 6.8, CH_2), 3.45-3.52 (m, 2H, CH_2), 4.02-4.10 (q, 2H, J

7.1, CH_2), 5.85 (s, 2H, CH_2), 7.07-7.67 (m,10H), 8.66-8.70 (t,1H, 5.5, NH); ^{13}C NMR (DMSO) δ 14.4, 34.1, 35.5, 47.1, 60.3, 105.5, 111.4, 120.7, 122.0, 124.1, 126.2, 127.0, 127.3, 127.8, 127.9, 128.7, 132.0, 138.2, 139.1, 162.3, 171.6; MS (ES+) *mz* = 373.0 (M+Na).

Ethyl 3-(1*H*-indole-2-carboxamido)propanoate [52][138]

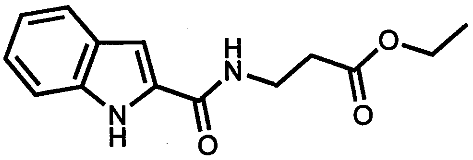

Method C. β-Alanine ethyl ester hydrochloride (1.550 g; 10.1 mmol; 1.1 equiv.), DMAP (0.949 g; 7.8 mmol; 0.8 equiv.), indole-2-carboxylic acid **[28]** (1.510 g; 9.4 mmol), EDCI (1.902 g; 9.9 mmol; 1.1 equiv.) produced a pale yellow solid 2.07 g (85 %; Lit. 95 %[114], 98 %[138]).

R_f 0.82 (100 % EtOAc); mp 162-164 °C (Lit. 159-160 °C[114], 158-160 °C[138]);

^{1}H NMR (d6- DMSO) δ 1.16-1.21 (t, 3H, CH_3), 2.58-2.63 (t, 2H, CH_2), 3.50-3.56 (q, 2H, CH_2), 4.05-4.12 (q, 2H, CH_2), 7.01-7.06 (t, 1H), 7.09, (s, 1H), 7.15-7.20 (t, 1H), 7.41-7.44 (d, 1H), 7.60-7.62 (d, 1H), 8.54-8.57 (t, NH), 11.56 (s, NH); ^{13}C NMR (d6-DMSO) δ 14.4, 34.3, 35.5, 60.3, 102.8, 112.6, 120.0, 121.8, 123.6, 127.4, 131.9, 136.8, 161.5, 171.7; MS (ES+) *mz* = 261.1 (M+H).

Ethyl 2-(1*H*-indole-2-carboxamido)acetate [117]

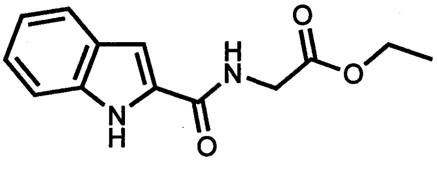

Method C. Glycine ethyl ester hydrochloride (1.55 g; 11.1 mmol; 1.1 equiv.), DMAP (0.96 g; 7.8 mmol; 0.8 equiv.), EDCI (1.54 g; 8.0 mmol; 0.8 equiv.) and **[28]** (1.58 g; 9.8 mmol) produced a pale yellow solid (2.3 g, 95 %).

R_f 0.68 (100% EtOAc); mp 218-220 °C (Lit 225 °C[171]); ^{1}H NMR (d6-DMSO) δ 1.20-1.24 (t, 3H, CH_3), 4.04-4.06 (d, 2H, CH_2), 4.11-4.12 (q, 2H, CH_2), 7.03-7.08 (t, 1H), 7.17-7.22 (m, 2H), 7.46-7.85 (d, 1H), 8.92-8.96 (t, NH), 11.63 (s, NH); ^{13}C NMR (d6-DMSO) δ 14.5, 41.3, 60.8, 103.3, 112.7, 120.1, 122.0, 123.8, 127.4, 131.4, 136.9, 161.9, 170.3; MS (ES+) *mz* = 247.1 (M+H).

Ethyl 2-(1-methyl-1*H*-indole-2-carboxamido)acetate [154]

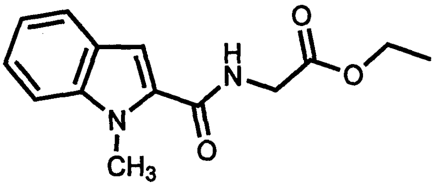

Method C. Glycine ethyl ester hydrochloride (1.54 g; 11.0 mmol; 1.1 equiv.), DMAP (1.01 g; 8.3 mmol; 0.8 equiv.), EDCI (1.58 g; 8.2 mmol; 0.8 equiv.) and **[34]** (1.76 g; 10.0 mmol) produced a yellow solid (2.29 g, 88 %).

R_f 0.89 (100% EtOAc); ^{1}H NMR (d6-DMSO) δ 1.22-1.29 (t, 3H, J 7.1, CH_3), 4.04 (s, 3H, CH_3), 4.06-4.08 (d, 2H, CH_2, J 6.0), 4.15-4.22 (q, 2H, J 7.1, CH_2), 7.14-7.19 (dd, 1H, J 7.9 7.0), 7.20 (s, 1H), 7.31-7.37 (dd, 1H, J 8.3 7.0), 7.60-7.63 (d, 1H, J 8.3), 7.70-7.73 (d, 1H, J 7.9) 8.93-8.97 (t, 1H, NH, J 6.0); ^{13}C NMR (d6-DMSO) δ 14.5, 31.7, 41.3, 60.8, 105.1, 110.9,120.6, 122.0, 124.1, 125.9, 131.7, 138.8, 162.6, 170.2.

Ethyl 3-(3-bromo-1-methyl-1*H*-indole-2-carboxamido)propanoate [63]

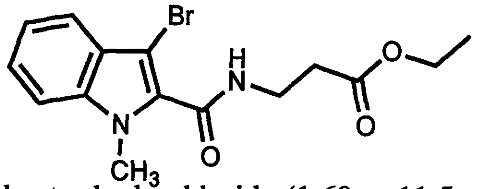

Method C. β-alanine ethyl ester hydrochloride (1.60 g; 11.5 mmol; 1.5 equiv.), DMAP (1.12 g; 9.2 mmol; 1.2 equiv.), EDCI (1.90 g; 9.9 mmol; 1.3 equiv.) and **[114]** (2.00 g; 7.9 mmol) produced a pale brown solid (2.48 g, 89 %).

R_f 0.46 (1 : 1 Pet 60/80 : EtOAc); mp: 48-50 °C; ^{1}H NMR (d6-DMSO) δ 1.20-1.25 (t, 3H, J 7.1, $CH_2C\underline{H}_3$), 2.63-2.67 (t, 2H, J 6.7, $NHNCH_2C\underline{H}_2$), 3.55-3.61 (dt, 2H, J 6.9 5.8, $NHC\underline{H}_2CH_2$), 3.81 (s, 3H, CH_3), 4.08-4.15 (q, 2H, J 7.1, $C\underline{H}_2CH_3$), 7.21-7.26 (dd, J 7.1 7.9, 1H), 7.34-7.39 (dd, 8.4 7.1, 1H), 7.49-7.52 (d, J 7.9, 1H), 7.58-7.61 (d, 1H, J 8.4, 1H), 8.64-8.67 (t, 1H, J 5.8, NH) [NH exchanges with D_2O]; ^{13}C NMR (d6-DMSO) δ 14.5, 60.4, 89.5, 111.2, 119.7, 121.3, 124.5, 125.8, 132.9, 136.6, 160.7, 171.5; MS (ES+) *mz* (%) =353.1 (100 %) / 355.1 (100 %) (M+H [^{79}Br] / M+H [^{81}Br]).

Ethyl 3-(1-(4-methoxybenzyl)-1*H*-indole-2-carboxamido) propanoate [82]

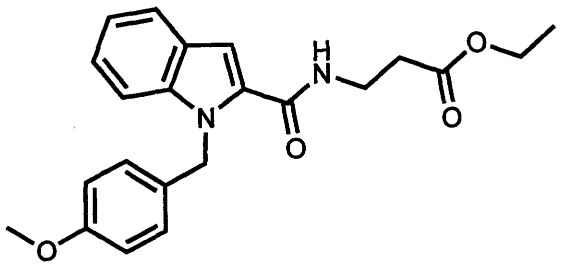

Method C. β-Alanine ethyl ester hydrochloride (0.50 g; 3.6 mmol; 1.2 equiv.), DMAP (0.30 g; 2.5 mmol; 0.8 equiv.), EDCI (0.50 g; 2.6 mmol; 0.9 equiv.) and crude **[81]** (see exp. 6.3.5) (0.82 g; 2.9 mmol) The product did not precipitate from water, so was taken up in EtOAc and washed with water. After purification by column chromatography (eluent 3 : 1 Pet 60/80 : EtOAc) a brown oil was produced (0.06 g, 2 % from **[34]**).

^{1}H NMR (d6-DMSO) δ 1.16-1.21 (t, 3H, J 7.1, $CH_2C\underline{H}_3$), 2.57-2.61 (t, 2H, J 7.0, $NHCH_2C\underline{H}_2$), 3.47-3.53 (m, 2H, $NHC\underline{H}_2CH_2$), 3.68 (s, 3H, CH_3), 4.04-4.11 (q, 2H, J 7.1, $C\underline{H}_2CH_3$), 5.77 (s, 2H, CH_2), 6.79-6.82 (d, 2H), 7.07-7.10 (m, 4H), 7.20-7.25 (dd, 1H), 7.53-7.56 (d, 1H), 7.63-7.66 (d, 1H), 8.65 (t, 1H, J 4.8, $N\underline{H}CH_2CH_2$); ^{13}C NMR (d6-DMSO) δ 14.4, 34.1, 35.5, 39.0, 46.5, 55.3, 60.3, 105.4, 111.5, 114.1, 120.6, 122.0, 124.0, 126.2, 128.5, 131.0, 132.0, 138.2, 158.6, 162.4, 171.6.

Ethyl 4-(1*H*-indole-2-carboxamido)butanoate [120]

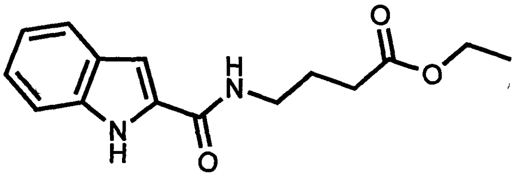

Method C. Ethyl 4-aminobutyrate hydrochloride (1.40 g; 8.4 mmol; 1.0 equiv.), DMAP (0.90 g; 7.4 mmol; 0.9 equiv.), EDCI (1.60 g; 8.3 mmol; 1.0 equiv.) and **[28]** (1.30 g; 8.1 mmol) produced a yellow solid (2.1 g, 94 %).

R_f 0.43 (1 : 1 Pet 60/80 : EtOAc); mp: 116-118 °C; ^{1}H NMR (d6-DMSO) δ 1.16-1.21 (t, 3H, J 7.1, $CH_2C\underline{H}_3$), 1.76-1.86 (m, 2H, $NHC\underline{H}_2CH_2$), 2.36-2.41 (t, 2H, J 7.4, $NHCH_2CH_2C\underline{H}_2$), 3.18-3.38 (m, 2H, $NHCH_2C\underline{H}_2CH_2$), 4.02-4.10 (q, 2H, J 7.1, $C\underline{H}_2CH_3$), 7.01-7.06 (dd, 1H, J 8.1 6.6), 7.11 (s, 1H), 7.15-7.20 (dd, 1H, J 8.0 6.6), 7.42-7.44 (d, 1H, J 8.1), 7.60-7.62 (d, 1H, J 8.0), 8.49-8.52 (t, 1H, J 5.4, $N\underline{H}CH_2$), 11.56 (s, 1H, NH) [Both NH peaks exchange with D_2O]; ^{13}C NMR (d6-DMSO) δ 14.5, 25.0, 31.4, 38.4, 60.1, 102.7, 112.6, 120.0, 121.8, 123.5, 127.4, 132.1, 136.7, 161.5, 173.0.

N-(2-(*N*-Methoxy-*N*-methylcarbamoyl)ethyl)-3-bromo-1-methyl-1*H*-indole-2-carboxamide [116]

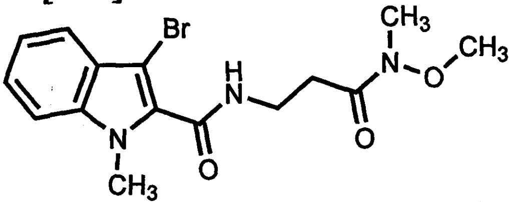

Method C. N,O-Dimethylhydroxylamine hydrochloride (0.19 g; 1.9 mmol; 0.9 equiv.), DMAP (0.20 g; 1.6 mmol; 0.8 equiv.), EDCI (0.35 g; 1.8 mmol; 0.9 equiv.) and **[115]** (0.50 g; 2.1 mmol). The product did not precipitate out of water, so was taken up in EtOAc and washed with water, then purified by column chromatography (eluent 3 : 1 pet 60/80 : EtOAc) to yield a light brown viscous oil (0.268 g, 47 %).

R_f 0.52 (100% EtOAc); ^{1}H NMR (d6-DMSO) δ 2.72-2.77 (t, 2H, J 6.6, NHCH$_2$C$\underline{H}_2$), 3.15 (s, 3H, CH$_3$), 3.50-3.60 (dt, 2H, J 6.6 5.7, NHC$\underline{H}_2$CH$_2$), 3.70 (s, 3H, CH$_3$), 3.82 (s, 3H, CH$_3$), 7.20-7.25 (dd, J 8.3 6.8, 1H), 7.33-7.38 (dd, J 8.5 6.8, 1H), 7.48-7.51 (d, J 8.5, 1H), 7.57-7.60 (d, J 8.3, 1H), 8.53-8.57 (t, J 5.7, 1H, N$\underline{H}$CH$_2$CH$_2$ exchanges with D$_2$O); ^{13}C NMR (d6-DMSO) δ 31.9, 35.5, 61.4, 89.5, 111.2, 113.6, 119.7, 121.3, 124.5, 125.8, 132.9, 136.6, 160.6; MS (ES+) *mz* (%) = 368.1 (100 %) / 370.1 (100 %) (M+H [^{79}Br] / M+H [^{81}Br]).

N-(3-(*N*-Methoxy-*N*-methylcarbamoyl)propyl)-3-bromo-1*H*-indole-2-carboxamide [121]

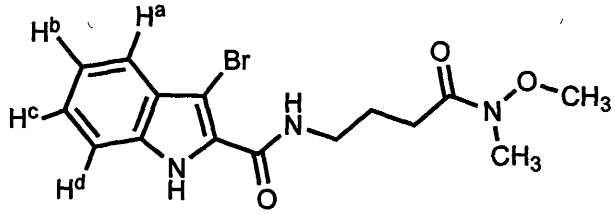

Method C. N,O- Dimethylhydroxylamine hydrochloride (0.60 g; 6.2 mmol; 1.3 equiv.), DMAP (0.65 g; 5.3 mmol; 1.1 equiv.), EDCI (1.10 g; 5.7 mmol; 1.2 equiv.) and **[155]** (1.51 g; 4.6 mmol). No precipitate formed when water was added, so the product was taken up in EtOAc and washed with water, and the solvents removed *in vaccuo* to leave a sticky tar which was crystallised from ether to give a light brown solid. (0.917 g, 54 %)

R_f 0.48 (100% EtOAc); mp: 134-138 °C; ^{1}H NMR (d6-DMSO) δ 1.78-1.87 (m, 2H, NHCH$_2$C$\underline{H}_2$CH$_2$), 2.49-2.54 (t, 2H, J 7.0, NHCH$_2$CH$_2$C$\underline{H}_2$), 3.10 (s, 3H, CH$_3$), 3.35-3.42 (q, 2H, J 7.2 5.4, NHC$\underline{H}_2$CH$_2$CH$_2$), 3.67 (s, 3H, CH$_3$), 7.16-7.21 (dd, 1H J 9.0, 5.9, H^b), 7.28-7.33 (dd, 1H, J 9.1 5.9, H^c), 7.46-7.49 (d, 1H, J 9.1, H^d), 7.49-7.52 (d, 1H, J 9.0, H^a), 7.98-8.02 (t, 1H, J 5.4, $N\underline{H}CH_2CH_2CH_2$), 11.99 (s, 1H, NH) [both NH peaks exchange with D_2O]; ^{13}C NMR ($CDCl_3$) 24.8 ($NHCH_2\underline{C}H_2CH_2$), 29.6 ($NHCH_2CH_2\underline{C}H_2$), 32.6, 39.8 ($NHC\underline{H}_2CH_2CH_2$), 61.7, 91.6, 112.8 ($\underline{C}H^d$), 120.8 ($\underline{C}H^a$), 121.7 ($\underline{C}H^b$), 126.0 ($\underline{C}H^c$), 127.5, 127.9, 135.2, 161.2; MS (ES+) *mz* (%) = 368.1 (100 %) / 370.1 (100 %) (M+H [^{79}Br] / M+H [^{81}Br]).

N-((*N*-Methoxy-*N*-methylcarbamoyl)methyl)-3-bromo-1*H*-indole-2-carboxamide [118]

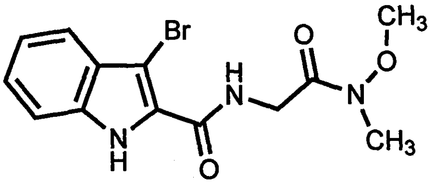

Method C. N,O- Dimethylhydroxylamine hydrochloride (0.30 g; 3.1 mmol; 1.2 equiv.), DMAP (0.55 g; 4.5 mmol; 1.8 equiv.), EDCI (0.35 g; 1.8 mmol; 0.7 equiv.) and **[156]** (0.76 g; 2.6 mmol) produced a pale orange solid (0.75 g, 86 %).

R_f 0.59 (100 % EtOAc); mp: 202-204 °C; ^1H NMR (d6-DMSO) δ 3.17 (s, 3H, CH_3), 3.77 (s, 3H, CH_3), 4.33-4.35 (d, 2H, J 4.9, $NHC\underline{H}_2$), 7.17-7.22 (dd, 1H, J 8.4 6.5), 7.29-7.34 (dd, 1H, J 8.6 6.5), 7.48-7.51 (d, 1H, J 8.6), 7.51-7.53 (d, 1H, J 8.4), 8.03-8.06 (t, 1H, J 4.9, $N\underline{H}CH_2$), 12.11 (s, 1H, NH) [both NH peaks exchange with D_2O]; ^{13}C NMR ($CDCl_3$) δ 31.4, 40.5, 60.6, 91.2, 111.2, 119.6, 120.3, 124.7, 125.8, 126.7, 133.7, 159.4, 168.3; MS (ES+) *mz* (%) = 340.0 (100 %) / 342.0 (100 %) (M+H [^{79}Br] / M+H [^{81}Br]).

N-(2-(*N*-Methoxy-*N*-methylcarbamoyl)ethyl)-3-bromo-1*H*-indole-2-carboxamide [119]

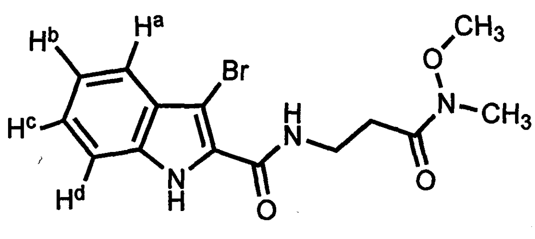

Method C. N,O- Dimethylhydroxylamine hydrochloride (0.20 g; 2.1 mmol; 1.3 equiv.), DMAP (0.21 g; 1.7 mmol; 1.1 equiv.), EDCI (0.37 g; 1.9 mmol; 1.2 equiv.) and **[157]** (0.50 g; 1.6 mmol) produced a white solid (0.365 g, 64 %).

R_f 0.52 (100 % EtOAc); mp: 140-142 °C; ^1H NMR (d6-DMSO) δ 2.75 (t, 2H, $NHCH_2C\underline{H}_2$), 3.13 (s, 3H, CH_3), 3.55-3.64 (m, 2H, $NHC\underline{H}_2CH_2$), 3.68 (s, 3H, CH_3), 7.16-7/21 (dd, 1H, J 7.8 7.5, H^c), 7.28-7.33 (dd, 1H, J 7.8 7.5, H^b), 7.46-7.49 (d, 1H, J 7.8, H^d), 7.49-7.52 (d, 1H, J 7.8, H^a), 8.02 (t, 1H, $N\underline{H}CH_2CH_2$), 12.04 (s, 1H, NH) [both NH peaks exchange with D_2O]; ^{13}C NMR ($CDCl_3$) δ 32.4($NHCH_2\underline{C}H_2$), 32.5, 35.3($NH\underline{C}H_2CH_2$), 61.7, 92.0, 112.5($\underline{C}H^d$), 121.0($\underline{C}H^a$), 121.7($\underline{C}H^c$), 126.0($\underline{C}H^b$), 127.6, 128.1, 135.0, 160.8; MS (ES+) *mz* = 354.0448 (M+H) (calculated 354.0449 for ^{79}Br).

3-(1-Methyl-1*H*-indole-2-carboxamido)propanoic acid [37]

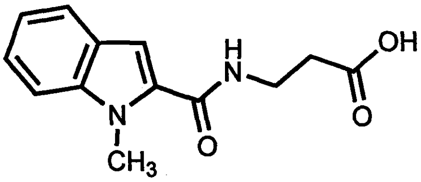

Method D. Indole ester **[35]** (0.087 g; 3.2 mmol), $LiOH.H_2O$ (0.040 g; 9.5 mmol; 3.0 equiv.) produced a brown solid (0.076 g, 97 %, Lit 93 %[138]).

R_f 0.32 (1 : 1 Pet 60/80 : EtOAc); mp: 144-148 °C (Lit. 161 °C[138], 160-162 °C[114]); ^1H NMR (d6-DMSO) δ 2.51-2.57 (t, 2H, CH_2), 3.44-3.50 (q, 2H, CH_2), 3.99 (s, 3H, CH_3), 7.06 (s, 1H), 7.08-7.13 (t, 1H), 7.23-7.30 (t, 1H), 7.51-7.54 (d, 1H), 7.62-7.65 (d, 1H), 8.55-8.58 (t, NH), 12.30 (s, broad OH) [NH & OH peaks exchange with D_2O]; ^{13}C NMR (d6-DMSO) δ 31.7, 34.14, 35.5, 104.6, 110.8, 120.4, 121.9, 123.8, 125.9, 162.2, 173.2; MS (ES-) *mz* = 244.7 (M-1).

2-(1-Methyl-1*H*-indole-2-carboxamido)acetic acid [102]

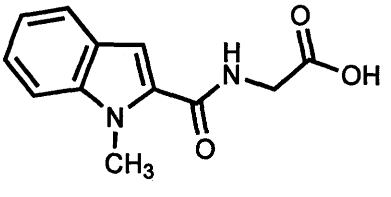

Method D. **[154]** (2.02 g; 7.8 mmol), $LiOH.H_2O$ (1.07 g; 25.5 mmol; 3.3 equiv.) produced a yellow solid (1.72 g, 95 %).

R_f 0.11 (100 % EtOAc); mp 146-148 °C; ^1H NMR (d6-DMSO) δ 3.86-3.92 (d, 2H, CH_2), 4.01 (s, 3H, CH_3), 7.06-7.14 (t, 1H), 7.16 (s, 1H), 7.25-7.31 (t, 1H), 7.50-7.54 (d, 1H), 7.66-7.69 (d, 1H), 8.77-8.84 (t, NH), 12.34 (br s, OH); ^{13}C NMR (d6-DMSO) δ 31.7, 41.2, 105.0, 110.9, 120.5, 122.0, 124.0, 125.9, 131.9, 238.8, 262.5, 171.7.

2-(1-Methyl-1*H*-indole-2-carboxamido)benzoic acid [103]

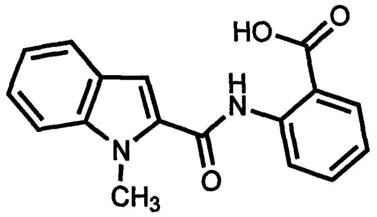

Method D. [153] (0.13 g; 0.4 mmol; 1.0 equiv.), LiOH.H$_2$O (0.05 g; 1.2 mmol; 3.0 equiv.) produced a white solid (0.093 g, 75 %).

R$_f$ 0.71 (100 % EtOAc); mp: 228-230 °C; ^{1}H NMR (d6-DMSO) δ 4.07 (s, 3H, CH$_3$), 7.14-7.23 (m, 3H), 7.32-7.37 (t, 1H), 7.59-8.06 (m, 3H), 8.08-8.09 (d, 1H), 8.67-8.70 (d, 1H), 12.35 (s, 1H); ^{13}C NMR (d6-DMSO) δ 31.9, 105.3, 111.1, 116.6, 120.0, 121.0, 122.3, 123.2, 124.8, 125.9, 131.7, 132.4, 134.7, 139.5, 141.4, 160.4, 170.4; MS (ES+) *mz* = 295.1079 (M+H), (calculated = 295.1079).

3-(1*H*-Indole-2-carboxamido)propanoic acid [27]

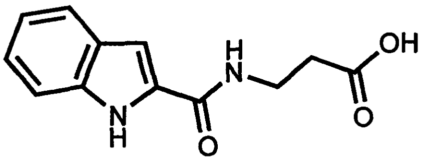

Method D. [52] (11.00 g; 42.3 mmol), LiOH.H$_2$O (5.50 g; 131.1 mmol; 3.1 equiv.) produced a pale yellow solid (9.5 g, 97 %, Lit 93 %[139]).

R$_f$ 0.68 (100 % EtOAc); mp 194-198 °C (lit 232 °C[138]); ^{1}H NMR (d6-DMSO) δ 2.54-2.59 (t, 2H, CH$_2$), 3.48-3.54 (q, 2H, CH$_2$), 7.02-7.07 (t, 1H), 7.12 (s 1H), 7.17-7.22 (t, 1H), 7.43-7.46 (d, 1H), 7.61-7.64 (d, 1H), 8.54-8.57 (t, NH), 11.58 (s, NH), 12.38 (br s, 1H, OH); ^{13}C NMR (d6-DMSO) δ 34.3, 65.3, 102.8, 112.6, 120.0, 121.8, 123.6, 127.4, 132.0, 136.8, 161.5, 173.2; MS (ES-) *mz* = 231.0 (M-1).

2-(1*H*-Indole-2-carboxamido)acetic acid [99]

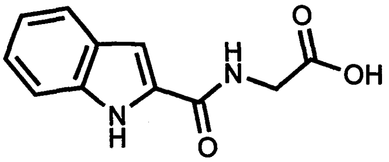

Method D. [117] (5.00 g; 20.3 mmol), LiOH.H$_2$O (2.50 g; 59.6 mmol; 2.9 equiv.) produced a yellow solid (3.12g, 70 %).

R$_f$ 0.57 (100 % EtOAc); mp 228-230 °C; ^{1}H NMR (d6-DMSO) δ 3.95-3.97 (d, 2H, CH2), 7.01-7.06 (t, 1H), 7.15 (s, 1H), 7.18-7.21 (t, 1H), 7.41-7.44 (d, 1H), 7.61-7.64 (d, 1H), 8.81-8.85 (t, NH), 11.52 (s, NH), 12.49 (br s, 1H, OH); ^{13}C NMR(d6-DMSO) δ 41.2, 103.2, 112.7, 120.1, 121.9, 123.8, 127.4, 131.6, 136.9, 161.8, 171.7; MS (ES+) mz = 219.1 (M+H).

3-(3-Bromo-1*H*-indole-2-carboxamido)propanoic acid) [157]

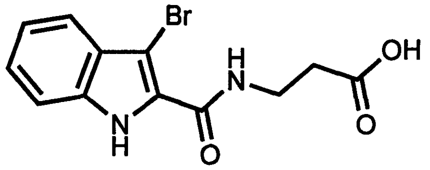

Method D. **[56]** (0.75 g; 2.2 mmol), LiOH.H$_2$O (0.40 g; 9.5 mmol; 4.3 equiv.) produced a white solid (0.68 g, 98 %).

R$_f$ 0.5 (100 % EtOAc); mp: 238-240 °C; ^{1}H NMR (d6-DMSO) δ 2.56-2.60 (t, 2H, J 6.7, NHCH$_2$C$\underline{H}_2$), 3.54-3.61 (dt, 2H, J 6.7 5.7, NHC$\underline{H}_2$CH$_2$), 7.16-7.21 (dd, 1H, J 7.7 7.3), 7.28-7.33 (dd, 1H, J 8.0 7.3), 7.46-7.49 (d, 1H, J 8.0), 7.49-7.52 (d, 1H, J 7.7), 8.00-8.07 (t, 1H, J 5.5, N$\underline{H}$CH$_2$CH$_2$), 12.06 (s, 1H, NH), 12.30 (br s, 1H, OH) [NH and OH peaks exchange with D$_2$O]; ^{13}C NMR (d6-DMSO) δ 36.6, 38.1, 93.1, 115.6, 122.4, 127.7, 128.0, 129.5, 131.1, 137.8, 162.7, 176.0; MS (ES+) *mz* (%) = 311.0 (100 %) / 313.0 (100 %) (M+H [^{79}Br] / M+H [^{81}Br]).

3-(3-Bromo-1-methyl-1*H*-indole-2-carboxamido)propanoic acid [115]

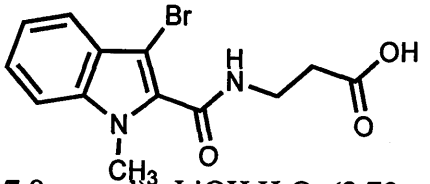

Method D. **[63]** (2.48 g; 7.0 mmol); LiOH.H$_2$O (2.70 g; 64.3 mmol; 9.2 equiv.) produced a pale brown solid (1.69 g, 74 %).

R$_f$ 0.56 (100 % EtOAc); mp: 152-154 °C; ^{1}H NMR (d6-DMSO) δ 2.55-2.60 (t, J 6.9, 2H, NHNC$_2$C$\underline{H}_2$), 3.51-3.57 (dt, J 6.9 5.5, 2H, NHC$\underline{H}_2$CH$_2$), 3.81 (s, 3H, CH$_3$), 7.21-7.26 (dd, J 7.0 7.9, 1H), 7.34-7.39 (dd, J 7.0 8.4, 1H), 7.49-7.51 (d, J 7.9, 1H), 7.59-7.61 (d, J 8.4, 1H), 8.61-8.64 (t, J 5.5, 1H, N$\underline{H}$CH$_2$CH$_2$), 12.36 (bs, 1H, OH) [NH and OH exchange with D$_2$O]; ^{13}C NMR (d6-DMSO) δ 31.8, 34.0, 35.7, 89.4, 111.2, 119.6, 121.3, 124.5, 125.8, 132.9, 136.6, 160.6, 173.1.

4-(3-Bromo-1*H*-indole-2-carboxamido)butanoic acid [155]

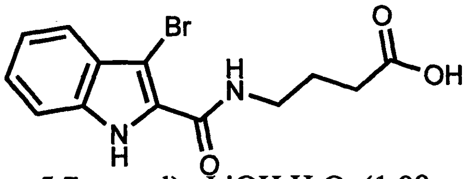

Method D. **[158]** (2.00 g; 5.7 mmol), $LiOH.H_2O$ (1.00 g; 23.8 mmol; 4.2 equiv.) produced a light grey solid (1.57g, 85 %).

R_f 0.56 (100 % EtOAc); mp: 208-210 °C; ^1H NMR (d6-DMSO) δ 1.75-1.85 (tt, J 7.4 6.8, 2H, $NHCH_2C\underline{H}_2CH_2$), 2.31-2.36 (t, J 7.4, 2H, $NHCH_2CH_2C\underline{H}_2$), 3.31-3.39 (dt, J 5.6 6.8, 2H, $NHC\underline{H}_2CH_2CH_2$), 7.14-7.19 (dd, J 8.8 6.1, 1H), 7.26-7.31 (dd, J 9.1 6.1, 1H), 7.44-7.47 (d, 1H , J 9.1), 7.47-7.50 (d, 1H, J 8.8), 7.98-8.02 (t, J 5.6, 1H, $N\underline{H}CH_2CH_2CH_2$), 11.60 (bs, 1H, OH), 11.98 (s, 1H, NH) [OH and NH peaks exchange with D_2O]; ^{13}C NMR (d6-DMSO) δ 24.8, 31.5, 38.9, 90.5, 113.0, 119.8, 121.2, 125.0, 127.0, 129.2, 135.2, 160.5, 174.6; MS (ES+) *mz* (%) = 325.0 (100 %) / 327.0 (100 %) (M+H [^{79}Br] / M+H [^{81}Br]).

2-(3-Bromo-1*H*-indole-2-carboxamido)acetic acid [156]

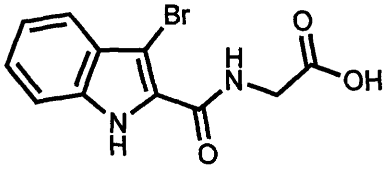

Method D. **[159]** (0.90 g; 2.8 mmol), $LiOH.H_2O$ (0.45 g; 10.7 mmol; 3.9 equiv.) produced a white solid (0.82 g, 99 %).

R_f 0.22 (100 % EtOAc); mp: 218-220 °C; ^1H NMR (d6-DMSO) δ 4.07-4.09 (d, 1H, J 5.6, $NHC\underline{H}_2$), 7.20-7.23 (dd, 1H, J 8.7 6.2), 7.30-7.35 (dd, 1H, J 9.1 6.2), 7.48-7.51 (d, 1H, J 9.1), 7.51-7.54 (d, 1H, J 8.7), 8.13-8.17 (t, 1H, J 5.6, $N\underline{H}CH_2$), 12.11 (s, 1H, NH), 12.82 (bs, 1H, OH) [NH and OH peaks exchange with D_2O]; ^{13}C NMR (d6-DMSO) δ 41.7, 91.0, 113.2, 120.0, 121.3, 125.3, 127.0, 128.0, 135.4, 160.4, 171.3; MS (CI+) *mz*(%) = 297.0 (100 %) / 299.0 (100 %) (M+H [^{79}Br] / M+H [^{81}Br]).

4-(1*H*-Indole-2-carboxamido)butanoic acid [100][172]

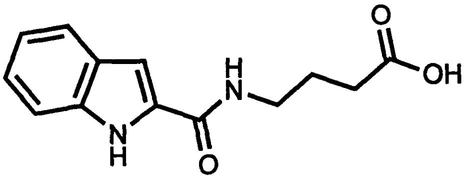

Method D. **[120]** (2.20 g; 8.0 mmol), $LiOH.H_2O$ (1.10 g; 26.2 mmol; 3.3 equiv.) produced a white solid (1.34 g, 68 %).

R_f 0.52 (100 % EtOAc); mp: 184-186 °C; ^1H NMR (d6-DMSO) δ 1.74-1.83 (m, 2H, CH_2), 2.29-2.34 (t, 2H, CH_2), 3.28-3.35 (m, 2H, CH_2), 7.01-7.06 (dd, 1H), 7.11 (s, 1H), 7.15-7.20 (dd, 1H), 7.42-7.44 (d, 1H), 7.60-7.62 (d, 1H), 8.48-8.52 (t, 1H, NH), 11.54 (s, 1H, NH0, 12.09 (bs, 1H, OH) [OH and NH peaks exchange with D_2O]; ^{13}C NMR (d6-DMSO) δ; MS (Cl+) *mz* = 247.1 (M+H).

3-(1-Benzyl-1*H*-indole-2-carboxamido)propanoic acid [41]

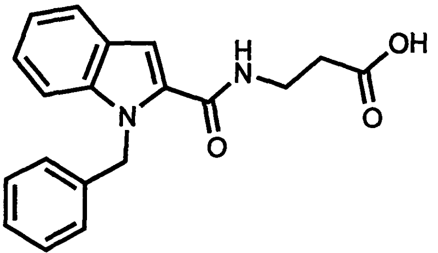

The ester **[40]** (0.21 g; 0.6 mmol) was dissolved in MeOH (2.50 mL; 61.7 mmol; 103.9 equiv.) and NaOH (4M) (2.50 mL; 250.0 mmol; 420.9 equiv.). The mixture was stirred at 60 °C for 4 h, then at room temperature for 64 h. Concentrated HCl was then added dropwise until pH 2 was reached. The solvents were evaporated and the residue dissolved/suspended in distilled water, then extracted with EtOAc, dried over magnesium sulphate and the solvents removed *in vaccuo* to produce a brown solid (0.16 g, 83 %).

R_f 0.04 (1 : 1 Pet 60/80 : EtOAc); mp: 160-175 °C; ^1H NMR (d6-DMSO) δ 2.54-2.59 (t, 2H, CH_2), 3.47-3.53 (dt, 2H, CH_2), 5.90 (s, 2H, CH_2), 7.04-7.71 (m, 10H), 8.69-8.73 (t, NH) [NH exchanges with D_2O]; MS (ES-) *mz* = 321.0 (M-1).

3,4-Dihydro-10-methylazepino[3,4-*b*]indole-1,5(2*H*,10*H*)-dione [31]

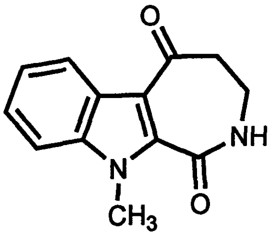

Method E. Phosphorous pentoxide (0.74 g; 5.2 mmol; 0.9 equiv.), methane sulfonic acid (5.2 mL; 80 mmol; 14 equiv.), carboxylic acid [37] (1.380 g; 5.6 mmol). The crude product was purified using column chromatography (eluent 5% EtOAc in Pet 60/80) to afford a brown solid. Yield (1.040 g, 82 %).

R_f 0.21 (100 % EtOAc); mp 207-209 °C (Lit 208 °C[114], 200-205 °C[138]); ^{1}H NMR ($CDCl_3$) δ 2.99-3.03 (m, 2H, CH_2), 3.64-3.70 (q, 2H, CH_2), 4.16 (s, 3H, CH_3), 7.20-7.23 (t,1H), 7.40-7.47 (m,1H), 7.49-7.51 (m,1H), 8.53-8.56 (d,1H); ^{13}C NMR ($CDCl_3$) δ 33.2, 38.2, 45.5, 110.7, 124.3, 125.7, 126.3, 133.5, 139.1, 159.9, 164.4, 195.9; MS (ES+) *mz* 229.0978 (M+H$^+$) (calc. 229.0977).

3,4-Dihydroazepino[3,4-*b*]indole-1,5(2*H*,10*H*)-dione [25]

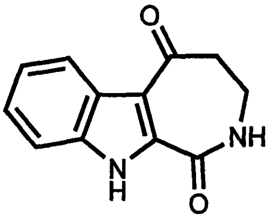

Method E. [27] (1.85 g; 8.0 mmol), phosphorus pentoxide (0.93 g; 6.5 mmol; 0.8 equiv.), methane sulfonic acid (6.50 mL; 100.7 mmol; 12.6 equiv.) was heated at 100 °C. Recrystallization from acetone and petrol produced a yellow solid (0.88 g, 58 %, Lit 85 %[139]).

R_f 0.25 (100 % EtOAc); mp 282-284 °C (lit 257-260 °C[138]); ^{1}H NMR (d6-DMSO) δ 2.83-2.86 (m, 2H, CH_2), 3.46-3.51 (q, 2H, CH_2), 7.23-7 28 (t, 1H), 7.31-7.38 (t, 1H), 7.52-7.55 (d, 1H), 8.30-8.32 (d, 1H), 8.75-8.78 (t, 1H), 12.48 (s, 1H); ^{13}C NMR (d6-DMSO) δ 34.3, 35.6, 102.8, 112.6, 120.0, 121.8, 123.6, 127.4, 132.0, 136.7, 161.5, 173.2; MS (ES+) *mz* = 215.0813 (M+H$^+$) (calc. 215.0815).

2,3-Dihydro-pyrazino[1,2-*a*]indole-1,4-dione [101][173]

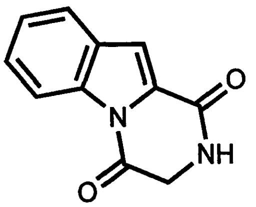

Method E. **[99]** (0.54 g; 2.5 mmol), phosphorous pentoxide (0.22 g; 1.5 mmol; 0.6 equiv.), methane sulfonic acid (1.60 mL; 24.8 mmol; 10.0 equiv.) produced a yellow orange solid (0.03 g, 6 %).

R_f 0.43 (100 % EtOAc); ^{1}H NMR (d6-DMSO) δ 4.41-4.42 (d, 2H, CH_2), 7.36 (s, 1H), 7.38-7.43 (t, 1H), 7.49-7.54 (t, 1H), 7.78-7.81 (d, 1H), 8.35-8.38 (d, 1H), 8.48 (s, NH); ^{13}C NMR (d6-DMSO) δ 47.1, 112.2, 116.1, 122.9, 125.2, 127.6, 128.8, 130.3, 134.6, 156.8, 163.8; MS (ES-) *mz* = 221.2 (M+Na).

1-(1-methyl-1*H*-indole-2-carbonyl)benzo[*b*]azet-2(1*H*)-one [104]

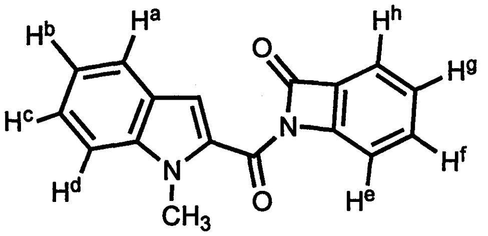

Method E. **[103]** (0.50 g; 1.8 mmol), phosphorus pentoxide (0.26 g; 1.8 mmol; 1.0 equiv.), methane sulfonic acid (2.00 mL; 31.0 mmol; 17.4 equiv.) produced an off white solid (0.10 g, 21 %).

R_f 0.78 (1 : 1 Pet 60/80 : EtOAc); mp: 166 °C; ^{1}H NMR (d6-DMSO) δ 4.29 (s, 3H, CH_3), 7.18-7.22 (dd, 1H, J 7.2 7.5, H^c), 7.39-7.44 (dd, 1H, J 8.1 7.2, H^b), 7.48 (s, 1H), 7.63-7.68 (m, 2H, H^g & H^a), 7.76-7.78 (d, 2H, $2H^d$ & H^e), 7.96-8.02 (dd, 1H, J 8.0 7.9, H^f), 8.18-8.20 (d, 1H, J 7.9, H^h); ^{13}C NMR (d6-DMSO) δ 32.8, 109.7, 111.2, 117.3, 121.0, 122.5, 125.4, 126.1, 127.2, 128.4, 128.5, 137.2, 140.5, 146.5, 152.0, 159.0; MS (ES+) *mz* = 277.0972 ($M+H^+$) (calc = 277.0972).

(*E*)-5-(2-Phenylhydrazono)-2,3,4,5-tetrahydro-10-methylazepino[3,4-*b*]indol-1(10*H*)-one [65]

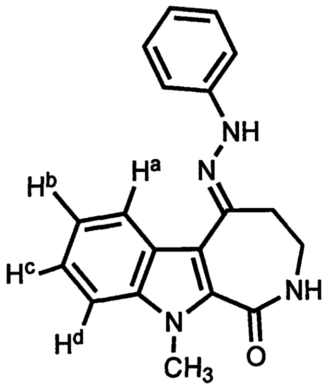

Method F. Phenyl hydrazine hydrochloride (2.26 g; 15.6 mmol; 50 equiv.), sodium acetate (2.02 g; 24.6 mmol; 79 equiv.), **[31]** (0.071 g; 0.3 mmol) in EtOH (75 mL), the product was purified using column chromatography (eluent 1 : 1 Pet 60/80 : EtOAc) to yield a yellow solid (0.062 g, 62 %).

R$_f$ 0.17 (in 100 % EtOAc); mp 268-272 °C; IR 1647, 2967, 3317; ^{1}H NMR (d6-DMSO) δ 2.89-2.92 (m, 2H, NHCH$_2$C$\underline{H_2}$), 3.39-3.42 (m, 2H, NHC$\underline{H_2}$CH$_2$), 3.93 (s, 3H, CH$_3$), 6.75-6.79 (m, 1H), 7.22-7.28 (m, 5H, H^b), 7.34-7.39 (dd, 1H, J 8.2 7.0, H^c), 7.55-7.58 (d, 1H, J 8.2, H^d), 8.33-8.36 (d, 1H, J 8.0, H^a), 8.43-8.48 (t, 1H, J 5.9, N$\underline{H}$CH$_2$CH$_2$), 9.10 (s, 1H); ^{13}C NMR (d6-DMSO) δ 31.9, 34.6, 37.6, 110.7, 113.0, 116.6, 119.2, 121.2, 123.5, 124.2, 124.9, 129.4, 129.6, 138.7, 141.8, 145.5, 164.6; MS (ES+) *mz* = 319.1559 (calculated 319.1558); CHN, C 69.81 %, H 5.86 %, N 16.38 %, Calcd. for $C_{19}H_{18}N_4O.0.2EtOAc.0.2H_2O$ C 70.03 %, H 5.94 %, N 16.50 %.

(*E*)-5-(2-(4-Fluorophenyl)hydrazono)-2,3,4,5-tetrahydro-10-methylazepino[3,4-*b*]indol-1(10*H*)-one [68]

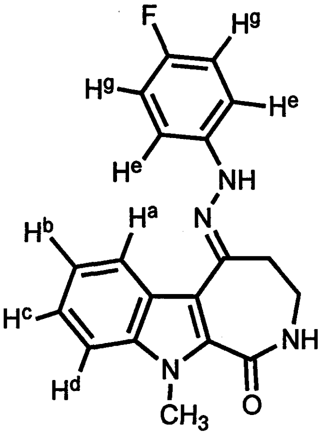

Method F. **[31]** (0.14 g; 0.6 mmol), 4-fluoro-phenyl hydrazine hydrochloride (1.52 g; 9.3 mmol; 15.6 equiv.), sodium acetate (2.38 g; 29.1 mmol; 48.4 equiv.). The solvent was evaporated and the residue dissolved in MeOH instead of EtOAc, water was added, and the solution left overnight. The precipitate was collected, and the pale yellow solid was found to be pure (0.045 g, 22 %).

R_f 0.17 (100 % EtOAc); mp: 218-222 °C; IR: 1659, 2926, 3056, 3212, 3296; ^{1}H NMR (d6-DMSO) δ 2.88-2.91 (m, 2H, $NHCH_2C\underline{H}_2$), 3.39-3.42 (m, 2H, $NHC\underline{H}_2CH_2$), 3.93 (s, 2H, CH_3), 7.075-7.134 (d, 2H, J 8.9, H^g) 7.20-7.26 (m, 4H, H^e&H^b), 7.34-7.39 (dd, 1H, J 8.4 6.9, H^c), 7.55-7.58 (d, 1H, J 8.4, H^d), 8.29-8.32 (d, 1H, J 8.1, H^a), 8.42-8.46 (t, 1H, J 6.0, $N\underline{H}CH_2CH_2$), 9.09 (s, NH) [The two NH peaks exchanged with D_2O]; ^{13}C NMR (d6-DMSO) δ 31.9, 34.7, 37.6, 110.7, 113.9, 114.0, 115.7, 116.0, 116.4, 121.3, 123.5, 124.9, 129.6, 138.7, 141.9, 143.3, 154.7, 157.8, 164.6; MS *mz* (ES+) = 337.1466 (calculated 337.1464).

(*E*)-5-(2-(4-Carboxylic acid methyl ester)hydrazono)-2,3,4,5-tetrahydro-10-methylazepino[3,4-*b*]indol-1(10*H*)-one [72]

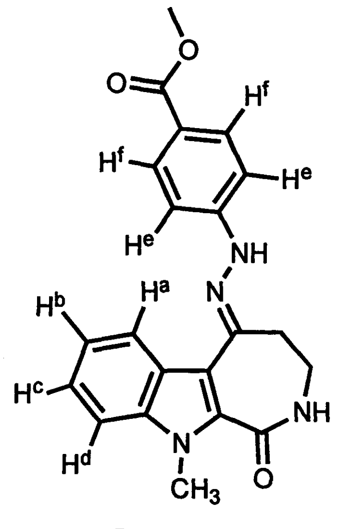

Method F. **[31]** (0.30 g; 1.3 mmol), **[70]** (2.00 g; 9.9 mmol; 7.5 equiv.), sodium acetate (2.00 g; 24.4 mmol; 18.6 equiv.) The solvent was evaporated and the residue dissolved in MeOH instead of EtOAc, water was added, and the solution left overnight. The precipitate was collected, producing a yellow solid (0.21 g, 43 %)

R_f 0.17 (100 % EtOAc); mp: 268-270 °C; IR 1606, 1694, 3276, 3348; ^{1}H NMR (d6-DMSO) δ 2.93-2.97 (m, 2H, $NHCH_2C\underline{H}_2$), 3.40-3.43 (m, 2H, $NHC\underline{H}_2CH_2$), 3.80 (s, 3H, OCH_3), 3.98 (s, 3H, NCH_3), 7.24-7.32 (m, 3H, H^e&H^b), 7.36-7.41 (dd, 1H, J 7.5 7.8, H^c), 7.58-7.61 (d, 1H, J 8.1, H^d), 7.87-7.89 (d, 2H, J 8.4, H^f), 8.31-8.34 (d, 1H, J 7.5, H^a), 8.47-8.51 (t, 1H, J 6.0, $N\underline{H}CH_2CH_2$), 9.66 (s, NH) [both NH exchange with D_2O]; ^{13}C NMR (d6-DMSO) δ 30.0, 32.8, 35.5, 49.8, 108.8, 110.3, 114.0, 117.5, 119.6, 121.4, 122.1, 122.9, 128.2, 129.3, 136.7, 142.4, 148.2, 162.4, 164.5; MS $[E+H]^+$ *mz* = 377.1610 (calculated = 377.1608); CHN: C 66.42 %, H 5.49 %, N 13.98 %, calcd. For $C_{21}H_{20}N_4O_3.0.1C_4H_8O_2$ C 66.69 %, H 5.60 %, N 14.27 %.

(*E*)-2,3,4,5-Tetrahydro-5-(hydroxyimino)-10-methylazepino[3,4-*b*]indol-1(10*H*)-one [73]

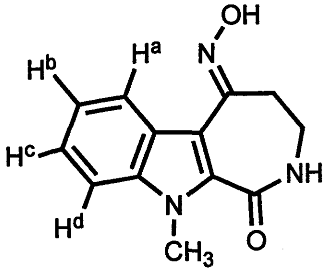

Method F. [31] (1.00 g; 4.4 mmol), hydroxylamine hydrochloride (1.50 g; 21.6 mmol; 4.9 equiv.), sodium acetate (2.95 g; 36.0 mmol; 8.2 equiv.) produced a white solid (0.87 g, 82 %).

R_f: 0.18 (in 100 % EtOAc); mp: 202-204 °C; IR 1644 cm^{-1}, 2922 cm^{-1}, 3353 cm^{-1}; ^1H NMR (d6-DMSO) δ 2.81-2.92 (t, 2H, J 5.4, $NHCH_2C\underline{H}_2$), 3.37-3.48 (dt, 2H, J 5.4 5.9, $NHC\underline{H}_2CH_2$), 4.05 (s, 3H, CH_3), 7.32-7.37 (dd, 1H, J 8.0 6.9, H^b), 7.42-7.48 (dd, 1H, J 8.3 6.9, H^c), 7.70-7.72 (d, 1H, J 8.3, H^d), 8.31-8.34 (d, 1H, J 8.0, H^a), 8.85-8.88 (t, 1H, J 5.9, $N\underline{H}CH_2CH_2$); ^{13}C NMR (d6-DMSO) δ 32.8, 37.0, 45.3, 111.4, 115.1, 123.1, 125.4, 135.1, 138.4, 159.9, 162.8, 196.1; MS *mz* (EI+) 243.1007 (calculated 243.1008); CHN, C 63.33 %, H 5.33 %, N 16.83 %, Calcd. for $C_{13}H_{13}N_3O_2.0.13H_2O$ C 63.60 %, H 5.44 %, N 17.12 %.

(*E*)-5-(2-Phenylhydrazono)-2,3,4,5-tetrahydroazepino[3,4-*b*]indol-1(10*H*)-one [64]

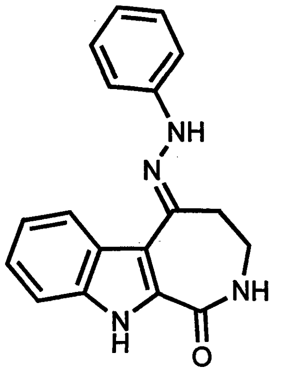

Method G. [25] (0.200 g; 0.9 mmol), phenylhydrazine hydrochloride (1.35 g; 9.3 mmol; 10 equiv.) boron trifluoride diethyletherate (0.4 mL; 3.2 mmol; 3.4 equiv.), pyridine (0.6 mL; 7.4 mmol; 8.0 equiv.), the precipitate was collected and purified by column chromatography (eluent 1 : 1 Pet 60/80 : EtOAc) to yield a pure yellow solid. This was still wet, and decomposed before a pure dry weight was taken.

R_f 0.20 (100 % EtOAc); ^{1}H NMR (d6-DMSO) δ 2.94-2.98 (t, 2H, CH_2), 3.36-3.43 (q, 2H, CH_2), 6.76-6.81 (t, 1H), 7.17-7.22 (t, 1H), 7.26-7.34 (m, 6H), 7.45-7.48 (d, 1H), 8.31-8.34 (t, 1H, NH), 8.46-8.48 (d, 1H), 9.12 (s, 1H, NH), 11.70 (s, 1H, NH) [all 3 NH peaks exchange with D_2O]; ^{13}C NMR (d6-DMSO) δ 32.8, 37.8, 112.5, 113.0, 115.8, 119.1, 120.9, 124.3, 124.7, 125.2, 129.0, 129.4, 136.8, 143.0, 146.6, 165.0.

(*E*)-2,3,4,5-Tetrahydro-5-(hydroxyimino)azepino[3,4-*b*]indol-1(10*H*)-one [87]

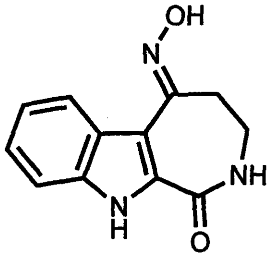

Method G. [25] (1.00 g; 4.7 mmol), hydroxylamine hydrochloride (3.30 g; 47.5 mmol; 10.2 equiv.), boron trifluoride diethyletherate (4.00 mL; 31.6 mmol; 6.8 equiv.), pyridine (6.00 mL; 74.2 mmol; 15.9 equiv.) produced a yellow solid (0.46 g, 43 %).

R_f 0.50 (100 % EtOAc); mp: 258-260 °C ; ^{1}H NMR (d6-DMSO) δ 2.95-2.99 (t, 2H, CH_2), 3.29-3.38 (m, 2H, CH_2), 7.09-7.14 (dd, 1H), 7.32-7.29 (dd, 1H), 7.44-7.47 (d, 1H), 8.20-8.25 (d, 1H), 8.32-8.36 (t, 1H, NH), 11.12 (s, 1H, NH), 11.80 (s, 1H, OH) [NH and OH peaks exchange with D_2O]; ^{13}C NMR (d6-DMSO) δ 30.5, 37.8, 112.5, 112.7, 120.9, 124.5, 124.7, 125.1, 130.0, 136.6, 154.0, 164.6; MS (EI+) *mz* = 229.1.

(*E*)-7-Bromo-2,3,4,5-tetrahydro-5-(hydroxyimino)azepino[3,4-*b*]indol-1(10*H*)-one [86]

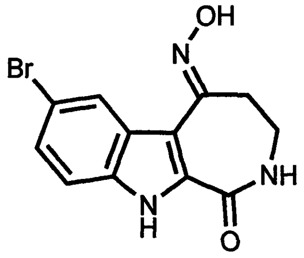

Method G. [57] (0.60 g; 2.0 mmol), hydroxylamine hydrochloride (1.50 g; 21.6 mmol; 10.5 equiv.), boron trifluoride diethyletherate (3.20 mL; 25.3 mmol; 12.3 equiv.), pyridine (4.80 mL; 59.3 mmol; 29.0 equiv.) produced an off white solid (0.36 g, 57 %).

R_f 0.43 (100 % EtOAc); mp: 274-276 °C; IR 1633 cm^{-1}, 3291 cm^{-1}, 3404 cm^{-1}; ^1H NMR (d6-DMSO) δ 2.95-2.98 (t, 2H, CH_2), 3.30-3.45 (m, 2H, CH_2), 7.40-7.41 (m, 2H), 8.42-8.44 (m, 2H, NH), 11.25 (s, 1H, NH), 12.03 (bs, 1H, OH) [NH and OH peaks exchange with D_2O]; ^{13}C NMR (d6-DMSO) δ 30.0, 37.7, 112.1, 113.4, 114.6, 126.6, 127.3, 131.2, 135.3, 153.7, 164.1; MS (EI+) *mz* =308.0029 (M+H;) (calculated 308.0030 for ^{79}Br).

(*E*)-5-(Benzyloxy)imino-2,3,4,5-tetrahydroazepino[3,4-*b*]indol-1(10*H*)-one [88]

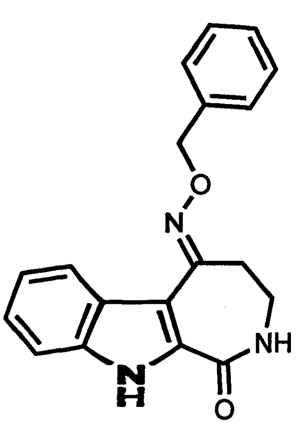

Method G. [25] (0.20 g; 0.9 mmol), *O*-benzylhydroxylamine (1.15 g; 9.3 mmol; 10.0 equiv.), boron trifluoride diethyletherate (0.40 mL; 3.2 mmol; 3.4 equiv.), pyridine (0.60 mL; 7.4 mmol; 8.0 equiv.) produced a creamy white solid (0.08 g, 27 %).

R_f 0.55 (100 % EtOAc); mp: 204 °C; IR 1643 cm^{-1}, 3271 cm^{-1}, 3373 cm^{-1}; ^1H NMR (d6-DMSO) δ 3.01-3.04 (m, 2H, $NHCH_2C\underline{H}_2$), 3.29-3.34 (m, 2H, $NHC\underline{H}_2CH_2$), 5.26 (s, 2H, CH_2), 7.08-7.13 (dd, 1H, J 8.1 7.2), 7.23-7.29 (dd, 1H, J 7.8 7.2), 7.35-7.38, (d, 1H, J7.8), 7.40-7.49 (m, 5H), 8.11-8.14 (d, 1H, J 8.1), 8.38-8.42 (t, 1H, J 5.1, $N\underline{H}CH_2CH_2$), 11.93 (s, 1H, NH) [Both NH peaks exchange with D_2O]; ^{13}C NMR (d6-DMSO) δ 31.1, 37.6, 75.8, 111.5, 112.6, 121.3, 124.4, 124.8, 124.9, 128.0, 128.5, 128.7, 130.9, 136.5, 138.6, 155.1, 164.3; MS (EI+) *mz* = 320.1394 (M+H) (calculated = 320.1394); CHN: C 70.90 %, H 5.45 %, N 12.81 %, Calcd. for $C_{19}H_{17}N_3O_2.0.08C_4H_8O_2$ C 71.11 %, H 5.44 %, N 12.88 %.

N-(2-(Benzyloxycarbamoyl)phenyl)-1-methyl-1*H*-indole-2-carboxamide [107]

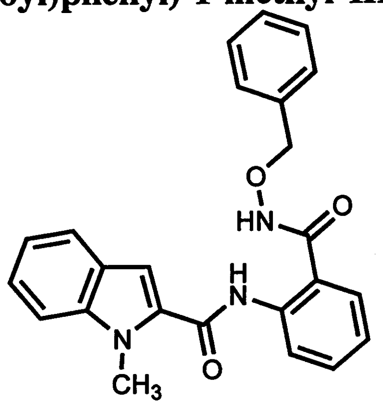

[104] (0.100 g; 0.36 mmol) was dissolved in acetonitrile (2 mL) under nitrogen. *O*-Benzylhydroxylamine (0.25 mL; 2 mmol; 5.6 equiv.) was added and the mixture left stirring for 48 h.

The solvents were evaporated, and the product was purified by column chromatography to yield an oil, from which a solid crashed out. This was recrystalised from acetone and Petrol 60/80 to yield a white solid (0.045 g, 31 %).

R_f 0.70 (1 : 1 Pet 60/80 : EtOAc); mp: 172-174 °C; Ir 1595.50 cm^{-1}, 1746.41 cm^{-1}; ^1H NMR (d6-DMSO) δ 4.07 (s, 3H, CH_3), 5.00 (s, 2H, CH_2), 7.15-7.23 (n, 3H), 7.29-7.42 (m, 4H), 7.47-7.50 (d, 2H), 7.57-7.66 (m, 3H), 7.77-7.79 (d, 1H), 8.51-8.54 (d, 1H), 11.87 (s, 1H, NH), 12.10 (s, 1H, NH) [both NH peaks exchange with D_2O]; ^{13}C NMR (d6-DMSO) δ 31.9, 77.5, 105.2, 111.1, 119.2, 120.9, 121.0, 122.3, 123.3, 124.7, 125.9, 127.8, 128.3, 128.5, 128.7, 128.7, 129.4, 132.2, 132.8, 136.1, 139.2, 139.4, 160.3; MS $[M+H]^+$ *mz* = 400.1653 (expected 400.1656); CHN: C 71.88 % H 5.23 % N 10.30 %; Calcd. for $C_{24}H_{21}N_3O_3$ C 72.16 % H 5.30 % N 10.52 %.

(*E*)-5-(Benzyloxy)imino-2,3,4,5-tetrahydro-10-methylazepino[3,4-*b*]indol-1(10*H*)-one [75]

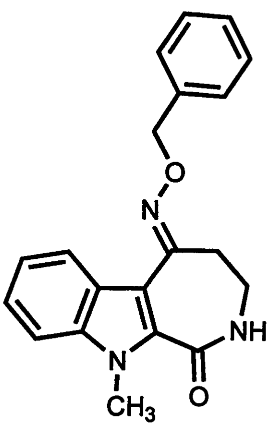

Method H. [73] (0.100 g; 0.41 mmol), Potassium tert-butoxide (0.047 g; 0.42 mmol; 1 equiv.), benzylbromide (0.05 mL; 0.44 mmol; 1.1 equiv), the crude product was purified by column chromatography (eluent 1 : 1 Pet 60/80 : EtOAc) to yield a light brown solid (0.020 g; 15 %).

R_f 0.84 (100 % EtOAc); mp 156-158 °C; ^{1}H NMR (d6-DMSO) δ 2.91-2.96 (t, 2H, CH_2), 3.28-3.37 (q 2H, CH_2), 4.01 (s, 3H, CH_3), 5.18 (s, 2H, CH_2), 7.13-7.21 (t, 1H), 7.31-7.53 (m, 6H), 7.55-7.61 (d, 1H), 7.98-8.02 (d, 1H), 8.45-8.82 (t, NH); ^{13}C NMR (d6-DMSO) δ 32.1, 33.4, 37.3, 75.8, 110.8, 112.2, 121.6, 123.6, 123.8, 125.0, 128.1, 128.4, 128.7, 131.1, 138.6, 138.7, 154.5, 164.1; MS (ES+) *mz* = 356.1 (M+Cl).

(*E*)-5-(Cyclohexylmethoxy)imino-2,3,4,5-tetrahydroazepino[3,4-*b*]indol-1(10*H*)-one [76]

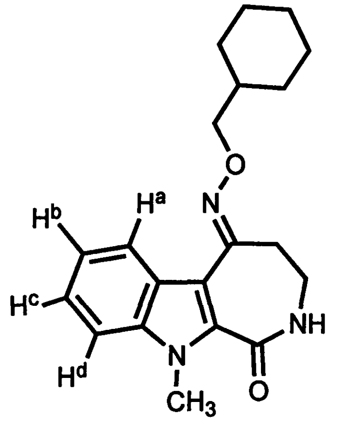

Method H. [31] (0.25 g; 1.1 mmol), Potassium tert-butoxide (0.13 g; 1.0 mmol; 0.9 equiv.), (bromomethyl)cyclohexane (0.15 mL; 1.1 mmol; 1.0 equiv.) produced a light brown solid (0.06 g, 16 %).

R_f 0.52 (100 % EtOAc); mp: 154-156 °C; ^{1}H NMR (d6-DMSO) δ 0.95-1.31 (m, 6H, 1.70-1.80 (m, 5H), 2.89-2.92 (m, 2H, $NHCH_2C\underline{H}_2$), 3.26-3.32 (m, 2H, $NHC\underline{H}_2CH_2$), 3.94 (s, 3H, CH_3), 4.00-4.02 (d, 2H, CH_2), 7.18-7.23 (dd, 1H, 8.1 6.8, H^b), 7.34-7.39 (dd, 1H, 8.4 6.8, H^c), 7.57-7.60 (d, 1H, J 8.4, H^d), 8.10-8.13 (d, 1H, J 8.1, H^a), 8.46-8.50 (t, 1H, J 6.0, $N\underline{H}CH_2CH_2$); ^{13}C NMR (d6-DMSO) δ 25.7, 26.5, 29.7, 32.1, 33.3, 37.7, 79.4, 110.8, 112.4, 121.6, 123.5, 123.8, 125.0, 131.0, 138.6, 153.7, 164.0 MS (EI+) *mz* =340.2023 (M+H) (calculated = 340.2020); CHN, C 68.87 %, H 7.48 %, N 11.06 %, Calcd. for $C_{20}H_{25}N_3O_2.0.5C_4H_8O_2$ C 68.90 %, H 7.62 %, N 10.96 %.

Ethyl 3-(3-bromo-1*H*-indole-2-carboxamido)propanoate [56]

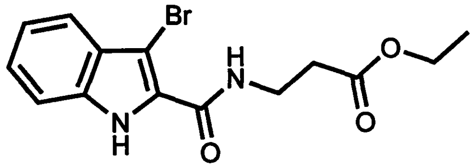

Method I. Indole ether **[52]** (1.032 g; 4.0 mmol), NBS (0.755 g; 4.0 mmol; 1 equiv.), produced a bright yellow solid (0.690 g; 51 %).

R_f 0.52 (1 : 1 Pet 60/80 : EtOAc); mp 144-148 °C; ^{1}H NMR (d6-DMSO) δ 1.19-1.24 (t, 3H, J 7.1, $CH_2C\underline{H}_3$), 2.64-2.75 (t, 2H, J 6.5, $NHCH_2C\underline{H}_2$), 3.59-3.65 (m, 2H, J 6.5, 5.2, $NHC\underline{H}_2CH_2$), 4.09-4.16 (q, 2H, J 7.1, $C\underline{H}_2CH_3$), 7.17-7.20 (dd, J 7.5 7.4, 1H), 7.29-7.34 (dd, J 7.7 7.4, 1H), 7.48-7.53 (dd, 2H, J 7.7 7.5), 8.01-8.04 (t, 1H, J 5.2, $N\underline{H}CH_2CH_2$), 12.04 (s, NH); ^{13}C NMR (d6-DMSO) δ 34.1, 35.6, 39.1, 90.6, 113.1, 119.9, 121.3, 125.2, 127.0, 128.6, 135.3, 160.3, 171.8; MS (ES+) *mz* (%) = 339.0 (100 %) / 341.0 (100 %) (M+H [^{79}Br] / M+H [^{81}Br]).

7-Bromo-3,4-dihydro-2*H*,10*H*-azepino[3,4-*b*]indole-1,5-dione [57]

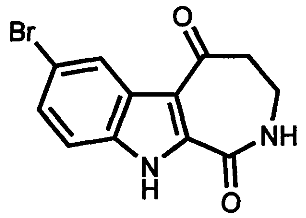

Method I. **[25]** (0.20 g; 0.9 mmol), NBS (0.18 g; 0.9 mmol; 1.0 equiv.) produced a yellow solid (0.24 g, 88 %).

R_f 0.26 (100 % EtOAc); mp >360 °C; ^{1}H NMR (d6-DMSO) δ 2.84-2.87 (t, 2H, CH_2), 3.43-3.48 (q, 2H, CH_2), 7.46-7.53 (m, 2H), 8.45 (s, 1H), 8.84-8.86 (t, NH), 12.69 (s, NH) [both NH peaks exchange with D_2O]; ^{13}C NMR (d6-DMSO) δ 36.9, 44.3, 113.5, 15.2, 115.8, 125.2, 128.0, 128.1, 134.7, 136.0, 162.4, 195.6; MS (EI+) *mz* = 291.9842 (calculated 291.9842 for ^{79}Br).

Ethyl 3-bromo-1*H*-indole-2-carboxylate [113]

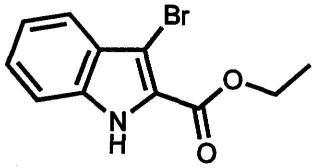

Method I. **[32]** (5.00 g; 26.4 mmol), NBS (5.76 g; 29.6 mmol; 1.1 equiv.) produced a light brown solid (6.17 g, 86 %).

R$_f$ 0.78 (1 : 1 Pet 60/80 : EtOAc); mp: 142-144 °C (Lit 148 °C[169]); ^{1}H NMR (d6-DMSO) δ 1.39-1.45, (t, 3H, CH_3), 4.39-4.46 (q, 2H, CH_2), 7.22-7.27 (t, 1H), 7.38-7.43 (t, 1H), 7.52-7.61 (m, 2H), 1.28 (s, 1H, NH – exchanges with D_2O); ^{13}C NMR (d6-DMSO) δ 14.6, 61.2, 96.3, 113.4, 120.5, 121.5, 124.3, 126.3, 127.2, 136.2, 160.5; MS (ES+) *mz* (%) = 268.0 (100 %) / 270.0 (100 %) (M+H [^{79}Br] / M+H [^{81}Br]).

Ethyl 4-(3-bromo-1*H*-indole-2-carboxamido)butanoate [158]

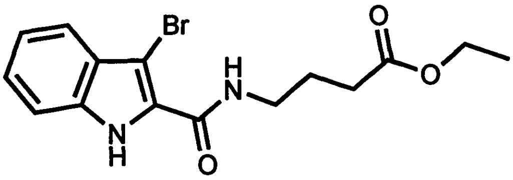

Method I. **[120]** (3.00 g; 10.9 mmol), NBS (2.00 g; 10.3 mmol; 0.9 equiv.) produced a bright yellow solid (2.29 g, 58 %).

R$_f$ 0.56 (1 : 1 Pet 60/80 : EtOAc); mp: 98-100 °C; ^{1}H NMR (d6-DMSO) δ 1.16-1.21 (t, 3H, J 7.2, $CH_2C\underline{H}_3$), 1.79-1.89 (m, 2H, $NHCH_2C\underline{H}_2CH_2$), 2.40-2.45 (t, 2H, J 7.4, $NHCH_2CH_2C\underline{H}_2$), 3.34-4.41 (m, 2H, $NHC\underline{H}_2CH_2CH_2$), 4.03-4.10 (q, 2H, J 7.2, $C\underline{H}_2CH_3$), 7.16-7.21 (dd, 1H, J 8.7 6.0), 7.28-7.33 (dd, 1H, J 8.4 6.0), 7.46-7.52 (dd, 2H, J 8.4 8.7), 8.00-8.04 (t, 1H, $N\underline{H}CH_2CH_2CH_2$), 11.99 (s, 1H, NH) [both NH exchange with D_2O]; ^{13}C NMR (d6-DMSO) δ 14.5, 24.8, 31.4, 38.8, 60.2, 90.5, 113.0, 119.8, 121.0, 125.0, 126.9, 129.2, 135.2, 160.5, 173.0; MS (ES+) *mz* (%) = 353.0 (100 %) / 355.0 (100 %) (M+H [^{79}Br] / M+H [^{81}Br]).

Ethyl 2-(3-bromo-1*H*-indole-2-carboxamido)acetate [159]

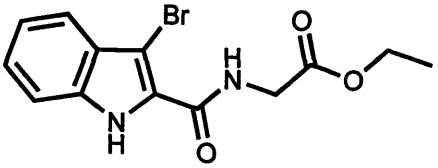

Method I. **[117]** (1.00 g; 4.1 mmol), NBS (0.70 g; 3.6 mmol; 0.9 equiv.) produced an off white solid (1.01 g, 78 %).

R$_f$ 0.60 (1 : 1 Pet 60/80 : EtOAc); mp: 172-174 °C; ^{1}H NMR (d6-DMSO) δ 1.22-1.26 (t, 3H, J 7.2, $CH_2C\underline{H}_3$), 4.14-4.20 (m, 4H, $C\underline{H}_2CH_3$ & $NHC\underline{H}_2$), 7.18-7.23 (dd, 1H, J 7.5 6.8), 7.30-7.35 (dd, 1H, 8.1 6.8), 7.48-7.54 (dd, 2H, J 8.1 7.5), 8.24-8.28 (t, 1H, J 5.5, $N\underline{H}CH_2$), 12.09 (s, 1H, NH) [both NH exchange with D_2O]; ^{13}C NMR (d6-DMSO) δ

14.5, 41.8, 61.0, 91.1, 113.2, 120.0, 121.3, 125.4, 127.0, 128.0, 160.6, 169.9; MS (ES+) *mz* (%) = 325.0 (100 %) / 327.0 (100 %) (M+H [^{79}Br] / M+H [^{81}Br]).

N-((methylcarbamoyl)methyl)-3-bromo-1*H*-indole-2-carboxamide

[122]

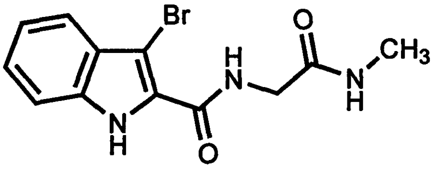

Method J. Weinreb amide **[118]** (0.513 g; 1.5 mmol), *tert*-Butyllithium (1.8 mL; 3.0 mmol; 2 equiv.), the crude product was purified by column chromatography (eluent 2 : 1 Pet 60/80 : EtOAc) to yield a pale yellow solid (0.102 g; 21 %).

R$_f$ 0.25 (100 % EtOAc); mp: 244 °C; ^{1}H NMR (d6-DMSO) δ 2.65-2.66 (d, 3H, J 4.5, NHC$\underline{H}_3$), 3.98-4.03 (d, 2H, J 5.1, NHC$\underline{H}_2$), 7.17-7.22 (dd, 1H, J 8.3 6.6), 7.29-7.34 (dd, 1H, J 8.4 6.6), 7.48-7.5 (d, 1H, J 8.4), 7.51-7.54 (d, 1H, J 8.3), 8.01 (q, 1H, J 4.5, N$\underline{H}$CH$_3$), 8.11-8.15 (t, 1H, J 5.1, N$\underline{H}$CH$_2$), 12.09 (s, 1H, NH) [all NH peaks exchange with D$_2$O]; MS (ES+) *mz* = 310.0188 (M+H) (calculated = 310.0186 for ^{79}Br).

3-Bromo-*N*-(5,5-dimethyl-4-oxohexyl)-1*H*-indole-2-carboxamide [123] and *N*-(3-(methylcarbamoyl)propyl)-3-bromo-1*H*-indole-2-carboxamide [124]

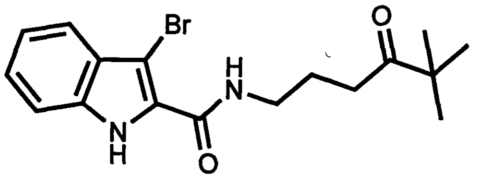

[123]

+

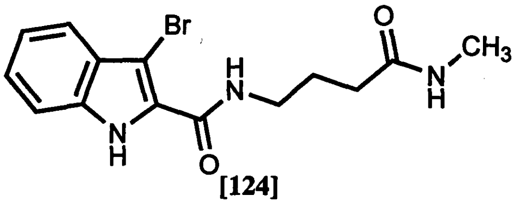

[124]

Method J. **[121]** (0.54 g; 1.5 mmol), *tert*-butyllithium (1.70 mL; 3.1 mmol; 2.1 equiv.). Column chromatography (eluent 1% EtOAc in Pet 60/80) yielded **[123]** which was recrystallized to give a white solid (0.025 g, 5 %). Column chromatography (eluent 100% EtOAc) yielded **[124]**, a white solid (0.040 g, 8 %).

[123]

R$_f$ 0.65 (1 : 1 Pet 60/80 : EtOAc); mp: 140 °C; ^{1}H NMR (d6-DMSO) δ 1.099 (s, 9H, 3CH$_3$), 1.71-1.81 (m, 2H, NHCH$_2$C$\underline{H}_2$CH$_2$), 2.51-2.52 (t, 2H, J 7.2, NHCH$_2$CH$_2$C$\underline{H}_2$), 2.65-2.70 (m, 2H, NHC$\underline{H}_2$CH$_2$CH$_2$), 7.16-7.21 (dd, 1H, J 9.3 5.6), 7.27-7.32 (dd, 1H, J 9.0 5.6), 7.45-7.49 (d, 1H, J 9.3), 7.49-7.52 (d, 1H, J 9.0), 7.97-8.00 (t, 1H, J 5.3, NH$CH_2CH_2CH_2$), 12.00 (s, 1H, NH) [NH peaks exchange with D_2O]; MS (ES+) *mz* = 365.0862 (M+H), (calcd. 365.0859 for ^{79}Br).

[124]

R_f 0.10 (100% EtOAc); mp: 186-188 °C; ^{1}H NMR (d6-DMSO) δ 1.78-1.82 (m, 2H, $NHCH_2C\underline{H_2}CH_2$), 2.16-2.20 (t, 2H, $NHCH_2CH_2C\underline{H_2}$), 2.57-2.58 (d, 3H, $NHC\underline{H_3}$), 3.27-3.34 (m, 2H, $NHC\underline{H_2}CH_2CH_2$), 7.16-7.21 (dd, 1H, J 8.7 6.3), 7.27-7.32 (dd, 1H, J 9.0 6.3), 7.46-7.52 (dd, 2H, J 9.0 8.7), 7.78 (m, 1H, $N\underline{H}CH_3$), 7.99 (t, 1H, $NHCH_2CH_2CH_2$), 12.00 (s, 1H, NH) [all NH peaks exchange with D_2O]; MS (ES+) *mz* = 338.0498 (M+H) (calcd. 338.0499 for ^{79}Br).

β-Alanine ethyl ester hydrochloride [36]

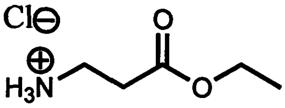

Method K. Thionyl chloride (16.4 mL; 224 mmol; 2 equiv.), ethanol (100 mL; 1712 mmol; 15.3 equiv.), β-Alanine **[29]** (10.0 g; 112 mmol) produced a white solid (16.6 g, 96 %)

mp: 68-70 °C (lit 70-72 °C[174]); ^{1}H NMR (d6-DMSO) δ 1.20 (t, 3H, CH_3), 2.71 (t, 2H, CH_2), 2.98 (m, 2H, CH_2), 4.09 (q, 2H, CH_2), 8.25 (s, 3H, NH_3); ^{13}C NMR (d6-DMSO) δ 14.4, 31.8, 35.0, 60.8, 170.6; MS (ES+) *mz* = 117.9 (M-HCl).

Methyl 4-hydrazinylbenzoate hydrochloride [70]

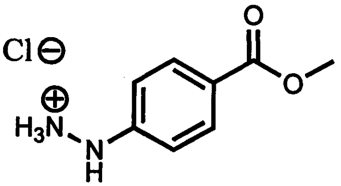

Method K. Thionyl chloride (2.46 mL; 33.7 mmol; 2.1 equiv.), methanol (15.00 mL; 370.3 mmol; 23.3 equiv.), 4-hydrazinylbenzoic acid hydrochloride, (3.00 g; 15.9 mmol) produced a yellow solid (3.1 g, 96 %, lit 51 %[175])

mp 219 °C (Lit 227 °C[175]) ^{1}H NMR (d6-DMSO) δ 3.82 (s, 3H, CH_3), 6.98-7.01 (d. 2H), 7.89-7.92 (d, 2H), 8.89 (s, 1H, NH), 10.33 (s, 3H, NH_3).

Ethyl 1-tosyl-1*H*-indole-2-carboxylate [44][176,177]

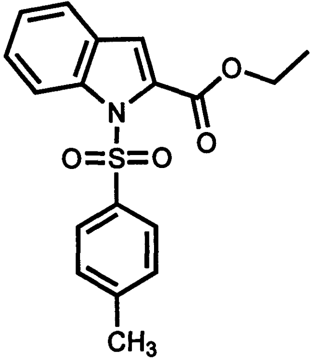

To a stirred solution of potassium *tert*-butoxide (0.36 g; 32 mmol; 0.9 eqiv.) and 18-crown-6 (0.074 g; 3 mmol; 0.08 equiv.) in anhydrous THF (5.6 mL) was added dropwise a solution of indole-2-carboxylic acid ester [32] (0.5 g; 36 mmol) in THF (5.6 mL). The solution was cooled to 0 °C, and a solution of tosyl chloride (0.5 g; 26 mmol; 0.7 equiv.) in THF (5.6 mL) was added dropwise. The reaction was stirred at room temperature 3 h, then most of the solvent was removed *in vaccuo* leaving a small volume which was extracted with EtOAc. This was washed with brine and dried over magnesium sulphate before being purified by column chromatography (eluent 4 : 1 Pet 60/80 : EtOAc) to yield a yellow solid (0.470 g, 72 %).

Rf 0.25 (1 : 1 Pet 60/80 : EtOAc); mp 98-102 °C (Lit 98-99 °C[178]); ^{1}H NMR ($CDCl_3$) δ 1.43-1.48 (t, 3H, CH_3), 2.43 (s, 3H, CH_3), 4.43-4.50 (q, 2H, CH_2), 7.20-7.21 (d, 1H), 7.30-7.36 (m, 2H), 7.45-7.51 (t, 1H), 7.60-7.36 (d, 1H), 7.96- 7.99 (m, 2H), 8.15-8.18 (d, 1H) ; MS (ES+) *mz* = 366.0 (M+Na).

Phenylmagnesium bromide [47][179]

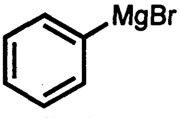

Magnesium (1.2 g) was placed in a flask with anhydrous ether (30 mL) under a condenser, and bromobenzene [46] (6 mL) was added in 1 mL portions. Scratching with a glass rod was required to initiate reaction, and the 1 mL portions were added at a rate so as to keep a gentle reflux. After the final addition, the flask was swirled and allowed to stand until reflux stopped. The product was used *in situ* without analysis.

Diphenyl-4-pyridylmethanol [49][113]

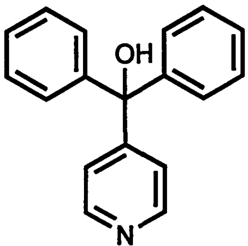

4-Benzoyl pyridine **[48]** (5.55 g; 30 mmol) was dissolved in Et$_2$O (60 mL) at 0 °C. **[47]** (9.5 g; 1.7 equiv.; 52.4 mmol) was brought to 0 °C, and added slowly, washing the flask with Et$_2$O (30 mL). The solution was then refluxed for 15 h, and allowed to cool to 0 °C in an ice bath. This was then poured onto ice-water containing concentrated HCl (16 mL; 196 mmol; 6.3 equiv.). A concentrated NaOH solution was used to bring the solution to pH 7, and the resulting precipitate was filtered and washed with water and Et$_2$O, before being left overnight in a desiccator. A pure white solid was produced (6.476 g; 82 %, Lit 88 %[113]).

R$_f$ 0.61 (100 % EtOAc), mp, 242-244 °C (Lit 240-242 °C[113]); ^{1}H NMR (d6-DMSO) δ 6.73 (s, 1H, OH exchanges with D$_2$O), 7.20-7.36 (m, 12H), 8.51-853 (d, 2H); ^{13}C NMR (d6-DMSO) δ 80.3, 123.0, 127.4, 128.0, 128.2, 146.8, 149.5, 156.3.

Diphenyl-4-pyridylmethyl Chloride Hydrochloride [50][113]

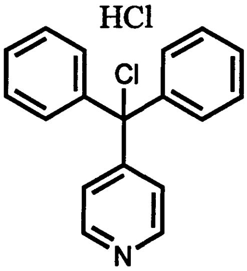

Diphenyl-4-pyridylmethanol **[49]** (2.00 g; 7.7 mmol) was dissolved in chloroform (100 mL) and thionyl chloride (3.5 mL; 3.9 equiv.; 29.9 mmol) was added. The mixture was refluxed for 76 h, and the solvent removed *in vaccuo*. A light brown solid (1.954 g; 81 %, Lit 86 %[113]) was recovered.

R$_f$ 0.57 (100 % EtOAc); mp 188-190 °C (Lit = 134-135 °C[113]); ^{1}H NMR (CDCl$_3$) δ 7.22-7.48 (m, 10H), 7.88-7.90 (d, 2H), 8.88-8.90 (d, 2H); ^{13}C NMR (CDCl$_3$) δ 127.8, 129.2, 129.5, 129.7, 141.2, 141.9, 165.1.

Methyl 2-(3-Ethoxycarbonyl-propionylamino)-benzoate [137][88]

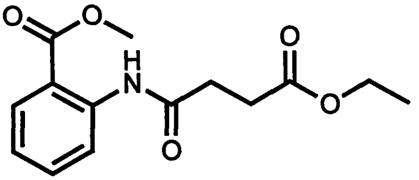

Methyl anthranilate **[103]** (0.7 mL, 5.3 mmol) was dissolved in toluene (9 mL), and cooled. Ethyl succinyl chloride (1.0 mL, 1.2 equiv., 6.3 mmol) was then added. The solution was allowed to warm to room temp, and was then refluxed for 2.5 h. The mixture was cooled, water was added, the extracted with dichloromethane. The solvent phase was washed with HCl (1M), and saturated sodium bicarbonate, then dried over magnesium sulphate, and evaporated. The crude product was purified by column chromatography (eluent 1 : 1 Pet 60/80 : EtOAc) to yield a colourless oil (0.79 g, 52 %). R_f 0.82 (100% EtOAc); ^{1}H NMR ($CDCl_3$) δ 1.19-1.23 (t, 3H, CH_3), 2.66-2.75 (m, 4H, 2xCH_2), 3.88 (s, 3H, CH_3), 4.08-4.13 (q, 2H, CH_2), 7.00-7.05 (t, 1H), 7.45-7.48 (t, 1H), 7.96-7.99 (d, 1H), 8.63-8.66 (d, 1H), 11.26 (s, 1H); ^{13}C NMR ($CDCl_3$) δ 14.6, 29.7, 33.2, 52.8, 61.1, 115.2, 120.8, 122.9, 131.2, 135.1, 141.9, 169.1, 170.8, 173.0.

4,5-Dihydro-1*H*-benzo[*b*]azepin-2(3*H*)-one [141][160]

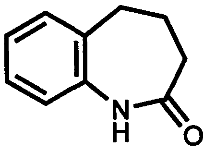

Trichloroacetic acid (81.6 g; 499 mmol; 7.5 equiv.) was melted in a round bottom flask and transferred to an ice bath. Tetralone **[140]** (8.8 mL; 66.2 mmol), and sodium azide (5.44 g; 83.8 mmol; 1.3 equiv.) were added, and the mixture was then heated at 100 °C for 21 h, and allowed to cool to room temperature. The mixture was taken up in DCM and washed with saturated sodium bicarbonate and the solvents removed *in vaccuo*. The tar was recrystallized from EtOAc and Pet 60/80 to give dark brown crystals; 3.2 g (31 %; lit 57 %[160]).

R_f 0.61 (100 % EtOAc); mp: 146 °C (Lit 139-141 °C[160]); ^{1}H NMR (d6-DMSO) δ 2.05-2.18 (m, 4H, CH_2CH_2), 2.66- 2.71 (t, 2H, CH_2), 6.95-6.98 (d, 1H), 7.06-7.11 (t, 1H), 7.20-7.26 (m, 2H), 9.53 (s, 1H, NH) [NH exchanges with D_2O]. ^{13}C NMR (d6-DMSO) δ 28.3, 30.2, 33.2, 121.9, 124.9, 127.5, 130.0, 134.0, 139.3, 173.6.

3,4-Dihydro-1*H*-benzo[*b*]azepine-2,5-dione [139][160]

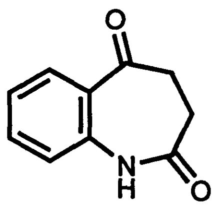

To a solution of **[141]** (0.653 g; 4.1 mmol) in *tert*-butyl alcohol (10 mL) was added distilled water (30 mL), potassium permanganate (3.15 g; 19.9 mmol; 4.9 equiv.) and magnesium nitrate hexahydrate (5.1 g; 19.9 mmol; 4.9 equiv.). The mixture was stirred at room temperature for 20 h.

The mixture was cooled to 0 °C, and 3M HCl (20 mL; 48 mmol; 9.5 equiv.) was added, followed by sodium bisulfite in portions until the mixture became a yellow solution. This was extracted with DCM, dried with magnesium sulphate and *in vaccuo*. The crude product was recrystalized from EtOAc and hexane, purified by column chromatography, then recrystalized again from EtOAc and hexane to yield a white solid (0.077 g, 11 %; lit 26 %[160]).

R_f 0.61 (100 % EtOAc); mp: 188-190 °C (Lit. 185-186 °C[160]); ^{1}H NMR (d6-DMSO) δ 2.65-2.70 (t, 2H, CH_2), 2.90-2.94 (t, 2H, CH_2), 7.16-7.21 (m, 2H), 7.53-7.59 (t, 1H), 7.82-7.85 (d, 1H), 10.10 (s, 1H, NH) [NH exchanges with D_2O]; ^{13}C NMR (d6-DMSO) δ 29.6, 38.7, 122.0, 123.7, 127.1, 130.6, 134.5, 139.6, 173.9, 199.1; MS (EI+) *mz* =175.1.

Kenpaullone [14][87,158,159]

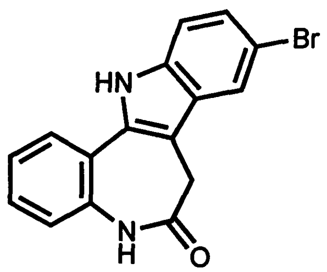

A suspension of ketone **[139]** (0.05 g; 0.3 mmol), 4-bromophenylhydrazine.HCl (0.094 g; 0.4 mmol; 1.5 equiv.) and sodium acetate (0.057 g; 0.7 mmol; 2.4 equiv.) in glacial acetic acid (2 mL; 3.7 mmol; 12.9 equiv.) was stirred at 70 °C for 1 h. Concentrated sulphuric acid (0.1 mL; 1.9 mmol; 6.6 equiv.) was added and the mixture stirred for a further 1 h at 70 °C.

After cooling to room temperature, the mixture was poured into 20 mL of a 5 % aqueous sodium acetate solution, and the precipitate was filtered off and purified by column chromatography (eluent 2 : 1 Pet 60/80 : EtOAc) to yield a brown solid. (0.034 g; 37 %; lit 58 %[158]).

R_f 0.70 (100 % EtOAc); mp: >360 °C (lit >330 °C[158]); ^1H NMR (d6-DMSO) δ 3.52 (s, 2H, CH_2), 7.26-7.32 (m, 3H), 7.38-7.42 (m, 2H), 7.74-7.76 (d, 1H), 7.92 (s, 1H), 10.13 (s, 1H, NH), 11.8 (s, 1H, NH) [both NH exchange with D_2O]; ^{13}C NMR (d6-DMSO) δ 31.7, 107.5, 112.1, 113.8, 120.8, 122.7, 124.1, 124.9, 127.4, 128.7, 128.8, 134.4, 136.0, 136.4, 171.8; MS (ES+) *mz* (%) = 327.1 (100 %) / 329.1 (100 %) (M+H [^{79}Br] / M+H [^{81}Br]).

2-Phenoxyisoindoline-1,3-dione [135][154]

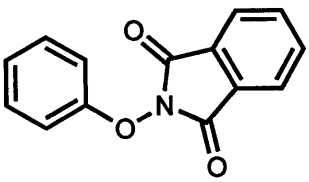

Hydroxyphthalimide (0.483 g; 3 mmol), CuI (0.586 g; 3.1 mmol; 1 equiv.), phenyl boronic acid (0.735 g; 6 mmol; 2 equiv,) and 3 Å molecular sieves (0.733 g) were dissolved in DCM (15 mL), and pyridine (0.3 mL; 3.7 mmol; 1.3 equiv.) was added. The mixture was allowed to stir at room temperature for one week. Silica was added and the solvents removed *in vaccuo*, and purified by column chromatography (eluent 10% EtOAc in Pet 60/80) to yield a cream solid (0.514 g, 65 % Lit 90 %[154]).

R_f 0.65 (1 : 1 Pet 60/80 : EtOAc); mp: 146-148 °C (Lit 150-152 °C, 144-146 °C[154]); ^1H NMR (d6-DMSO) δ 7.15-7.20 (t, 1H), 7.25-7.28 (d, 2H), 7.37-7.43 (t, 2H), 7.92-7.99 (m, 4H); ^{13}C NMR (d6-DMSO) δ 113.5, 124.1, 124.4, 129.1, 130.3, 135.5, 158.9, 163.2; MS (EI+) *mz* = 239.1.

Biological Assays

Cellular Proliferation Assays[180]

All tissue culture work was carried out under sterile conditions in a class II biological safety cabinet. Cells were grown in a humid atmosphere with 5 % CO_2, incubated at 37 °C and counted using a Beckman Coulter Counter Multisizer II. Wild-type MCF-7 human mammary or A549 lung carcinoma cells were removed from liquid nitrogen storage and grown in phenol red RPMI culture medium supplemented with 5 % foetal calf serum, antibiotics (streptomycin and penicillin) and fungicide. Cells were passaged using a 0.5 g/L trypsin solution. Following centrifugation, the supernatant was discarded and the cells re-suspended in culture medium ensuring even distribution. From this cell suspension, cells were seeded out and incubated (5 % CO_2, 37 °C) until needed. For each compound, growth inhibitions experiments were performed in triplicate against a control of untreated cells. Cells were seeded into 24 well plates at 10^6 cells per well and allowed to settle for 24 h. Culture medium was removed and replaced with medium containing inhibitors at varying concentrations. Cells were grown for 7 days before removal with trypsin solution for counting.

CDK2/Cyclin A Assay

CDK2/cyclin A assay kit, containing recombinant protein expressed in Sf21 cells, was purchased from Upstate Inc., lake Placid NY, USA. Radiolabelled ATP was purchased from Amersham PLC, UK. The enzyme was diluted in assay buffer (10 % v/v) and γ^{32}P-ATP was diluted in assay buffer containing magnesium chloride (1 % v/v). A suitable range of dilutions of the test inhibitor were made from a 10 mM stock (in DMSO), using sterile water with 0.1 % DMSO as dilutent. The solutions were made from stock at room temperature and checked for complete solubility of compound (which may precipitate at 4 °C). Assays were performed in 1.5 mL Eppendorf tubes. 5 μL of kit buffer per assay on ice, followed by 5 μL of diluted histone-H1 stock on ice was added to the Eppendorf tube, followed by 2.5 μL of 50 ng CDK2/cyclin A solution. The tubes were then removed from the ice and diluted inhibitor solutions were added. They were then transferred to a beta-cabinet and 10 μL of pre-diluted γ^{32}P-ATP per assay was added. After incubation for 10 minutes at 30 °C in a shaking inhibitor, 20 μL was spotted onto numbered phosphocellulose paper from the kit and allowed to air-dry. These were then transferred on filters to 50 μL Falcon tubes containing 0.75 % phosphoric acid, washed on a rotating mixer for 5 minutes (repeated X3), and the radioactive solution disposed of. The wash solution was replaced with acetone and washed for a further 5 minutes and the filters air-dried. These were then transferred to scintillation tubes and the scintillation counted.

Chk2 Assay

The Chk2 assay was developed and performed in-house by KuDOS Pharmaceuticals Ltd, using purified human Chk2.

Molecular Modelling

All molecular modelling studies were performed on a Apple PowerBook G4 15" 1.33 GHz running Mac OS X version 10.3.9 using Molecular Operating Environment (MOE) 2004.03[181] and SYBYL 7.0[182] molecular modelling software.

All the minimizations performed with MOE were carried out until RMSD gradient of 0.05 Kcal mol^{-1} Å^{-1} with the MMFF94s forcefield and the partial charges were automatically calculated. The minimizations performed with SYBYL were carried out using the Tripos forcefield applying the default values.

References

[1] Cancer Research UK <URL http://www.cancerresearchuk.org.html> [accessed 1st September 2005]

[2] World Health Organisation <URL http://www.who.int/en.html> [accessed 1st September 2005]

[3] Carnero, A.; Targeting the Cell Cycle for Cancer Therapy, *Brit. J. Cancer*, **2002**, *87*, 129-133

[4] Garrett, M. D.; Cell Cycle Control and Cancer, *Curr. Science*, **2001**, *81*, 515-522

[5] Nurse, P.; Masui, Y.; Hartwell, L.; Understanding the Cell Cycle, *Nature Medicine*, **1998**, *4*, 1103-1106

[6] Swanton, C.; Cell-Cycle Targeted Therapies, *Oncology*, **2004**, *5*, 27-36

[7] Kraker, A. J.; Booher, R. N.; Chapter 25. New Targets in Cell Cycle Regulation, *Ann. Rep. Med. Chem.*, **1999**, *34*, 247-255

[8] Nurse, P.; Ordering S Phase and M Phase in the Cell Cycle, *Cell*, **1994**, *79*, 547-550

[9] Grewal, S. S.; Edgar, B. A.; Controlling Cell division in Yeast and Animals: Does Size Matter?, *J. Biol.*, **2003**, *2*, article 5

[10] Lui, V.W.Y.; Grandis, J.R.; EGRF-Mediated Cell Cycle Regulation, *Anticancer Res.*, **2002**, *22*, 1-12

[11] Chong, M. P.; Barritt, G. J.; Crouch M. F.; Insulin Potentiates EGFR Activation and Signaling in Fibroblasts, *Biochem. Biophys. Res. Commun.*, **2004**, *322*, 535–541

[12] Takaki, T.; Fukasawa, K.; Suzuki-Takahashi, I.; Hirai H.; CDK-Mediated Phosphorylation of pRb Regulates HDAC Binding in vitro, *Biochem. Biophys. Res. Commun.*, **2004**, *316*, 252–255

[13] Yamasaki, L.; Pagano, M.; Cell Cycle Proteolysis and Cancer, *Curr. Opin. Cell. Biol.*, **2004**, *16*, 623-628

[14] Sherr, C. J.; G1 Phase Progression Cycling on Cue, *Cell*, **1994**, *79*, 551-555

[15] Vodermaier, H. C.; APC/C and SCF: Controlling Each Other and the Cell Cycle, *Curr. Biol.*, **2004**, *14*, 787-796

[16] Reed, S.I.; Maller, J.L.; Cell Multiplication, *Curr. Opin. Cell. Biol.*, **1996**, *8*, 763-766

[17] S.D. Kimball and K.R. Webster; Chapter 14. Cell Cycle Kinases and Checkpoint Regulation in Cancer. *Annu. Rep. Med. Chem.*, **2001**, *36*, 139-148

[18] Lees, E.; Cyclin Dependent Kinase Regulation, *Curr. Opin. Cell Biol.*, **1995**, *7*, 773-778

[19] McInnes, C.; Andrews, M. J. I.; Zheleva, D. I.; Lane, D. P.; Fischer, P. M.; Peptidomimetic Design of CDK Inhibitors Targeting the Recruitment Site of the Cyclin Subunit, *Curr. Med. Chem. Anti-Cancer Agents*, **2003**, *3*, 57-69

[20] Ekholm, S. V.; Reed, S. I.; Regulation of G1 Cyclin-Dependent Kinases in the Mammalian Cell Cycle, *Curr. Opin. Cell. Biol.*, **2000**, *12*, 676-684

[21] Vidal, A.; Koff, A.; Cell-Cycle Inhibitors: Three Families United by a Common Cause, *gene,* **2000**, *247*, 1-15

[22] Boylan, J. M.; Gruppuso, P. A.; D-Type Cyclins and G1 Progression During Liver Development in the Rat, *Biochem. Biophys. Res. Commun.*, **2005**, *330*, 722–730

[23] Lundberg, A. S.; Weinberg, R. A.; Control of the Cell Cycle and Apoptosis, *Eur. J. Cancer*, **1999**, *35*, 531-539

[24] A.B. Pardee, Regulation of the Cell Cycle; Chapter 2; *www.cancerhandbook.net.*

[25] Johnson, D. G.; Schneider-Broussard, R.; Role of E2F in Cell Cycle Control and Cancer, *Front. Biosci.*, **1998**, *3*, 447-458

[26] Schwob, E.; Flexibility and Governance in Eukaryotic DNA Replication, *Curr. Opin. Microbiol.*, **2004**, *7*, 680-690

[27] Curman, D.; Cinel, B.; Williams, D. E.; Rundle, N.; Block, W. D.; Goodarzi, A. A.; Hutchins, J. R.; Clarke, P. R.; Zhou, B.; Lees-Miller, S. P.; Andersen, R. J.; Roberge, M.; Inhibition of the G2 DNA Damage Checkpoint and of Protein Kinases Chk1 and Chk2 by the Marine Sponge Alkaloid Debromohymenialdisine, *J. Biol. Chem.*, **2001**, *276*, 17914-17919

[28] Rudner, A. D.; Murray, A. W.; The Spindle Assembly Checkpoint, *Curr. Opin. Cell. Biol.*, **1996**, *8*, 773-780

[29] Matsumoto, Y.; Hayashi, K.; Nishida, E.; Cyclin-Dependent Kinase 2 (Cdk2) is Required for Centrosome Duplication in Mammalian Cells, *Curr. Biol.*, **1999**, *9*, 429–432

[30] McGowan, C. H.; Russell, P.; the DNA Damage Response: Sensing and Signalling, *Curr. Opin. Cell Biol.*, **2004**, *16*, 629-633

[31] Tenzer, A.; Pruschy, M.; Potentiation of DNA-Damage-Induced Cytotoxicity by G_2 Checkpoint Abrogators, *Curr. Med. Chem. – Anti-Cancer Agents*, **2003**, *3*, 35-46

[32] Bartek, J.; Falck, J.; Lukas, J.; Chk2 Kinase: A Busy Messenger, *Nature Rev.*, **2001**,

2, 877-886

[33] White, A. W.; Nicholson, R. I.; Unpublished personal communication, **2005**

[34] Feng, H.; Reining in CDK, *Nature Struct. Biol.*, **2001**, *8*, 391

[35] Press Release: The 2001 Nobel Prize in Physiology or Medicine, [www] URL <http://nobelprize.org/medicine/laureates/2001/press.html> [accessed 15th September 2005].

[36] Gray, N.; Detivaud, L.; Doerig, C.; Meijer, L.; ATP-site Directed Inhibitors of Cyclin-dependent Kinases, *Curr. Med. Chem.*, **1999**, *6*, 859-875

[37] Monaco III, E. A.; Beaman-Hall, C. M.; Mathur, A.; Vallano, M. L.; Roscovitine, Olomoucine, Purvalanol: Inducers of Apoptosis in Maturing Cerebellar Granule Neurons, *Biochem. Pharmacol.*, **2004**, *67*, 1947-1964

[38] Kasten, M.; Giordano, A.; CDK10, a Cdc2-Related Kinase, Associates With the Ets2 Transcription Factor and Modulates its Transactivation Activity, *Oncogene*, **2001**, *20*, 1832-1838

[39] Roberts, J. M.; Evolving Ideas about Cyclins, *Cell*, **1999**, *98*, 129-132

[40] Bazan, J. F.; Helical Fold Prediction for the Cyclin Box, *Proteins: Struct. Funct. Genet.*, **1996**, *24*, 1-17

[41] Graph of Rise and Fall of Several Proteins Including Cyclin, MPF, cdc2, Modified From Campbell, *Biology* [www] <URL: http://home.earthlink.net/~dayvdanls/MPF-cyclin.htm> [accessed 3rd June 2005]

[42] S. Mader; *Biology (5th Edition)*, **1996**, McGraw-Hill

[43] Lim, J. H.; Chang, Y.; Park, Y. B.; Park, J.; Kwon, T. K.; Transcriptional Repression of E2F Gene by Proteasome Inhibitors in Human Osteosarcoma Cells, *Biochem. Biophys. Res. Commun.*, **2004**, *318*, 868–872

[44] Brown, N. R.; Noble, M. E. M.; Endicott, J. A.; Johnson, L. N.; The structural Basis for Specificity of Substrate and Recruitment Peptides for Cyclin-Dependent Kinases, *Nature Cell Biol.*, **1999**, *1*, 438-443

[45] Willems, A. R.; Schwab, M.; Tyers, M.; A Hitchhiker's Guide to the Cullin Ubiquitin Ligases: SCF and its Kin, *Biochim. Biophys. Acta*, **2004**, *1695*, 133– 170

[46] Koepp, D. M.; Harper, J. W.; Elledge, S. J.; How the Cyclin Became a Cyclin: Regulated Proteolsis in the Cell Cycle, *Cell*, **1999**, *97*, 431-434

[47] Morgan, D. O.; Cyclin-Dependent Kinases: Engines, Clocks, and Microprocessors, *Ann. Rev. Cell Dev. Biol.*, **1997**, *13*, 261-91

[48] Russo, A. A.; Tong, L.; Lee, J.; Jeffery, P. D.; Pavletich, N. P.; Structural Basis for Inhibition of the Cyclin-Dependent Kinase CDK6 by the Tumour Suppressor $p16^{INK4a}$, *Nature*, **1998**, *395*, 237-243

[49] Sherr, C.J.; Cancer Cell Cycles, *Science*, **1996**, *274*, 1672

[50] Swellam, M.; El-Aal, A. A. A.; AbuGabel, K. M.; Deletions of p15 and p16 in Schistosomal Bladder Cancer Correlate With Transforming Growth Factor-α Expression, *Clin. Biochem.*, **2004**, *37*, 1098-1104

[51] Pavletich, N. P.; Mechanisms of Cyclin-dependent Kinase Regulation: Structures of CDKs, their Cyclin Activators, and Cip and INK4 Inhibitors, *J. Mol. Biol.*, **1999**, *287*, 821-828

[52] G. Draetta & M. Pagano; Section V. Topics in cancer, *Annu. Rep. Med. Chem.*, **1998**, *31*, 241-247

[53] Bryja, V.; Pachernik, J.; Faldikova, L.; Krejci, P.; Pogue, R.; Nevriva, I.; Dvorak, P.; Hampl, A.; The Role of $p27^{Kip1}$ in Maintaining the Levels of D-Type Cyclins in vivo, *Biochim. Biophys. Acta*, **2004**, *1691*, 105- 116

[54] Bastians, H.; Townsley, F. M.; Ruderman, J. V.; The Cyclin-Dependent Kinase Inhibitor $p27^{Kip1}$ Induces N-Terminal Proteolytic Cleavage of Cyclin A, *Proc. Natl. Acad. Sci. USA*, **1998**, *95*, 15374–15381

[55] Smits, V. A. J.; Medema, R. H.; Checking out the G_2/M Transition, *Biochim. Biophys. Acta*, **2001**, *1519*, 1-12

[56] Dong, Y.; Chi, S. L.; Borowsky, A. D.; Fan, Y.; Weiss, R. H.; Cytosolic $p21^{Waf1/Cip1}$ Increases Cell Cycle Transit in Vascular Smooth Muscle Cells, *Cellular Signalling*, **2004**, *16*, 263–269

[57] Yang, J.; Kornbluth, S.; All Aboard the Cyclin Train: Subcellular Trafficking of Cyclins and Their CDK Partners, *Cell Biol.*, **1999**, *9*, 207-210

[58] Schulze-Gahmen, U.; Brandsen, J.; Jones, H.D.; Morgan, D.O.; Meijer, L.; Vesely, J.; Kim, S.H.; Multiple Modes of Ligand Recognition: Crystal Structures of Cyclin-Dependent Protein Kinase 2 in Complex With ATP and Two Inhibitors, Olomoucine and Isopentenyladenine, *Prot. Struct. Func. Gen.*, **1995**, *22*, 378-391

[59] Schulze-Gahmen, U.; De Bondt, H.L.; Kim, S.H.; High Resolution Crystal Structures of Human Cyclin-Dependent Kinases: With and Without ATP: Bound Waters and Natural Ligands as Guides for Inhibitor Design, *J. Med. Chem.*, **1996**, *39*, 4540-4536

[60] Russo, A. A.; Jeffery, P. D.; Pavletich, N. P.; Structural Basis of Cyclin-Dependent Kinase Activation by Phosphorylation, *Nat. Struct. Biol.*, **1996**, *3*, 696-700

[61] Jeffery, P. D.; Russo, A. A.; Polyak, K.; Gibbs, E.; Hurwitz, J.; Massague, J.; Pavleitch, N. P.; Mechanism of CDK Activation Revealed by the Structure of a Cyclin A-CDK2 Complex, *Nature*, **1995**, *376*, 313-320

[62] Noble, M. E. M.; Endicott, J. A.; Chemical Inhibitors of Cyclin-Dependent Kinases: Insights into Design from X-Ray Crystallographic Studies, *Pharmacol. Ther.*, **1999**, *82*, 269-278

[63] De Bondt, H. L.; Rosenblatt, J.; Jancarik, J.; Jones, H. D.; Morgan, D. O.; Kim, S.; Crystal Structure of Cyclin-Dependent Kinase 2, *Nature*, **1993**, *363*, 595-602

[64] Endicott, J. A.; Noble, M. E. M.; Tucker, J .A.; Cyclin-Dependent Kinases: Inhibition and Substrate Recognition, *Curr. Opin. Struct. Biol.*, **1999**, *9*, 738-744

[65] Brown, N. R.; Noble, M. E. M.; Lawrie, A. M.; Morris, C. M.; Tunnah, P.; Divita, G.; Johnson, L. N.; Endicott, J. A.; Effects of Phosphorylation of Threonine 160 on Cyclin-dependent Kinase 2 Structure and Activity, *J. Biol. Chem.*, **1999**, *274*, 8746-8756

[66] Beattie, J. F.; Breault, G. A.; Ellston, R. P. A.; Green, S.; Jewsbury, P. J.; Midgley, C. J.; Naven, R. T.; Minshull, C. A.; Pauptit, R. A.; Tucker, J. A.; Pease, J. E.; Cyclin-Dependent Kinase 4 Inhibitors as a Treatment for Cancer. Part 1: Identification and Optimization of Substituted 4,6-Bis Anilino Pyrimidines, *Bioorg. Med. Chem. Lett.*, **2003**, *13*, 2955–2960

[67] Toledo, L. M.; Lydon, n. B.; Elbaum, D.; the Structure-Based Design of ATP-Site Directed Protein Kinase Inhibitors, *Curr. Med. Chem.*, **1999**, *6*, 775-805

[68] Senderowicz, A. M.; Targeting Cell Cycle and Apoptosis for the Treatment of Human Malignancies, *Curr. Opin. Cell Biol.*, **2004**, *16*, 670-678

[69] Sausville, E. A.; Complexities in the Development of Cyclin-Dependent Kinase Inhibitor Drugs, *Trends Mol. Med.*, **2002**, *8*, 32-37

[70] Boyle, F. T.; Costello, G. F.; Cancer Therapy: a Move to the Molecular Level, *Chem. Soc. Rev.*, **1998**, *27*, 251-260

[71] Toogood, P. L.; Progress Towards the Development of Agents to Modulate the Cell Cycle, *Curr. Opin. Chem. Biol.*, **2002**, *6*, 472-478

[72] Kim, K. S.; Kimball, S. D.; Misra, R. N.; Rawlins, D. B.; Hunt, J. T.; Xiao, H.; Lu, S.; Qian, L.; Han, W.; Shan, W.; Mitt, t.; Cai, Z.; Poss, M. A.; Zhu, H.; Sack, J. S.; Tokarski, J. S.; Chang, C. Y.; Pavletich, N.; Kamath, A.; Humphreys, W. G.; Marathe,

P.; Bursuker, I.; Kellar, K. A.; Roongta, U.; Batorsky, R.; Mulheron, J. G.; Bol, D.; Fairchild, C. R.; Lee, F. Y.; Webster, K. R.; Discovery of Aminothiazole Inhibitors of Cyclin-Dependent Kinase 2: Synthesis, X-ray Crystallographic Analysis, and Biological Activities, *J. Med. Chem.*, **2002**, *45*, 3905-3927

[73] Roy, K. K.; Sausville, E. A.; Early development of Cyclin Dependent Kinase Modulators, *Curr. Pharm. Des.*, **2001**, *7*, 1669-1687

[74] Nathans, D.; Puromycin Inhibition of Protein Synthesis: Incorporation of Puromycin into Peptide Chains, *Biochem.*, **1964**, *51*, 585-592

[75] Garrett, M. D.; Fattaey, A.; CDK Inhibition and Cancer Therapy, *Curr. Opin. Genet. Dev.*, **1999**, *9*, 104-111

[76] Arraham, R. T.; Acquarone, M.; Andersen, A.; Asensi, A.; Belle, R.; Berger, F.; Bergounioux, C.; Brunn, G.; Buquet-Fagot, C.; Fagot, D.; Glab, N.; Goudeau, H.; Goudeau, M.; Guerrier, P.; Houghton, P.; Hendriks, H.; Kloareg, B.; Lippai, M.; Marie, D.; Maro, B.; Meijer, L.; Mester, J.; Mulner-Lorillon, O.; Poulet, S. A.; Schierenberg, E.; Schutte, B.; Vaulot, D.; Verlhac, M. H.; Cellular Effects of Olomoucine, an Inhibitor of Cyclin-Dependent Kinases, *Biol. Cell*, **1995**, *83*, 105-120

[77] Gibson, A. E.; Arris, C. E.; Bentley, J.; Boyle, F. T.; Curtin, N. J.; Davies, T. G.; Endicott, J. A.; Golding, B. T.; Grant, S.; Griffin, R. J.; Jewsbury, P.; Johnson, L. N.; Mesguiche, V.; Newell, D. R.; Noble, M. E. M.; Tucker, J. A.; Whitfield, H. J.; Probing the ATP Ribose-Binding Domain of Cyclin-Dependent Kinases 1 and 2 with *O6*-Substituted Guanine Derivatives, *J. Med. Chem.*, **2002**, *45*, 3381-3393

[78] Gray, N. S.; Wodicka, L.; Thunnissen, A. W. H.; Norman, T. C.; Kwon, S.; Espinoza, F. H.; Morgan, D. O.; Barnes, G.; LeClerc, S.; Meijer, L.; Kim, S.; Lockhart, D. J.; Schultz, P. G.; Exploiting Chemical Libraries, Structure, and Genomics in the Search for Kinase Inhibitors, *Science*, **1998**, *281*, 533-538

[79] Sielecki, T. M.; Boylna, J. F.; Benfield, P. A.; Trainor, G. L.; Cyclin-dependent Kinase Inhibitors: Useful targets in cell Cycle regulation *J. Med. Chem.*, **2000**, *43*, 1-18

[80] Fischer, P. M.; Lane, D. P.; Inhibitors of Cyclin-Dependent Kinases as Anti-Cancer Therapeutics, *Curr. Med. Chem.*, **2000**, *7*, 1213-1245

[81] Mason, K.; Hunter, N. R.; Raju, U.; Ariga, H.; Husain, Amir.; Valdecanas, D.; Neal, R.; Ang, K. K.; Milas, L.; Flavopiridol Increases Therapeutic Ratio of Radiotherapy by Preferentially Enhancing Tumour Radioresponse, *Int. J. Radiation. Oncology Biol. Phys.*, **2004**, *59*, 1181-1189

[82] Sausville, E. A.; Zaharevitz, D.; Gussio, R.; Meijer, L.; Louarn-Leost, M.; Kunick, C.; Schultz, R.; Lahusen, T.; Headlee, D.; Stinson, S.; Arbuck, S. G.; Senderowicz, A.; Cyclin-Dependent Kinases: Initial Approaches to Exploit a Novel Therapeutic Target, *Pharmacol. Ther.*, **1999**, *82*, 285–292

[83] Kim, K. S.; Sack, J. S.; Tokarski, J. S.; Qian, L.; Chao, S. T.; Leith, L.; Kelly, Y. F.; Misra, R. N.; Hunt, J. T.; Kimball, S. D.; Humphreys, W. G.; Aulet, B. S.; Mulheron, J. G.; Webster, K. R.; Thio- and Oxoflavopiridols, Cyclin-Dependent-Kinase 1-Selective Inhibitors: Synthesis and Biological Effects, *J. Med. Chem.*, **2000**, *43*, 4126-4134

[84] Senderowica, A. M.; Headlee, D.; Stinson, S. F.; Lush, R. M.; Kalil, N.; Villalba, L.; Hill, K.; Steinberg, S. M.; Figg, W. D.; Tompkins, A.; Arbuck, S. G.; Sausville, E. A.; Phase I Trial of Continuous Infusion Flavopiridol, a Novel Cyclin-Dependent Kinase Inhibitor, in Patients With Refractory Neoplasms, *J. Clin. Oncology*, **1998**, *16*, 2986-2999

[85] Shapiro, G. I.; Supko, J. G.; Patterson, A.; Lynch, C.; Lucca, J.; Zacarola, P. F.; Muzikansky, A.; Wright, J. J.; Lynch, J.; Rollins, B. J.; A Phase II Trial of the Cyclin-dependent Kinase Inhibitor Flavopiridol in Patients with Previously Untreated Stage IV Non-Small Cell Lung Cancer, *Clin. Cancer Res.*, **2001**, *7*, 1590-1599

[86] Grendys, E. C.; Blessing, J. A.; Burger, R.; Hoffman, J.; A Phase II Evaluation of Flavopiridol as Second-Line Chemotherapy of endometrial carcinoma: A Gynecologic Oncology Group Study, *Gynecologic Oncology*, **2005**, *98*, 249-253

[87] Schultz, C.; Link, A.; Leost, M.; Zaharevitz, D. W.; Gussio, R.; Sausville, E. A.; Meijer, L.; Kunick, C.; Paullones, a Series of Cyclin-Dependent Kinase Inhibitors: Synthesis, Evaluation of CDK1/cyclin B Inhibition, and in vitro Antitumour Activity, *J. Med. Chem.*, **1999**, *42*, 2909-2919

[88] Kunick C.; Schultz, C.; Lemcke, T.; Zaharevitz, D. W.; Gussio, R.; Julluri, R. K.; Sausville, E. A.; Leost, M.; Meijer, L.; 2-Substituted Paullones: CDK1/Cyclin B-Inhibiting Property and In Vitro Antiproliferative Activity, *Bioorg. Med. Chem. Lett.*, **2000**, *10*, 567-569

[89] Zaharevitz, D. W.; Gussio, R.; Leost, M.; Senderowicz, A. M.; Lahusen, T.; Kunick, C.; Meijer, L.; Sausville, E. A.; Discovery and Initial Characterization of the Paullones, a Novel Class of Small-Molecule Inhibitors of Cyclin-dependent Kinases, *Cancer Res.*, **1991**, *59*, 2566-2569

[90] Zaharevitz, D. W.; Gussio, R.; Leost, M.; Senderowicz, A.; Lahusen, T.; Kunick, C.; Meijer, L.; Sausville, E. A.; A Model of Kenpaullone (NCS-664704) Fit in the ATP Site of CDK2 [www] UCL <http://www.dtp.nci.nih.gov/branches/itb/tsddg/paullones/kp%5Fcdk2nc.html> [accessed 5th June 2005]

[91] Annoura, H. Tatsuoka, T.; Total Synthesis of Hymenialdisine and Debromohymenialdisine: Stereospecific Construction of the 2-Amino-4-oxo-2-imidazolin-5(Z)-Disubstituted Ylidene Ring System, *Tetrahedron Lett.*, **1995**, *36*, 413-416

[92] Meijer L.; Thunnissen, A. W. H.; White, A. W.; Garneier, M.; Nikolic, M.; Tsai, L.; Walter, L.; Cleverley, K. E.; Salinas, P. C.; Wu, Y.; Biernat, J.; Mandelkow, E.; Kim, S.; Pettit, G. R.; Inhibition of Cyclin-Dependent Kinases, Gsk-3 and Chkl by Hymenialdisine, a Marine Constituent, *Chem. Biol.*, **2000**, *7*, 51-63

[93] Akinago, S.; Sugiyama, K.; Akiyama, T.; UCN-01 (7-Hydroxystaurosprine) and Other Indolocarbazole Compounds: a New Generation of Anti-Cancer Agents for the New Century?, *Anti-Cancer Drug Des.*, **2000**, *15*, 43-52

[94] Johnson, L. N.; De Moliner, E.; Brown, N. R.; Song, H.; Barford, D.; Endicott, J. A.; Noble, M. E. M.; Structural Studies With Inhibitors of the Cell Cycle Regulatory Kinase Cyclin-Dependent Protein Kinase 2, *Pharmacol. Ther.*, **2002**, *93*, 113-124

[95] Hoessel, R.; Leclerc, S.; Endicott, J. A.; Nobel, M. E. M.; Lawrie, A.; Tunnah, P.; Leost, M.; Damiens, E.; Marie, D.; Marko, D.; Niederberger, E.; Tang, W.; Eisenbrand, G.; Meijer, L.; Indirubin, the Active Constituent of a Chinese Antileukaemia Medicine, Inhibits Cyclin-Dependent Kinases, *Nat. Cell Biol.*, **1999**, *1*, 60-67

[96] Crews, C. M.; Mohan, R.; Small-Molecule Inhibitors of the cell cycle, *Curr. Opin. Chem. Biol.*, **2000**, *4*, 47–53

[97] Marko, D.; Schatzle, S.; Friedel, A.; Genzlinger, A.; Zankl, H.; Meijer, L.; Eisenbrand, G.; Inhibition of Cyclin-Dependent Kinase 1 (CDK1) by Indirubin Derivatives in Human Tumour Cells, *Brit. J. Cancer*, **2001**, *84*, 283-289

[98] Huwe, A.; Mazitschek, R.; Giannis, A.; Small Molecules as Inhibitors of Cyclin-Dependent Kinases, *Angew. Chem. Int. Edit.*, **2003**, *42*, 2122-2138

[99] Meijer, L.; Chemical Inhibitors of Cyclin-Dependent Kinases, *Cell Biol.*, **1996**, *6*, 393-397

[100] Furet, P.; X-Ray Crystallographic Studies of CDK2, a Basis for Cyclin-Dependent Kinase Inhibitor Design in Anti-Cancer Drug Design, *Curr. Med. Chem. Anti-Cancer Agents*, **2003**, *3*, 15-23

[101] International Union of Pure and Applied Chemistry [www] <URL: http://www.chem.qmul.ac.uk/iupac/> [accessed 10th September 2005]

[102] Unpublished student project; S. English, project student, Cardiff University, 2000

[103] Webb, R. G.; Haskell, M. W.; Stammer, C. H.; A Nuclear Magnetic Resonance Method for Distinguishing Alpha Amino Acids from Beta and Gamma Isomers, *J. Org. Chem.*, **1969**, *34*, 576-580

[104] Cho, H.; Matsuki, S.; Ring Construction of Several Heterocycles With Phosphorous Pentoxide – Methane Sulfonic Acid (PPMA), *Heterocycles*, **1996**, *43*, 127-131

[105] Mizuno, A.; Miya, M.; Kamei, T.; Shibata, M.; Tatsuoka, T.; Nakanishi, K.; Takinguchi, C.; Hidaka, T.; Yamaki A.; Inomata, N.; Studies on Antihypertensive Agents With Antithrombotic Activity. 2. Syntheses and Pharmacological Evaluation of Pyrrole[2,3-c]azepine Derivatives, *Chem. Pharm. Bull.*, 2000, **48**, 1129-1137

[106] Latypovt, S.; Fernandez, R.; Quinoa E.; Riguera, R.; The Conformation of Aldisin and Analogues. A Potential Model for Expanded Nucleosides, *Tetrahedron*, **1995**, *51*, 1301-1310

[107] Greene, T. W.; Wuts, P. G. M. Protective Groups in Organic Synthesis (3rd Ed.), Wiley-Interscience, **1999**

[108] Bell, M.; D'Ambra, T.; Kumar, V.; Eissenstat, M.; Hermann, J.; Wetzel, J.; Rosi, D.; Philion, R.; Daum, S.; Hlasta, D.; Kullnig, R.; Ackerman, J.; Haubrich, D.; Luttinger, D.; Baizman, E.; Miller M.; Ward, S.; Antinociceptive (Amiloalkyl)indoles, *J. Med. Chem.*, **1991**, *34*, 1099-1110

[109] Wanner, M.; Koomen, G.; Pandit, U.; Inter- and Intramolecular Addition of Ester Anions to Nicotinium salts, *Tetrahedron*, **1983**, *39*, 3673-3681

[110] Ketcha, D. M.; Lieurance B. A.; Homan, D. F. J.; Synthesis of Alkyl-Substituted N-Protected Indoles via Acylation and Reductive Deoxygenation, *J. Org. Chem.*, **1989**, *54*, 4350-4356

[111] Gribble, G.; Keavy, D.; Davis, D.; Saulnier, M.; Pelcman, B.; Barden, T.; Sibi, M.; Olson, E.; BelBruno, J.; Synthesis and Diels-Alder Cycloaddition Reactions of 4*H*-Furo[3,4-*b*]indoles. A Regiospecific Diels-Alder Synthesis of Ellipticine, *J. Org. Chem.*, **1992**, *57*, 5879-5891

[112] Dhanak, D.; Reese, C. B.; studies in the Protection of Pyrrole and Indole Derivatives, *J. Chem. Soc., Perkin Trans 1*, **1986**, *1*, 2181-2186

[113] Coyne, S.; Hallett, A.; Munns M.; Young G.; Amino-acids and Peptides. Part 45. The Protection of the Thiol Function of Cysteine and the Imidazole-N of Histidine by the Diphenyl-4-pyyridylmethyl Group; *J. Chem. Soc., Perkin Trans I*, **1981**, 522-528.

[114] Chacun-Lefevre, L.; Joseph B.; Merour, J.; Synthesis and Reactivity of Azepino[3,4-*b*]indol-5yl Trifluoromethanesulfonate, *Tetrahedron*, **2000**, *56*, 4491-4499

[115] Mariminon, C.; Pierre, A.; Pfeiffer, B.; Perez, V.; Leonce, S.; Joubert, A.; Bailly, C.; Renard, P.; Hickman, J.; Prudhomme, M.; Synthesis and Antiproliferative Activities of 7-Azarebeccamycin Analogues Bearing One 7-Azaindole Moiety, *J. Med. Chem.*, **2003**, *46*, 609-622

[116] Villemin, D.; Gomez-Escalonilla M.; Saint-Clair, J.; Palladium-Catalysed Phenylation of Heteroaromatics in Water or Methylformamide Under Mircrowave Irradiation, *Tetrahedron Lett.*, **2001**, *42*, 635-637

[117] Zanon, J.; Klapars A.; Buchwald, S.; Copper-Catalysed Domino Halide Exchange-Cyanation of Aryl Bromides, *J. Am. Chem. Soc.*, **2003**, *125*, 2890-2891

[118] Barraja, P.; Diana, P.; Lauria, A.; Passannanti, A.; Almerico, A.; Minnei, C.; Longu, S.; Congiu, D.; Muisu C.; LaColla, P.; Indolo[3,2-c]cinnolines with Antiproliferative, Antifungal, and Antibacterial Activity, *Bioorg. Med. Chem.*, **1999**, *7*, 1591-1596

[119] Smith, M. B.; Guo, L.; Okeyo, S.; Stenzel, J.; Yanella J.; LaChapelle, E.; Regioselective One-Pot Bromination of Aromatic Amines, *Org. Lett.*, **2002**, *4*, 2321-2323

[120] Arris, C. E.; Boyle, F. T.; Calvert, A. H.; Curtin, N. J.; Endicott, J. A.; Garman, E. F.; Gibson, A. E.; Golding, B. T.; Grant, S.; Griffin, R. J.; Jewsbury, P.; Johnson, L. N.; Lawrie, A. M.; Newell, D. R.; Noble, M. E. M.; Sausville, E. A.; Schultz R.; Yu, W.; Identification of Novel Purine and Pyrimidine Cyclin-Dependent Kinase Inhibitors with Distinct Molecular Interactions and Tumor Cell Growth Inhibition Profiles, *J. Med. Chem.*, **2000**, *43*, 2797-2804

[121] Cywin, C. L.; Firestone, R. A.; McNeil, D. W.; Grygon, C. A.; Crane, K. M.; White, D. M.; Kinkade, P. R.; Hopkins, J. L.; Davidson, W.; Labadia, M. E.; Wildeson, J.; Morelock, M. M.; Peterson, J. D.; Raymond, E. L.; Brown M. L.; Spero, D. M.; The Design of Potent Hydrazones and Disulfides as Cathepsin S Inhibitors, *Bioorg. Med. Chem.*, **2003**, *11*, 733-740

[122] Rossello, A.; Bertini, S.; Lapucci, A.; Macchia, M.; Martinelli, A.; Rapposelli, S.; Herreros, E.; Macchia, B.; Synthesis, Antifungal Activity, and Molecular Modeling Studies of New Inverted Oxime Ethers of Oxiconazole, *J. Med. Chem.*, **2002**, *45*, 4903-4912

[123] Palani, A.; Shapiro, S.; Josien, H.; Bara, T.; Clader, J. W.; Greenlee, W. J.; Cox, K.; Strizki, J. M.; Baroudy, B. M.; Synthesis, SAR, and Biological Evaluation of Oximino-piperidino-piperidine Amides. Orally Bioavaliable CCR5 Receptor Antagonists With Potent Anti-HIV Activity, *J. Med. Chem.*, **2002**, *45*, 3143-3160

[124] Karakurt, A.; Dalkara, S.; Ozalp, M.; Ozbey, S.; Kendi, E.; Stables, J. P.; Synthesis of Some 1-(2-Naphthyl)-2-(imidazole-1-yl)ethanone Oxime and Oxime Ether Derivatives and Their Anticonvulsant and Antimicrobial Activities, *Eur. J. Med. Chem.*, **2001**, *36*, 421-433

[125] Clore, G. M.; Robien M. A.; Gronenhorn, A. M.; Exploring the limits of precision and Accuracy of Protein Structures Determined by Nuclear Magnetic Resonance Spectroscopy, *J. Mol. Biol.*, **1993**, *231*, 82-102

[126] Nettleton, D. E.; Balitz, D. M.; Doyle, T. W.; Brandner, W. T.; Johnson, D. L.; O'Herron, F. A.; Schreiber, R. H.; Coon, A. B.; Moseley, J. E.; Myllymaki, R. W.; Antitumour Agents from Bohemic Acid Complex, III. The Isolation of Marcellomycin, Musettamycin, Rudolphomycin, Mimimycin, Collinemycin, Alcindoromycin and Bohemamine, *J. Nat. Prod.*, **1980**, *43*, 242

[127] Lipshutz, B. H.; Pegram, J. J.; β-(Trimethylsilyl)ethoxymethyl chloride. A New Reagent for the Protection of the Hydroxyl Group, *Tetrahedron Lett.*, **1980**, *21*, 3343-3346

[128] Muchowski, J. M.; Solas, D. R.; Protecting Groups for the Pyrrole and Indole Nitrogen Atom. The [2-(Trimethylsilyl)ethoxy]methyl Moeity. Lithiation of 1-[[2-(Trimethylsilyl)ethoxy]methyl]pyrrole, *J. Org. Chem.*, **1984**, *49*, 203-205

[129] Fresneda, P. M.; Molina, P.; Sanz, M. A.; The first Synthesis of the Bis(indole) Marine Alkaloid Rhopaladin D, *Synlett*, **2000**, *8*, 1190-1192.

[130] Lipshutz, B. H.; W Vaccaro W.; Huff, B.; Protection of Imidazoles as Their β-Trimethylsilylethoxymethyl (SEM) Derivatives, *Tetrahedron Lett.*, **1986**, *27*, 4095-4098

[131] Whitten, J. P.; Mathews, D. P.; McCarthy, J. R.; [2-(Trimethylsilyl)ethoxy]methyl (SEM) as a Novel and Effective Imidazole and Fused Aromatic Imidazole Protecting Group, *J. Org. Chem.*, **1986**, *51*, 1891-1894.

[132] McCort, G.; Duclos, O.; Cadilhac, C.; Guilpain, E.; A Versatile New Synthesis of 4-Aryl- and Heteroaryl- [3,4-*c*]pyrrolocarbazoles by [4+2] Cycloaddition Followed by Palladium Catalysed Cross Coupling, *Tetrahedron Lett.*, **1999**, *40*, 6211-6215

[133] Garg, N. K.; Sarpong, R.; Stoltz, B. M.; The First Total Synthesis of Dragmacidin D, *J. Am. Chem. Soc.*, **2002**, *124*, 13179-13184

[134] Suzuki, H.; Tsukuda, A.; Kondo, M.; Aizwa, M.; Senoo, Y.; Nakajima, M.; Watanabe, T.; Yokoyama, Y.; Murakami, Y.; Unexpected Debenzylation of *N*-Benzylindoles with Lithium Base. A New Method of *N*-Debenzylation, *Tetrahedron Lett.*, **1995**, *36*, 1671-1672

[135] Denyer, K.; Waite, D.; Motawia, S.; Moller, B. L.; Smith, A. M.; Granule-Bound Starch Synthase I in Isolated Starch Granules Elongates Malto-oligosaccharides Processively, *Biochem. J.*,**1999**, *340*, 183-191

[136] Jiang, S.; Singh, G.; Chemical Synthesis of Shikimic Acid and Its Analogues, *Tetrahedron*, **1998**, *54*, 4697-4753

[137] De Koning, C. B.; Michael, J. P.; Rousseau A. L.; A Versatile and Convenient Method for the Synthesis of Substituted Benzo[*a*]carbazoles and Pyrido[2,3-*a*]carbazoles, *J. Chem. Soc., Perkin Trans. 1*, **2000**, 1705–1713

[138] Sharma, V.; Lansdell, T. A.; Jin, G.; JJ Tepe, J. J.; Inhibition of Cytokine Production by Hymenialdisine Derivatives, *J. Med. Chem.*, **2004**, *47*, 3700-3703

[139] Sharma V.; Tepe, J. J.; Potent inhibition of Checkpoint Kinase Activity by a Hymenialdisine-derived Indoloazepine, *Biorg. & Med. Chem. Letts.*, **2004**, *14*, 4319-4321

[140] Clayden, J.; Greeves, N.; Warren, S.; Wothers, P.; Organic Chemistry, Oxford University Press Inc., New York, **2001**

[141] Pigulla, J.; Roder, E.; *Liebigs Ann. Chem.*, **1978**, 1390-1398

[142] Suzuki, H.; Iwata, C.; Sakurai, K.; Tokumoto, K.; Takahashi, H.; Hanada, M.; Yokoyama, Y.; Murakami, Y.; A General Synthetic Route for 1-Substituted 4-Oxygenated β-Carbolines (Synthetic Studies on Indoles and Related Compounds 41), *Tetrahedron*, **1997**, *53*, 1593-1606

[143] Kobylecki, R. J.; McKillop, A.; 1,2,3-Triazines, *Adv. Heter. Chem.*, **1976**, *19*, 215-277

[144] Patrick, G. L.; An Introduction to Medicinal Chemistry, Oxford University Press Inc., New York, **1999**

[145] Pal, M.; Parasuraman, K.; Gupta, S.; Yeleswarapu, K. R.; Regioselective Synthesis of 4-Substituted-1-Aryl-1-butanones Using a Songogashira-Hydration Strategy: Copper-Free Palladium-Catalyzed Reaction of Terminal Alkynes with Aryl Bromides, *Synlett*, **2002**, *12*, 1976-1982

[146] Faltz, A.; Radspieler, A.; Liebscher, J.; Synthesis of Optically Active Condensed Tetrahydropyridin-3-ones as Precursors of Alkaloid Analogues, *Synlett*, **1997**, 1071-1072

[147] Faul, M. M.; Winneroski, L. L.; Palladium-Catalyzed Acylation of a 1,2-Disubstituted 3-Indolylzinc Chloride, *Tetrahedron Lett.*, **1997**, *38*, 4749-4752

[148] Keck, G. E.; McHardy, S. F.; Murry, J. A,; Some Unusual Reactions of Weinreb Amides, *Tetrahedron Lett.*, **1993**, *34*, 6215-6218

[149] Braun, M.; Waldmuller, D; Simple Three-Step Synthesis of (*R*)- and (*S*)-4-Amino-3-hydroxybutanoic Acid (GABOB) by Stereoselective Aldol Addition, *Synthesis*, **1989**, 856-858

[150] Alberola, A.; Ortega, A. G.; Sidaba M. L.; Safiudo C.; Versatility of Weinreb Amides in the Knorr Pyrrole Synthesis, *Tetrahedron,* **1999**, *55*, 6555-6566

[151] Oster, T. A.; Harris, T. M.; Acetylations of Strongly Basic and Nucleophilic Enolate Anions with N-Methoxy-N-Methylacetamide, *Tetrahedron Lett.*, **1983**, *24*, 1851-1854

[152] Huang, C. C.; Couch, G. S.; Pettersen, E. F.; Ferrin, T. E.; Chimera: An Extensible Molecular Modeling Application Constructed Using Standard Components, *Pac. Symp. Biocomp.*, **1996**, *1*, 724

[153] UCSF Chimera, an Extensible Molecular Modelling System. [www]<URL: http://www.cgl.ucsf.edu/chimera [Accessed 26th August 2005]

[154] Petrassi, H. M.; Sharpless, K. B.; Kelly, J. W.; The Copper-Mediated Cross-Coupling of Phenylboronic Acids and *N*-Hydroxyphthalimide at Room Temperature: Synthesis of Aryloxyamines, *Org. Lett.*, **2001**, *3*, 139-142

[155] Legault, C.; Charette, A. B.; Highly Efficient Synthesis of *O*-(2,4-Dinitrophenyl)hydroxylamine. Application to the Synthesis of Substituted *N*-Benzoyliminopyridinium Ylides, *J. Org. Chem.*, **2003**, *68*, 7119-7122

[156] Safety (MSDS data for hydrazine hydrate [www]<URL: http://physchem.ox.ac.uk/MSDS/HY/hydrazine_hydrate.html [accessed 28th August 2005

[157] IPCS International Program on Chemical Safety, Health and Safety Guide No. 56; [www]<URL; http://energyconcepts.tripod.com/energyconcepts/hydrazinedata.htm [accessed 28th August 2005]

[158] Kunick, C.; Synthese von 7,12-Dihydro-indolo[3,2-*d*][1]benzazepin-6-(5*H*)-onen und 6,11-Dihydro-thieno-[3',2':2,3]azepnio[4,5*b*]indol-5(4*H*)-*on*, *Arch. Pharm. (Weinheim)*, **1992**, *325*, 297-299.

[159] Wieking, K.; Knockaert, M.; Leost, M.; Zaharevitz, D. W.; Meijer, L.; Kunick, C.; Synthesis of Paullones with Aminoalkyl Side Chains, *Arch. Pharm. Med. Chem.*, **2002**, *7*, 311-317.

[160] Chen, W. Y.; Gilman, N. W.; Synthesis of 7-Phenylpyriido[5,4-*d*][1]benzepin-2-ones, *J.Heterocyclic Chem.*, **1983**, *20*, 663-666.

[161] Soule, H. D.; Vasquez, J.; Long, A.; Albert, S.; Brennan, M.; A Human Cell Line from a Pleural Effusion Derived from a Breast Carcinoma, *J. Nat. Can.*, **1973**, *51*, 1409-1416

[162] Lieber, M.; Smith, B.; Szakal, A.; Nelson-Rees, W.; Todaro, G.; A Continuous Tumour-Cell Line from a Human Lung Carcinoma With Properties of type II Alveolar Epithelial Cells, *Int. J. Cancer.*, **1976**, *17*, 62-70

[163] Gibson, A. E.; Arris, C. E.; Bentley, J.; Boyle, F. T.; Curtin, N. J.; Davies, T. G.; Endicott, J. A.; Golding, B. T.; Grant, S.; Griffin, R. J.; Jewsbury, P.; Johnson, L. N.; Mesguiche, V.; Newell, D. R.; Noble, M. E. M.; Tucker, J. A.; Whitfield, H. J.; Probing the ATP Ribose-Binding Domain of Cyclin-Dependent Kinases 1 and 2 with O6-Substituted Guanine Derivatives, *J. Med. Chem.*, **2002**, *45*, 3381-3393.

[164] Lipinski, C. A.; Lombardo, F.; Dominy, B. W.; Feeney, P. J.; Experimental and Computational Approaches to Estimate Solubility and Permeability in Drug Discovery and Development Settings, *Adv. Drug Dev. Rev.*, **1997**, *23*, 3-25

[165] Lottin, J.R.P.; Design of Novel Cyclin Dependent Kinase Inhibitors. *PhD Thesis, University of Wales*, **2004**

[166] Bartek, J.; Lukas, J; Chk1 and Chk2 Kinases in Checkpoint Control and Cancer, *Cancer cell*, **2003**, *3*, 421-429

[167] Portevin, B.; Golsteyn, R. M.; Pierre, A.; De Nanteuil, G.; An Expeditious Multigram Preparation of the Marine Protein Kinase Inhibitor Debromohymenialdisine, *Tetrahedron Lett.*, **2003**, *44*, 9263-9365

[168] Palani, A.; Shapiro, S.; Josien, H.; Bara, T.; Calder, J. W.; Greenlee, W. J.; Cox, K.; Strizki J. M.; Baroudy, B. M.; Synthesis, SAR and Biological Evaluation of Oximeino-Pipidino-Piperdine Amides. 1. Orally Bioavaliable CCR5 Receptor Antagonists with Potent Anti-HIV activity, *J. Med. Chem.*, **2002**, *45*, 3143-3160

[169] Bretechea, A.; Duflosa, M.; Dassonvillea, A.; Nourrissona, M.; Breleta, J.; Le Bauta, G.; Grimaudb, N.; Petit, J. Y.; New N-Pyridinyl(methyl)-indole-2- and 3-(Alkyl)carboxamides and Derivatives Acting as Systemic and Topical Inflammation Inhibitors, *J. Enzyme Inhib. Med. Chem.*, **2002**, *17*, 415–424

[170] Liu, Y.; Gribble, G. W.; Selective Lithiation of 2,3-Dibromo-1-methylindole. A Synthesis of 2,3-Disubstituted Indoles, *Tetrahedron Lett.*, **2002**, *43*, 7135–7137

[171] Varnavas, A.; Lassiani, L.; Luxich, E.; Zacchigna, M.; Boccu, E.; Pichierri, F.; Quinolone derivatives: Synthesis and Binding Evaluation on Cholecystokinin Receptors, *Il Farmaco*, **1996**, *51*, 341-350

[172] Leopoldo, M; Berardi, F.; Colabufo, N. A.; DeGiorgio, P.; Lacivita, E.; Perrone, R.; and Tortorella V.; Structure-Affinity Relationship Study on *N*-[4-(4-Arylpiperazin-1-yl)butyl]arylcarboxamides as Potent and Selective Dopamine D3 Receptor Ligands, *J. Med. Chem.*, **2002**, *45*, 5727-5735

[173] Suzuki, H.; Shinpo, K.; Yamazaki, T.; Niwa, S.; Yokoyama Y.; Murakami, Y.; Synthetic Studies of 1,2,3,4-Tetrahydro-1,3,4-trioxo-β-carboline Alkaloids I, *Heterocycles*, **1996**, *42*, 83-6

[174] Loudon, G. S.; Radhakrishna, A. S.; Almond, M. R.; Blodgett, J. K.; Boutin, R. H.; Conversion of Aliphatic Amides Into Amines With [I,I-Bis(trifluoroacetoxy)iodo]benzene. 1. Scope of the Reaction, *J. Org. Chem.*, **1984**, *49*, 4272-4276

[175] Stieber, F.; Grether, U.; Waldmann, H.; Development of the Traceless Phenylhydrazide Linker for Solid-Phase Synthesis, *Chem. Eur. J.*, **2003**, *9*, 3270-3281

[176] Abell, A. D.; Nabbs B. K.; Battersby, A. R.; The Reaction of N-Magnesium Derivatives of Pyrroles with N-Mesylchloromethylpyrroles: A Synthesis of Dipyrrylmethanes, *J. Org. Chem.*, **1998**, *6*, 8163-8169

[177] Makosza, M.; Kwast, E.; Vicarious Nucleophilic Substitution of Hydrogen in Nitroderivatives of Five-Membered Heteroaromatic Compounds, *Tetrahedron*, **1995**, *51*, 8339-8354

[178] Yokoyama, Y.; Ikeda, M.; Saito, M.; Yoda, T.; Suzuki, H.; Murakami, Y.; Palladium-catalyzed Reaction of 3-Bromoindole Derivative with Allyl Esters in the Presence of Hexa-*n*-butyldistannane, *Heterocycles,* **1990**, *31*, 1505 -1511

[179] Durst, H.D.; Gokel, G.W.; Experimental Organic Chemistry, 2nd Ed., McGraw-Hill (publisher), Experimental 11.1, Synthesis of Phenylmagnesium Bromide, **1987**, 313-317

[180] Gee, J. M. W.; Harper, M. E.; Hutcheson, I. R.; Madden, T. A.; Barrow, D.; Knowlden, J. M.; McClelland, R. A.; Jordan N.; Wakeling, A. E.; Nicholson, R. I. ; The Antiepidermal Growth Factor Receptor Agent Gefitinib (ZD1839/Iressa) Improves Antihormone Response and Prevents Development of Resistance in Breast Cancer in Vitro, *Endocrinology*, **2003**, *144*, 5105–5117

[181] Molecular Operating Environment 2004.03 (MOE) Chemical Computing Group Inc Montreal Quebec Canada http://www.chemcomp.com

[182] Tripos SYBYL 7.0, Tripos Inc 1699 South Hanley Rd St Louis Missouri 63144 USA http://www.tripos.com

CARDIFF UNIVERSITY * PRIFYSGOL CAERDYDD *